



# GRADUATE SCHOOL YEARBOOK 2020



# **GRADUATE SCHOOL YEARBOOK 2020**



# Our PhD students contribute to solving present and future challenges

Welcome to Graduate School Yearbook 2020 in which we highlight the important work of our PhD students.

At DTU Chemical Engineering, we host about 100 PhD students from all over the world. We highly appreciate the international environment that this creates and in this publication, you get an insight into the many and varied research areas they cover.

Some have just initiated their work, whereas others are close to writing their thesis. Common to them all is, however, that sustainability is a focal point. At DTU Chemical Engineering, we are doing our best to support our national climate goals as well and the UN's sustainability goals. Thus, the PhD students have selected the most relevant goal for their project.

This is part of a wider effort at DTU in general. We want to highlight the importance of technology development in order to support future sustainable growth. To do so, we need to have a very wide and strong focus on sustainability – and it is obvious that many of the environmental challenges we face today can be solved only by using science and technology.

Consequently, at DTU Chemical Engineering we develop and utilize knowledge, methods, technologies and sustainable solutions within:

- Chemical and biochemical process engineering and production
- Design of chemical and biochemical products and processes
- Energy and environment

Sustainable growth asks for clever solutions and requires the ability to think big and innovative - and for that, we believe in our young PhD students. Their work is of utmost importance and contributes to shaping future development not only in Denmark, but around the world.



Kim Dam-Johansen  
Professor, Head of Department

## CONTENT

### A

Akhilesh Nair 10  
*Hydrogenation in Flow*

Andersen Jakob Afzali 12  
*Exploring Plasma-Catalysis for Sustainable Production of Chemicals*

Aouichaoui, Adem Rosenkvist Nielsen 14  
*Machine Learning (AI) Applications for New and Improved Property Predictions*

Aprile, Giovanni 16  
*Development of Lab-Scale Continuous Crystallizers for Pharmaceutical APIs*

### C

Caño de Las Heras, Simoneta 18  
*Development of a Virtual Educational Bioprocess Plant*

### D

Dotti, Margherita 20  
*Ash Transformation in Waste Boilers and Optimization of Novel Steam Superheater*

Du, Yifan 22  
*Pollutant formation and control in wood stoves*

Duan, Yuanmeng 24  
*Melamine tail gas cleaning with ionic liquids*

### E

Enekvist, Karl Markus Jannert 26  
*Computer-Aided Product Design of Organic Coatings*

### F

Frydenberg, Tenna 28  
*The use of silica aerogels-encapsulated biocides to achieve long-term efficacy of antifouling coatings*

Fu, Aixiao 30  
*Novel Intumescent Coatings Development*

### G

Gong, Wentao 32  
*Liquefaction for transport of CO<sub>2</sub> from steel blast furnaces*

Guo, Bingwen 34  
*Experimental and Theoretical Study of Cyclone Reactors*

### H

Hasanzadeh, Aliyeh 36  
*Development of an electrochemical sensor for real-time monitoring of bioprocess*

Hu, Pengpeng 38  
*Silicone elastomer constructed of concatenated rings shows excellent elasticity*

**J**

Jensen, Jesper Wang <i>Design and Upscaling of Pseudomonas putida Fermentations for Robust Biomanufacturing</i>	40
Jeong, Seonghyeon <i>Autonomous self-healing dielectric elastomer actuator</i>	42
Jian, Jie <i>O<sub>3</sub> assisted Combustion to alternative Fuel</i>	44
Jurášková, Alena <i>Condensation curing silicone elastomer coatings with high scratch resistance</i>	46

**K**

Kaiser, Johann <i>Evaluation of Single-Pass Tangential Flow Filtration (SPTFF) to Increase Productivity in Protein Purification Processes</i>	48
Kang, Zhaoqing <i>High-permittivity Silicone Elastomers for Sensitive Flexible Pressure Sensors</i>	50
Krpovic, Sara <i>Coating with inherent sensing functionality based on dielectric elastomer</i>	52

**L**

Lamprakou, Zoi <i>Role of Additives on Corrosion Protection of Metals by Organic Coatings</i>	54
Li, Qiong <i>Quantification of internal stress in thermoset coatings</i>	56
Li, Shu <i>Investigation of Anti-corrosive Coatings Degradation Mechanism – The Use of Non-destructive Evaluation Techniques</i>	58
Luo, Shicong <i>Dispersion principles of coatings production</i>	60
Løge, Isaac Appelquist <i>Kinetic of scaling formation</i>	62

**M**

Mancini, Enrico <i>Sustainable and Cost-Effective Routes for Production and Separation of Succinic Acid</i>	64
Mirzaei, Mohamadali <i>A Numerical and Experimental Investigation of Industrial Cyclones</i>	66
Monje López, Vicente T. <i>Evaluation of optimization potentials and capacity liberation options in a full-scale industrial wastewater system using a Digital Twin</i>	68
Muthachikavil, Aswin Vinod <i>Exploring the Structure and Properties of Water</i>	70

**N**

Nazemzadeh, Nima 72  
*An integrated multi-scale framework for bioprocess design, control and analysis*

Nielsen, Kasper Rode 74  
*Novel Catalysts and Reaction Pathways to Complex Nitrile Molecules*

Nielsen, Niels Dyreborg 76  
*Catalytic Methanol Synthesis*

Nielsen, Rasmus Fjordbak 78  
*Novel Strategies for Control and Monitoring of Bio-Processes using Advanced Image-Analysis*

**O**

Olsen, Martin Due 80  
*Further Development of the Primitive Electrolyte Equation of State Approach*

Olsson, Emil Lidman 82  
*Phosphorus Chemistry in Biomass Combustion*

**P**

Pandey, Jyoti Shanker 84  
*Experimental Investigation of CH<sub>4</sub>/CO<sub>2</sub> Mixed Hydrate Phase Behavior During CH<sub>4</sub> Recovery and CO<sub>2</sub> Storage*

Pedersen, Morten Lysdahlgaard 86  
*Real-Time Evaluation of the Settlement of Marine Biofouling*

Pinto, Tiago 88  
*Ecological Control Strategies for Biobutanol Production*

Pudi, Abhimanyu 90  
*Multiscale Modeling of Liquid-Liquid Phase Transfer Catalysis*

**Q**

Qi, Chunping 92  
*Investigation and improvement of zinc-rich coatings*

**R**

Rasmussen, Jess Bjørn 94  
*Cyclic Distillation Technology*

Rezazadeh, Amirali 96  
*Experimental study and modelling of PET plastic recycling process*

**S**

Schandel, Christian Bækhøj 98  
*Cracking of Sugars for Production of Chemicals*

Segura, Isabel Pol 100  
*Optimization of geopolymers cement technologies*

Shao, Jiang 102  
*Stretchable conductive MWCNTs-PDMS composite*

Shi, Meng	104
<i>Macroscopic study on depressurization production of hydrate spheres below ice freezing point</i>	
Su, Ziran	106
<i>High performance production of oligosaccharides by using enzymatic membrane reactors</i>	
<b>T</b>	
Thorsen, Lauge	108
<i>Combustion Chemistry Studies for Marine Engines</i>	
Thrane, Joachim	110
<i>Novel Catalysts for the Selective Oxidation of Methanol to Formaldehyde</i>	
Tong, Jiahuan	112
<i>Theory, Simulation and Models for Electrolyte Systems with Focus on Ionic Liquids</i>	
Topalian, Sebastian	114
<i>Development of Digital Twins in Water Treatment Systems</i>	
Tran, Jakob-Anhtu	116
<i>Slide-ring silicone networks for dielectric elastomer actuators</i>	
Tsochantaris, Evangelos	118
<i>Advanced Thermodynamic Models for Water</i>	
<b>V</b>	
Vinjarapu, Sai Hema Bhavya	120
<i>Biogas Upgrading Simulation through Experimental Work and Thermodynamic Modelling</i>	
Vollmer, Nikolaus	122
<i>Synergistic Optimization Framework for the Process Design of Biorefineries</i>	
<b>W</b>	
Wang, Wendi	124
<i>Linear viscoelastic and nonlinear extensional rheology of diamine neutralized entangled poly(styrene-co-4-vinylbenzoic acid) ionomer melts</i>	
Wang, Xiaozan	126
<i>Particle deposition in high temperature processes</i>	
<b>Z</b>	
Zafiryadis, Frederik	128
<i>Hydrodynamics of circulating fluidized beds</i>	
Zhao, Liyan	130
<i>Agglomeration in Fluidized Bed Gasification of Wheat Straw</i>	
Zverina, Libor	132
<i>Tubular membrane reactors for immobilization of enzymes</i>	

# Hydrogenation in Flow

(September 2019- August 2022)

9 INDUSTRY, INNOVATION  
AND INFRASTRUCTURE



## Contribution to the UN Sustainable Development Goals

Innovation advances the technological capabilities of industrial sectors and prompts the development of new skills. This project involves the development a continuous flow reactor that can run hydrogenation reactions semi-autonomously. Replacing the existing batch reactor at Lundbeck A/S with a flow reactor enhances safety and lowers energy consumption. It also reduces production costs and helps in faster process optimization. The flexibility of a flow reactor allows the easy scale-up of complex hydrogenations steps, which is a bottleneck for new pharmaceutical drug development.



**Akhilesh Nair**

akbna@kt.dtu.dk

**Supervisors:** Kim Dam-Johansen, Martin Høj, Anker Degn-Jensen and Tommy Skovby (Lundbeck)

### Abstract

The project is in collaboration with Lundbeck A/S and involves developing a flow reactor that can run hydrogenation reactions 24x7 semi-autonomously. The current reactor Lundbeck uses is a batch reactor, which is time consuming in terms of obtaining a high product yield and exhaustive in terms of the catalyst usage. The project primarily looks at designing and demonstrating a multifunctional flow reactor system(s), which can handle a wide range of substrates, catalysts and reaction conditions applicable in the production at Lundbeck in Lumsås (Denmark).

### Introduction

Hydrogenation is a very important unit operation in the chemical industry for synthesizing intermediates and products [1]. Catalytic, heterogeneous hydrogenation is one of the most important and widespread techniques in the reduction of functional groups. Even with the development of very reaction specific homogeneous catalysts for gas/liquid multiphase reactions, the use of heterogeneous catalysts for gas/liquid/solid multiphase reactions is still preferable and holds many advantages over their homogeneous counterparts. These include stability of the catalyst, ease of separating the catalyst from the product, the wide range of reaction conditions available, and the ability to reduce highly unreactive functional groups [2].

In the pharmaceutical and fine chemical industries, most of the multiphase hydrogenation reactions are conducted in large batch reactors, where the catalyst is suspended in the liquid, which is continuously stirred. Hydrogenation falls under the class of reactions, which are fast on noble metals and are usually limited by external mass transfer of gas phase hydrogen to the liquid phase in conventional reactors. These reactions are also highly exothermic in nature, which requires effective

heat removal. In addition, the non-uniform temperature distribution in the conventional reactors may develop hot spots on the catalyst surface or may lead to the formation of several byproduct(s) or intermediate(s), which can also react with one another, and further lead to violent decomposition of starting material or partially hydrogenated intermediates. A continuous flow reactor system is an attractive process intensification that could overcome the challenge of mass and heat transfer seen in batch systems [3].

### Hypothesis

Commercial hydrogenation in flow reactors is done in massive systems, e.g. in the hydrotreating of crude diesel to remove sulfur, producing tons/day. In the pharmaceutical industry, the amount of product is much smaller and flow systems producing around 30-200 kg/day is needed. This means that the systems must be much smaller. In addition, pharmaceutical ingredients typically have multiple chemical functionalities, which means that the hydrogenation must be selective, so it is performed at moderate temperature (< 100 °C), but the small volume makes the expensive, but more active and selective, noble metal catalysts feasible.

In addition, the products and substrates in production are often changed, which means that a generic process system (reactor) that can handle different catalysts, solvents and substrates, as well as different reaction conditions such as temperature, pressure and residence time is needed. This could either be a fixed bed reactor system, where the liquid substrate solution trickles down by gravity with a flow of hydrogen gas or a slurry flow system where the catalyst is suspended in the substrate solution and flows with a stream of hydrogen gas.

In collaboration with the production and process development department at H. Lundbeck A/S this project aims at designing and demonstrating a multifunctional flow reactor system, which can handle a wide range of substrates, catalysts and reaction conditions applicable in the production at Lundbeck in Lumsås (Denmark).

Existing systems such as the FLowCAT trickle bed reactor from HEL, the H-cube reactor Thales Nano and the Corning Advanced flow reactor provide the basis and inspiration for developing a pharmaceutical industry sized pilot scale reactor capable of producing on the order of 0.1 to 1kg product per day. [4]

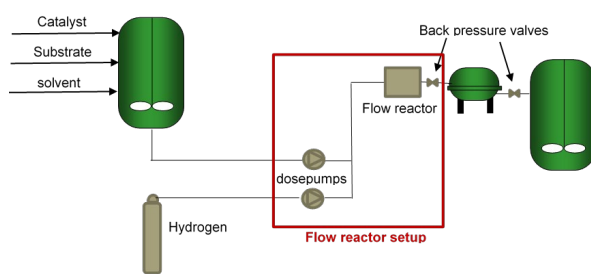


Figure 1: A typical Flow reactor setup. The catalyst, the solvent and the substrate (organic precursor molecule) is mixed together and fed into a flow reactor as a slurry along with hydrogen. These are then separated downstream.

### Objectives

1. Literature survey of selective catalytic hydrogenation of functional organic molecules in flow reactors including options for catalyst and reactor design
2. Investigations of hydrogenation of relevant substrates (typically multifunctional organic compounds) in an existing trickle-bed, high-

pressure reactor setup at DTU Chemical Engineering.

3. Synthesis and characterization of hydrogenation catalysts
4. Development of a new flow reactor system for trickle or slurry flow of catalyst, solvent and substrate with high-pressure hydrogen, which can be applied in the pilot-plant or production at Lundbeck A/S.
5. Performing detailed chemical analysis of hydrogenation products using e.g. HPLC, GC-MS

As an example, the hydrogenation of a functional organic precursor produced by Lundbeck, in a trickle bed reactor is shown in Figure 2.

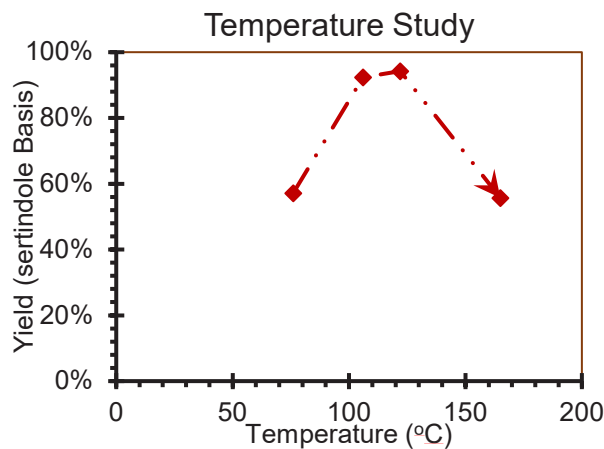


Figure 2: Hydrogenation of a precursor Lu23-148 to Sertindole in a trickle bed reactor using 5wt% Pt/C catalyst. Liquid flow: 0.05 ml/min. Pressure: 90bar. Substrate Concentration: 0.3M. Hydrogen Flow: 1000 Nml/min. The Hydrogenation is seen to be dependent on the reaction temperature.

### References

1. P. Baumeister, H.U. Blaser, M. Studer, *Catalysis Letters* 49 (1997) 219-222.
2. R.V.Jones, L.Godorhazy, N.Varga, D.Szalay, L.Urge, F. Darvas, *J.Comb Chem* 8 (2006) 110-116.
3. S.Nishimura, *Handbook of Heterogenous Catalytic Hydrogenation for Organic Synthesis*, Wiley Publishers, Japan, 2001, Vol. 1.
4. J.M. Hawkins, *Enantio- and Diastereoselective Hydrogenation of Pharmaceutical Intermediates*, Chemical Research and Development Pfizer PharmaTherapeutics, U.K, August 2010.

# Exploring Plasma-Catalysis for Sustainable Production of Chemicals

(October 2018 - September 2021)



## Contribution to the UN Sustainable Development Goals

Historically, production of chemicals has been made based on fossil resources with a focus on minimizing the energy and feedstock consumption leading to large chemical plants. This project will explore the use of non-thermal plasma in combination with catalysis for a sustainable production of chemicals. The plasma can be powered by renewable energy and act as the reaction enabler instead of high temperature or pressure. This minimizes the use of fossil fuels and allows a local production that cuts away transportation expenses.



**Jakob Afzali Andersen**  
Jakaan@kt.dtu.dk

**Supervisor:** Anker Degn Jensen, Jakob Munkholt Christensen, Martin Østberg (Haldor Topsøe A/S), Annemie Bogaerts (University of Antwerpen)

## Abstract

An alternative to thermal activation of gas mixtures is the use of a non-thermal plasma. This technology has been shown to be applicable in the decomposition of molecules. In this study, a coaxial dielectric barrier discharge reactor with a discharge zone of 5 cm and a gap of 4.5 mm was used to study ammonia decomposition. A fixed power input of 21 W at a frequency of 3 kHz was used along with ambient pressure and temperature. The influence of different dielectric materials and impregnation of transition metals was examined. An improved decomposition was found when introducing dielectric materials, typically used as supports in thermal catalysis however, impregnation with metals decreased the NH<sub>3</sub> conversion.

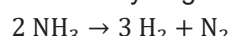
## Introduction

Hydrogen is considered an important fuel of the future, because it is a clean energy source with water as the only by-product from combustion. However, delivery and storage of H<sub>2</sub> is hindering the commercialization of fuel cell-based processes, along with catalyst and reactor stability of a fuel cell system [1].

Non-thermal plasma (NTP) processes have been studied for many years in numerous environmental applications [2], especially for air and water pollution control, and in the production of ozone from air [3]. NTP can be generated by atmospheric pressure discharges, such as corona discharge or dielectric barrier discharge (DBD), by applying a sufficiently strong electric field to the enclosed gas mixture, which then initiates electron avalanches and streamer formation. The electrons are characterised by a much higher temperature than the gas molecules, resulting in a mixture that is in a non-thermodynamic equilibrium [4].

Recently, the use of plasma-catalytic processes have shown an enhanced ability for NH<sub>3</sub> decomposition (Reaction 1) [5,6]. The process can

be powered by renewable electricity, as the flexibility of the plasma allows for operation that accommodates the fluctuations from such sources. This offers a process that can provide CO<sub>x</sub>-free H<sub>2</sub> from an easily storable hydrogen carrier.



In this study, the combination of NTP and catalysis was used to convert NH<sub>3</sub> into H<sub>2</sub> and N<sub>2</sub>.

## Materials and Methods

An NH<sub>3</sub> (99.999% purity) flow rate of 75 Nml/min was fed to a coaxial DBD reactor with quartz as the dielectric barrier (reactor wall). A discharge length and gap of 5 cm and 4.5 mm, respectively, were used in this study. The power was supplied by a high voltage amplifier controlled by a function generator. A fixed frequency of 3 kHz and power input of 21 W was utilised for all experiments, along with atmospheric pressure and no addition of thermal heat.

In the plasma-catalysis experiments, the plasma zone was fully packed with different types of dielectric materials (SiO<sub>2</sub>, MgAl<sub>2</sub>O<sub>4</sub>, γ-Al<sub>2</sub>O<sub>3</sub>, m-ZrO<sub>2</sub>, TiO<sub>2</sub>, BaTiO<sub>3</sub>) as well as metal (10 wt.% Ni, 10

wt.% Fe, 10 wt.% Co, 5-5 wt.% Fe-Ni) impregnated  $\text{MgAl}_2\text{O}_4$  and a commercial Fe-based  $\text{NH}_3$  synthesis catalyst (Topsoe - KM1R) all with a particle size of 0.85-1.4 mm.

The reactor effluent was bubbled through a dilute aqueous solution of sulfuric acid to remove unconverted  $\text{NH}_3$ . After absorption of unconverted  $\text{NH}_3$ , the flow rate of the produced  $\text{H}_2$  and  $\text{N}_2$  was measured over a time period of 15 minutes to determine the conversion of  $\text{NH}_3$ . Furthermore, the composition of the product was determined by an online gas chromatograph equipped with a thermal conductivity detector (TCD).

## Results and Discussion

From the gas chromatograph measurements, it was determined that the product flow contained a  $\text{H}_2:\text{N}_2$  fraction of 3:1 as prescribed by Reaction 1, with no  $\text{NH}_3$  remaining after the absorption in acid.

Fig. 1 show that when utilizing dielectric materials, commonly used as supports in thermal catalysis, with a lower dielectric constant (4-30) a significant increase in the  $\text{NH}_3$  conversion compared to plasma-only (5%) was achieved, with  $\text{MgAl}_2\text{O}_4$  yielding the highest conversion of 12.7%. However, as the dielectric constant is increased the conversion decreases below 1%. From analysis of the electrical parameters ( $U$ ,  $I$ , and  $Q$ ) it was furthermore found that the materials showing increased conversion promoted higher intensity current spikes and a lower charge transfer number.

Great importance of the materials' electrical characteristics are thereby shown, as opposed to thermal catalysis, where surface area, porosity, acidity etc. are of high significance. Here, the difference in acidity between  $\text{MgAl}_2\text{O}_4$  and  $\gamma\text{-Al}_2\text{O}_3$  was not found to give rise to a significant change in conversion.

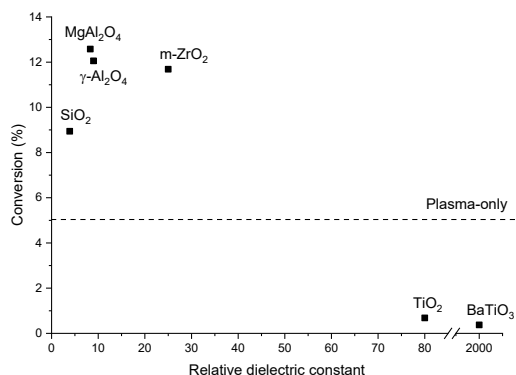


**Figure 1:**  $\text{NH}_3$  conversion as function of relative dielectric constant of different dielectric materials obtained after 2 hours in a 21 W plasma.

Impregnating  $\text{MgAl}_2\text{O}_4$  with different metals was found to result in a decreased conversion as shown in Fig. 2. The catalyst containing 10% wt. Ni still showed an improved conversion (7%) compared to

the plasma-only, while the catalysts containing Fe and Co showed conversions of ca. 1%.

From the electrical parameters, it was observed that the catalysts with low conversion showed a high charge transfer number and low intensity current spikes, similarly to the dielectric materials providing low conversion.

According to thermal catalysis, addition of the metal should increase the surface chemistry, since the  $\text{NH}_3$  can bind more strongly to the metal sites. However, these results indicate that the plasma-assisted decomposition mainly occur in the gas phase by interaction with the high energy electrons.

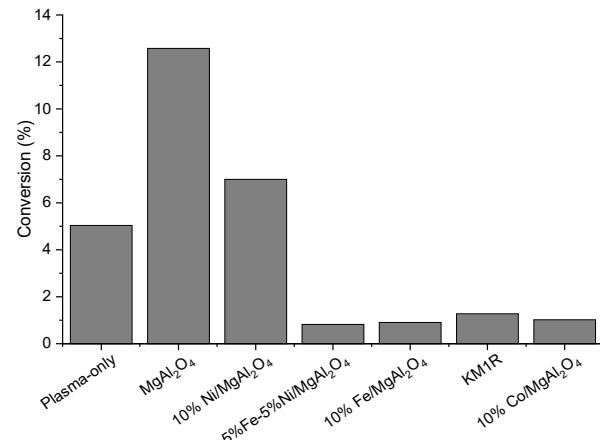


**Figure 2:** Effect of different impregnations on  $\text{NH}_3$  conversion obtained after 2 hours in a 21 W plasma.

## Conclusion

It has been shown that plasma is able to activate  $\text{NH}_3$  at atmospheric pressure and room temperature resulting in a decomposition of 5% for plasma-only under the applied conditions. Implementing  $\text{MgAl}_2\text{O}_3$  in the plasma zone increased the decomposition by a factor of 2.5. Generally, supports with relative dielectric constant in the range 10-30 were found to give strong synergies and enhanced  $\text{NH}_3$  conversion.

Impregnating  $\text{MgAl}_2\text{O}_4$  with metals was found to decrease the conversion due to lower energy electrons in the gas phase.

## References

1. A. Chellappa, C. Fischer, W. Thomson, *Appl Catal A* 227 (2002) 231–40.
2. H.-H. Kim, A. Ogata, S. Futamura, *J. Phys. D. Appl. Phys.* 38 (2005) 1292–1300.
3. S. Pekárek, *Acta Polytech.* 43 (6) (2003) 47–51.
4. R. Snoeckx, A. Bogaerts, *Chem. Soc. Rev.* 46 (19) (2017) 5805–5863.
5. L. Wang, Y. Yi, Y. Guo, Y. Zhao, J. Zhang, H. Guo, *Plasma Process Polym.* 14 (2017).
6. M. Akiyama, K. Aihara, T. Sawaguchi, M. Matsukata, M. Iwamoto, *Int. J. Hydrogen Energy* 43 (2018).

# Machine Learning (AI) Applications for New and Improved Property Predictions

(December 2019- December 2022)



## Contribution to the UN Sustainable Development Goals

Being able to determine various properties related to a large variety of chemicals with more accuracy and extended range of applicability, will allow for the identification of new chemical alternatives to substitute existing ones. These alternatives will be less toxic (with regard to humans and the environment), less hazardous (requiring fewer safety installations during processing) and more cost-effective chemical processes (lower material usage and energy demands). This will ultimately lead to more efficient and responsible consumption and production within the chemical processing industry.



**Adem Rosenkvist  
Nielsen Aouichaoui**  
arnaou@kt.dtu.dk

**Supervisor:** Gürkan Sin  
Jens Abildskov  
Seyed Soheil Mansouri

## Abstract

The ability to predict properties of interest for various chemicals is of paramount importance in many engineering applications such as process design, product design and process safety. The availability of experimental data for many properties is limited to the most commonly used chemicals in industry. In order to discover novel compounds for example chemical substitution, mathematical models exist that leverage available experimental data. Current methods have many drawbacks especially with regards to the way the molecular descriptors and with regards to the nature of the chosen mathematical model relates structure to property. Both drawbacks can be solved by novel discoveries in machine learning.

## Introduction

Chemical engineering is undeniably central to ensuring the development of modern society. It contributes to the improvement in production of fuels, the food processing industry, agriculture, and equipment automation, among many others. These contributions are proof of the diversity in disciplines within chemical engineering. However, central to all these disciplines is the need for knowledge about the behavior and the properties of chemical compounds involved and most importantly their thermo-physical, toxicological and safety related properties.

## Importance of chemical properties

Knowledge about the various properties related to chemical compounds is the corner stone in many engineering applications. The critical properties such as critical pressure and critical temperature are used in equations of state (EoS) such as the Peng-Robinson or the Soave-Redlich-Kwong (SRK) EoS to perform phase equilibria calculations which are of importance in many separation processes such as distillation. Phase equilibria is an essential element

in performing chemical process design through process simulation. Solubility parameters such as the Hansen and the Hildebrand parameters and the melting point can be used to evaluate the solubility of Active Pharmaceutical Ingredients (APIs)[1]. Energy related properties such as the enthalpy of formation in reaction engineering to determine the heat released by the formation reaction of a given compound. Flammability related properties such as lower flammability limit (LFL) and auto-ignition temperature are important metrics to consider when evaluating the safety of processing and storing chemicals [2]. Properties such as the Lethal Dose LC<sub>50</sub> and the Global Warming Potential (GWP) are also used to evaluate the impact of chemicals has on organisms and the environmental in general [3].

The diverse nature of the properties and the fields wherein they are used underscore the need for and challenge in accurately predicting them for a wide variety of compounds.

## The need for predictive models

In general, the chemical properties of interest are determined through tedious and time-consuming experimental work, which often results in high quality data. However, performing experiments as and when the need arises is not an efficient solution [4]. Luckily, many properties have already been measured for many chemicals frequently used in industry and can be obtained through various databases such as the NIST database. However, such databases can be an expensive option and the availability of compounds treated might be limited. This is especially true for novel compounds that may not have been considered in previous research. Therefore, it is of great importance to develop property prediction models that can relate the molecular structure of a compound to the property of interest. An example of such models is the group contribution models where the molecule is described in terms of the occurrence of a predetermined set of groups or molecular descriptors and the value of the property is determined by a contribution for each group[3]. However these models face a series of inherent drawbacks such as the inability to describe large sections of the chemical design space (ability to generalize), a simplistic model structure that might not capture the true underlying trend of the property and sometimes they have questionable accuracy. Recently, a data-driven approach based on deep learning has emerged as a potential candidate to replace previous models and overcome the challenges faced.

## Data-Driven end-to-end Approach

Recent developments in the field of Deep-Learning (DL) and, more specifically, the emergence of Graph Neural Networks (GNN) have made it possible to combine the generation of suitable molecular descriptors and develop a predictive model. GNN are a special type of Deep Neural Networks (DNN) that can process data represented in the graph domain [5]. The molecule is represented as a molecular graph: a set of nodes representing the atoms connected by edges representing the bonds between the nodes/atoms. Associated with each node and each edge is a feature vector reflecting the type of atom (e.g. H, C, N, etc.) and nature of the bond (double bond, ring structure, etc.). This molecular graph is the used as input to the GNN, which is able to learn an embedded state or a vector representation containing information concerning the neighboring atoms [5]. The vector representation is directly used as input to another Fully Connected DNN (FCDNN) (see Figure 1). The FCDNN tries to relate the vector

representation to the desired output, which in this case is the property value. Using back propagation through the GNN and FCDNN, end-to-end learning can be achieved where the vector representation is adjusted to enable meaningful features that are correctly able to link to molecular structure to the property [6]. The initial molecular graph can be constructed through freely available cheminformatics and would therefore overcome the limitation of previous models concerning the ability to generalize. FCDNN as well as many other types of DNN are able to approximate any function (universal approximation theorem), given a suitable architecture. This will make it possible to approximate the true underlying trend and behavior of the property of interest.

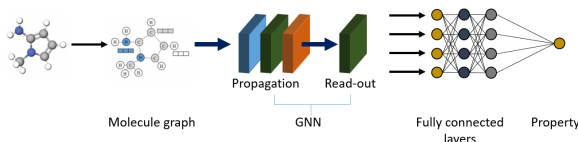


**Figure 3:** Data-Driven GNN based property model

## Specific Objectives

The aim is to develop a systematic methodology to construct machine-learning based property prediction models with uncertainty characterization. The methodology is then to be applied on various types of GNN and properties to build a library of property prediction models.

## References

1. S. Jankovic, G. Tsakiridou, F. Ditzinger, N.J. Koehl, D.J. Price, A.-R. Ilie, L. Kalantzi, K. Kimpe, R. Holm, A. Nair, B. Griffin, C. Saal, M. Kuentz, *J. Pharm. Pharmacol.* 71 (2019) 441–463
2. J. Frutiger, C. Marcarie, J. Abildskov, G. Sin, J. Hazard. Mater. 318 (2016) 783–793.
3. R. Gani, *Curr. Opin. Chem. Eng.* 23 (2019) 184–196.
4. L. Zhang, K.Y. Fung, C. Wibowo, R. Gani, *Rev. Chem. Eng.* 34 (2018) 319–340.
5. J. Zhou, G. Cui, Z. Zhang, C. Yang, Z. Liu, L. Wang, C. Li, M. Sun, *ARXIV*, (2018) 1–22.
6. C.W. Coley, R. Barzilay, W.H. Green, T.S. Jaakkola, K.F. Jensen, *J. Chem. Inf. Model.* 57 (2017) 1757–1772.

# Development of Lab-Scale Continuous Crystallizers for Pharmaceutical APIs

(September 2020- August 2023)

9 INDUSTRY, INNOVATION AND INFRASTRUCTURE



## Contribution to the UN Sustainable Development Goals

Crystallization is a ubiquitous separation and purification process extensively adopted by the chemical, pharmaceutical and food industry. A current trend in the pharmaceutical industry is toward continuous manufacturing to improve process efficiency. The continuous formalism offers opportunities to exploit various inherent advantages compared to batch-wise operation such as easier control, smaller inventories, reduced footprint, and reduced material and energy usage.



**Giovanni Aprile**

gioapri@kt.dtu.dk

**Supervisor:** Kim-Dam-Johansen; Gürkan Sin; Hao Wu

## Abstract

Crystallization from solution and the melt continues to be an important separation and purification process in a wide variety of industries. In the past three decades, interest in crystallization technology, particularly in the pharmaceutical and biotech industry, has increased dramatically. Although promising, continuous crystallization is still not as universal as batch crystallization in industries. To foster a widespread adoption of continuous crystallization, work has to be spent in the characterization and control of the available equipment and investigation of novel alternative setups.

## Introduction

Crystallization from solution and the melt continues to be an important separation and purification process in a wide variety of industries.

In the past three decades, interest in crystallization technology, particularly in the pharmaceutical and biotech industry, has increased dramatically. Previously a largely empirical art, the design of process systems for manufacturing particulate crystals is now characterized on a rational basis and the more complex precipitation processes whereby crystallization follows fast chemical reactions have been analyzed more deeply. This progress stems from the growing power of the population balance and kinetic models, computational fluid dynamics, and mixing theory. Conventional batch and continuous processes, which are becoming increasingly mature, are being coupled with various control strategies and the recently developed crystallizers are thus adapting to the needs of the pharmaceutical industry.

The development of crystallization process design and control has led to the appearance of several new and innovative crystallizer geometries for continuous operation and improved performance. Continuous crystallizers stand out for their capability to deliver consistent particle attributes, reduce

manufacturing costs through process intensification, shorten process development times, and provide flexibility in supply. The flourishing research in this field has brought to light a wealth of different configurations to exploit such benefits. Mixed solvent mixed product removal (MSMPR), Plug Flow, Continuous Oscillatory Baffled, Continuous laminar shear and continuous Couette-Taylor (CT), microfluidic, fluidized bed, forced recirculation, draft tube and falling film crystallizers are among the setups being currently under constant investigation and optimization.

Although promising, continuous crystallization is still not as universal as batch crystallization in industries. Problems, such as blockage and encrustation, need to be solved by some cost-effective solutions before wider application of continuous crystallization.

Besides, MSMPR crystallizer, one of the typical continuous crystallizers, often causes cyclical oscillations in the crystal size distribution (CSD), which is also challenging for continuous crystallization. Furthermore, the process of continuous crystallization is different from a batch formalism, and must be carefully designed and controlled. Early stage process development is

lacking of robust controlled continuous setups to allow laboratory scale investigation that could accelerate the scale up procedure suitable for multipurpose processes. In general, two problems must be solved in order to employ a continuous process in pharmaceutical crystallization. The first is the design problem, which determines whether a new designed crystallization process is able to produce the desired crystals; and the second is the control problem, which determines whether a continuous crystallization process can produce the desired crystals in a stable manner.

The selection of a suitable crystallization platform is usually guided by system-dependent factors such as crystallization kinetics and fouling/agglomeration propensity, in addition to the ability of the platform to consistently control a desired critical quality attribute (CQA) while satisfying yield constraints. Additional factors such as solid-liquid density difference, viscosity, and solids loading are important, since they can affect crystallization process performance. The material residence time distribution (RTD) is an important parameter that describes the time histories of crystals and, as such, the supersaturation histories of all crystals within a continuous crystallizer. Therefore, RTD can affect drug substance CQAs such as the crystal size distribution (CSD), which determines filterability, drying times, and final drug product performance. Also the prediction of the influence of the crystallizer scale on the process behavior and performance (e.g. CQAs) is one of the major challenges in the design of industrial crystallization processes.

The effect of volume in batch crystallization has been investigated, outlining the importance of fluid dynamics on the process outcome. Such matter is the major obstacle encountered in process scale up. The term scale-up is normally based on the concept of making appropriate measurements on the small scale and using these measurements to design a process and equipment, which allow the same results to be obtained on a much larger scale. Batch crystallization in the pharmaceutical industry is normally performed on multi-use batch equipment, which is not specifically designed for any process.

The challenge therefore in development of a crystallization process is the determination of how to develop the operating conditions in existing equipment to allow to produce crystals identical to those obtained in the laboratory and pilot plant. The first phase of this process is to connect work done in early phases of pharmaceutical development where small amounts of material are available to experiments that will be conducted later in a slightly larger scale. To such purpose, analyze multiple lab-

scale crystallizers behavior would provide a wealth of data and expertise to be transferred in early stage process development. Focus will be spent on the implementation of continuous setups that could serve the task of screening experiments for the suitability of continuous processing for a given system. The formulation of an operational framework would be a paramount benefit for both the industry and the academy. To achieve this goal, different control strategies will be screened and applied to different continuous crystallizers, in order to allow a robust procedure for process characterization. Of utmost relevance is the selection of a pool of process analytical technologies and their inclusion in the different crystallizers configuration, to allow an adequate and robust process control. The parallel screening will allow useful correlation and analysis of the complex intertwining between system and equipment, highlighting advantages and pitfalls of the different setups. In fact, while extensive effort has been spent in characterizing and controlling several crystallizers, little comparative analysis is to be retrieved in the literature. Most existing crystallizations in the pharmaceutical industry are batch or semi-batch with significant existing expertise and knowledge on equipment design, process monitoring/control, and training of operating personnel. The same is not to be said for continuous equipment. To this matter, work has to be spent to efficiently characterize continuous lab scale equipment to provide both industry and academia with effective controlled tools for early stage process development, capable of paving the way for sounder and more predictable process scale up, fostering a wide-spread adoption of continuous crystallization and the benefits deriving from it.

## Objectives

The multiple objectives of the project can be condensed in four targets. The first encompasses the development of controlled continuous setups, able to provide extensive and high quality data.

Second objective will be the elaboration of a control strategy based on the wealth of insights provided by the experiments.

The model validation of such experimental results in terms of crystal growth rate, crystal size distribution and average crystal size, constitute the third objective. Lastly the evaluation of the transferability/adaptability of the framework to multiple pharmaceutical compounds will establish the successful accomplishment of the fourth target.

# Development of a Virtual Educational Bioprocess Plant

(September 2018- August 2021)



Contribution to the UN Sustainable Development Goals

To advance into a more sustainable future, we need to facilitate and make more available technical education. The Department of Chemical and Biochemical Engineering of DTU, through my PhD, is developing an open-source software for the teaching of bioprocess. This software can help in the building and to upgrade learning environments for all, through making more affordable and easy technical bioprocesses education. Moreover, we can promote sustainable industrialization (Goal 9) and "doing more and better with less" (Goal 12).



**Simoneta Caño de Las Heras**  
simoca@kt.dtu.dk

**Supervisors:**  
Seyed Soheil Mansouri  
Carina L. Gargalo  
Ulrich Krünhe

## Abstract

Bioprocesses are experiencing a fast growth with the involvement of complex technologies and therefore, creating an educational need for trainees and new graduates. However, providing an understandable hands-on experience for an increasing number of students and trainees is almost impossible due to time and limitation of resources as well as safety considerations. The combination of educational laboratories and computer simulation could be considered as a match made in heaven as it tackles these issues. Thereby, they are able to support a learning based on action as the users are in control of the decision-making. The simulators commonly used in engineering education are not prepared to explain the choices made by the user and consequently, failing in providing a complete educational experience to the unexperienced users. In addition, they are not tackling the current need to provide preparation for a digitalized industry that relays more in data analysis, modeling and its integration. Therefore, in this project, a simulation software that integrates the solution of complex models with a thoughtful learning design and involving motivational elements in envisaged is created.

## Introduction

The use of simulators as learning tools in higher education started in the 1970s and many areas such as wastewater treatment [1], robotic [2], electronic circuit [3], control [4], etc. have so far benefited from its use. One of these disciplines is biochemical engineering. Biochemical engineering is based on unit operations across the scales processes; and providing a hands-on experience for the student can be a challenge. Mainstream process simulation tools for teaching bioprocess development, design and implementation lack learning design and require previous knowledge of the systems. This is due to the design of commercial simulators which commonly aims at solving a specific question and/or develop a process. On the other hand, students require for an instructional computational laboratory to learn something practicing engineers are assumed to already know. That something needs to be defined by carefully designed learning objectives. In addition, the acquisition of knowledge and skills can be facilitated through an enjoyable experience and considering the new habits and interests of the students [5].

Therefore, integrating game elements inside the software platform is one way to tackle this objective.

## Specific Objectives

The novelty in this project is within creation of a software tool. The computational-aided tool is designed according to three milestones:

- 1) A careful learning design.
- 2) The use of template models that can be displayed, reused and modified[6].
- 3) A motivational approach based on gamification.

These milestones are then integrated inside in a framework (Figure 1).

Based on these requirements, a software is developed with:

- A software architecture (Figure 2).
- A database to store information in libraries related to bioprocesses. It consists on a library of mathematical models, a library of common parameter in bioprocess models, an expert system with operational problems and their solutions and a library with theoretical knowledge.

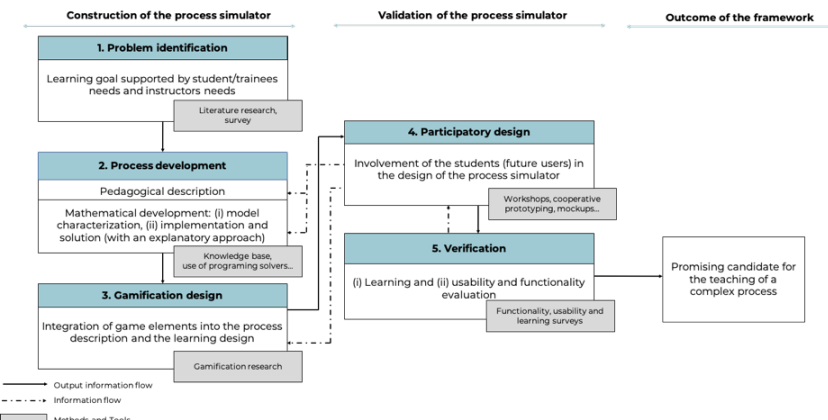


Figure 1. Representation of the proposed framework workflow. Based on [8].

- Mechanistic models and consequently, the models are explained, as well as its implementation in Python.
- Gamification elements which are integrated in the design of the platform to motivate the users.

Moreover, other features are added such a chatbot to solve questions and to stimulate a collaborative learning. The chatbot have an evil phase in which students will need to develop their critical thinking as not all the solutions of the chatbot will be correct.

### Current state of development

The software has been developed to become an interactive webpage, with a three-tier software architecture using open-source exclusively.

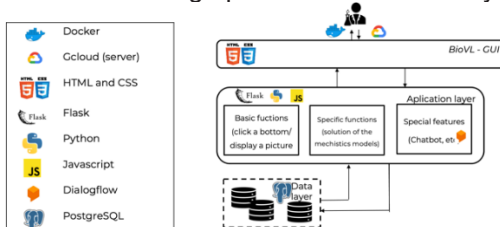


Figure 2. Software architecture of BioVL

Most of the software is written in python programming language as it is *interpreted, interactive, object-oriented*. As a free object-oriented open-source language, python is suited to create the template model library.

The current platform is preliminary called BioVL and so far, it is focused in the content related to fermentation and the teaching of programming. Further than a simulator for different bioconversion, BioVL has implemented different mini-games using fermentation concepts, the possibility to modify the different parameters of the chosen models with information related to the parameter theory and range, the creation of a problem-solution database, and multimedia resource.

### Conclusions

A bioprocess simulator designed for and by students with a prime pedagogical aim can provide the

students and trainees with a tailored tool for the understanding of the complex theoretical knowledge as well as train critical-thinking and decision-making abilities inside bioprocess operations and modeling and its implementation.

### References

1. Group, D. WEST <https://www.mikepoweredbydhi.com/products/west> (accessed Jan 15, 2018).
2. Ifak e.V. SIMBA <http://www.inctrl.ca/software/simba/> (accessed Jan 15, 2018).
3. Guimarães, E.; Maffeis, A.; Pereira, J.; Russo, B.; Cardozo, E.; Bergerman, M.; Magalhães, M. F.; Guimaraes, E.; Magalhaes, M. F. REAL: A Virtual Laboratory for Mobile Robot Experiments. *IEEE Trans. Educ.* **2003**, *46* (1), 37. <https://doi.org/10.1109/TE.2002.804404>.
4. Kerala, G. J. KTechLab <http://www-mdp.eng.cam.ac.uk/web/CD/engapps/ktechlab/ktechlab.pdf> (accessed Jan 15, 2018).
5. Sanchez, J.; Morilla, F.; Dormido, S.; Aranda, J.; Ruiperez, P. Virtual and Remote Control Labs Using Java: A Qualitative Approach. *IEEE Control Syst.* **2002**, *22* (2), 8–20. <https://doi.org/10.1109/37.993309>.
6. Kiili, K. Digital Game-Based Learning: Towards an Experiential Gaming Model. *Internet High. Educ.* **2005**, *8* (1), 13–24. <https://doi.org/10.1016/j.iheduc.2004.12.001>
7. Fedorova, M.; Sin, G.; Gani, R. Computer-Aided Modelling Template: Concept and Application. *Comput. Chem. Eng.* **2015**. <https://doi.org/10.1016/j.compchemeng.2015.02.010>.
8. de las Heras, S. C.; Mansouri, S. S.; Cignitti, S.; Uellendahl, H.; Weitze, C. L.; Gernaey, K. V.; Rootzén, H.; Krühne, U. A Methodology for Development of a Pedagogical Simulation Tool Used in Fermentation Applications. *Comput. Aided Chem. Eng.* **2018**, *44*, 1621–1626. <https://doi.org/10.1016/B978-0-444-64241-7.50265-2>.

# Ash Transformation in Waste Boilers and Optimization of Novel Steam Superheater

(April 2019 - April 2022)



## Contribution to the UN Sustainable Development Goals

Waste to Energy (WtE) plant is an economical method to use waste to create a stable production of heat and power. The limited electrical efficiency relates to the ash deposition and ash induced corrosion in the boiler. Numerical simulations to control, predict and reduce deposit formations can help increasing the electrical efficiency. This would make WtE particularly relevant for the green development of warm and highly dense populated countries, where the need of both energy supply and reducing uncontrolled open-air landfills is quickly growing.



Margherita  
Dotti  
[mardott@kt.dtu.dk](mailto:mardott@kt.dtu.dk)

**Supervisor:**  
Peter Arendt Jensen  
Sønnik Clausen, Hao Wu  
Mohammadhadi Nakhaei

## Abstract

**Abstract:** The focus of this PhD project is to investigate the influence of changes of operation conditions on ash deposit properties and formation on an additional superheater placed in a Waste to Energy power plant. Flue gas pattern, as well as ash formation and deposition phenomena are modeled through Computational Fluid Dynamics (CFD) simulations, in which mechanistic deposition models will be implemented. The numerical results will be validated by comparison with full-scale experimental data acquired during the 3 years. For this, a novel flow visualization technique has been developed.

## Introduction

In the last half-century, the modern life-style, along with the rapid urbanization and population growth, has forced humankind to face the effects of the global warming, as well as energetic and waste management problems.

Waste to Energy (WtE) can replace fossil fuels and re-employ waste, by burning it under controlled conditions, to create a stable production of heat and power. This method became an important part of the strategy for reducing CO<sub>2</sub> emissions in many countries. Unfortunately, in most cases, WtE plants have a low electrical efficiency, around 26%, since typically the superheater (SH) operates at a maximum temperature of approx. 400°C to prevent excessive corrosion. This limitation is due to the ash species that are released from the grate combustion process and forms corrosive deposits on the superheater (SH) surfaces. The most corrosive deposit is formed by alkali and chlorine species, whose release mainly takes place at the first half of the grate. Contrary, relatively hot gases with a low chlorine content appears near the end of the grate.

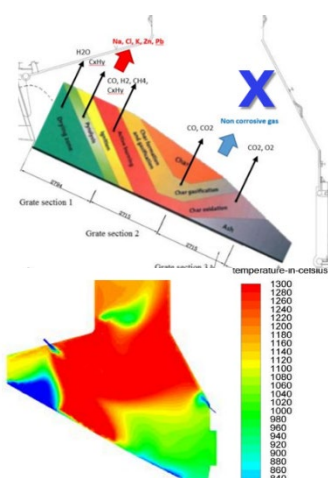


Figure 4a - Schematic view of volatile elements' potential release in the considered grate-firing boiler. The X corresponds to the place of the novel test. Adapted from [1] and Vølund's 2009 report.

Based on those observations, BWV and DTU have together invented and patented a new superheater technology called Steamboost. The flue gas from

the grate are split in a corrosive and a less corrosive fractions, and uses the latter so that the SH can reach higher temperatures without corrosion issues. This idea allows to control the deposit formation, lowering the corrosion on the SH surfaces and increasing the electrical efficiency to approximately 30%.

### Specific Objectives

The PhD project shall support the development of a well-functioning full-scale Steamboost technology. The aim is to obtain an adequate regulation of both heat transfer and deposit formation, which requires a good control of the flows in the lower part of the boiler. This will be done through investigations on the influence of changes of the power plant operation conditions on ash deposit formation in the superheater area. Computational Fluid Dynamics (CFD) simulations are a valuable tool in this regard. The project plan can be divided in the following steps:

- Setting up CFD simulations to replicate the ash formation and flow in the furnace;
- Implementing mechanistic deposition models into numerical codes for a more accurate prediction of the deposit formation and growth;
- Developing a new flow visualization technique that allows to determine the ash flow pattern in the furnace chamber;
- Carrying out measurements campaigns, concerning the investigation of the flue gas flow and for analyzing the composition of the built up deposit, in a full-scale WtE plant;
- Tuning the numerical model and verifying its accuracy with comparisons against the collected experimental data;

### Results and Discussion

ANSYS FLUENT is chosen as framework for the numerical simulations, which, inspired by Kær et al. [2], adopt a quasi-transient approach. Meaning that the converged flow field and particle paths resulting from a steady state simulation are used to calculate the deposit accumulation. The prediction is then advanced in time, using these values as initial condition for the new calculation. The vapor species are modeled in an Eulerian reference system, while the entrained ash with a Lagrangian one, using a one-way coupled steady DPM. The phenomena that have been considered for the deposition are impaction, thermophoresis and direct condensation, implementing the model developed by S. Hansen [3]. UDF codes have been written for setting material properties, temperature at the boundaries and ash dimensions distribution, as well as for calculating and storing the sticking efficiency of the impacting particles, the deposit build up and the heat transfer through the deposit. In order to find the

temperature of the deposit surface, a 4<sup>th</sup> degree equation is solved by implementing the recursive Newton's approximation. Though, it became clear that several inputs and parameters are still unknown and/or are in need of a more accurate description: among others, the composition of waste (and consequently to the elements that are released from the grate), or the viscoelastic properties of the ash, such as the Young modulus, on which the deposition rate significantly depends on.

For studying the flow behavior, two visualization techniques have been developed. The first one requires the use of a thermal camera to look through the combustion zone of the grate. The second, a novel technique, consist of injecting aluminum oxide particles in the furnace, while illuminating it with several 2W blue LED and recording several pictures with a regular video camera. Thanks to the strong blue light (450nm) and a blue lens filter applied on the camera, the flame light is filtered away but, since the emissivity of the seeding particles at this wavelength is high enough, they stand out and can be tracked. Seeding, optics and LEDs are inserted into the furnace through previously designed water-cooled probes. Some deposit samples from various zones of the bottom part of the furnace have been collected already during the boiler shut-down. They will be analyzed using SEM/EDX along with the deposits that will be sampled from the additional superheater.

### Conclusion

A novel flow visualization technique has been tested but still needs to be implemented. Experimental campaigns will be carried out in the near future. More work still has to be put into the CFD modelling but the resulting codes written until now seem promising. Improving the mathematical description of the ash materials rose as an additional goal of this project.

### Acknowledgements

This PhD study is conducted at the Department of Chemical Engineering of DTU in collaboration with B&W Vølund. The author also acknowledges Affald+, for allowing the experimental campaigns to be carried out at its power plant in Næstved, and EUDP for funding the project.

### References

1. M.S. Jepsen, PhD thesis "NOx reduction in grate-fired WtE plants", 2018
2. S.K. Kær et al., Towards a CFD-based mechanistic deposit formation model for straw-fired boilers, 2005
3. S.B Hansen et al., Mechanistic Model for Ash Deposit Formation in Biomass Suspension Firing. Part 1: Model Verification by Use of Entrained Flow Reactor Experiments, 2017

# Pollutant formation and control in wood stoves

(September 2017- September 2020)

7 AFFORDABLE AND CLEAN ENERGY



## Contribution to the UN Sustainable Development Goals

Wood stoves are among the most widely used biomass-based distributed energy systems for domestic heating. However, particulate matter (PM) emissions from wood stoves have raised great concerns about indoor and outdoor air pollution. The application of cost-effective control systems to such small-scale combustion units is therefore important for the reduction of PM emissions. In this work, multi-pollutant sensors for the automatic air control system of wood stoves are being evaluated, which could contribute to a more sustainable future of residential wood combustion.



**Yifan  
Du**

yifandu@kt.dtu.dk

**Supervisors:**

Peter Glarborg  
Weigang Lin

## Abstract

The application of sensor-based air control systems is expected to efficiently optimize the combustion process and reduce multiple pollutants of wood stoves. In this work, the capability of low-cost LED sensors to monitor the transient soot and tar emission levels of wood stoves was evaluated. Results show that the optical measurements using LED sensors correlated well with the particulate and organic matter concentrations measured by other advanced instruments under both normal and poor combustion conditions. In addition, the good performance of the LED sensors was validated over an approximately 5-month running period.

## Introduction

With biomass utilization being an important coping strategy for climate change, the utilization of wood stoves has become an increasingly popular and economic option for domestic heating due to government incentives and subsidies. However, gaseous and particulate emissions from residential wood combustion can be harmful to human health and the environment. A recently high-resolution anthropogenic particulate matter (PM) emission inventory indicates that about half of the total PM<sub>2.5</sub> emissions in Europe is carbonaceous PM and that residential wood combustion is the largest carbonaceous PM source [1]. Major pollutant emissions from wood stoves are formed under incomplete combustion conditions. Regarding wood stoves, the batch firing mode, large wood log sizes, varying firewood properties and bad firing habits can lead to even more challenging combustion conditions [2]. The lack of emission reduction technologies for small-scale combustion units is another problem, because most of the well-established pollutant control technologies are expensive and only economically feasible for medium and large scaled combustion units.

Therefore, there is a strong motivation to develop cost-effective combustion control and emission reduction technologies that are suitable for small-scale combustion units such as wood stoves. Promising solutions to optimize combustion conditions and reduce pollutant emissions of wood stoves include the application of the sensor-based automatic air control system, but relevant laboratory studies are still lacking.

## Specific objectives

This PhD project aims at improving the understanding of wood stove PM emissions from the perspectives of both the application of sensor-based emission control technologies and the fundamentals of PM (especially soot) formation mechanisms. Specifically, this work focuses on:

- The capability of using optical sensors to capture the transient emission levels of soot and tars of a modern wood stove.
- Influences of fuel-related properties (i.e., bark contents and inorganic constitutes) and the tertiary air inlet design on PM emissions from a modern wood stove.

- A fundamental study on the influence of alkali metals on the soot formation process in fuel-rich oxidation of methane, an important volatile compound of biomass.

## Materials and methods

Two low-cost absorption-based single-wavelength LED sensors (280 nm and 417 nm wavelengths) aiming at the *in situ* and real time monitoring of the emission levels of soot and tars were tested on a modern wood stove. According to Beer–Lambert law, light transmittance detected by the sensors can be correlated with the concentrations of absorbing species, i.e., soot and tar, in the flue gas. Light absorption measurements using the LED sensors were supplied and evaluated by the measurements through wide-spectrum UV spectroscopy, Flame Ionization Detector (FID), Scanning Mobility Particle Sizer (SMPS) and Electrical Low Pressure Impactor (ELPI+).

## Results and discussion

Previously, the good performance of the LED sensors was validated under the normal combustion condition. To further investigate the versatility and capability of the sensors, optical measurements were conducted under poor combustion conditions when using wood logs with peeled barks separately attached on the surface (WBS). During the combustion of WBS, significantly higher concentrations of soot and tars were emitted. Figure 1 suggests the good agreements of soot and tar absorption signals detected by the LED sensors with the total hydrocarbon (THC) concentrations measured by FID and PM concentrations derived from SMPS. Overall, the LED sensors were shown to be able to monitor both the low and high emission levels of soot and tars.

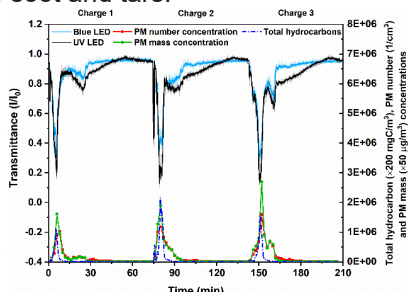


**Figure 5.** Comparison of UV absorption by soot and organic matter with the total hydrocarbon concentration measured by FID.

In addition, the long-time performance of the LED sensors was evaluated. Figure 2 shows the incident light intensity of both sensors detected in the cold chimney on different days, with the symbols indicating the days when combustion tests on the stove were performed. It can be seen that the UV LED only had a slight decrease in the incident light intensity over the testing period, while the incident

light intensity of the blue LED decreased from around 1.5 to 0.2. However, according to Figure 3, even with the much lower incident light intensity of around 0.2, the measurements by the LED sensors still correlated well with the transient THC and PM emission levels obtained from other advanced instruments.

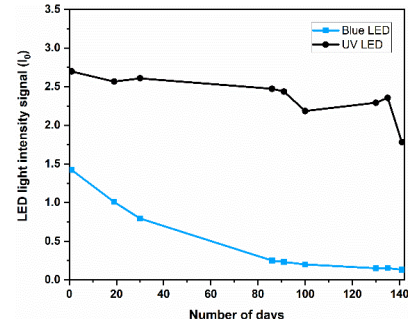


**Figure 6.** Variations of incident LED sensor signals ( $I_0$ ) detected in the cold chimney with time.

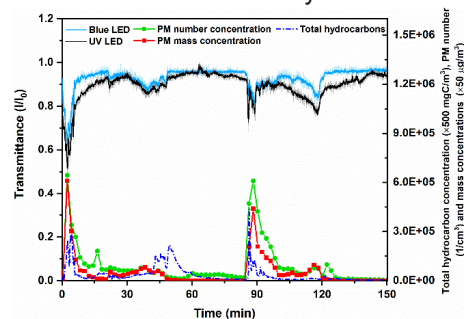


**Figure 7.** Correlations of transmitted LED sensor signals with other measurements when the incident light intensity of blue LED decreased to a lower level ( $I_0 \approx 0.2$ ).

## Conclusions

The feasibility of absorption-based LED sensors was validated under both the normal combustion condition and the poor combustion condition with notably higher emission levels. Furthermore, a desirable performance of the LED sensors was observed over a long period of nearly 5 months. Overall, the low-cost LED sensors exhibited the capability of monitoring the transient soot and tar emissions of the wood stove, thus proving a promising application for process and emission control of wood stoves.

## Acknowledgements

This PhD project is funded by the Danish EUDP (Energy Technology Development and Demonstration Program) and DTU.

## References

1. C. Guerreiro, A. Gonzalez Ortiz, F. de Leeuw, M. Viana, J. Horalek. Air quality in Europe — 2016 report, Publications Office of the European Union, 2016.
2. E.D. Vicente, C.A. Alves, Atmos. Res. 199 (2018) 159–185.

# Melamine tail gas cleaning with ionic liquids

(November 2019- September 2022)



## Contribution to the UN Sustainable Development Goals

The emission of industrial tail gas containing CO<sub>2</sub> and NH<sub>3</sub> cause significant pollution to the environment and humans. The existing tail gas treatment technologies are applied for different tail gas composition and processes; however, the energy consumption of these technologies is relatively high. As a low-volatility solvent with good performance for gas separation and recovery, ionic liquids can be used in the separation process of NH<sub>3</sub>-containing gas. The main advantages of this method are lower energy consumption, a simple process, and high-value chemical products can be recovered.



**Yuanmeng  
Duan**

yuadu@kt.dtu.dk

**Supervisor:**  
Jakob Kjøbsted Huusom,  
Jens Abildskov,  
Xiangping Zhang

## Abstract

With the development of industry, the emission of harmful gas from industrial tail gas is becoming more and more serious, which is harmful to human body and environment. At present, the main treatment methods of industrial tail gases are water scrubbing, solvent absorption, biological treatment, etc. Ionic liquids have been experimentally proved to be effective for ammonia-containing gas separation and recovery with lower energy consumption, it is of great significance to establish process simulation of this technology as a mean to model-based analysis, optimization and process development.

## Introduction

With the development of industry, various chemical processes are prone to produce industrial tail gases (waste streams) containing components such as CO<sub>2</sub>, NH<sub>3</sub>, SO<sub>2</sub>, etc. The direct emission of these industrial tail gases will cause serious pollution to the environment. At present, the main treatment methods of industrial tail gases are water scrubbing, solvent absorption, biological treatment, etc. However, some ammonia-containing exhaust gases, such as vapour contained in melamine exhaust gas, will condense during the pressurization process.

Melamine production in particular is known to produce tail gas with a significant amount of both ammonia and CO<sub>2</sub>. In the following, the four prevailing methods for the treatment of ammonia containing tail gases from the melamine industry will be briefly described.

The water scrubbing method treat melamine tail gas by utilizing the high solubility of ammonia in water. However, the main challenge of the melamine tail gas washing method is that it requires a large utility consumption. Further the ammonia absorption is an exothermic process and the generated heat results in a reduction in ammonia absorption efficiency [1]. The processing principle of the solvent absorption separation method is to use sulfuric acid or another acidic solvent to chemically react with the ammonia

in the tail gas to form ammonium salt. The main disadvantage of using this method to treat melamine tail gas is that during the ammonium salt drying process, ammonium salt-containing dust particles are generated, and the subsequent processing section is complicated and difficult to operate. At the same time, acid solvents are highly corrosive to process equipment and pipelines thus increase the cost of installation.

Currently, in many factories, various co-production treatment methods such as the melamine tail gas co-production urea method, the co-production ammonium bicarbonate method and the co-production of ammonium nitrate method are used in ammonia tail gas cleaning. Melamine tail gas co-production urea method [2] is through the co-production of melamine tail gas with the original urea device. Many large-scale melamine manufacturers are equipped with urea devices to produce urea by recovering melamine tail gas to achieve recycling.

As a new type of solvent, the ionic liquid ([Bim][NTf<sub>2</sub>]) is composed of positive and negative ions and is a liquid organic salt at room temperature or below 100°C. Because of its designable structure, extremely low vapor pressure, and high gas solubility, it has received wide attention in the field of gas separation. The use of ionic liquids to treat ammonia-containing tail gas has many

advantages such as high ammonia absorption, good selectivity, no waste water discharge, and low operating energy consumption [3].

### Specific Objectives

The objective of this project is to develop a full simulation package of melamine tail gas cleaning method by ionic liquids. The project starts from the ionic liquid NH<sub>3</sub>-CO<sub>2</sub> separation process. First, based on experimental data, a thermodynamic model suitable for process simulations are established. Then the steady-state model of the process will be built and investigated through sensitivity analysis. Finally, the dynamic and control aspects of the process is considered.

### Results and Discussion

Accurate thermodynamic models are the basis of process simulation, and it is needed to establish the thermodynamic model of the ionic liquid including single value component properties, temperature-dependent functional pure component properties and phase equilibrium relationship. As example Figure 1 shows the comparison of the estimated values with experimental data [4] of [Bim][NTf<sub>2</sub>]’s density properties.

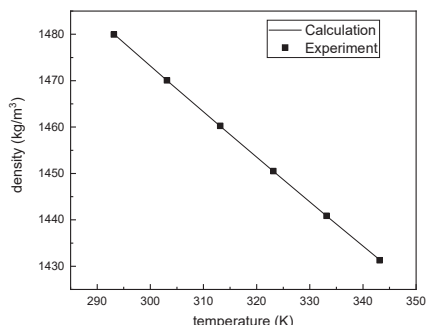


**Figure 8:** Comparison of the estimated values with experimental data of [Bim][NTf<sub>2</sub>]’s density.

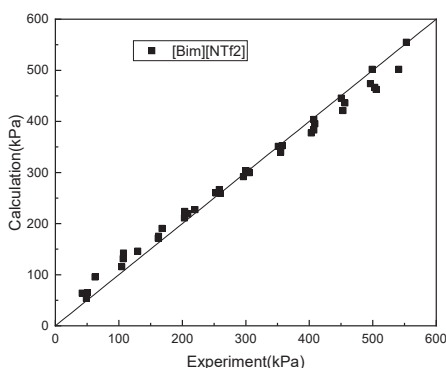


**Figure 2:** Comparison of the estimated values with experimental values of total pressure of NH<sub>3</sub>-[Bim][NTf<sub>2</sub>] system.

Further the solubility of NH<sub>3</sub> in [Bim][NTf<sub>2</sub>] was measured using vapor liquid equilibrium (VLE) apparatus. By measuring the total pressure of NH<sub>3</sub>-[Bim][NTf<sub>2</sub>] system, we can calculate the solubility of NH<sub>3</sub> in [Bim][NTf<sub>2</sub>] using the PR equation. Figure 2 shows the estimated results are in good accordance with the literature experimental data. This suggest sufficient reliability of the NRTL model for the NH<sub>3</sub>-ionic liquid system to be used for process simulation.

Figure 3 shows the conceptual design of NH<sub>3</sub> recovery from melamine tail gas by [Bim][NTf<sub>2</sub>]. This process is divided into two parts, namely, the NH<sub>3</sub> absorption parts and absorbent regeneration parts. The operating conditions of the absorption tower is 2 bar and Flashes are 383 K at 10 kPa and 383 K at, 2 kPa in the absorbent regeneration parts respectively. The steady state simulation of this process indicates that in the purified gas the mol concentration of NH<sub>3</sub> can be lower than 1% when feed gas has 50% of NH<sub>3</sub> in the feed gas [1].

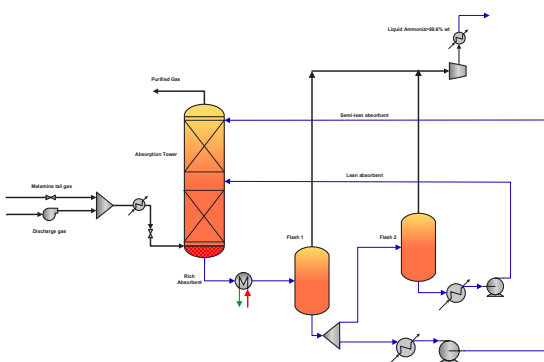


**Figure 3:** Flow chart of NH<sub>3</sub> recovery from tail gas by [Bim][NTf<sub>2</sub>]

### Conclusions

The treatment of melamine-containing ammonia tail gas by ionic liquid method can effectively reduce the ammonia in the purified gas and efficiently recover the ammonia in the tail gas.

There are still more aspects of this technology need to be investigated, such as the more detailed comparation of this technology with other methods in aspect of energy consumption and purification cost.

### Acknowledgements

This project is funded by the cooperation of DTU-IPE project.

### References

1. Y. Tang.CN 103100059 A, 2013.05.22.
2. F. C. Li. CN 101607168 B, 2011.05.04.
3. S.J. Zeng, D.W. Shang, X. P. Zhang. J Chem Ind Eng. (China). 70.3(2019).
4. D.W. Shang, X. P. Zhang, S.J. Zeng. Green Chem.19.4(2017).

# Computer-Aided Product Design of Organic Coatings

(September 2018 - August 2021)

9 INDUSTRY, INNOVATION  
AND INFRASTRUCTURE



## Contribution to the UN Sustainable Development Goals

Developing new tools for product design can lead to innovation and increased effectiveness when formulating products, in this case organic coatings. Predictive methods can be used to substitute unwanted pigments, polymers and volatile organic compounds (VOCs) to reduce hazards and environmental impact during the coating lifespan. Computer-aided product design can drive both growth and innovation by giving the sector access to new technical capabilities in addition to the experience already present.



**Karl Markus  
Jannert Enevist**  
Maene@kt.dtu.dk

**Supervisors:** Georgios Kontogeorgis, Xiaodong Liang, Kim Dam-Johansen, and Xiangping Zhang.

### Abstract

A combination of databases and models capable of estimating properties will be used to predict functionality in coatings to simplify the extensive process of creating new formulations. These predictions can improve formulation time and accuracy, and substitute unwanted ingredients while maintaining performance, which could be of great interest to an industry that relies heavily on experience. The approach is to create a computational framework by finding the relevant properties for each constituent and to create databases or develop new group-contribution methods depending on available data and project needs.

### Introduction

During the formulation process of a coating, the formulator tries to reach a set of requirements for the product, both in its liquid state, during application, evaporation, and for the dry film. These requirements depend on the customer needs, the intended substrate, and regulatory or environmental considerations.

Current formulation practices depend heavily on a time-intensive iterative process of trial-and-error, where a recipe is produced and later adjusted according to testing [1]. An alternative to the classic approach to formulation is to use an integrated experiment-modelling design that includes predictive methods and databases to guide experimentation, and reduce reliance on traditional trial-and-error coating formulation known as computer-aided product design (CAPD).

This approach to formulation can not only reduce development time, but also limit the use of or substitute chemicals shown to have a detrimental effect to nature or human health, especially as coatings often include a significant volatile organic compound (VOC) content and additives including biocides [2].

### A framework for CAPD of organic coatings

The product design field consists of a combination of computational tools, algorithms, large databases

and predictive methods for the estimation of different product properties. The aim is to be able to solve a large range of design problems in coating formulation within a systematic framework that is both flexible and practical [3]. A suggested product design framework for coatings is shown in figure 1.

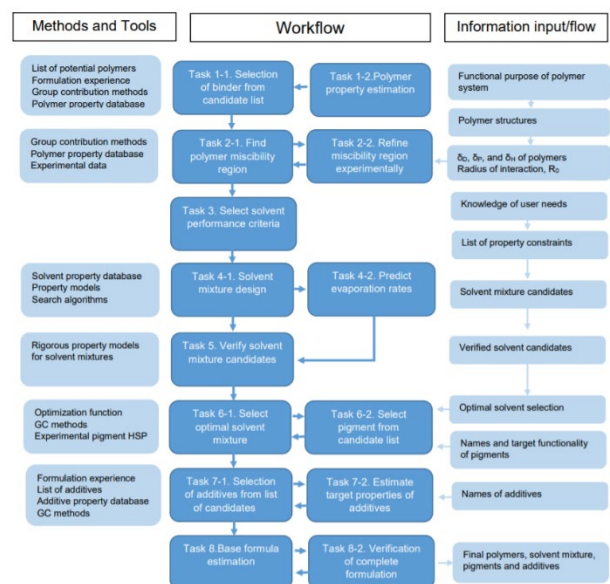


**Figure 1.** Suggested framework for computer-aided product design of coatings

As the problem of formulating a paint is very complex and can be difficult to approach, the formulation methodology is broken down into individual tasks that each requires certain inputs and tools. Advances have been made with regard to thermodynamic models and property estimation methods, especially group contribution (GC) methods which can provide qualitatively correct estimates quickly for a large number of compounds. Application of these tools can provide a formulator with a more accurate starting point for a new product, and focus experiments on a selected number of screened ingredients from a very large search space.

### Development of Novel Group Contribution Methods

An important step to further the field of CAPD is to develop new, applicable property estimation methods where current methods either do not exist, or does not perform well. The Hansen Solubility Parameters (HSP) are frequently used for solvent selection and characterization of polymers, and are directly related to the suspension behavior of pigments in solvent mixtures. Currently available GC methods were evaluated, and found to be unreliable for selection of large, organic, molecules like organic pigments. The GC model is based on the molecular structure, using first- and second-order groups based on conjugation theory [4]. The developed model, shown in figure 2, performs well when compared to most available measurements of organic pigments, and can be used for a broad range of applications, including computer-aided product design and solvent selection for complex pure components such as pharmaceuticals, organic dyes, or organic pigments.

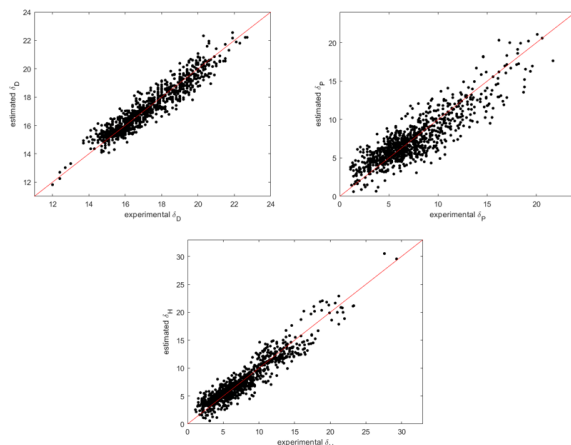


**Figure 2.** Prediction of HSP for organic compounds using a novel second-order group contribution method.

While much progress has been made with regard to modern predictive models, issues still occur due to the large number of parameters, lack of data, and the approximate nature of results [5], which is why the developed group contribution method also provides a detailed uncertainty analysis and 95 % confidence intervals.

### Conclusion and Future Work

The application of CAPD in the paints and coatings industry is still in an early stage and adding new knowledge and tools could be highly beneficial for saving time and resources during trial-and-error experiments. While a number of group contribution methods are already available for some pigment and polymer properties, additional methods for more accurate results might need to be developed. Current and future work includes interpreting the needs for polymers into target properties, as well as sustainability indicators such as biodegradability or toxicity. Constraints on these properties can then be used as a selection guide, after necessary tools are either found, or developed.

### Acknowledgements

I would like to extend special thanks the Sino-Danish Center for Education and Research (SDC) as well as the Hempel Foundation Coatings Science and Technology Center (CoaST) for their generous funding and help with this PhD Project.

### References

1. Müller, B., & Poth, U. (2011). *Coatings formulation*. Hanover: Vincentz Network.
2. Turner, G. P. A. Introduction to Paint Chemistry and Principles of Paint Technology. In *Introduction to Paint Chemistry and Principles of Paint Technology*. 2011
3. Gani, R. Chemical Product Design: Challenges and Opportunities. *Computers and Chemical Engineering* 28(12) (2004) 2441-2457
4. E. Stefanis, C. Panayiotou, Int J Thermophys 29(2) (2008) 568-585
5. J. Frutiger, C. Marcarie, J. Abildskov, G. Sin, A Comprehensive Methodology for Development, Parameter Estimation, and Uncertainty Analysis of Group Contribution Based Property Models -An Application to the Heat of Combustion. *J. Chem. Eng. Data*, 61 (1) (2016) 602-613

# The use of silica aerogels-encapsulated biocides to achieve long-term efficacy of antifouling coatings

(June 2019- May 2022)



## Contribution to the UN Sustainable Development Goals

While biocide-based antifouling coatings do a great job of keeping ship's hulls clean and even have some environmental benefits such as improving fuel efficiency and preventing the spread of invasive non-native species, it is toxic to aquatic life. By encapsulating the biocides in silica aerogels, a more effective use of biocides in antifouling coatings can be achieved, thereby prolonging service life of the coating and decreasing the environmental impact.



**Tenna  
Frydenberg**  
[tenfry@kt.dtu.dk](mailto:tenfry@kt.dtu.dk)

**Supervisors:** Søren Kiil,  
Claus Erik Weinell, Kim  
Dam-Johansen, Eva  
Wallström, Birte Høgh  
Andersen

## Abstract

This project is in collaboration with the Danish company EnCoat, who has developed an encapsulation technology that reduces the overall biocide demand in an antifouling coating. The encapsulation technology is based on highly porous silica aerogels, which form a cage-like structure around the biocides that helps to control the biocide release rate and thereby minimizes the surplus of biocide. The project aims to develop a better understanding of the underlying mechanisms in an aerogel-based antifouling coating and thereby contributing to the development of an optimized coating with a prolonged antifouling performance.

## Introduction

The global antifouling coatings market is projected to reach 193 thousand tons by the end of 2025 [1]. This high demand for antifouling coatings is driven by the shipping industry. Antifouling coatings are applied on ship hulls to prevent the growth of fouling organisms, including bacteria, algae, invertebrates, mussels and barnacles. Biofouling is undesirable for the shipping industry both from an environmental and economic point of view. The accumulation of fouling organisms leads to a significant decrease in ship performance, resulting in an increased fuel consumption (and associated GHG emissions) compared to a smooth hull. A high degree of fouling on a ship's hull significantly increases the drag, reducing the overall hydrodynamic performance of the ship. Most of antifouling coatings are based on polishing binder systems that contain biocides, which are slowly released into the seawater and thereby prevent fouling [2].

In recent years, the use of biocides (tributyltin, copper, co-biocides) has been strictly controlled by both national and international regulations, such as the Biocidal Product Regulation (BPR) in the EU and International Maritime Organization (IMO). This

has prompted the development of antifouling coatings with a reduced environmental pressure.

## Aerogel-Encapsulation Technology

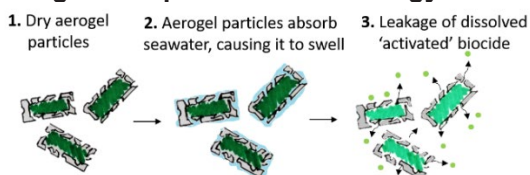


**Figure 1:** Graphic illustration of biocide (green) release from silica aerogel particles.

To be able to reduce the amount of biocide needed in an antifouling coating, it is necessary to be able to control the biocide present in the surface layer of the coating. This control is achieved by encapsulating the biocide in a silica aerogel. A graphic illustration of the mechanisms that will occur when aerogels with biocide are exposed to seawater is given in Figure 1. The biocide particles are effectively entrapped inside a thin and porous silica structure. Aerogels exposed to seawater start swelling due to their porous nature. This creates a local aquatic environment inside the aerogels and over time a saturated solution of biocide. The

biocide is released depending on its solubility, diffusivity and degradation of the aerogel structure in the coating-water interface.

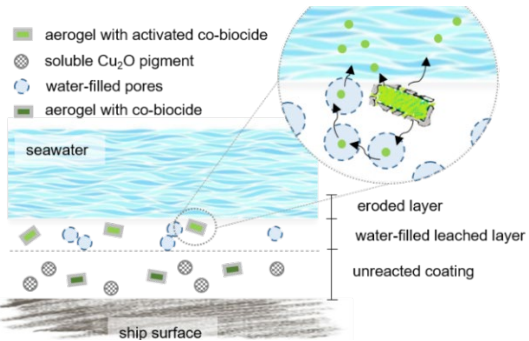


**Figure 2:** Schematic cross-section of an aerogel-based antifouling coating exposed to seawater. A porous leaching layer ( $10\text{ }\mu\text{m}$ ) is formed after dissolution of soluble pigments. Activated biocides need to diffuse through the leached layer pores in order to give the biocidal protection at the coating surface. Aerogels in the outer surface layer are polished by the flow of water.

Figure 2 illustrates the working mechanisms of an antifouling coating containing aerogel-encapsulated biocides. As shown in the figure, encapsulated biocides and soluble pigments are distributed throughout the binder matrix. When the coating is exposed to water, the binder matrix and soluble pigments start to react with seawater ions, which creates a porous leaching layer. Aerogels embedded in the outer coating layer will undergo the mechanisms described in Figure 1, and activated biocides are subsequently released through the porous leaching layer. The aerogel has a special ability to ensure adherence of the biocide to the binder in the outer surface layer of the coating. The biocide release mechanisms will also depend on the environmental conditions (e.g. seawater temperature, pH, salinity and water flow) during the release.

### Specific Objectives

The objectives of this project are:

- To characterize silica aerogels and find the optimum biocide loading.
- Investigate different parameters' (e.g. aerogel concentration, biocide loading, binder intrusion and formulation parameters) influence on the biocide release rate.
- Determine which and how parameters are used to manage water absorption of a coating film.
- Study the antifouling performance of coatings.
- To be able to describe the biocide release mechanism from an anti-fouling coating containing silica aerogel encapsulated biocide.

### Results and Discussion

Silica aerogels have been prepared with different copper pyrithione (CuPT) concentrations, ranging from 50 wt% to 80 wt%. The aerogels were

incorporated in identical coating systems to investigate their influence on coating properties such as water absorption. Water absorption is a critical parameter connected to biocide leaching, polishing rate and thus, antifouling properties. A sufficient water uptake in the coating film is necessary to ensure a dissolved and active biocide in the coating surface. A low water absorption can cause an ineffective coating without the biocidal effect needed to provide the necessary protection. At the same time, a high water absorption may cause blistering or reduce the overall service life of the coating. Comparing different aerogels in the same coating formulation has shown that the CuPT loading of the aerogels has an impact on water absorption. Water absorption measurements seen in Figure 3 were obtained by weight change of coatings immersed in artificial seawater at 25 degrees, pH 8.2 and with a salinity of 33 %.

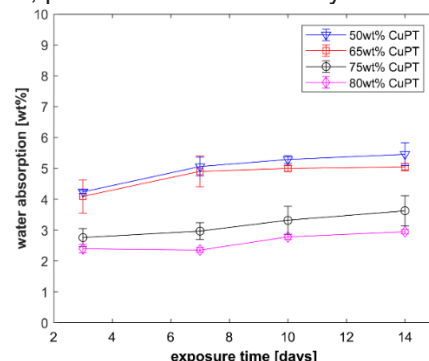


**Figure 3:** Water absorption of coatings containing aerogels with different CuPT loadings.

The results show that the water absorption decreases with increasing CuPT loading of the aerogels. A lower silica aerogel content is present in the coating at high loading levels and therefore the aerogels are expected to swell less when exposed to water.

### Conclusion

It can be concluded that the biocide loading levels of the aerogels used in an antifouling coating affect the water absorption and must be carefully adjusted to match the marine environment and provide the adequate antifouling performance.

### Acknowledgements

This project is a collaboration between CoaST (The Hempel Foundation Coatings Science and Technology Centre) at DTU Chemical Engineering and EnCoat ApS. The financial support from Innovation fond Denmark is gratefully acknowledged (Grant number 8053-00249B).

### References

1. Global Antifouling coating market research report. Forecast 2025.
2. Callow, Maureen E., and James A. Callow. Marine biofouling: a sticky problem. Biologist 49.1, 2002, p. 1-5.

# Novel Intumescent Coatings Development

(September 2020-August 2023)

11 SUSTAINABLE CITIES  
AND COMMUNITIES



## Contribution to the UN Sustainable Development Goals

Exposed to fire, the strength and stiffness of structural steel is significantly reduced, causing a detrimental effect on the stability of the constructed structure. In severe cases, this could lead to the loss of lives and property. Fire losses have been one of the major preventable tragedies in modern civilization. Intumescent coatings exhibit good fire protection capacity for construction materials, whose application is a promising method to protect lives and assets, and moreover realize sustainable cities.



Aixiao  
Fu

aixfu@kt.dtu.dk

Supervisor: Kim Dam-Johansen, Hao Wu, Burak Ulusoy

## Abstract

Structural fires can in severe cases lead to the loss of lives and property. To prevent such disastrous outcomes, intumescent coatings can be used to protect construction materials upon fire. When exposed to high temperatures, intumescent coatings swell to form a low heat conductivity barrier, slowing the temperature increase of the underlying substrates. In this article, a popular scientific introduction to organic and inorganic intumescent coatings is provided, including their working mechanisms and compositions.

## Introduction

Exposed to high temperatures such as in fire events, all commonly used construction materials lose strength, which may cause the materials to buckle and collapse within a few minutes. An example hereof is structural steel, a common construction material, which loses 50% of its load bearing capacity above 500 °C. It is therefore of high importance to establish effective fire safety strategies in order to preserve the integrity of buildings and prevent the loss of lives and assets in the event of fire.

Fire protection strategies are generally divided into active fire protection (AFP) and passive fire protection (PFP) methods. AFP includes sprinklers, alarms, fire extinguishers, or gas release systems, which are activated and respond quickly during a fire. Their application, however, is restricted by their high capital cost, requirement for complex equipment, and inability to prevent flame spread in large fires <sup>1</sup>. In comparison, PFP systems use thermal barriers on the surface of the substrate, e.g. steel, to slow heat transfer and prolong the time before structural collapse. Examples of barriers are concrete encasements, mineral fibers, gypsum plaster boards, and intumescent coatings. Of the passive techniques, intumescent coatings are increasingly used due to advantages such as good fire protective performance, aesthetic finish, corrosion resistance, and cost effectiveness <sup>1</sup>.

Upon heating, traditional intumescent coatings swell to form a carbonaceous char with low density and low thermal conductivity, thereby slowing down the temperature increase of the underlying steel structure during fire (Figure 1). Intumescent coatings can swell up to 50-100 times of their original thickness and help retain the integrity of structural steel up to 4 h under severe fire scenarios such as that of hydrocarbon fires <sup>2</sup>.

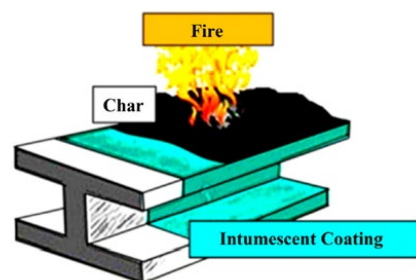
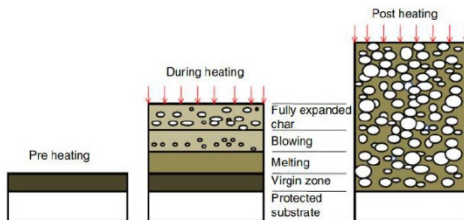


Figure 9: Intumescent coating applied on steel in fire scenario <sup>3</sup>.

Current state-of-the-art intumescent coatings are predominantly based on organic systems due to their good performance and decorative capacity. The composition and working mechanism of organic intumescent coatings have been extensively studied. Generally, an organic intumescent coating consists of an acid source, carbon source, blowing agent, binder, and additives. When the coating is exposed to a source of heat and reaches a critical

temperature, a mineral acid is released through the decomposition of the acid source, which acts as a catalyst for the dehydration and carbonization of the carbon source. Further, the blowing agent decomposes to release a large amount of gaseous products, which are trapped in the melted binder matrix making it swell up and form an expanded char layer that acts as thermal barrier (Figure 2)<sup>3</sup>.



**Figure 2:** Illustration of intumescence process of organic intumescent coatings<sup>3</sup>.

Ammonium polyphosphate (APP), pentaerythritol (PER) and melamine (MEL) are the most commonly used acid source, carbon source and blowing agent, respectively. These components are commonly used together as they act in a certain order leading to charring and swelling. As for the binder, acrylic resins are typically used for cellulosic fire conditions, while epoxy resins are applied for hydrocarbon fires. Additives include flame retardants, fillers, pigments, etc., which are compatible with the coating matrix and help improving certain properties of coating.

Intumescent coatings are typically evaluated based on standardized fire curves. A cellulosic fire is caused by the ignition of paper, wood, textiles, plastics and etc. while hydrocarbon fires occur in the presence of oil or natural gas. They follow standard fire curves as described in the International Standardization Organization (ISO) 834 standard and Underwriters Laboratories (UL) 1709 standard, respectively (Figure 3)<sup>1</sup>.

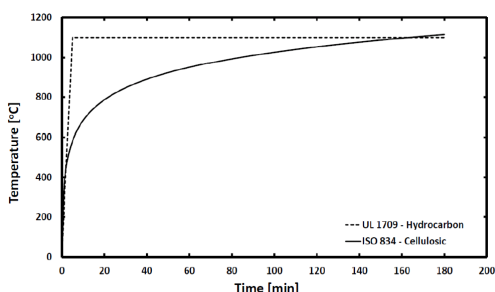


**Figure 3:** Temperature-time curve of standard ISO 834 and UL 1709.

Organic intumescent coatings have several disadvantages such as toxic gas release (e.g. CO, HCN, etc.), toxic species incorporation (e.g. B-compounds etc.), exothermic decomposition, and low mechanical strength<sup>4</sup>. A way to circumvent these problems is to develop inorganic intumescent coating formulations, which have little to no health

and environmental concerns. Moreover, inorganic materials employed in intumescent systems are inexpensive, abundant, and have higher thermal stability and oxidation resistance<sup>3</sup>.

A promising purely inorganic intumescent coating may be based on soluble alkali silicates, e.g.  $(M_2O)_x \cdot (SiO_2)_y$ , where M could be Na, K, or Li. The intumescent system expands upon heat exposure due to the endothermic loss of  $H_2O$  and the softening of the silicate matrix<sup>3</sup>. Hence, the working principle is similar to that of organic intumescent coatings. These coatings are however prone to deactivation by weathering, i.e. humidity conditions and  $CO_2$  presence. Another type of inorganic intumescent coating is based on silicone, which has high thermal and oxidative stability. However, silicone is not inherently intumescent, making it necessary to incorporate additives such as expandable graphite to provide expansion<sup>4</sup>.

### Specific objectives

This research project will focus on the development of inorganic intumescent coatings due to their inherent lower toxicity and thermal stability. As of yet, no inorganic intumescent coating has been commercialized, mainly due to durability problems, including weather sensitivity and low substrate adhesion<sup>5</sup>. It is therefore pivotal to formulate novel inorganic coating systems with good fire protective performance and high durability against physical and chemical factors.

### Acknowledgement

The authors acknowledge the financial support of the Hempel Foundation and Chinese Scholarship Council (CSC) and the professional support from CoaST Research Center at the Department of Chemical and Biochemical Engineering at DTU.

### References

- Yasir, M., Ahmad, F., Yusoff, P. S. M. M., Ullah, S. & Jimenez, M. Latest trends for structural steel protection by using intumescent fire protective coatings: a review. *Surf. Eng.* **36**, 334–363 (2020).
- Williams, R. Rapid Rise Hydrocarbon Fires.
- Puri, R. G. & Khanna, A. S. Intumescent coatings: A review on recent progress. *J. Coatings Technol. Res.* **14**, 1–20 (2017).
- Gardelle, B., Duquesne, S., Vandereeken, P. & Bourbigot, S. Characterization of the carbonization process of expandable graphite/silicone formulations in a simulated fire. *Polym. Degrad. Stab.* **98**, 1052–1063 (2013).
- Langille, K. B., Nguyen, D., Bernt, J. O., Veinot, D. E. & Murthy, M. K. Mechanism of dehydration and intumescence of soluble silicates - Part I Effect of silica to metal oxide molar ratio. *J. Mater. Sci.* **26**, 695–703 (1991).

# Liquefaction for transport of CO<sub>2</sub> from steel blast furnaces

(September 2019- August 2022)

13 CLIMATE ACTION



## Contribution to the UN Sustainable Development Goals

EU Horizon 2020 has funded this project and it is therefore a part of the EU project: "DMX Demonstration in Dunkirk (3D)". The 3D project aims to reduce the CO<sub>2</sub> emission from the steelmaking industrial. The objectives are to demonstrate the efficiency of the carbon capture technology, DMX technology developed by IPFEN, and to implement the first CO<sub>2</sub> capture units on ArcelorMittals steel mill in Dunkirk. This project contribute to the EU project by designing a novel CO<sub>2</sub> conditioning process which is a necessary step in the Carbon Capture & Storage chain. Therefore, this project contributes to the SDG goal: Climate action.



**Wentao Gong**

wengon@kt.dtu.dk

**Supervisor:** Nicolas Von Solms & Philip Loldrup Fosbøl

## Abstract

In this study, liquefaction processes for CO<sub>2</sub> from steel blast furnaces are simulated and compared. Here, two liquefaction methods are compared: Open cycle and closed cycle. In addition, liquefaction pressures of both 7 bar and 15 considered. Optimizations of the designs are also included. It is found that closed cycle liquefaction method requires less energy compared to the open cycle method. Furthermore, it is shown that liquefaction at 7 bar is more energy-consuming compared to 15 bar. Finally, the optimization study shows that ammonia is the best choice as the refrigerant and overall energy consumption of the process can be reduced using multistage cooling.

## Introduction

The CCS chain consists of three main processes: Capture, transportation, and storage. The liquefaction of CO<sub>2</sub> is an essential process between the capturing process and safe tank transport. Despite the fact that CO<sub>2</sub> liquefaction is an energy-consuming process, most of the CCS researches are devoted to capture, transport and storage processes. The conditioning processes are comparatively overlooked.

Only very few studies have modeled and compared the energy consumption of various liquefaction approaches. A. Alabdulkarem et al. compared different compression and liquefaction designs.<sup>[1]</sup> They found that open cycle liquefaction is slightly more energy efficient than closed-cycle liquefaction. Y. Seo et al.<sup>[2]</sup> compared three open cycle designs (Linde Hampson system) with the closed cycle and calculated the CAPEX and OPEX of the designs and found that the closed cycle has the lowest Life Cycle Cost (LCC). Other authors conducted similar studies but there is no agreement in the literature on which approach is optimal. More research on optimization of CO<sub>2</sub> liquefaction processes is therefore needed.

## CO<sub>2</sub> liquefaction designs

For the designing process, it is assumed that the feed gas comes from DMX capture technology developed by IPFEN<sup>[3]</sup>. The gas flowrate is 125

tonnes/hour. The gas is assumed to be saturated with water, and it contains 300 ppm CO and 20 ppm H<sub>2</sub>S on the dry basis. The temperature of the gas is 60°C, and the pressure is 6 bar.

Also, It is assumed that the compressor adiabatic efficiency is 80%, coolers reduces the hot streams to 30°C. The pressure drop in HX is 10kPa. Water is assumed to be removed using a dryer, H<sub>2</sub>S is reduced to 20 ppm using activated coal, and CO is reduced to 100 ppm using a stripper.

### Open cycle approach

In the open cycle liquefaction approach, water and H<sub>2</sub>S are firstly removed. The captured CO<sub>2</sub> gas is then compressed to high pressure, approximately 70-100 bar, using 3 compression stages. After that, it is liquefied during expansion. Finally, CO<sub>2</sub> is removing using a stripper. A simplified process flowsheet for the open cycle design is shown in figure 1.

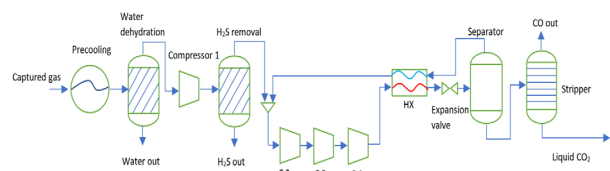


**Figure 1:** Flowsheet of the open cycle liquefaction design. Each compressor stage also includes a watercooler that cools the hot gas to 30°C, which is not shown.

### Closed cycle approach

In the closed cycle approach, the gas is only compressed to 15 (or 7) bar. It is then liquefied using a refrigerant. See figure 2.

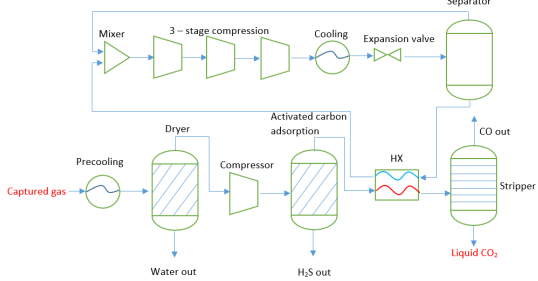


**Figure 2:** Flowsheet for the closed cycle liquefaction design. Each compression stage in the refrigerant loop includes a watercooler, which is not shown on the figure.

The closed cycle requires an external refrigerant. In this study, both ammonia and propane are simulated. In the refrigerant cycle, three compression stages are used to compress the refrigerant gas.

### Closed cycle with multistage cooling

In a different closed cycle design, the high pressure ammonia stream is split into three streams each expanded to a different pressure. The 1 bar stream is used for liquefying CO<sub>2</sub> while the 4 and 7 bar streams are used to precool CO<sub>2</sub>. See figure 3. The ammonia streams with intermediate pressure and temperature allow a better fit of the heat exchange curves between CO<sub>2</sub> and refrigerant. Hence reduces the energy consumption of the process. See figure 4.

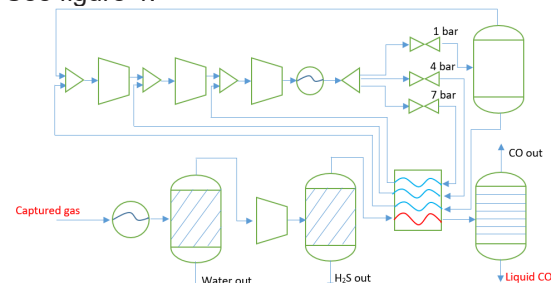


**Figure 3:** Closed cycle liquefaction with multistage cooling. Ammonia streams are split into 1 bar (-33°C) which is used to liquefy CO<sub>2</sub>, 4 bar(-1.9°C) and 7 bar (18°C) are used to precool CO<sub>2</sub> before liquefaction.

### Results and discussion

In this study, the compressor power, electric energy per tones CO<sub>2</sub> and cooling duty required are compared for different designs. See table 1.

The study shows that for both designs (Open and closed liquefaction), 15 bar case is more energy-efficient compared to the 7 bar case. However, liquefying CO<sub>2</sub> at 7 bar might be advantageous during transport processes because it is safer and require cheaper equipment. When comparing the two approaches, the closed cycle design is significantly better (7.5 MW compression duty) than the open cycle design (9.3 MW compression duty). The study also shows that ammonia is the best choice as refrigerant compared to propane as

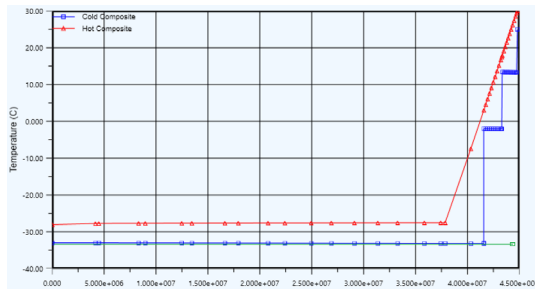


**Figure 4:** Heat exchange curves for the closed cycle liquefaction. Red curve shows the heat flow of CO<sub>2</sub>. Blue and green curves show the heat flow of ammonia in the multistage cooling design and base design respectively.

Design	Compression duty(MW)	Energy (kWh/t CO <sub>2</sub> )	Cooling duty (GJ)
Open, 7 bar	12.5	99.8	103.2
Open, 15 bar	9.3	74.2	86.3
Closed, NH <sub>3</sub> , 7 bar	9.6	76.5	92.6
Closed, NH <sub>3</sub> , 15 bar	7.5	60.2	80
Closed, C <sub>3</sub> H <sub>8</sub> , 15 bar	8.2	65.9	82.6
Multistage HX, NH <sub>3</sub> , 15 bar	7.2	57.4	78.1

**Table 1:** Design results in terms of compression power, (electric) energy per tonne CO<sub>2</sub> and cooling duty.

propane requires slightly more utility than ammonia. Other alternatives like freons could also be considered. However they have high GWP and most of them have low boiling points. Therefore, they are not the best choices for CO<sub>2</sub> liquefaction. Finally, it is shown that the closed cycle design with multistage cooling is slightly more energy efficient than the base design for the closed cycle approach.

### Conclusion

Multiple CO<sub>2</sub> conditioning processes are designed and compared. It is found that the closed cycle design with multistage cooling and ammonia as refrigerant is most optimal.

### Acknowledgement

This project has received funding from the European Union's Horizon 2020 research and innovation program under Grant Agreement No 838031.

### References

1. Alabdulkarem, Y. Hwang, R. Rademacher. Development of CO<sub>2</sub> liquefaction cycles for CO<sub>2</sub> sequestration. Applied Thermal Engineering 2012, 33-24:144-56
2. Youngkyun Seo, Hwalong You, Sanghyuk Lee, Cheol Huh, Daejun Chang. Comparison of CO<sub>2</sub> liquefaction pressures for ship-based carbon capture and storage (CCS) chain. International Journal of Greenhouse Gas Control 52(2016)1-12
3. P. Broutin, P. Briot, S. Ehlers, A. Kather. Benchmarking of the DMXTM CO<sub>2</sub> capture process, Energy Procedia 114(2017)2561-2572

# Experimental and Theoretical Study of Cyclone Reactors

(February 2019- February 2022)



## Contribution to the UN Sustainable Development Goals

Energy intensive industries, such as cement industry, contribute significantly to the global NOx emissions. Selective Non-catalytic Reduction (SNCR) is a NOx reduction technology by injecting N-containing agents to reduce NOx in an appropriate temperature window. In this study, we explore the application of SNCR in high temperature cyclones to achieve efficient NOx reduction and process intensification. Our work could contribute to SDG 12 Responsible Consumption and Production by reducing NOx emissions in industrial high-temperature processes, and improving process efficiency through a combined particle separation and NOx reduction process.



**Bingwen  
Guo**

[bingu@kt.dtu.dk](mailto:bingu@kt.dtu.dk)

**Supervisor:** Weigang Lin,  
Hao Wu,  
Kim Dam-Johansen

## Abstract

Experimental work was carried out in a pilot-scale cyclone reactor to investigate the SNCR performance under different particle loading and temperature conditions. The results showed that the presence of particles reduced the DeNOx efficiency and meanwhile lowered the NH<sub>3</sub> slip.

## Introduction

Nitrogen oxides (NOx) is one of the main sources of air pollution, which may cause photochemical smog and acid rain, and thereby harm the environment and health of people. A large proportion of NOx is emitted from energy intensive industries, such as cement industry. In order to reduce the NOx emission from these industries, ammonia or urea solution are injected to the flue gas at a suitable temperature window to react with NO to form N<sub>2</sub>. This method is named Selective Non-catalytic Reduction (SNCR).

Currently, the SNCR process has been primarily applied in freeboard of industrial processes. As an alternative, the application of SNCR in high-temperature cyclones with intensive mixing may offer a good NOx reduction efficiency, and a possibility of process intensification. Preheater cyclones are important components in cement industry, which partly operate at temperatures (850–1000°C) relevant for SNCR process.

However, compared to the conventional SNCR process, high particle loads in a cyclone, which can affect the temperature distribution and flow pattern, and thereby the SNCR performance. In addition, the presence of particles may catalyze the SNCR reactions. So far, the knowledge on the SNCR performance in particle loading cyclones is still limited.

## Objectives

The objectives of this project are:

- Understand the gas mixing behaviors inside cyclones and their importance to SNCR reactions
- Reveal the influence of the presence of particles on the SNCR process
- Understand the effect of NH<sub>3</sub> injection location and ways of injection on NO reduction
- Compare the influence of different reducing agents on the SNCR performance

## Experimental

Experiments were conducted on a pilot-scale cyclone reactor setup schematically illustrated in Figure 1. So far, silicon carbide particles are used to investigate the effect of relative chemical inert particles on the SNCR performance. Different particle feeding rates (from 20g/min to 60g/min) and stoichiometric ratios (from 0.5 to 2) are applied, with other experimental conditions fixed as shown in Table 1.

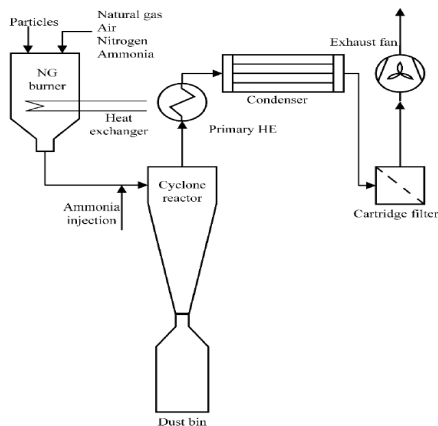


Figure 1. The diagram of the SNCR setup

Table 1. The experimental conditions

Cyclone inlet temperature (°C)	Inlet NO concentration (ppm)	Oxygen concentration (%)
980	500	4

## Results and discussion

The influence of particle on the SNCR performance and temperature distribution inside the cyclone are shown in Figure 2 and Figure 3, respectively.

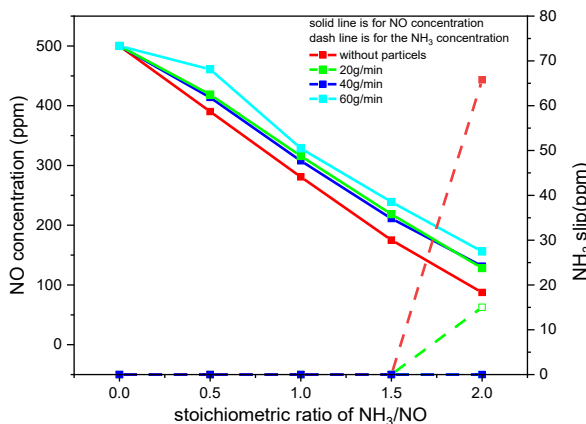


Figure 2. The influence of particle on the SNCR performance

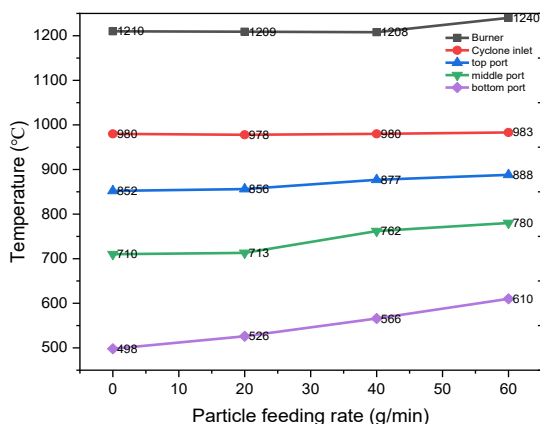


Figure 3. The influence of particles on the temperature distribution

From the figure 2, it is clear that the NO emissions increase slightly with an increase of the particle

feeding rate, i.e. reduced the NO reduction. While, the significant drop of NH<sub>3</sub> slip in the presence of particle.

One possible reason may be the temperature effect. From the figure 3, it is clear that when the cyclone inlet temperature is fixed, the particles can significantly change the temperature distribution inside cyclone. Around more than 100°C increase especially for the cyclone bottom, which may influence the N-chemistry.

Another possible reason is the surface effect. For the studies of NH<sub>3</sub> absorption on the silica surface, the process involves dissociative chemisorption of NH<sub>3</sub> forming Si-NH<sub>2</sub> on the surface and depending on the site, either a surface Si-OH group (if the surface is dehydrated) or gas-phase H<sub>2</sub>O (hydroxylated surface)<sup>1</sup>. More investigations are needed to clarify these hypotheses.

## Conclusions

In this work, the particles effect on the SNCR process was investigated. The presence of particles can reduce the DeNOx efficiency and meanwhile reduce the NH<sub>3</sub> slip. The possible reasons are the temperature effect and catalytic surface effect.

## Future work

The steps to follow in the future is to investigate the effect of different injection location, particle types and reducing agent on the SNCR performance

## Acknowledgements

This project is funded by China Scholarship Council (CSC), Technical University of Denmark (DTU), and is associated to ProBu funded by Innovation Fund Denmark.

## References

1. Glarborg, P., Dam-Johansen, K., Miller, J. A., Kee, R. J. & Coltrin, M. E. Modeling the thermal DENOx process in flow reactors. Surface effects and Nitrous Oxide formation. *Int. J. Chem. Kinet.* **26**, 421–436 (1994).

# Development of an electrochemical sensor for real-time monitoring of bioprocess

(January 2019- December 2021)

9

INDUSTRY, INNOVATION  
AND INFRASTRUCTURE



## Contribution to the UN Sustainable Development Goals

The efficiency of bioprocesses critically depends on the precise control of cultivation parameters. Rapid quantification is required for improved process control. On-line monitoring of the bioprocess enables fast decision-making through applying dynamic feeding strategies that are tailored to the process conditions. Development of electrochemical sensors and biosensors will lead to more precise on-line measurement of key state variables and metabolites in bio-based processes, and will thereby open up for better monitoring and control of future bio-based processes, resulting in increased efficiency.



**Aliyeh  
Hasanzadeh**  
alhas@kt.dtu.dk

**Supervisors:** Krist V. Gernaey, Mogens Kilstrup, Ulrich Krühne

## Abstract

In almost all fermentations, parameters such as pH, temperature, and dissolved oxygen, are monitored as standard. Other parameters, such as substrate utilization and product formation, can be monitored off-line using enzymatic assays and analytical techniques such as chromatography methods, but this involves inevitable delays, with implications for process control and management. Electrochemical sensors and biosensors offer the potential for rapid or even real-time monitoring of such parameters. This project aims at developing an electrochemical sensor for the monitoring of ammonium as a key state variable of the fermentation process.

## Introduction

Most bioprocesses are three-phase systems. The cells are dispersed as a solid phase in a liquid medium phase, which is aerated by a gas phase. The interactions among these three phases are complex. Biological components often react very sensitively to environmental changes (e.g., pH, temperature, pO<sub>2</sub>, nutrients), which may result in adverse effects on the activity of the cells or the reproducibility of the process [1]. Detailed analysis and monitoring of these three phases, combined with deep process knowledge, is necessary to control and optimize cultivation processes towards high product concentration and quality as well as for documentation purposes. Over the last few years, the process analytical technology (PAT) initiative of the Food and Drug Administration (FDA) has been introduced in biotechnology, biopharma production, and the food industry. By combining process analysis, process knowledge, and process modeling, a “built-in” quality in bioprocesses is enabled [2]. Over the past decades, there has been a great effort in developing methods for real-time monitoring of fermentation processes using various advanced sensors. Electrochemical sensors and biosensors offer the possibility of real-time

monitoring in combination with the advantages of low cost, high sensitivity and selectivity, and independence of the sample color and turbidity [3].

Ammonium is one of the central nutrients in media for most fermentation processes and needs to be present in relevant levels to promote growth and enzyme production. Besides, there are also major challenges associated with ammonium. It imposes for example additional costs on downstream wastewater treatment if more ammonium is added to the medium than needed by the microorganisms during the fermentation [4].

## Specific objectives

One of the objectives of this study is to fabricate an electrochemical sensor, based on a metal organic framework (MOF) in combination with polyaniline (PANI), for the on-line determination of ammonium in the fermentation broth. MOFs were selected as a sensing part because they offer unique structural diversity in contrast to other porous materials, allowing the successful control of framework topology, porosity, and functionality [5].

## Results and Discussion

The thin film morphology of MOF on a screen printed electrode was characterized using scanning electron microscopy (SEM) (see Figure 1). It can be seen that the electrodeposited MOF crystals are well-defined in shape, that is, a cube structure composed of six square facets of {100} [5].

Amperometric ammonium sensing was performed on a MOFs modified electrode obtained after different electrodeposition durations from 10 to 60 minutes, in order to find the optimal setting and sensitivity performance. However, increasing the electrodeposition time showed a clear increase in linear sensitivity of the electrodes. The increase in sensitivity of the electrodeposited MOFs of 30 and 60 minutes can be explained by the formation of more active sites on the electrode surface to capture ammonium ions.

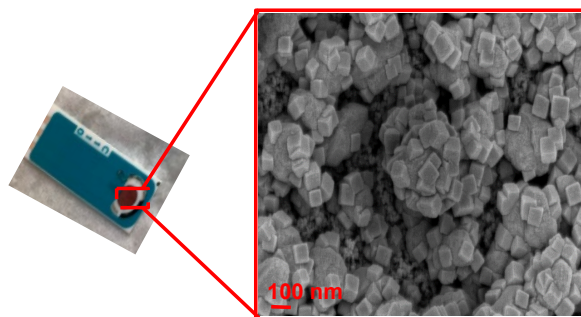


**Figure 1:** SEM image of the surface of electrode modified by MOFs.

To prove the reliability of the MOFs modified sensor for the electrochemical determination of ammonium requires demonstrating that there is little or no interference with other substances. For that, various compounds in typical culture media were considered and the corresponding responses are shown in Figure 2. The plots evidently demonstrate that the current output for ammonium is much higher as compared to that for the interfering compounds.

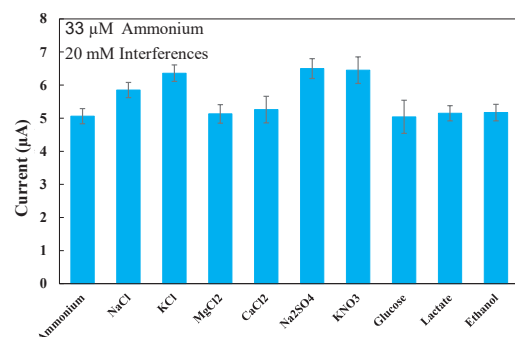


**Figure 2:** Interference tests on the MOFs modified electrode in ammonium detection.

Response stability and long-term durability of the MOFs modified electrode obtained in 33  $\mu\text{M}$  ammonium solution are shown in Figure 3. The data represents a high level of response stability over 20 days. The result confirms that the electrochemical behavior of the MOFs modified electrode does not change over time when exposed to an ammonium solution.

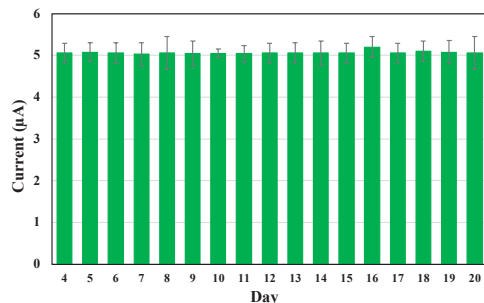


**Figure 3:** Long-term reusability of the MOF modified sensor for ammonium detection.

## Conclusions

In this work, an electrochemical sensor for ammonium quantification has been elaborated using MOFs. The sensor fabrication was optimized in terms of electrogeneration conditions. The analytical performance was thoroughly assessed and it was demonstrated that the developed electrochemical sensor presented a high sensitivity and a wide linear range. Besides, the lifetime of the developed sensor of more than 20 days is of key importance for monitoring ammonium in a real scenario.

## Acknowledgements

This project is part of the Fermentation-Based Biomanufacturing Initiative funded by the Novo Nordisk Foundation. It is conducted as a collaboration between DTU Chemical Engineering, DTU Bioengineering, FreeSense ApS, and Novozymes A/S.

## References

- 1 L. Mears, R. Nørregård, G. Sin, K.V. Gernaey, S.M. Stocks, M.O. Albaek, K. Villez, AIChE J. 62 (2016) 1986-1994.
- 2 D.W. Kimmel, G. LeBlanc, M.E. Meschievitz, D.E. Cliffel, (2019) Anal. Chem. 84 (2019) 685-707.
- 3 D. Semenova, T. Pinto, M. Koch, K. V Gernaey, and H. Junicke, Biosens Bioelectron 170, (2020) 112702
- 4 K. Pontius, H. Junicke, K. V Gernaey, and M. Bevilacqua, Appl. Microbiol Biotechnol, 104 (2020) 5315–5335.
- 5 M. R. Azhar, G. Hussain, M. O. Tade, D. S. Silvester, and S. Wang, ACS Appl Nano Mater 3 (2020) 4376–43

# Silicone elastomer constructed of concatenated rings shows excellent elasticity

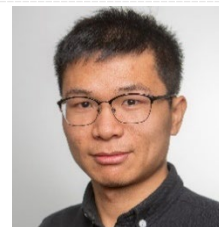
(Oct 2018- Oct 2021)

9 INDUSTRY, INNOVATION AND INFRASTRUCTURE



## Contribution to the UN Sustainable Development Goals

Soft silicone elastomers can be used as long-term stretchable and implantable devices, such as for soft robots, stretchable electronics, and sensors. A novel silicone elastomer with extreme softness and super high stretch-ability has been reported but the mechanism of elasticity has not been elucidated yet. Understanding the mechanism of elasticity of the novel elastomers will open a route for molecular design of materials with tailored properties, therefore providing industrial sectors the access to new technical capabilities.



Pengpeng Hu

penghu@kt.dtu.dk

### Supervisor:

Anne Ladegaard Skov  
Peter Jeppe Madsen

## Abstract

Preparing silicone elastomers with softness resembling human tissue is a key interest in research during recent years. Recently, a silicone elastomer prepared without the use of crosslinkers from heterobifunctional polydimethylsiloxane (PDMS) macromonomers has shown surprising softness, mechanical stability and extreme elongation [1]. In this work, the excellent elasticity is shown to originate from concatenated rings.

## Introduction

Silicone elastomers have been widely applied in stretchable electronics [2], medical devices [3], implants [4], and microfluidic devices [5]. Preparing silicone elastomers with softness resembling human tissue has been a key interest in research during recent years [6].

Conventional crosslinked silicone elastomers are generally produced from telechelic vinyl functional silicone polymers, multifunctional hydride crosslinkers and a platinum catalyst. Recently, an extremely soft elastomer was produced in the absence of a crosslinker, simply using near-monodisperse  $\alpha$ -monovinyl- $\omega$ -monohydride terminated PDMS and a platinum catalyst [1]. The elastomer shows an elongation of more than 5000% and a strain recovery of 82%. These observations depart from the elasticity of conventional cross-linked elastomers, since an elastomer without cross-links should not show such a high strain recovery [7].

From the reported reaction route, two possible topological structures can be formed during the reaction from highly purified macromonomers: chain extended linear PDMS from the *intermolecular* reaction and cyclic PDMS from the *intramolecular* reaction. Because the intermolecular reaction always produces end-functional macromolecules, the intramolecular reaction may happen for any intermediate linear PDMS. The final two possible

structures in the elastomer are rings and super-long polymer chains with end groups. Considering concatenated rings provide topological linkages which can act as crosslinkings, the novel elastomer is hypothesized to mainly consist of concatenated rings.

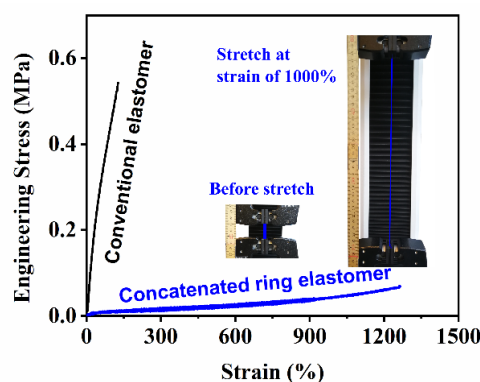


Figure 1 Stress-strain behaviors of elastomers

## Specific objectives

The main target of the project is to substantiate the hypothesis that the novel soft elastomer consists of concatenated rings, providing the support for molecular design of silicone elastomers with tailored softness.

## Results and discussions

We synthesized the reported elastomers without fillers, and a conventional elastomer was used as a reference sample. In figure 1, the concatenated ring elastomer is seen to be much softer and can be stretched to a much greater extent (maximum strain of 1270% and strain recovery of 96% after 3 cycles) than that of the conventional elastomer.

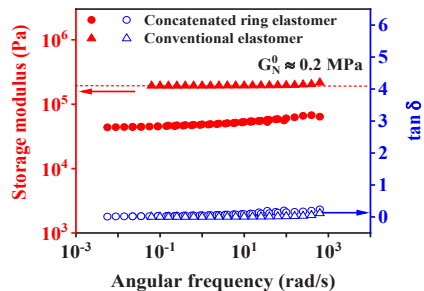


**Figure 2** Linear viscoelastic properties of elastomers

In figure 2, the conventional elastomer shows an entanglement plateau of 200 kPa at the full range of investigated frequency. However, at the same range of frequency, the concatenated ring elastomer exhibits a plateau of  $G'$  (44 kPa) which is far below the entanglement threshold. This plateau suggests that most of the elastomer network is elastically active. Theoretically, the plateau of a diluted, well-entangled network can be predicted to be  $G_0 = G_N^0(1 - \varphi)^a$  (with  $a=1.8-2.3$ ) where  $\varphi$  is the volume fraction of solvent [8]. The low  $G_0$  of the concatenated network cannot be exclusively due to contribution from sol fraction (15 wt%), but must also be from dangling rings trapped in the concatenated ring network.

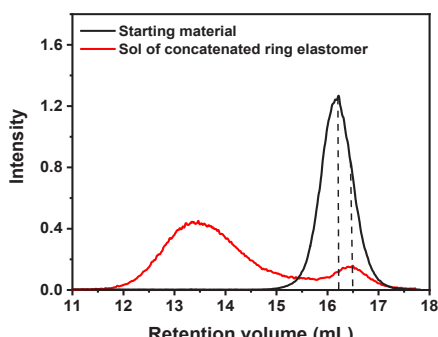


**Figure 3** Size-exclusion chromatography curves of starting material and sol fraction of the elastomer

The cyclic sol fraction can be distinguished from linear chains of the same molecular mass using size exclusion chromatography (SEC) due to a smaller hydrodynamic volume of a cyclic polymer [9]. As figure 3 shows, the SEC chromatogram of the sol fraction of concatenated ring elastomer exhibits a peak with a higher maximum retention volume

compared to starting material, indicating that a polymer with smaller hydrodynamic volume than the macromonomer—i.e. cyclic PDMS—is present in the concatenated elastomer. It should be pointed out that the smaller peak on the chromatogram of sol fraction only represents the existence of monocyclic PDMS. Since no reactive groups were detected in the sol fractions based on  $^1\text{H}$  NMR studies, the rest of the sol fraction can be slightly concatenated rings.

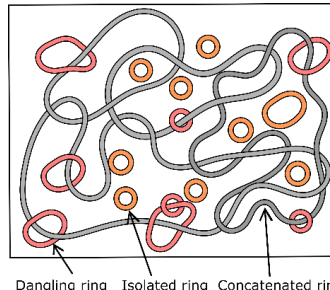


**Figure 4:** Illustration of concatenated ring network

## Conclusions

In this work, we demonstrated that the elasticity of the soft elastomers originates from concatenated rings, dangling rings and isolated rings structures, as illustrated in Figure 4. The dangling rings and isolated rings structures act as internal solvent and external solvent respectively, and both contribute to the low elastic modulus.

## Acknowledgements

The author would like to thank DTU Chemical Engineering and China Scholarship Council for the financial support.

## References

1. J. Goff, S. Sulaiman, B. Arkles, J. P. Lewicki, Advanced Materials 28 (12) (2016) 2393-2398.
2. F. B Madsen, L. Yu, A. L. Skov, ACS Macro Lett. 5 (11) (2016) 1196–1200.
3. F. Xu, W. Lu, Y. Zhu, ACS Nano 5 (1) (2011) 672–678.
4. K. Tybrandt, D. Khodagholy, B. Dielacher, F. Stauffer, A. F. Renz, G. Buzsáki, J. Vörös, Adv. Mater. 30 (15) (2018) 1706520.
5. M. P. Wolf, G. B. Salieb-Beugelaar, P. Hunziker, Progress in Polymer Science 83 (2018) 97–134.
6. K. Mazich, A. Samus, Macromolecules 23 (9) (1990) 2478-2483.
7. H. Liang, B. J. Morgan, G. Xie, M. R. Martinez, E. B. Zhulina, K. Matyjaszewski, S. S. Sheiko, A. V. Dobrynin, Macromolecules 51 (2018) 10028–10039.
8. V. G. Vasiliev, L. Z. Rogovina, G. L. Slonimsky, Polymer 26 (11) (1985), 1667–1676.
9. C. W. Bielawski, D. Benitez, R. H. Grubbs, Science 297 (5589) (2002) 2041–2044.

# Design and Upscaling of *Pseudomonas putida* Fermentations for Robust Biomanufacturing

(October 2019- October 2022)

12

RESPONSIBLE  
CONSUMPTION  
AND PRODUCTION



## Contribution to the UN Sustainable Development Goals

Fermentations as a mean of production is usually regarded as sustainable in the sense that they convert a renewable substrate to a given product but can be inefficient in this regard. We aim to provide insights into the cellular behavior under large scale production conditions to facilitate cell engineering. A cell engineered to withstand the conditions experienced at large scale will eventually be more efficient at converting the substrate into product, producing a more sustainable production process.



**Jesper Wang  
Jensen**

jewaj@kt.dtu.dk

**Supervisor:** Helena Junicke, John M. Woodley, Pablo I. Nikel.

## Abstract

Cell factories have become ever more relevant as an option to develop sustainable means of chemical production. A wide range of products have been developed to be produced from cell factories ranging from simple bulk chemicals to complex biopharmaceuticals. However, a well known issue in regard to cell factories is the lack of performance in industrial scale bioreactors compared to the laboratory scale bioreactor, which is believed to be linked to the fluctuating conditions of the industrial scale bioreactor. This project aims to elucidate the effect of fluctuating conditions on the bacterium *Pseudomonas putida* to guide further development of a robust cell factory platform.

## Introduction

Sustainable means of production has become a more significant topic in recent years as a result of increasing environmental concerns. However, in the chemical industry many everyday products are derived from petrochemicals [1]. One endeavor to switch from fossil derived petrochemicals to a renewable substrate is the use and development of cell factories. Highlighting the interest in fermentation derived biochemicals is the market estimated to more than 58 billion UsD, excluding biofuels [2]. An obstacle faced by the implementation of cell factories are the interaction between cell metabolism and the fluctuating conditions of industrial bioreactors.

Cell factories are capable of converting a renewable substrate like sugars into valuable biochemicals. These include but are not limited to small acid molecules of the tricarboxylic acid cycle that can be used for polymerization, biofuels from higher alcohols and terpenoids with application as coloring agents [1]. Often these endeavors are explored using traditional model organism like *Escherichia coli* and *Saccharomyces cerevisiae* though plenty of other candidates are available.

One such candidate is the relatively unexplored bacterium *Pseudomonas putida*.

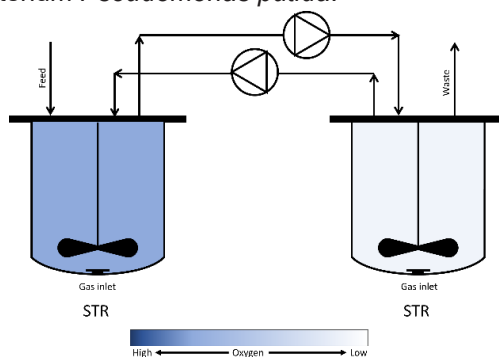


**Figure 1:** Two-compartment system consisting of two stirred tank reactors (STR). Separate control of each STR permit different oxygen levels in each compartment.

Robustness towards oxidative stress and a versatile metabolism are two of the key features that make *P. putida* an attractive cell factory platform. The *P. putida* metabolism consists of a special circular pathway for glucose metabolism which gives the bacterium the opportunity to tune both redox and energy regeneration to accommodate the given environment. This can be exploited to design

a high yielding cell factory [3]. However, there is a lack of information on how the fluctuating conditions of industrial bioreactors affect the energy and redox metabolism of *P. putida*.

### Specific Objectives

The overall objective of the project is to elucidate the effect of fluctuating oxygen levels on the cell physiology of *P. putida* to, in the future, enable development of the bacterium as a robust cell factory platform. To achieve this we aim to establish basic growth kinetics with an additional focus on the initial intermediates of the glucose assimilation pathway and how they depend on oxygen levels. Furthermore, we will elucidate how the energy state of the cell is affected by the oxygen level and its fluctuation. The latter should be based on predicted oxygen levels of a large scale bioreactor to reflect actual conditions.

### Experimental setup

To achieve the previously mentioned objectives a set of experiments are to be conducted. Basic cell kinetics will be explored in ordinary batch cultivations with a focus on the growth kinetics and metabolite levels to yield a basic understanding of the influence of oxygen levels on the cell. Here the partial pressure of oxygen will be varied to adjust the oxygen mass transfer of the bioreactor. Adjusting the partial pressure of oxygen rather than the agitation serves as a method to avoid mechanical stress and ensure that only oxygen levels are affecting the cell.

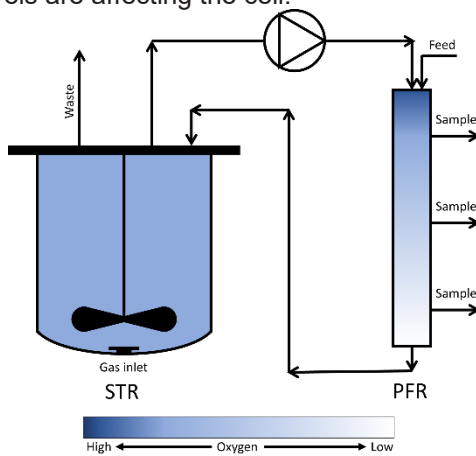


**Figure 2:** Two-compartment system consisting of a stirred tank reactor (STR) and a plug flow reactor (PFR). Gas inlet only in the STR to allow an oxygen gradient in the PFR compartment.

The second part will consist of scale down experiments to simulate the fluctuation oxygen levels expected to be present in a large scale

bioreactor. Each setup will consist of a two-compartment loop circulating the bacteria between high and low oxygen levels. These oxygen levels and circulation times will be based on oxygen gradients and mixing times predicted by a computational fluid dynamic model of a large scale bioreactor.

A setup consisting of two connected stirred tank reactors (STR), as illustrated in Figure 1, will be used to investigate the long term adaptation of *P. putida* to fluctuating oxygen levels. One STR will be operated at a high oxygen level whereas the other will be operated at a low oxygen level. By observing the energy state and metabolite production of the cell over long time we aim to elucidate how the organism adapts to the fluctuating conditions. A second setup, illustrated in Figure 2, has been devised to investigate the short term adaptation to fluctuating oxygen conditions. Here a STR operated at high oxygen level is connected to a plug flow reactor (PFR) without aeration. The PFR will simulate an oxygen gradient along the length of the reactor exposing the cell to a fast continuous decrease in oxygen levels. Several sampling points will be included along the PFR to follow the adaptation of the cell over the course of the PFR.

### Future Work and Perspective

With the influence of fluctuating oxygen levels established at a population level further investigations should be directed towards understanding how cell to cell heterogeneity is affected by fluctuating conditions.

To develop a more robust cell factory less affected by the fluctuating conditions of the industrial bioreactor cellular insights are required. These insights could, among other, be how the energy state and physiology is affected by fluctuating conditions. A cell factory which is physiologically more robust towards these conditions will necessarily also be more efficient at converting the substrate into product.

### References

1. J. Becker, C. Wittmann. Angew Chem Int Ed Engl 54 (11) (2015) 3328-3350.
2. A. M. Davy, H. F. Kildegaard, M. R. Andersen. Cell Syst 4 (3) (2017) 262-275.
3. P. I. Nikel, V. de Lorenzo. Metab Eng 50 (2018) 142-155.

# Autonomous self-healing dielectric elastomer actuator

(December 2019- November 2022)

12

RESPONSIBLE  
CONSUMPTION  
AND PRODUCTION



## Contribution to the UN Sustainable Development Goals

Dielectric elastomer actuators (DEAs) are made of an elastomer layer in between two conductive electrodes. A voltage is subjected to the device, which moves with an efficient conversion of electrical into kinetic energy. Due to the close resemblance with human muscles, DEAs are often termed artificial muscles. However, the device is prone to electrical damage and cannot easily be recycled. Thus, fabrication of a device that is not susceptible to electrical damage is in high demand. Moreover, a device that can be easily repaired from damage will not only extend the lifetime of the device but also reduce the involved waste.



**Seonghyeon  
Jeong**

seojeon@kt.dtu.dk

**Supervisor:** Anne L. Skov  
Anders E. Daugaard

## Abstract

Electrical breakdown of dielectric elastomer actuators (DEAs) generally leads to catastrophic failures, such as pinhole formation and subsequent tearing. In this event, the device must be replaced, since common DEAs cannot be reshaped and reprocessed. Here, we designed a DEA that autonomously self-heals after electrical breakdown as a result of the base material being an ultra-soft polydimethylsiloxane (PDMS) thermoplastic elastomer (TPE). This leads to an extended life-time and delayed ultimate failure of the DEA.

## Introduction

The capability for direct conversion of electrical energy to mechanical energy without gearing makes DEAs a promising candidate for soft robotics. [1] The efficiency of the energy conversion of the DEAs is related to the Young's modulus and the given voltage where a softer elastomer and higher voltage result in better conversion efficiency.[2] PDMS elastomers are widely used as dielectric elastomers due to their inherent softness.[3] On the other hand, the low electrical breakdown strength of PDMS elastomers limits their applications for soft robotics due to the necessary high voltage to achieve actuation.

When the elastomer experiences an electrical breakdown, the device is permanently damaged due to pinhole formation through the elastomer and subsequent tearing. There is extensive research on self-healing actuators with extended lifetime.[4] However, so far, there are no reports on instantaneous and autonomous self-healing DEAs. Here, we fabricated a DEA from a silicone based TPE, which can be shaped and molded reversibly using heat. The DEA can be fabricated using hot-pressing, which also enables scrapping and reuse of residual materials. Moreover, the DEA can survive from continuous electrical breakdowns as a result of self-clearing electrodes combined with

instant healing of the elastomer during actuation (as illustrated in Figure 1).

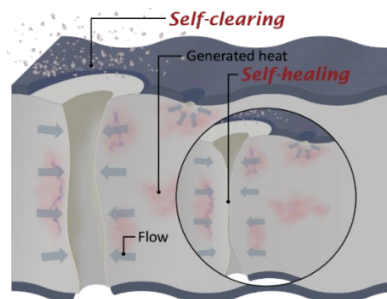


**Figure 1:** Schematic mechanism of the autonomous self-healing actuator

## Specific objectives

Fabrication of new types of thermoplastic elastomers enabling materials recycling and increased life-time of DEA systems.

## Results and Discussion

The PDMS TPE consists of a silicone backbone having two different types of hydrogen bonding groups, where weakly hydrogen bonding urea groups are spaced along the backbone, while the end-groups are strongly hydrogen bonding ureidopyrimidones. The Young's modulus of the elastomer is 178 kPa, where the softness arises from the weaker more dynamic urea bond, as illustrated in Figure 2.

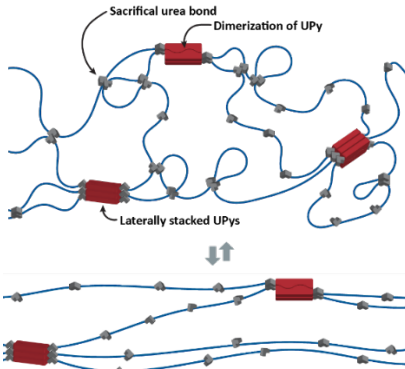


**Figure 2:** Schematic structure of the elastomer with urea (grey color), and ureidopyrimidone dimer (red color). When the elastomer is under deformation, the energy is dissipated by the dissociation of urea bond (bottom part).

The melting point is observed at 119 °C from a temperature sweep test, illustrating that the TPE can flow as a result of the localized heat during the electrical breakdown.[5] The DEA is prepared with a micro-corrugation on the surface, by hot-pressing of the elastomer at 140 °C, followed by silver-sputtering the electrodes on both surfaces. As a result, the DEA shows uniaxial deformation rather than biaxial deformation. The actuation strain is calculated from the length change of the DEA. With the increase in actuation strain along with the increased voltage, the maximum actuation strain is observed to be 6.8 % at 18.8 V  $\mu\text{m}^{-1}$ . Further increase of the voltage results in electrical breakdown of the DEA. However, no catastrophic failure of the device is observed and the device remains operative and can continue actuating. The electrical breakdown gives rise to localized heating, resulting in removal of the electrode and thereby preventing short-circuiting, since there is no longer a direct field. This ability is denoted a self-clearing effect,[6] which can be observed by the color change of the electrode [Figure 3].

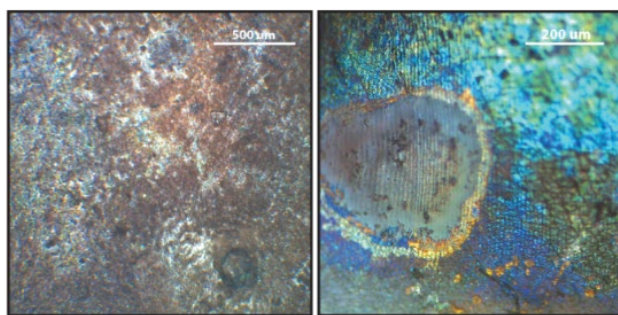


**Figure 3:** Microscopic images of the electrode surface before (left) and after self-clearing (right). In the absence of short-circuiting during the breakdowns, the localized heat softens the TPE, which allows it to flow and fill the voids that are

created by the electrical breakdown. Moreover, the presence of the actuation pressure assists the autonomous liquid-like behavior of the elastomer to fill out the cavity, leading to self-healing of the DEA as illustrated in Figure 1. As a result, the DEA can avoid the aforementioned catastrophic failure from the electrical breakdown. Instead, the defects caused by the electrical breakdown are mainly limited to the surface of the electrode.

## Conclusions

The DEA made of the soft PDMS TPE with silver electrodes has been shown to be autonomously self-healing from electrical breakdowns. The self-clearing effect enable the device to be operative during the electrical breakdowns, while the heat from the electrical breakdowns induces the flow of the elastomer into these cavities due to the actuation pressure. As a result, the damage created by the electrical breakdown is instantaneously and autonomously repaired and the device remains functional.

## Acknowledgements

Funding from Sino-Danish Center for Education and Research is acknowledged.

## References

1. Hines, L., Petersen, K., Lum, G. Z. & Sitti, M. Soft Actuators for Small-Scale Robotics. *Adv. Mater.* **29**, 1603483 (2017).
2. Madsen, F. B., Daugaard, A. E., Hvilsted, S. & Skov, A. L. The Current State of Silicone-Based Dielectric Elastomer Transducers. *Macromol. Rapid Commun.* **37**, 378–413 (2016).
3. Madsen, F. B., Yu, L., Daugaard, A. E., Hvilsted, S. & Skov, A. L. Silicone elastomers with high dielectric permittivity and high dielectric breakdown strength based on dipolar copolymers. *Polymer (Guildf.)* **55**, 6212–6219 (2014).
4. Yang, Y., Dang, Z. M., Li, Q. & He, J. Self-Healing of Electrical Damage in Polymers. *Adv. Sci.* **2002131**, 1–21 (2020).
5. Christensen, L. R., Hassager, O. & Skov, A. L. Electro-Thermal model of thermal breakdown in multilayered dielectric elastomers. *AIChE J.* **65**, 859–864 (2018).
6. Benslimane, M., Gravesen, P. & Sommer-Larsen, P. Mechanical properties of dielectric elastomer actuators with smart metallic compliant electrodes. in *Smart Structures and Materials 2002: Electroactive Polymer Actuators and Devices (EAPAD)* (ed. Bar-Cohen, Y.) vol. 4695 150–157 (2002).

# O<sub>3</sub> assisted Combustion to alternative Fuel

(Nov 2019 - Nov 2022)

7 AFFORDABLE AND CLEAN ENERGY



## Contribution to the UN Sustainable Development Goals

Combustion is the most fundamental method for humans to obtain energy from nature. The UN Sustainable Development Goals encourage the society to transfer from fossil fuel to clean fuel or use new technology for clean combustion. These new fuels and technology address challenges on conventional combustion equipment. Ozone-assisted combustion is able to solve these problems. Hence understanding the mechanism and the role of ozone in combustion is beneficial to promotion of clean combustion.



**Jie Jian**  
jiejia@kt.dtu.dk

**Supervisor:**  
Peter Glarborg; Hao Wu

## Abstract

Ozone-assisting combustion is a promising combustion technology that can stabilize and improve combustion performance in many unfavorable conditions. Understanding the role of ozone in combustion theoretically enable precise control to this technology. Our work focus on the basic O<sub>3</sub>-H<sub>2</sub> mechanism which is the foundation of any H<sub>2</sub> derived fuel. The O<sub>3</sub> decomposition and O<sub>3</sub>-H<sub>2</sub> reaction were tested in a flow reactor at 400K – 575K. The result showed that the participation of O<sub>3</sub> significantly promotes H<sub>2</sub> conversion. Present mechanisms show good agreement with the H<sub>2</sub> conversion but under-estimate O<sub>3</sub> decomposition conversion.

## Introduction

The demand of high-efficiency and clean combustion intrigues the scientific interest to develop modern combustion technologies such as low-temperature combustion, ultra-lean combustion, and homogeneous charge compression ignition. However, all these technologies involve challenges for the combustion control because they are running close to the extinction limit.

In order to overcome these challenges, ozone-assisting combustion has been a prominent and popular research field recently. Ozone is a highly reactive oxidizer which can be generated rapidly in-situ from air by electrical plasma. Addition of ozone into combustor has been tested on the modern combustion technology mentioned at the beginning and also various types of fuel, including methane, propane, octane, ethylene, and diesel.

Playing a very fundamental role in all hydrogen-derived fuel, the O<sub>3</sub>-H<sub>2</sub> sub-mechanism is of great significance to O<sub>3</sub>-assisted combustion and therefore combustion control. However the present sub-mechanisms are not developed directly from O<sub>3</sub> – H<sub>2</sub> reactions and have never been validated specifically.

Therefore the present work aims to improve the O<sub>3</sub>-H<sub>2</sub> sub-mechanism based on latest progress in ozone and hydrogen chemistry and validate it by

comparison with O<sub>3</sub>-H<sub>2</sub> experiments in a flow reactor.

## Experimental and Modelling

The experiment details are depicted in Fig. 1. A quartz tube flow reactor was used with an electricity-heating furnace providing a steady reaction temperature ranging from 400 to 575 K.

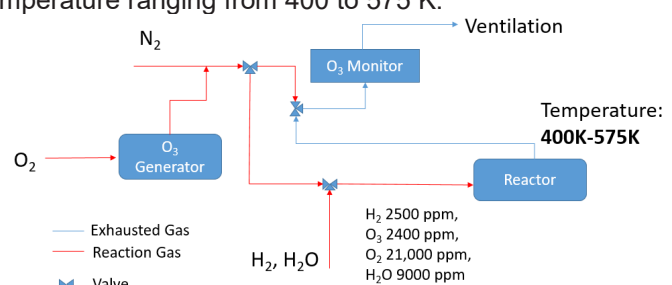


Figure 1. Schematic of the experiment.

The premixed reaction gas composed of ozone, oxygen, hydrogen, water vapor, and nitrogen. Different gas compositions were set to study O<sub>3</sub> decomposition and O<sub>3</sub>-H<sub>2</sub> mechanism, and the influence of water vapor. The O<sub>3</sub> and H<sub>2</sub> concentrations in the exhausted gas were analyzed by an ozone analyzer and a gas chromatography analyzer respectively.

Numerical simulations were performed using a one-dimensional flow reactor model of CHEMKIN-PRO with the measured reactor temperature profile implemented. The mechanism by Dagaut [1] and

the most recently updated model by Konnov [2] were employed and compared.

### Validation of O<sub>3</sub> Decomposition

The Figure 2 presents the experimental and modelling result of ozone decomposition in the flow reactor. Ozone gas starts to decompose at 450K. The decomposition rate dramatically increases at temperature higher than 475K. The conversion is completed above 525K. This indicates from 475K to 525K where the decomposition accelerates is the most important temperature range for ozone decomposition initiation.

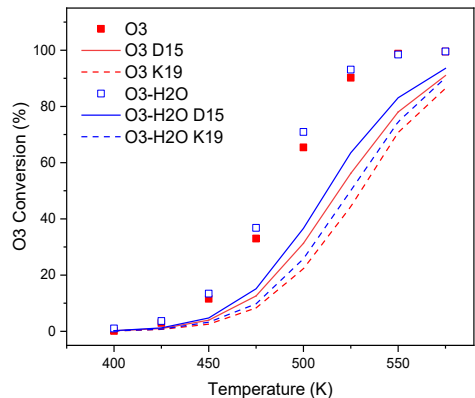


Figure 2. O<sub>3</sub> decomposition conversion at varied temperature and influence of water vapor. The symbols are experimental data while the lines are theoretical calculation.

The influence of water vapor in the decomposition was also investigated. It was found to slightly increase the conversion by around 3% under the initiation stage. This may be due to H<sub>2</sub>O contributing a small amount of O and OH radicals to the pool, but the overall influence of water vapor is actually almost negligible.

The mechanisms from Dagaut and Konnov are compared with the experimental data. The two mechanisms both considerably under-estimate the decomposition conversion by 30% - 40% at the initiation stage. Dagaut's mechanism performs slightly better than Konnov on this issue.

### Validation of O<sub>3</sub>-H<sub>2</sub> reaction

The O<sub>3</sub>-H<sub>2</sub> reaction is compared with O<sub>3</sub> decomposition and O<sub>2</sub>-H<sub>2</sub> reaction in the Figure 3. It is clear that with the participation of O<sub>3</sub> significantly promotes H<sub>2</sub> conversion compared with solely O<sub>2</sub>-H<sub>2</sub> reaction. The H<sub>2</sub> conversion rate has been drastically increased from around 2.5% to 15%. However, the influence of H<sub>2</sub> to is not as pronounced as its counterpart effect. The conversion of O<sub>3</sub> is only increased by 5% - 7% with H<sub>2</sub> participating. That means O<sub>3</sub> is mostly consumed by its own decomposition while H<sub>2</sub> is mainly consumed by reaction with O<sub>3</sub> and O radical from O<sub>3</sub> disassociation. Similarly the presence of water vapor has a trivial impact on the overall reaction.

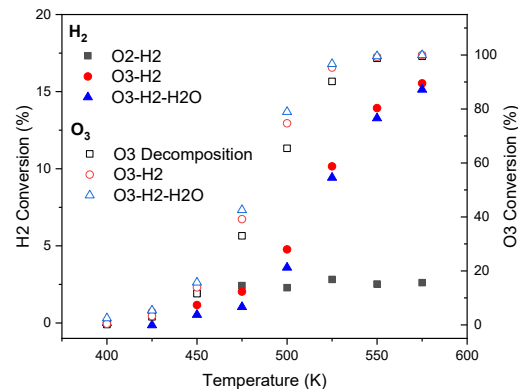


Figure 3. Experimental O<sub>3</sub> and H<sub>2</sub> conversions in varied reaction system. The solid symbols denotes H<sub>2</sub> while the hollow symbols denotes O<sub>3</sub>.

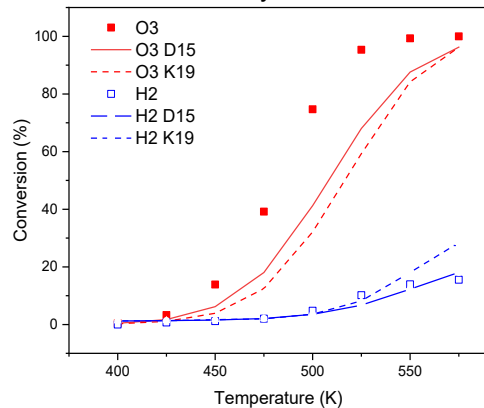


Figure 4. Comparison of experimental (symbols) and modelling (lines) results of O<sub>3</sub>-H<sub>2</sub> reaction.

The mechanisms are as well validated on the O<sub>3</sub>-H<sub>2</sub> reaction in Figure 4. As for O<sub>3</sub> conversion, the two mechanisms still show under-prediction as they do in O<sub>3</sub> decomposition (Figure 1). However, they perform much better on H<sub>2</sub> prediction, especially Dagaut's mechanism. Hence the hydrogen part in the mechanisms proved to be reliable. And the ozone decomposition has a potential for improvement.

### Conclusion

The current O<sub>3</sub>-H<sub>2</sub> reactions were studied in a flow reactor at temperatures of initiation stage. The results were compared with theoretical predictions. O<sub>3</sub> significantly enhances the conversion of H<sub>2</sub>. However, H<sub>2</sub> only contribute a small portion O<sub>3</sub> conversion. Water vapor was proved to have little impact on the reaction. The current mechanism give excellent prediction to H<sub>2</sub> concentration but underestimate the O<sub>3</sub> decomposition rate.

### Reference

1. J. B. Maserier, F. Foucher, G. Dayma, and P. Dagaut. Proc. Combust. Inst., vol. 35, no. 3, pp. 3125–3132, 2015.
2. A. A. Konnov. Combust. Flame, vol. 203, pp. 14–22, 2019.

# Condensation curing silicone elastomer coatings with high scratch resistance

(February 2018 – January 2021)



## Contribution to the UN Sustainable Development Goals

Condensation curing silicone elastomers are commonly used as protective coatings. Besides their excellent stability in a broad temperature range, oxidation stability, hydrophobicity, and biocompatibility, they can be cured in ambient environment, which represents a great application advantage. Nevertheless, the biggest limitation of silicone elastomers in general is the poor scratch resistance, which can lead to undesirable application failure or reduction of life time. Improving the scratch resistance of silicone elastomers will therefore help to reduce material consumption and production.



**Alena  
Jurásková**  
[alejur@kt.dtu.dk](mailto:alejur@kt.dtu.dk)

**Supervisors:** Anne Ladegaard Skov, Stefan Møller Olsen, Kim Dam-Johansen

### Abstract

In this work, the scratch resistance of silicone elastomer coatings is investigated. The coatings are prepared by condensation reaction of silanol terminated polysiloxane ( $\text{HO-PDMS-OH}$ ) with trimethoxysilane terminated polysiloxanes ( $(\text{MeO})_3\text{-PDMS-(OMe)}_3$ ) and ethoxy terminated octakis(dimethylsiloxy)-T8-silsesquioxane ( $(\text{QM}^{\text{OEt}})_8$ ), respectively. We showed that the scratch resistance of silicone elastomers can be significantly improved by a creation of so-called cross-linker domains in the elastomer network structure.

### Introduction

Condensation curing silicone elastomers benefit over other silicone elastomer types by the ability to cure in ambient environment.[1] The mild curing conditions together with the superior properties of silicone elastomers makes them to be commonly used as protective coatings.[2] Nevertheless, in order to provide proper material protection, fillers need to be added to silicone elastomer formulations to improve their scratch resistance. This often leads to undesirable Mullins effect or loss of coating transparency.[3]

In this study, we investigate the possibility to improve the scratch resistance by implementing so-called cross-linker domains into the elastomer network structure. The elastomers are prepared by reaction of  $\text{HO-PDMS-OH}$  with  $(\text{MeO})_3\text{-PDMS-(OMe)}_3$  and  $(\text{QM}^{\text{OEt}})_8$  cross-linker, respectively. The cross-linker domains are created by using cross-linker excess. The use of the higher molecular weight cross-linkers (alkoxy-terminated polysiloxanes and silsesquioxane) brings several advantages for the network formulation. Firstly, they do not evaporate from the reaction mixture as this is often the case of commonly used alkoxy silanes.[4] Secondly, the cross-linking density and elasticity of the cross-linker domains can be easily tailored.

### Specific Objectives

- What is the relation between the type and concentration of the cross-linker domains and the scratch resistance
- How do our coatings perform compare to a commercial silicone elastomer coating reinforced with fillers

### Experimental

The nomenclature, molecular weight, and chemical structure of the compounds used in the coating formulations are summarized in Table 1. The different network structures were prepared by changing either the cross-linker type ( $(\text{MeO})_3\text{-PDMS-(OMe)}_3$  or  $(\text{QM}^{\text{OEt}})_8$ ), cross-linker chain length (Di-10, 50, and 200), or the stoichiometric ratio ( $r = f^*[\text{cross-linker}]/f^*[\text{HO-PDMS-OH}]$ ,  $r = 3, 5$  or 15). Even though all films were cured withing a few hours, the scratch resistance measurements were conducted after 27 days of keeping the samples in a climite chamber, which is the time required for a complete creation of the cross-linker domains.

The scratch resistance was measured using Motorized Clemen Scratch Tester equipped with  $\varnothing 1\text{mm}$  ball tool. The destruction of the film was observed visually. Two different parameters were evaluated – “single” scratch resistanc and “multiple” scratch resistance. The “single” scratch resistance

was determined as the maximum load at which the coating is not penetrated. The “multiple” scratch resistance was determined as the maximum load at which the coating is not penetrated after three consecutive scratches at the same place. Both procedures (“single” and “multiple” scratch) were repeated three times for each coating composition. If the coating was penetrated during one or more of the three repetitions, the load was lowered and the whole procedure was repeated.

**Table 2:** Summary of compounds used in the coating formulations.

Nomenclature and molecular weight		
HO-PDMS-OH	C2T	$M_n \sim 20200 \text{ g/mol}$
(MeO) <sub>3</sub> -PDMS-(OMe) <sub>3</sub>	Di-10	$M_n \sim 1200 \text{ g/mol}$
	Di-50	$M_n \sim 5500 \text{ g/mol}$
	Di-400	$M_n \sim 20300 \text{ g/mol}$
(QM <sup>OEt</sup> ) <sub>8</sub>	-	$M = 1370.404 \text{ g/mol}$
Chemical structure and suppliers		
HO-PDMS-OH (Wacker Chemie)		
(MeO) <sub>3</sub> -PDMS-(OMe) <sub>3</sub> (Silitech)		
(QM <sup>OEt</sup> ) <sub>8</sub> (Synthesized)[5]		

## Results and Discussions

The formation of the cross-linker domains was shown to have significant effect on the scratch resistance (Figure 1). Specifically, the scratch resistance is improved with increasing  $r$ , for the elastomers cross-linked by Di-10 and (QM<sup>OEt</sup>)<sub>8</sub>, respectively. Elastomers E\_C2T+Di-10\_r15 and E\_C2T+(QM<sup>OEt</sup>)<sub>8</sub>\_r15, which do not contain any fillers, have a scratch resistance comparable to the one of the reference coating (E\_Ref). Distinctly, a negative effect of increasing  $r$  on the scratch resistance was observed for elastomers cross-linked by Di-50. This can be explained by the high weight percentage of the Di-50 cross-linker in the elastomer compared to Di-10 and (QM<sup>OEt</sup>)<sub>8</sub>. None or minimum difference in the scratch resistance is reported for E\_C2T+Di-400 and E\_Di-400. This is because of the high molecular weight of the Di-400 cross-linker, which is comparable to the molecular weight of the C2T (Table 1). Thus the Di-400 domains do not have reinforcing character. Noticeable, even though E\_C2T+(QM<sup>OEt</sup>)<sub>8</sub>\_15 has an excellent “single” scratch resistance, significant drop is observed for the “multiple” scratch resistance. On the other hand E\_C2T+Di-10\_r15 performs well in both “single” and “multiple” scratch resistance. Both elastomers (E\_C2T+(QM<sup>OEt</sup>)<sub>8</sub>)\_15

and E\_C2T+Di-10\_r15) contain similar weight percentage of the cross-linker, namely 20 and 23wt%, respectively. Therefore, the drop in the “multiple” scratch resistance can be attributed to the rigidity of the (QM<sup>OEt</sup>)<sub>8</sub> domains. The more elastic Di-10 domains perform well in both “single” and “multiple” scratch test, emphasizing the importance of the rigidity/elasticity of the cross-linker domains on the scratch resistance properties.

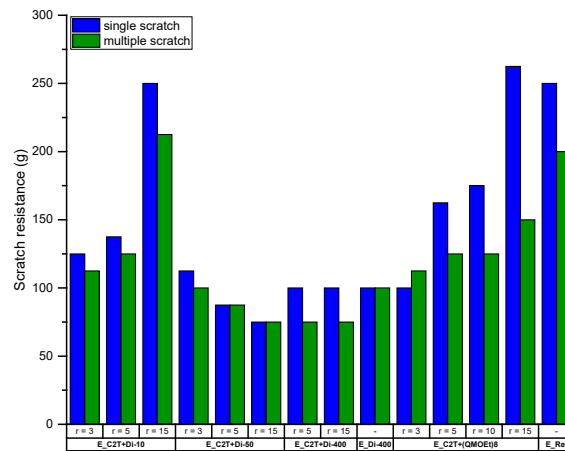


**Figure 1:** Scratch resistance of a commercial coating (E\_Ref) and elastomer films prepared by reactions between C2T and Di-10, Di-50, Di-200, and (QM<sup>OEt</sup>)<sub>8</sub>, respectively. The film thickness was ~ 100  $\mu\text{m}$ .

## Conclusion

- The scratch resistance is highly dependent on the concentration and type of the cross-linker domains in the elastomer network structure.
- Di-10 and (QM<sup>OEt</sup>)<sub>8</sub> cross-linker domains were found to have a positive effect on the scratch resistance.
- The scratch resistance of elastomers E\_C2T+Di-10\_r15 and E\_C2T+(QM<sup>OEt</sup>)<sub>8</sub>\_r15 is comparable to the one of the commercial coating (E\_Ref) containing reinforcing fillers.

## Acknowledgement

Financial support from the Hempel Foundation to CoaST (The Hempel Foundation Coating Science and Technology Centre).

## References

- T. Kimura and M. Ikeno, U.S. Patent 6,306,998 B1. 2001.
- U. Eduok, O. Faye, and J. Szpunar, Prog. Org. Coatings, 111, 124–163, 2017.
- F. B. Madsen, A. E. Daugaard, S. Hvilsted, and A. L. Skov, Macromol. Rapid Commun., 37, 378–413, 2016.
- A. Jurášková, K. Dam, J. Stefan, M. Olsen, and A. Ladegaard, J. Polym. Res, 1–14, 2020.
- A. Jurášková, A. L. Skov, and M. A. Brook, Ind. Eng. Chem. Res, 2020.

# Evaluation of Single-Pass Tangential Flow Filtration (SPTFF) to Increase Productivity in Protein Purification Processes

(June 2019 – May 2022)



## Contribution to the UN Sustainable Development Goals

During the past decades, the global consumption of material and energy resources has increased drastically as a result of economic and population growth. Thus, the responsible consumption and sustainable production of goods becomes increasingly important. This project aims to make drug manufacturing more efficient by increasing the capacity of manufacturing processes. As a result, the use of materials such as chemicals or consumables could be decreased, production equipment downsized, and energy consumption lowered.



**Johann Kaiser**

jokais@kt.dtu.dk

**Supervisors:**  
Ulrich Krühne, Manuel Pinelo, Janus Krarup

## Abstract

Increasing capacity of pharmaceutical manufacturing processes is important to reduce production costs in order to withstand rising cost pressures and to make drugs available to more people. Due to the complexity of pharmaceutical manufacturing, long processing times and high costs arise. This PhD project aims to increase the capacity of such processes by using single-pass tangential flow filtration (SPTFF) as an inline concentration step to reduce large volumes and processing times, and as a result reduce the facility footprint and the production costs. A multi-scale modelling approach combined with experiments is applied.

## Introduction

As the market for biopharmaceuticals such as monoclonal antibodies (mAbs) continues to rise, it becomes increasingly important to make manufacturing cheaper and more efficient. The processes to isolate and purify these biotechnologically produced pharmaceuticals face various challenges such as a poor operation flexibility, limited available space, and high costs. Especially large volumes and low product concentrations are a challenge in large-scale production because they cause long processing times and large facility footprints, which in turn results in low capacities and high costs. Figure 1 schematically shows the different process steps that are part of a typical mAb purification process. [1]

To overcome these challenges, large volumes can be reduced by technologies which can upconcentrate the product where needed in the process. One example of a technology used for upconcentrating is single-pass tangential flow filtration (SPTFF), which enables a volume reduction in a single pass. Figure 2 shows a schematic example of a SPTFF module consisting of multiple flow stages, each containing multiple

membranes, which results in a longer flow path, a longer residence time of the product, and a higher concentration factor compared to conventional crossflow filtration. Besides the higher achievable concentration, other advantages of this technology over existing filtration techniques are the ability to flexibly place a filter inline before or after other process steps, an upconcentration under more gentle conditions, and that no intermediate tanks and recirculation systems are required. [2] [3]

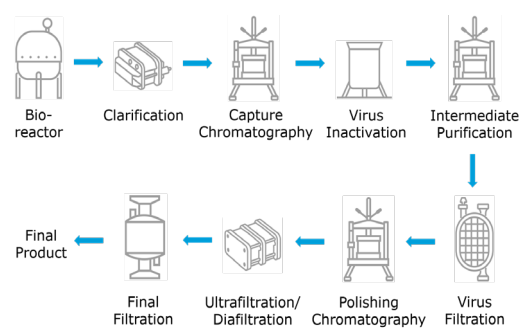


**Figure 1:** Overview of a typical mAb purification process from the clarification of the cell culture fluid to the final product. Adapted from [4].

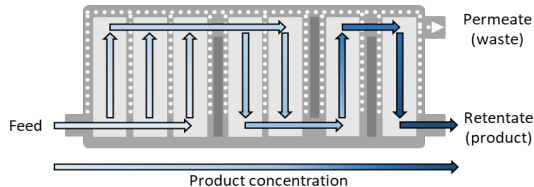


**Figure 2:** Schematic of SPTFF (3-3-2-2-1 layout) illustrating the flow path of the filtered solution. The concentrated product leaves the filter through the retentate outlet.

### Specific Objectives

A computer-aided multi-scale approach is applied to systematically evaluate the idea of implementing SPTFF as an inline concentration step in a mAb downstream process. This approach consists of an evaluation of the filtration technique at the process level (1) and at the equipment level (2). The simulation results are supported by experiments (3). The three parts and their objectives are described in the following:

1. Modelling of a mAb process and simulation of the implementation of SPTFF in this process ("flowsheet modelling") using a process simulation software with the objective to evaluate where in the process SPTFF can be implemented to increase the capacity. This model represents all process steps (e.g. a chromatography step) including the equipment (e.g. a chromatography column) and the tasks (e.g. different chromatography phases) carried out in each process step. Process data such as mass balances and a process schedule serve as input for the model. Once a model has been formulated and validated, the production process can be analyzed with respect to possibilities for improvement, and it can be used to test out ideas by performing discrete-event simulations to improve the capacity.
2. Modelling of the filtration process at the unit operation level for selected places in the process using a computational fluid dynamics (CFD) software with the objective to better understand the filtration process and define suitable operation parameters and a suitable filter design. For example, the CFD model can be used to investigate the fluid flow when changing parameters such as the backpressure or feed flow rate, the mixing of the solution in the filter, and the accumulation of product on the filtration membrane. Also, an engineering model can be formulated to help scale the filtration process from lab scale to production scale and find an optimal filter design for the production.

3. Experiments with the objective to obtain parameters needed for the mechanistic modelling and to verify the simulation results.

### Results and Discussion

The flowsheet model of the mAb downstream process has been used to simulate the effect of upconcentrating at different places in the process on the capacity taking into account different volumetric concentration factors. Figure 3 shows the simulation results for three different process schedules. By introduction upconcentration steps to the process, a maximum increase in capacity of 5% to 8% can be achieved, depending on the process schedule

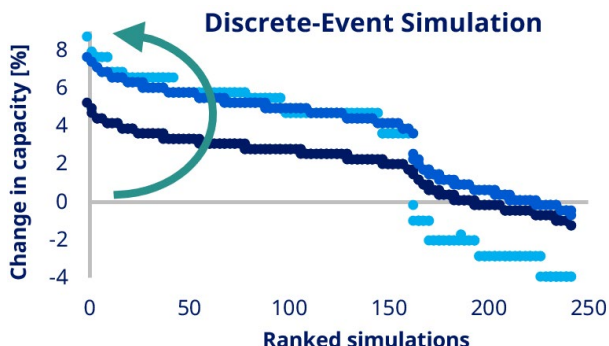


**Figure 3:** Flowsheet simulation results illustrating the change in capacity when implementing upconcentration steps in the processes for different process schedules.

### Conclusion

The flowsheet modelling results show that an increase in capacity can be achieved by introducing upconcentration steps in a mAb process. The results show that the process scheduling is of great importance for realizing the capacity.

The filtration process is further studied through mechanistic modelling to gain a deeper understanding of the separation process.

### References

1. A. Guerra, O.E. Jensen, Evaluating In-line Volume Reduction During mAb Production, *Pharmaceutical Engineering* (2018).
2. C. Casey, K. Rogler, X. Gjoka, R. Gantier, E. Ayturk, CadenceTM Single-pass TFF Coupled with Chromatography Steps Enables Continuous Bioprocessing while Reducing Processing Times and Volumes, *Pall Application Note* (2015).
3. E. Ayturk, C. Forespring, Simplifying Bioprocessing with Single-Pass TFF, *Genetic Engineering & Biotechnology News*, 36 (4) (2016).
4. White Paper "Single-pass tangential flow filtration, a versatile application to streamline biomanufacturing", Merck KGaA (2018)

# High-permittivity Silicone Elastomers for Sensitive Flexible Pressure Sensors

(November 2019- November 2022)

9 INDUSTRY, INNOVATION  
AND INFRASTRUCTURE



## Contribution to the UN Sustainable Development Goals

Polydimethylsiloxane (PDMS) elastomers are extensively used for the fabrication of flexible devices owing to their commercial availability and unique dielectric and mechanical properties. Highly sensitive and flexible PDMS sensors experience increased demand with the development of a wide variety of smart sensor solutions for sustainable and efficient energy management. The sensitivity of capacitive pressure sensor is primarily determined by the dielectric permittivity and elastic modulus of the dielectric layer, that reversibly deforms to produce an electrical signal. In this study, a facile method involving eco-friendly, high-permittivity ionic liquids and soft PDMS is investigated for production of sensitive pressure sensors.



Zhaoqing  
Kang

zhkang@kt.dtu.dk

**Supervisor:**  
Anne Ladegaard Skov,  
Liyun Yu  
Suojiang Zhang, Yi Nie

## Abstract

A novel high-permittivity soft filler (LMS-EIL) is developed by grafting imidazole-based ionic liquids (ILs) to chloropropyl functional silicone (LMS-152). The dielectric permittivity at 0.1 Hz of LMS-EIL is increased almost 100,000 times compared with LMS-152. Furthermore, high-permittivity, soft dielectric silicone elastomers are prepared with incorporated with LMS-EIL. The results show that the relative permittivity ( $\epsilon_r$ ) increases from 3.34 for the elastomer with the addition of 10 parts per hundred rubber (phr) LMS-152, up to 22 for the elastomer with the same amount of LMS-EIL. The Young's modulus (Y) decreases steadily with increasing amounts of LMS-EIL. Overall, the sensitivity of the resulting elastomer incorporated with 10 phr LMS-EIL increased 46 times compared to that of elastomer incorporated solely with LMS-152.

## Introduction

Flexible pressure sensors, which can generate output signals from a given pressure, have recently gained increasing demand in the flexible electronic device applications, such as detectors, electronic skins, and wearable electronics. Based on their working mechanisms, pressure sensors can be classified as piezoresistive, capacitive, triboelectric, or optical devices. Capacitive pressure sensors possess high sensitivity, low power consumption, fast response, and low cost are the fastest growing category[1].

For a classical capacitor, the capacitance is determined by the relative permittivity, the distance between electrodes, and the electrode area. Therefore, compressibility (softness) and  $\epsilon_r$  of the dielectric layers of the capacitor are two important factors for the sensitivity of flexible capacitive sensors. Due to their flexibility, PDMS elastomers are more widely used as the dielectric layer of the sensor than polyurethane and polyimide [2]. However, the sensitivity is limited by the modulus and low dielectric permittivity of PDMS. The most effective method to improve the sensitivity of the

sensors is to form a layered microstructure, such as gaps or micro array structures [3]. Due to the decrease of the overall modulus after formation of microstructure with resulting air voids, a more clear deformation from a small pressure is achieved. However, the preparation process of microstructures, such as chemical etching or photolithography, is expensive and complex, and is also not feasible for large-scale industrial production at low cost. Another approach to increased sensitivity is to add additives, such as silicone oil to a foam structure. Nevertheless, these sensors suffer from bad repeatability and durability because of the excessive unreacted oil (up to 50 wt%) in the substrate [4].

In this study, a high permittivity soft filler is synthesized by combination of imidazole-based ILs and chloropropyl-functional silicone. The dielectric elastomer layer of the sensor is prepared by inclusion of filler followed by crosslinking. Due to the combined improvement of dielectric permittivity and softness, the prepared pressure sensor possesses increased sensitivity as well as a linear response.

## Specific Objectives

The objectives of this project are:

- (1) To prepare a novel high permittivity soft filler by grafting ILs to chloropropyl-functional silicone oil
- (2) To evaluate the sensitivity of the capacitive sensor with the developed soft filler included

## Results and Discussion

The LMS-EIL is used to modify a PDMS elastomer, and thus its initiative dielectric property will have a pivotal effect on the sensor. In Figure 1, the dielectric permittivity ( $\epsilon_r$ ) of LMS-EIL is shown and it can be seen that  $\epsilon_r$  increases approximately 100,000 times compared to the pure silicone oil. The loss tangent ( $\tan\delta$ ) of LMS-EIL is shown to decrease 30 times compared to LMS-152 at 0.1 Hz.

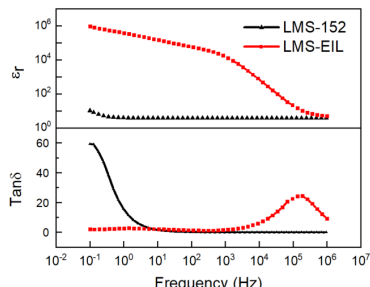


**Figure 10:** Dielectric properties of LMS-152 and LMS-EIL.

LMS-EIL has inhibiting effect on traditional Pt catalyst and thus condensation cure is used at room temperature due to less sensitivity towards inhibition from ILs. In Figure 2, there is an obvious increase in  $\epsilon_r$  for the elastomers incorporated with fillers. Additionally,  $\epsilon_r$  increases to 3.43 and 22.3, respectively, for the elastomers incorporated with 10 phr of LMS-152 or LMS-EIL, meaning it is more efficient to modify elastomer with grafted ILs, as expected. For the elastomer incorporated with LMS-EIL, a significant increase in  $\epsilon_r$  at low frequency is observed with increased LMS-EIL content.

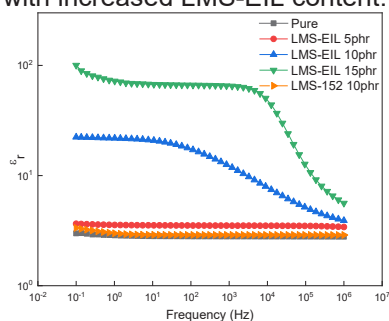


**Figure 2:** Relative permittivity ( $\epsilon_r$ ) of elastomer with different amounts of LMS-EIL.

The mechanical properties of elastomers are evaluated by tensile testing. In Table 1, it can be seen that the elastomer tends to be softer (i.e. lower Y) with increasing amount of LMS-EIL, indicating LMS-EIL functions both as high dielectric permittivity filler and as softening oil. Compared to the elastomer incorporated with 10 phr LMS-152, the corresponding LMS-EIL elastomer shows a

slightly higher Y due to the inherent inflexibility of the ILs. In addition, the elastomer with 10 phr LMS-EIL exhibits the highest tensile strain.

**Table 3:** Mechanical properties of the elastomers with different amounts of LMS-EIL.

Sample	Y <sub>1-10%strain</sub> (MPa)	Tensile strain (%)
Pure	0.88±0.04	236±5
LMS-152 10phr	0.76±0.02	240±24
LMS-EIL 5phr	0.84±0.09	281±8
LMS-EIL 10phr	0.78±0.01	321±11
LMS-EIL 15phr	0.73±0.02	230±3

Figure 3 presents the relative capacitance change ( $\Delta C/C_0$ ) of the sensors. Sensitivity is defined as  $S = (\partial(\Delta C/C_0))/\partial P$  where P is the pressure. The sensor with 10 phr LMS-EIL has the highest sensitivity in the pressure range of 0 to 7.5 kPa (46 times higher than LMS-152). However, the elastomer with 15phr LMS-EIL shows poor linearity in data ( $R^2=0.67$ ). This indicates that the sensor with 10 phr LMS-EIL constitutes the best sensor.

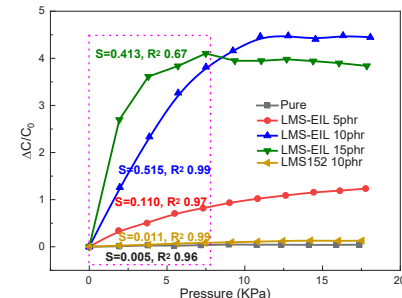


**Figure 3:** Relative change in sensors' capacitance incorporated with different amounts LMS-EIL.

## Conclusions

A simplistic approach to creating sensitive flexible pressure sensors has been developed through use of a novel soft filler, namely ILs grafted chloropropyl-functional silicone oil (LMS-EIL). The elastomers become increasingly softer and show higher permittivity as more LME-EIL is added. The elastomer with 10 phr LMS-EIL has the best dielectric and mechanical properties and exhibits the highest response to an applied pressure.

## Acknowledgements

This work is supported by the Department of Chemical and Biochemical Engineering, DTU, and Institute of Process Engineering, CAS.

## References

1. Li C, Pan L, et al. Journal of Materials Chemistry C, 2017, 5(45): 11892-11900.
2. Ma L, Shuai X, et al. Journal of Materials Chemistry C, 2018, 6(48): 13232-13240.
3. Nie B, Li X, et al. ACS applied materials & interfaces, 2017, 9(46): 40681-40689.
4. Liu M, Yu L, et al. International Journal of Smart and Nano Materials, 2020, 11(1): 11-23.

# Coating with inherent sensing functionality based on dielectric elastomer

(February 2018- March 2021)



## Contribution to the UN Sustainable Development Goals

Attachment of biofouling to the surfaces of ships, offshore wind farms, and other submerged marine surfaces presents serious economic and ecological problems. Hence, there is need to develop technology which will be beneficial for both marine economy and environment. An environmentally friendly antifouling technology based on silicone coatings is investigated. The coating will involve sensors and actuators and is anticipated to minimize high costs of cleaning damaged surfaces, fuel consumption, use of toxic materials, waste and pollutants which are currently being generated as direct and indirect consequence of biofouling.



**Sara  
Krpovic**

sarakr@kt.dtu.dk

**Supervisor:** Anne  
Ladegaard Skov, Kim  
Dam-Johansen

## Abstract

Dielectric elastomers (DEs) are micrometer thin, soft transducers that can be used as actuators, generators and sensors, due to their ability to deform under mechanical or electrical stimulation. When a substrate-bonded silicone dielectric elastomer is subjected to high voltage, electro-mechanical instabilities can be formed at the surface of the DE. In this work, this active deformation of DE surface is used for sensing.

## Introduction

Biofouling accumulation is a natural process of attachment of biological organisms on synthetic surfaces, which are exposed to the aqueous environment.<sup>1</sup> Massive fouling attachment on the surface of the ships, vessels, and different sea-platforms, presents serious economic and ecological problem for marine industry.<sup>2</sup> High fuel consumption, transport delays, frequent cleaning of marine surfaces, use of toxic ingredients in antifouling coatings, green-house gas emissions, extinction of certain biological species and unintentional transport of biological species from one place to another are some of the main concerns caused by biofouling accumulation. These concerns led to development of ecologically and economically friendly antifouling technologies. Newest antifouling technologies that are proposed and proof of concept demonstrated, include use of dielectric elastomers, where electromechanical deformation of the DE is employed to prevent and detach biofouling.<sup>2-4</sup>

Continuous improvement of current antifouling technologies and development of new antifouling technologies that are based on prevention and detachment of fouling is performed. However, the detection of biofouling on the synthetic surfaces exposed to the aqueous environment, is still visual only. Hence, it is of great interest to add the

capability of measuring the efficiency of DE-based antifouling.

## Objectives

When a substrate-bonded DE is subjected to high voltage, electro-mechanical instabilities in form of creases, wrinkles and craters can be formed at the surface of the DE.<sup>2-5</sup> It has been demonstrated that electromechanical instabilities can be used for prevention and detachment of biofouling from the surface of the soft-dielectric elastomer. The underlying idea for this project is that the deformation in the form of creases in the silicone could be also used for detection of biofouling and not only detachment. Therefore, the objective of the PhD project is to fabricate a sensor based on DE, which actively and effectively detects and detaches biofouling from the synthetic surface exposed to the aqueous environment.

## Experimental

A sensor is made of commercially available platinum catalyzed two-part addition curing polydimethylsiloxane (PDMS) (Ecoflex 00-30, Smooth-on) which was used as dielectric material, coated on a 69 µm Kapton polyimide tape that is bonded on to a copper plate. Copper plate acts as an electrode. The silicone film is immersed in a transparent conductive solution (3.5 wt% NaCl

solution) which acts as second electrode. Concentration of salt in the natural sea water is approximately 3.5 wt%. Small hollow cylinder made of poly(methyl metacrylate), which was glued to the top silicone surface, is used as pool for conductive solution (Figure 1)

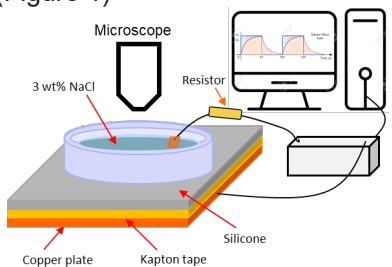


**Figure 1.** Schematic illustration of the fabricated sensor connected and measurement setup. The copper plate serves as electrode and is covered with Kapton polyimide tape, and coated with Ecoflex 00-30 silicone. Conductive solution (3.5 wt% NaCl) in poly(methyl metacrylate) pool, on the top of the silicone layer acts as second electrode.

The sensor, which acts as a capacitor was connected in series with a  $50 \text{ M}\Omega$  resistor. This formed a RC circuit which was connected to high voltage power supply. A square wave voltage was applied to the RC circuit and the capacitor charges and discharges with the voltage applied. Therefore, capacitance changes in the sensor are measured as a function of applied voltage, and the threshold voltage at which creases occur when there is an increase of capacitance is identified.<sup>6</sup>

## Results and Discussion

Capacitance as a function of voltage of sensor with approximately 47  $\mu\text{m}$  thick DE (Ecoflex 30) is presented in Figure 2.

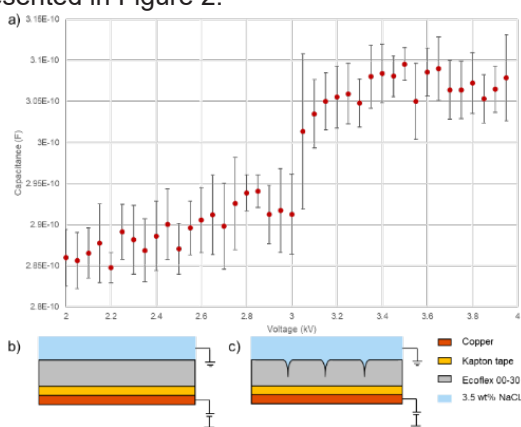


**Figure 2.** a) Capacitance as a function of applied voltage of the sensor with creasing voltage at 3.05kV; b) Schematic illustration of the sensor with the DE in flat (undeformed) state; c) Schematic illustration of the sensor with electro-mechanical instabilities (creases) on the top surface of the DE.

Onset voltage is detected as voltage at which electro-mechanical instabilities occur, and there is change of the capacitance. In Figure 2a) it can be

seen that creasing voltage for the sensor with the thickness of the DE of approximately 47  $\mu\text{m}$ , the onset voltage is 3.05 kV. Since the membrane is bonded to a rigid substrate, and since elastomers are incompressible, voltages below the creasing threshold create no deformation in the membrane (see Figure 2b)), and thus no significant change in capacitance is recorded. However, when a certain value of voltage is reached, electro-mechanical instabilities appear at the surface of the silicone in form of creases (see Figure 2c)). This formation of creases increases the capacitance of the device.<sup>6</sup>

## Outlook

Future electrical measurements will be performed with attached biofouling material to the surface of the silicone elastomer. The threshold voltage necessary to develop the electromechanical instabilities on the surface of the silicone will increase. Measuring the capacitance versus voltage enables identification of the voltage threshold, and thereby monitoring of biofouling is realized.

## Acknowledgements

This work is part of the Danish Polymer Centre (DPC) and The Hempel Foundation Coatings Science and Technology Centre (CoaST) at the Department of Chemical and Biochemical Engineering at Technical University of Denmark. Financial support from the Hempel Foundation to CoaST.

## References

- Nurioglu, A. G.; Esteves, A. C. C.; De With, G. Non-Toxic, Non-Biocide-Release Antifouling Coatings Based on Molecular Structure Design for Marine Applications. *J. Mater. Chem. B* **2015**, 3 (32), 6547–6570.
- Shivapooja, P.; Wang, Q.; Szott, L. M.; Orihuela, B.; Rittschof, D.; Zhao, X.; López, G. P. Dynamic Surface Deformation of Silicone Elastomers for Management of Marine Biofouling: Laboratory and Field Studies Using Pneumatic Actuation. *Biofouling* **2015**, 31 (3), 265–274.
- Shivapooja, P.; Wang, Q.; Orihuela, B.; Rittschof, D.; López, G. P.; Zhao, X. Bioinspired Surfaces with Dynamic Topography for Active Control of Biofouling. *Adv. Mater.* **2013**, 25 (10), 1430–1434.
- Zhao, X.; Wang, Q. Harnessing Large Deformation and Instabilities of Soft Dielectrics: Theory, Experiment, and Application. *Appl. Phys. Rev.* **2014**, 1 (2).
- Wang, Q.; Zhang, L.; Zhao, X. Creasing to Cratering Instability in Polymers under Ultrahigh Electric Fields. *Phys. Rev. Lett.* **2011**, 106 (11), 1–4.
- Krpovic, S.; Dam-Johansen, K.; Ladegaard Skov, A.; Rosset, S.; Anderson, I. A. Active Deformation of Dielectric Elastomer for Detection of Biofouling. *2020*, 67.

# Role of Additives on Corrosion Protection of Metals by Organic Coatings

(February 2019- January 2022)



## Contribution to the UN Sustainable Development Goals

This project aims to investigate the role of environmentally friendly inhibitive pigments in the anti-corrosive performance of organic coatings. The introduction of organic inhibitive pigments that can be extracted from natural resources or recovered during recycling processes can provide the coating industry with non-toxic, renewable, low cost, and efficient raw materials. Thus, the anti-corrosive coatings production would be able to increase resource efficiency and promote sustainable solutions.



**Zoi  
Lamprakou**  
[zoila@kt.dtu.dk](mailto:zoila@kt.dtu.dk)

**Supervisor:**  
Kim Dam-Johansen  
Huichao Bi  
Claus Erik Weinell

### Abstract

The use of organic inhibitive pigments for anti-corrosive coatings that can be extracted from natural resources has driven researchers attention over the past years. Tannins are natural, non-toxic, polyphenols present in various plants. Tannate complexes have been reported to be a great corrosion inhibitive pigments. In this work, tannate was obtained from tea extraction in the form of calcium tannate. Pigment composition was verified by Fourier transform infrared spectroscopy (FTIR). Epoxy coating containing calcium tannate was formulated and the corrosion performance was tested in a salt spray chamber and evaluated using electrochemical techniques. The performance of calcium tannate was compared with commercially available inhibitive pigments.

### Introduction

Organic coatings are employed as an effective way to protect metal structures from corrosion due to their capacity to act as a physical barrier between the metal surface and the corrosive environment [1-2]. However, polymeric films are permeable to corrosive species such as oxygen and water in practice [2]. The protectiveness of organic coatings against corrosion is enhanced by the introduction of pigments. Pigments can be classified into different categories according to their protective mechanism: as barrier, sacrificial and inhibitive pigments. The anticorrosive mechanism of inhibitive coatings (coatings embedded with inhibitive pigments) relies on passivation of the metal substrate by the formation of insoluble metallic complexes which work as barriers to aggressive species [3].

Zinc chromate had been a successful inhibitive pigment for many years but the high toxicity of chromate compounds led the industry to adopt alternative solutions [4]. Zinc phosphate is considered the most important alternative to chromate pigments [4]. However, the inhibitive efficiency of zinc phosphate is significantly lower. Tannins are polyphenolic compounds and they are present in high concentrations in several plants [5],

seeds and leaves like cocoa and tea. Tannins phenolic character makes them a potential source of products in the chemical industry [6]. In the corrosion field, tannins have been used extensively in boiler feed-water and water cooling systems to protect the internal parts of the equipment [7]. Tannins act as corrosion inhibitors due to the physical or chemical adsorption [8].

### Specific Objectives

The main objective of this project is to develop a novel inhibitive pigment for a more sustainable anticorrosive coating design. To do this, tannins extracted from natural resources will be introduced into organic coatings. The anticorrosive performance of the coatings containing the extracted tannins and the coatings containing commercial pigments will be tested and evaluated under marine conditions.

### Results and Discussion

The FTIR spectra of the tannin and calcium tannate (synthetic and obtained from tea) are illustrated in Figure 1. The broad bands in the  $3300\text{ cm}^{-1}$  indicate the presence of a phenolic hydroxyl group and the bands at  $1020\text{ cm}^{-1}$  exhibit a characteristic bending

vibration of O-C in a phenolic hydroxyl group. Peaks at  $1620\text{ cm}^{-1}$  and  $1445\text{ cm}^{-1}$  are characteristics of the C=C bond in aromatic rings. It can be observed that in case of both calcium tannates the peaks are broader because of the amorphous nature of the tannate complexes.

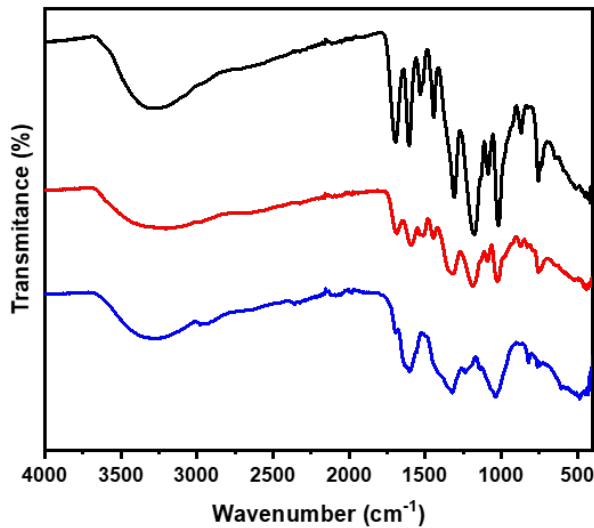


**Figure 11:** FTIR spectra of tannin (black line), synthetic calcium tannate (red line) and calcium tannate obtained from tea extraction (blue line).

The synthetic calcium tannate was introduced into an epoxy coating formulation (CTE). The anti-corrosive performance was compared with reference coatings (1. Unpigmented epoxy (UE), 2. Epoxy with zinc phosphate (ZPE), and 3. Epoxy with calcium phosphate (CPE)).

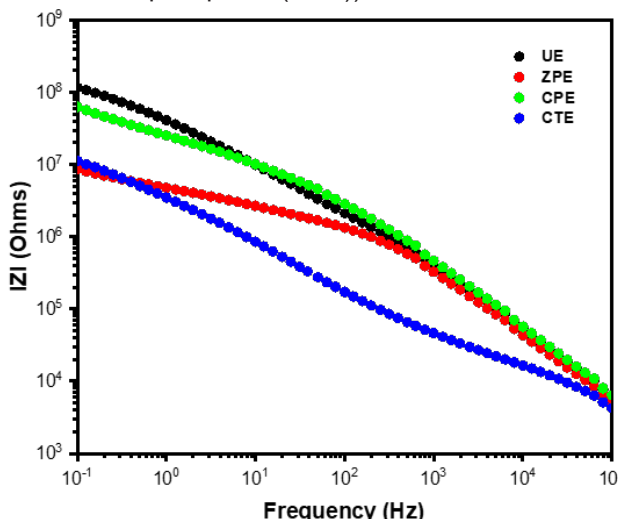


**Figure 12:** Bode plots for initial exposure conditions of the coated panels.

Figure 2 shows the Bode plots for the four formulations after their exposure in the salt spray

chamber for 24h. The coating impedance of calcium tannate is similar ( $10^7\Omega$ ) to the commercial zinc phosphate and only one order of magnitude lower than calcium phosphate coating ( $10^8\Omega$ ).

## Conclusions

Calcium tannate has been successfully obtained from natural resources (tea). Preliminary results showed that calcium tannate performs similarly to the commercial zinc phosphate pigment during the coatings initial exposure time.

## Acknowledgements

Financial support from the Hempel Foundation to CoaST (The Hempel Foundation Coatings Science and Technology Centre).

## References

- Y. González-García, S. González, and R. M. Souto, "Electrochemical and structural properties of a polyurethane coating on steel substrates for corrosion protection," *Corros. Sci.*, vol. 49, no. 9, pp. 3514–3526, 2007.
- G. M. Ferrari and J. H. W. D. E. Wit, "Van westing," vol. 36, no. 6, pp. 957–977, 1994.
- P. A. Sørensen, S. Kiil, K. Dam-Johansen, and C. E. Weinell, "Anticorrosive coatings: A review," *J. Coatings Technol. Res.*, vol. 6, no. 2, pp. 135–176, 2009.
- A. C. Bastos, M. G. Ferreira, and A. M. Simões, "Corrosion inhibition by chromate and phosphate extracts for iron substrates studied by EIS and SVET," *Corros. Sci.*, vol. 48, no. 6, pp. 1500–1512, 2006.
- E. Onem, G. Gulumser, S. Akay, and O. Yesil-celiktas, "Optimization of tannin isolation from acorn and application in leather processing," *Ind. Crop. Prod.*, vol. 53, pp. 16–22, 2014.
- P. L. De Hoyos-martínez, J. Merle, J. Labidi, and F. Charrier, "Tannins extraction : A key point for their valorization and cleaner production," *J. Clean. Prod.*, vol. 206, pp. 1138–1155, 2019.
- T. Substances, "Tannin Substances," vol. 14, no. 6, 2000.
- S. Martinez and I. Štern, "Inhibitory mechanism of low-carbon steel corrosion by mimosa tannin in sulphuric acid solutions," *J. Appl. Electrochem.*, vol. 31, no. 9, pp. 973–978, 2001.

# Quantification of internal stress in thermoset coatings

(February 2019-February 2022)



## Contribution to the UN Sustainable Development Goals

Thermoset coatings are widely used as anticorrosive coatings in harsh environment. However, curing induced internal stress within coatings can accelerate coatings degradation in service environment. If the influence of coating formulation and curing conditions on curing induced internal stress can be revealed, novel coating formulation and curing procedure can be designed to reduce the internal stress. This can help to produce coatings with prolonged service lifetime giving extended protection of the assets and to save raw materials.



**Qiong  
Li**

qioli@kt.dtu.dk

**Supervisor:**  
Søren Kjil  
Claus Erik Weinell

## Abstract

Internal stress can develop within thermoset coatings during the curing process and in some cases, internal stress can be large enough to provoke cracking and coatings barrier performance is severely deteriorated. This project will focus on constructing reliable methods to quantify curing induced internal stress with a cantilever deflection method, exploring the possibility of monitoring localized internal stress with embedded Fiber Bragg Grating sensors (FBGs) and simulation method. The influence of coating formulation, curing conditions and substrate geometry, including flat substrates and substrates with right angle corner, will also be investigated.

## Introduction

Thermoset polymer coatings are widely used as anticorrosive coatings to maintain the service performance of metallic structures in harsh environment due to their excellent mechanical strength and thermal/chemical stability. However, during the curing process, solvent evaporation and crosslinking reactions between binders and curing agents can lead to coating shrinkage and the shrinkage is hindered by strong adhesion at coating-substrate interface, thus internal stress is produced within the coatings [1].

Usually, anticorrosive coatings contain pigments and other additives, and the produced internal stress may concentrate around these pigments and additives at localized areas. The concentrated stress could be surprisingly large and in many cases, it can exceed the coatings fracture strength and provoke crack initiation and propagation [2]. The unexpected development of internal stress and cracks can deteriorate the coatings anticorrosive performance significantly. The barrier property loss within coatings and adhesion property loss at coating-substrate interface may promote and accelerate coatings degradation behavior in service environment, such as coatings delamination, disbonding and cracking [3]. Cracks within Novolac epoxy/cycloaliphatic amine coatings after cured at room temperature for 24 hours were observed with

optical microscopy in Figure 1. The cracking and disbonding behavior of coatings can leave the metallic devices unprotected and promote localized corrosion, which can result in sudden fracture of structures leading to catastrophic accidents [4, 5]. Researchers have tried to use the "deflection method" to evaluate the influence of binder/hardener type, coating thickness, solvent content, curing temperature/relative humidity variation, and substrate geometry on curing induced internal stress. However, this method cannot measure localized internal stress, which is directly related to cracks formation in coatings, and localized internal stress quantification remains challenging to be achieved [1-3].

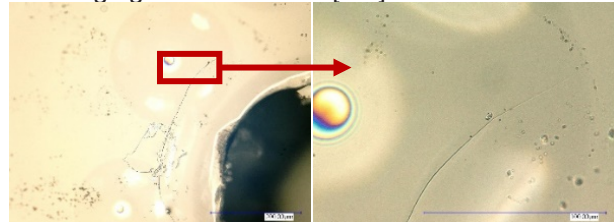


**Figure 1:** Optical micrograph of cracks in Novolac epoxy/cycloaliphatic amine coatings (500 µm wet film thickness, cured for 24 hours at 23±0.5 °C).

## Specific objectives

The objectives of this project include:

- To build up a reliable internal stress measurement technique
- To reveal the influence of coatings formulation, curing conditions and substrate conditions on the development and magnitude distribution of internal stress within coatings.
- To investigate the relationship between internal stress development and cracks initiation and propagation behavior within coatings.

## Methodology

The average curing induced internal stress are monitored with a cantilever beam deflection method. A schematic diagram of the cantilever set-up is given in Figure 2. A climate chamber is used to control the curing temperature and humidity, and the beam deflection distance is monitored with laser position sensor (Keyence, IL 1000).

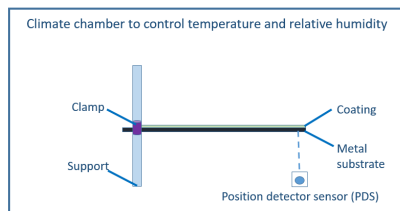


**Figure 2:** Schematic diagram of internal stress measurement set-up with cantilever beam method.

To clarify the influence of coating curing process on coating mechanical property evolution and internal stress development, ATR-FTIR, gravimetric method, and advanced rheometer are used to investigate coating curing kinetics, solvent evaporation rate, and modulus evolution, respectively.

The influence of curing induced internal stress and micro-cracks resulting from localized internal stress on coatings barrier properties will be investigated with Electrochemical Impedance Spectroscopy (EIS).

## Progress and future work

Curing-induced internal stress was monitored with deflection method and the result is shown if Figure 3.

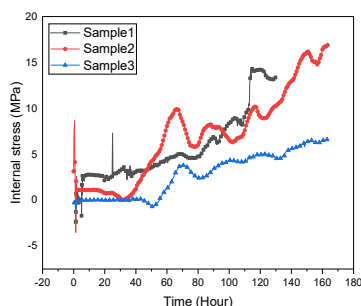


**Figure 3:** Internal stress in solvent-free epoxy/amine coatings with stoichiometric ratio of 100% cured at  $23\pm0.5$  °C,  $35\pm1$  % RH.

It can be found from Figure 3 that curing-induced stress increased with curing time and exhibited decrease at some point, it is suggested that thus decrease is resulted from stress relaxation by stimulate cracks initiation and propagation within coatings[2, 5].

The influence of initial solvent content on coating conversion was studied with ATR-FTIR and the result is given in Figure 4. It exhibited that before vitrification, solvent-containing sample showed lower conversion. After vitrification, solvent-containing sample exhibited higher conversion since trapped solvent can enhance mobility of molecules after vitrification.

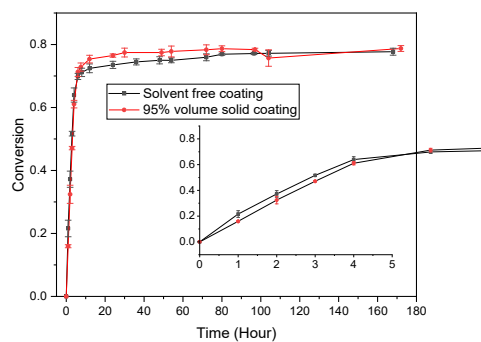


**Figure 4:** Epoxy conversion of bisphenol A and MXDA coatings with stoichiometric ratio of 100% cured at  $23\pm0.5$  °C,  $35\pm1$  % RH.

Future work will be focused on relating modulus with DMA test, conversion with ATR-FTIR and DSC, and internal stress measurement method to build a method to predict curing-induced internal stress.

## Acknowledgement

Financial support from the Hempel Foundation to CoaST (The Hempel Foundation Coating Science and Technology Center).

## References

1. D.Y. Perera, Paint and Coating Testing Manual: 15th. Edition of the Gardner-Sward Handbook, MNL 17-2ND-EB, Koleske, J., Ed., ASTM International, West Conshohocken, PA, 2012, p.655-672.
2. L.F. Francis, A.V. McCormick, D.M. Vaessen, J.A. Payne. Journal of Materials Science, 37(2002) 4717-4731.
3. D.Y. Perera, Progress in Organic Coatings, 28 (1996) 21-23.
4. F. Awaja, S. Zhang, M. Tripathi, A. Nikiforov, N. Pugno, Progress in Materials Science, 83 (2006) 536-573.
5. M.H. Nazir, Z.A. Khan, A. Saeed, K. Stokes, Corrosion, 72(4) 2016, 500-517.
6. P.P. Parlevliet, H.E.N. Bersee, A. Beukers, Polymer Testing, 29(2010) 291-301.

# Investigation of Anti-corrosive Coatings Degradation Mechanism – The Use of Non-destructive Evaluation Techniques

(December 2019- November 2022)

12 RESPONSIBLE CONSUMPTION AND PRODUCTION



## Contribution to the UN Sustainable Development Goals

Efficient and non-destructive coating performance assessments will provide a tool for a faster evaluation of new coating formulation performances. Furthermore, understanding of degradation mechanisms can help to predict the coating lifetime and better determine the maintenance time of the coating structures in the real operation field. This contributes to the reduction of natural resource consumption and volatile organic compounds emission during production and application.



Shu  
Li

Shuli@kt.dtu.dk

**Supervisor:** Kim Dam-Johansen, Huichao Bi, Claus Erik Weinell

## Abstract

Zinc rich epoxy coating is widely used to protect steel constructions e.g. ships in the marine environment. Electrochemical impedance spectroscopy (EIS) is used to study the degradation of zinc rich epoxy coating. Both physical coating degradation as water uptake (permeability changes) and electrochemical processes as galvanic protection of steel by zinc oxidation, and iron corrosion in the steel substrate is monitored by fitting of a suitable Equivalent Electrical Circuit (EEC) model to the impedance data.

## Introduction

The main protective mechanism of zinc rich primer is through sacrificial protection. Zinc metal has a lower standard reduction potential compared to Iron, this makes zinc acting as a sacrificial metal which oxidizes in the presence of aggressive species (e.g. oxygen, water) instead of iron[1]. The EIS measurement is performed through three-electrode configuration, where an alternating current is applied to the sample in different frequency and measuring the sample's responds to this signal in form of impedance and phase shift. This technique is relatively non-destructive and can be used in early coating degradation assessment due to the change in the impedance, phase shift and corrosion potential of a coated steel substrate as exposure time increases. The most challenging part using EIS for complex systems as coated metal is fitting of a suitable EEC model which should provide reasonable physical and chemical information of the studied coating system.

The EEC models used in this work to describe the degradation of zinc rich primer exposure to salts spray chamber is given in Figure1. A simplified sketch of zinc rich primer degradation processes is illustrated in Figure 2. Herein, the intact coating without penetration of seawater (a), penetration of

seawater in the coating film and initiation of cathodic protection (b), and corrosion of iron (c).

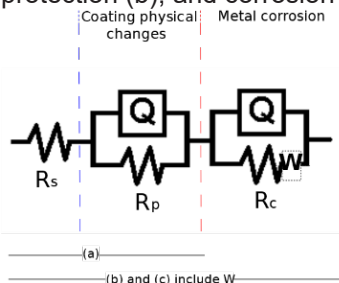


**Figure 13:** EEC models used to fit the impedance data of coated steel with zinc rich primer: (a)  $R(QR)$ , (b)  $R(QR)(QR)$  and (c)  $R(QR)(QRW)$ . Circuit elements: Resistance ( $R$ ), Constant Phase Element ( $Q$ ), and Warburg diffusion resistance ( $W$ ).

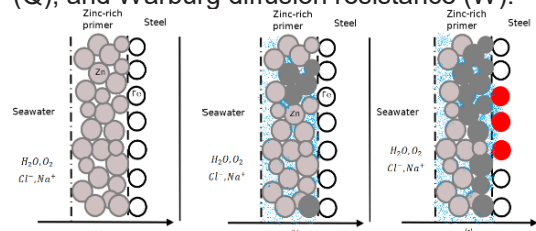


**Figure 2:** Simplified mechanisms of zinc-rich epoxy coating degradation processes exposed to artificial seawater: (a) an intact coating film, (b) zinc galvanic protection (c) iron corrosion, adapted from [1].

## Methodology

Commercial zinc rich epoxy primer coated on steel panels with an average dry film thickness of  $50\mu\text{m}$  is exposed to salt spray (ISO 9227) chamber with 5 wt.% of NaCl at  $35^\circ\text{C}$ . Three replications have been made and the samples are evaluated with EIS measurements at different exposure time to monitor the degradation process of the applied primer.

## Results and Discussion

The change of open circuit potential (OCP) of each exposed sample is shown in Figure 3. It is seen that the OCP development has the same trend which means the results are reproducible. From the OCP curve, the degradation of zinc primer can roughly be divided into Period I-Activation, Period II-Cathodic protection and Period III- Iron (slightly Zn) corrosion. The activation period is relatively fast indicating the initial penetration process of salt ions, water and oxygen occur in the first 48 hours of exposure. After Phase I, the OCP is stable in a short period which can be attributed to saturation of the coating film. The penetrated electrochemical active species activates zinc in the coating and corrodes and thereby protects the Iron (Phase II). Phase III is the period where cathodic protection is almost faded out (OCP above  $-0.78\text{ V}(vs.\text{SCE})$ [2]) while corrosion of Iron becoming more significant. This can be observed as increasing OCP value, where at the end of the exposure time the OCP value reaches about  $-0.65\text{V}(vs.\text{SCE})$ , which has been reported[3] as OCP of steel. At this point, cathodic protection is exhausted and pure barrier protection is existing.

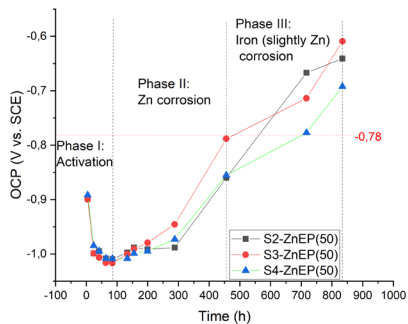


**Figure 3:** OCP development of three replications for zinc rich epoxy ( $50\mu\text{m}$ ) coated steel exposed to the salt spray.

The changes in coating resistance and water uptake in the primer are shown in Figure 4. The water uptake occurs primarily during the first 48 hours which is consistent with the activation Phase I on OCP curve (Figure 3), afterwards the water uptake in the coating film remains almost a constant level as the film is saturated. The coating resistance is decreasing rapidly during the first 48 hours and then it increases slightly around 450 hours due to

Zn corrosion products which are relatively dense. After 450 hours coating resistance remains in a relatively constant level also indicating that the iron corrosion in the steel substrate becomes more dominating, and the rust is more porous which will not contribute to the coating resistance. This is identified as Period III in Figure 3.

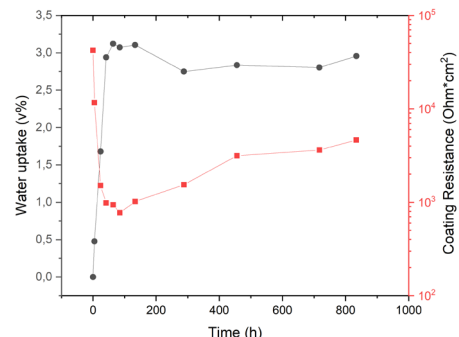


**Figure 4:** Water uptake and coating resistance of zinc rich primer are estimated by fitting EEC models to the EIS spectra.

## Conclusion

EIS can be used as an efficient technique to evaluate the protective properties of anti-corrosive coatings. Fitting of impedance spectra with suitable EEC models over time combined with OCP development graph can illustrate the period of degradation processes of zinc rich primer.

## Future work

Two-layer coating systems and waterborne coating systems will be investigated with EIS measurements in both laboratory and real field test in Hundested to follow the coating degradation processes. Additional non-destructive techniques may also be applied. A mathematical model for coating degradation processes is also in purpose to be developed base on the achieved experimental data.

## Acknowledgement

Financial support from the Hempel Foundation to CoaST (The Hempel Foundation Coatings Science and Technology Centre) and the Sino-Danish Center for Education and Research.

## References

1. P. Sørensen, S. Kill, K. Dam-Johansen, C.E. Weinell, Coatings Technology and Research 6(2009) 135-176.
2. N.Hammouda, H. Chadli, G. Guillemot, K.Belmokre, Advanced in Chemical Engineering and Science 01(2011) 51-60
3. M. Narozny, K. Zakowski, K. Darowichi, Construction and Building Materials 181(2018) 721-726.

# Dispersion principles of coatings production

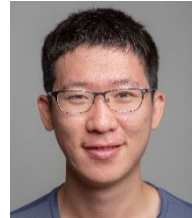
(Sep 2019- Aug 2022)

12 RESPONSIBLE CONSUMPTION AND PRODUCTION



## Contribution to the UN Sustainable Development Goals

The understanding of the change of the full particle size distribution during the dispersion process can help to reveal the process, understand the influence of the rotation speed, temperature, physical properties of pigment, solid concentration and the dispersing time. Based on the results, the best dispersion parameters can be selected to reduce the amount of pigment or energy needed for the process. In addition, with the help of on-line quality control methods, the time needed for the quality control and correction of the products will be greatly reduced, which means a higher production efficiency.



**Shicong  
Luo**

shiluo@kt.dtu.dk

**Supervisor:** Søren Kjil,  
Claus Erik Weinell, Kim  
Dam-Johansen

## Abstract

Traditional coatings production procedure is currently facing massive challenges, including the increasing price of the raw materials, and a large amount of energy is wasted during the dispersion process. Therefore, it is important to fully understand the current dispersion process. The purpose of this PhD study is to analyze the feasibility of different on-line quality control methods and evaluate the advantages and disadvantages of these instruments. At the same time, the dispersing process of pigments in different dispersion instruments will be studied and mathematical models will be established to describe the process. Besides, the development of a dispersion instruments special design for coatings is also desired.

## Introduction

The new paradigm of in-line continuous or semi-continuous production processes represent massive opportunities when facing the increasing challenges in the current coatings industry. For such an improvement from the current production process, two main tasks need to be considered: one is semi-continuous or continuous manufacturing equipment, and the other is the on-line quality control instrument.

The present project focuses on the performance of different dispersion instruments in the coatings industry. The dispersion mechanism of different instruments will be understood to reach a higher dispersion efficiency and develop a more sustainable process. Mathematical models will be developed to describe the full particle size distribution change during dispersion processes. Besides, a special design dispersion instrument for the coatings product will be discussed and developed to improve the manufacturing process.

On-line quality control instruments of evaluating the essential properties of coatings, such as the particle size distribution (PSD) and the coating rheology, are investigated in the project. The PSD of coatings is measured by the MasterSizer (laser diffraction), LiteSizer500 (dynamic light scattering (DLS)), Particletrack g400 (focus beam reflection

measurement (FBRM)), and the Hegman gauge. The viscosity profiles of coatings are characterized by the capillary rheometer, advanced rheometer and the Stormer viscometer.

## Objectives of the project

- Develop theoretical models to reveal the dispersion process within the high-speed disperser and pearl mill.
- Investigate new and fast on-line quality control methods of evaluating the essential properties of coatings, such as the degree of dispersion, and the coating rheology.
- Simulate and analyze different in-line dispersing instruments by simulating software
- To design, or construct a new dispersion instrument special for coating products.

## Results and Discussion

Methods of evaluating the coating viscosity property was first investigated in this project. Based on the literature study, it was found that several methods could be considered as a possible on-line quality control instrument for coatings production, the viscosity was measured by the advance rheometer, Stormer viscometer, and a specific capillary rheometer. 16 different coating samples were prepared to investigate the performance of the

instrument. Figure 1 presents a comparison among these three investigated methods.

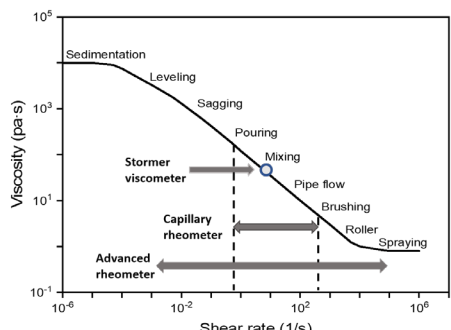


**Figure 1:** Shear rate analysis range for the advanced rheometer, Stormer viscometer, and capillary rheometer.

Later experiments move to investigate the suitable method to determine the PSD of coatings. Currently, the particle size of coatings is always measured by the fineness of grind gauge, which only gives the largest particle size. However, the full particle size distribution of coatings influence several parameters of coatings, such as colour strength and viscosity. Therefore, methods to analysis full PSD of coatings were investigated. The investigated methods are given in table below.

**Table 4:** PSD measurements and their analytical range

Methods	Analytical range	Reference
Laser diffraction	0.01 to 3500 $\mu\text{m}$	[1]
Dynamic light scattering	0.3 nm – 10 $\mu\text{m}$	[2]
Focus bean reflection measurement	1-1000 $\mu\text{m}$	[3]
SEM	0.1 nm-1000 $\mu\text{m}$	[4].

The laser diffraction is selected as the method to determine the PSD of coatings product in this project due to its broad analytical range and rapid measurement. A detailed sensitivity analysis was done to determine how the operation parameters influenced the measured PSD results. It was found that the obscuration value, the input refractive index value of the pigment and solvents, and the selection of the pigment shapes has certain influence on the measure PSD results when using the laser diffraction method.

## Conclusions

The experiment analyzed whether the capillary rheometer could be used in the industrial production

of coatings. Compared with the off-line measurements, the on-line capillary rheometer could be a better choice for industrial coatings production process due to its characteristics, such as efficiency, real-time analysis and reduction of product correction time. However, certain limitations existed for current on-line quality control methods that needed to be considered and resolved.

The possible analytical instruments to determine the full PSD of coatings during the dispersion process was also determined. Four instruments were investigated. Limitations were found for all instruments (i.e. obscuration limit or unable to determine the PSD of wet coatings). As a preliminary conclusion, it is decided to use the laser diffraction to determine the PSD of wet coating samples and use SEM to determine the PSD of a dry coating film.

## Future experiments

Future experiment will first try to conduct SEM method to determine the PSD of coatings. A free film of prepared coating sample will be made and the PSD will be measured both from the surface of the free film and also the cross section. Matlab code or Phyton code for the image analysis will be learned to help the PSD measurement. The PSD results from the SEM analysis will be compared with the result from the laser diffraction method.

After compared the SEM results with the laser diffraction results, the particle size change during the dispersion process will be investigated. Possible investigated instruments will include high-speed disk disperser, pearl mill and ultrasound disperser. Mathematical models will be established to describe the particle size change during the dispersion process based on the experimental results. The model will correlate the change in particle size during dispersion with the dispersion time, rotation speed, and physical properties of the pigment and solvent.

## Acknowledgement

Financial support from Hempel Foundation to CoaST (The Hempel Foundation Coating Science and Technology Centre).

## References

1. Eshel, G., Levy, G. J., Mingelgrin, U., Singer, M. J. Soil Science Society of America Journal 68.3 (2004): 736-743.
2. J. Panchal, J. Kotarek, E. Marszal, E. M. Topp, The AAPS journal, 16(3), 440-451.
3. V. Kumar, M. K. Taylor, A. Mehrotra, W. C. Stagner. Aaps Pharmscitech, 2013, 14(2): 523-530.
4. P. Linda, M. Bittelli, P. P. Rossi, Geoderma 135 (2006): 118-132.

# Kinetic of scaling formation

(January 2020- December 2022)



My contribution to the 12<sup>th</sup> UN Sustainable Development Goal “Responsible consumption and Production”

By shedding light on the kinetic of formation for various scaling agent, the amount of harmful chemical used in maintenance for oil and gas pipelines can be significantly reduced. By improving current prediction models for maintenance, the duration of production periods can be increased and frequency of shutdowns can be reduced, leading to a more sustainable production of our energy resources.



**Isaac  
Appelquist Løge**  
isacl@kt.dtu.dk

**Supervisor:** Phillip,  
Fosbøl, Søren Kjell

## Abstract

Scaling is defined as the deposition of mineral solids on surfaces in contact with water and is a problem seen across multiple industries for example in geothermal wells to oil and gas production. Scale formation in the equipment of the oil and gas industry poses a general challenge. Through gradual precipitation on the interior pipe, scaling is decreasing the internal diameter of the pipe and by time obstructing the flow of liquid through the pipe. This can create hazards downhole or result in a complete stop of production. Scales are also intimately linked with corrosion, and therefore there is a great need to understand why and where the scale is formed, in order to better prevent corrosion. Aside from the production problems caused by scaling, the process of scaling formation also poses a complex multistep process, where interdependent variables form an under-investigated parameter space.

## Introduction

Scaling has been traditionally seen as a problem of solubility, a thermodynamic property describing whether or not a mineral will be present in soluted or solid form in a liquid [1]. However, the path from dissolved ion to adhered surface scaling is of a significantly more complex nature, since multiple mechanisms play into the final scale formation [2]. As the answer to a kinetics problem can only be found in the lab, multiple experimental methods have emerged to describe the process to a complete extend [3-4]. Surface properties, temperature, flow velocity and brine composition are some, but not all, of the variables that currently are investigated, however, methods capable of a complete experimental in-situ investigation are scarce [5].

## Project objectives

The aim of this project is to develop a method to measure and characterize scaling formation, and corroborate the novel interplay at stake. The end goal is to measure FeCO<sub>3</sub> as it poses experimental challenges due to its high reactivity the oxygen in atmosphere. To validate the system BaSO<sub>4</sub> is chosen as a model system, where the relevant working conditions and methods of analysis are developed.

## Experimental setup and characterization methods

The experimental set up is designed to operate under relevant production conditions, and measure the scale formation ex-situ. Figure 1 shows the experimental set-up in its current form.

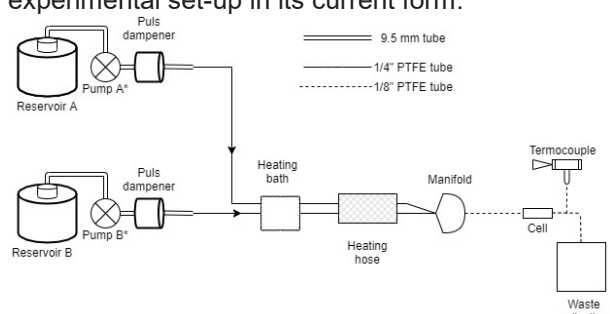


**Figure 14:** PI diagram of experimental set-up in current form

Temperature control, flow conditions and brine saturation has been validated through the scaling formation of BaSO<sub>4</sub>. To fully describe the scaling, a collaboration between multiple insitutes at DTU have been established. This collaboration enables different talent to come into play various and different methods to analyse the scale formation have been used:

- Effluent analysis (ICP)
- Surface roughness

- Flow characteristics (CFD)
- Scale visualization ( $\mu$ CT scanning)

Combining these methods new insights into the scale formation has been obtained.

### Results and discussion

Scale visualization has allowed for new mechanistic insight into scale formation, where the role of hydrodynamics both as a force for removal and as a delivery of unreacted ions for surface reactions to occur, has been elucidated.

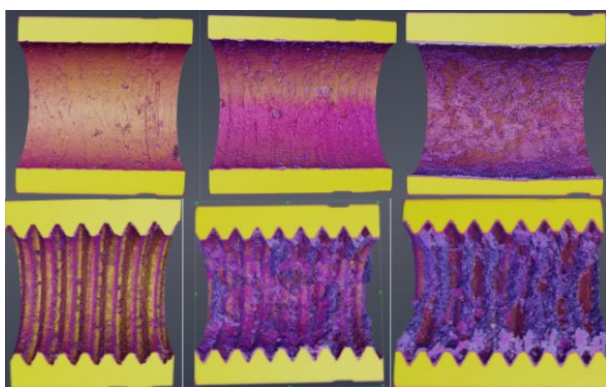


**Figure 15:**  $\text{BaSO}_4$  growth at various growth stages on a smooth and a threaded surface

Analysis of  $\mu$ CT tomographies showed a preferential growth, which was confirmed by CFD. The mechanism and position of the growth was found to be dependent the flow velocity, as higher flow created dead zones, where no new reactive material was supplied, and also increased the influx of material, creating a more kinetically hindered growth.

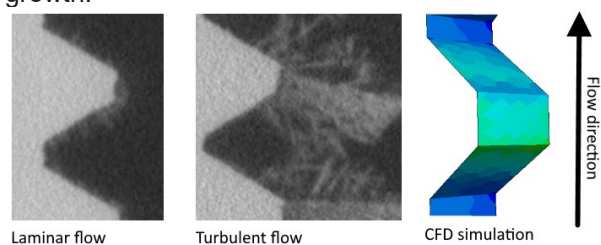


**Figure 16**  $\text{BaSO}_4$  growth on threaded surfaces.

### Conclusion and perspective

Based on the preliminary results from the validation tests, we have both developed an interdisciplinary way of scale analysis and shown that the set-up at its current status can operate under the relevant temperature, flow and brine conditions. The continued work of this set-up is a transition to an anoxic environment with a  $\text{CO}_2$  variable partial pressure.

### Acknowledgement

Heartfelt acknowledgements are extended to Povl Valdemar Andersen, who, by his dedication and hard work, made substantial contribution to this project. Furthermore, thanks are directed to Benaiah Anabaraonye for his guidance and structure, which concretized this project from idea to execution. The cornerstone of the projects financing comes from DHRTC, for which the authors are grateful. Many unnamed persons have contributed to the work performed, and they are not forgotten.

### References

1. A. W. Rudie and P. W. Hart, "Mineral scale management Part II. Fundamental chemistry," *Tappi Journal*, vol. 5, no. 7, pp. 17–23, 2006.
2. J. W. Mullin, *Crystallization*. Weinheim, Germany: Elsevier, jan 2001.
3. M. Barber and S. Heath, "A new Approach to Testing Scale Inhibitors in Mild Scaling Brines - Are Dynamic Scale Loop Tests Needed?," in SPE, 2019.
4. D. R. Gabe and F. C. Walsh, "The rotating cylinder electrode: a review of development," 1983
5. R. Barker, D. Burkle, T. Charpentier, H. Thompson, and A. Neville, "A review of iron carbonate ( $\text{FeCO}_3$ ) formation in the oil and gas industry," *Corrosion Science*, vol. 142, no. October, pp. 312–341, 2018

# Sustainable and Cost-Effective Routes for Production and Separation of Succinic Acid

(June 2018- May 2021)



## Contribution to the UN Sustainable Development Goals

This project aims to improve a biorefinery process to produce one of the most important products from biomass fermentation: succinic acid. Succinic acid is a biochemical building block used to produce more than 30 commercially valuable products; examples are bioplastics, pharmaceuticals, detergents and food additives. The broad applicability of succinic acid as a chemical building block can both reduce the use of petroleum and be a way to valorize industrial, agricultural and household waste as well as a way to dispose of numerous wastes.



**Enrico  
Mancini**

senrmini@kt.dtu.dk

### Supervisors:

Manuel Pinelo  
Seyed Soheil Mansouri  
Krist V. Gernaey

### Abstract

Succinic acid (SA) from biomass fermentation is already a commercial product, however the production costs are still high compared to succinic acid from petroleum and the technological readiness level is not fully developed. Furthermore, while the SA demand is increasing, the biomass-based SA production is far from large-scale bulk synthesis. Most relevant feed-stocks, pretreatments, fermentation and downstream techniques have been identified, and membranes emerge as a key technology in both the production (MBR) and separation of SA. To generate potential and realistic production processes, process simulation, superstructure optimization and lab laboratory experiments are under study.

### Introduction

Biorefinery is a promising concept that can contribute overcoming the petrol-era, especially with respect to sustainable fine chemical production, addressing at the same time several problems: the depletion of petroleum resources (with the associated consequences), human sustainability, waste management and political concerns. Production and separation of valuable products from biomass have indeed been successfully achieved and implemented at full scale [1]. However, the lack of cost-effective processes, especially in the downstream, is largely preventing biorefinery products to become economically competitive. Succinic acid from biomass fermentation has gained increasing interest since more than 30 commercially valuable products can be currently synthetized from it, including solvents and lubricants, synthetic resins and biodegradable polymers such as PBS and polyamides, cosmetics, food and pharmaceuticals [1]. Succinic acid has been selected from both the E.U. [2] and the U.S. department of energy [3], among the most important bio-building blocks in biorefinery. Several different technologies are used to produce SA, but standard optimal processes have not been identified yet. Nonetheless, we have identified potential optimal

units and working conditions for a cost-effective SA large-scale production [4].

### Objectives

Fermentation is a biotechnology from which many valuable bio-products can be obtained however, to economically compete with petrol-based products, cheap feedstocks must be used and, most importantly, both technological advances and process optimization further developed. All the steps required in the production of a biomass-based fermentation product are connected with each other; starting with a certain feedstock for which, specific pretreatments might be needed and both the type of feedstock and pretreatment generating a certain range of compounds. These compounds are nutrients but also inhibitors and both affect the fermentation step, which generates other compounds that need to be removed in the downstream. The selected pretreatment should maximize the production of nutrients while reducing inhibitors. The fermentation should be controlled in order to divert fluxes from unwanted products and finally, the downstream's number of units and efficiency should be reduced and maximized respectively. Thus, the objective of this work is to identify SA production process routes through

simulation and ultimately, the sensitive steps resulting from the simulation will be tested and verified through lab experiments.

## Outcomes and working progress

The work started with a literature study that helped to identify the potential feedstocks, fermentation and separation techniques for large-scale production of succinic acid (Figure 1).

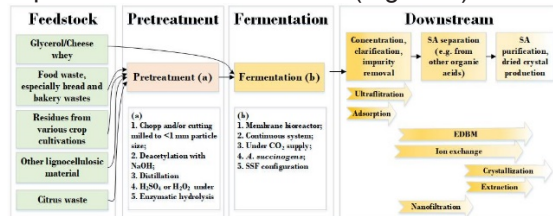


**Figure 17:** Generic process for succinic acid production listing the most relevant second generation feedstocks, the proposed pretreatments and fermentation conditions and the optimal range under which major separation techniques can operate.

Inexpensive, sustainable and available feedstocks were pinpointed (Figure 2), together with the identification of fermentation strategy and microbial strain with the highest records and advantages so far (Figure 1 and Table 1).

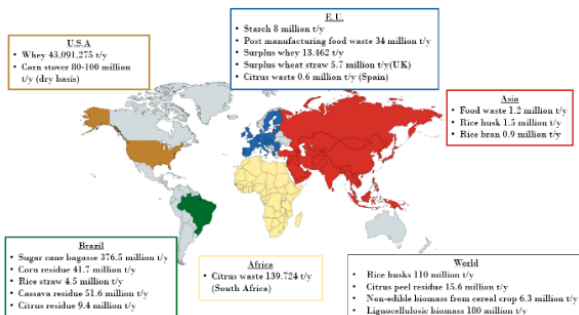


**Figure 18:** distribution of world food waste that would be suitable for succinic acid production. With the exception for data on rice waste in Asia, which are from the work of Gunarathne et al. (2019) [5], all the other data are based on the work of C. S. K Lin et al. (2013) [6].

These are then studied through process simulation and superstructure optimization, to identify potential best processes for large-scale SA production. The investigation of the commercial production of SA has been proceeding with a techno-economic analysis (TEA) of the commercial plant and the design of a new conceptual process with including membrane *in situ* SA separation.

## Experimental configuration

According to the conducted literature study, which includes process simulation on SA production, the downstream is the most expensive step in the whole

process [4] and membrane separation and crystallization are key technologies for production of pure SA. Therefore, different commercial ultrafiltration and nanofiltration (NF) membranes are tested to separate SA, investigating performance and selectivity also through mathematical simulation (the DSPM model).

The acquired knowledge in NF selectivity, together with the study of commercial SA processes, is condensing around a promising novel conceptual process that will be tested in laboratory.

**Table 1.** Some collected data for succinic acid production. Used feedstocks, fermentation strategy, productivity and yield.

Feedstock	Ferment. strategy	Conc. (g L <sup>-1</sup> )	Product. (g l <sup>-1</sup> h <sup>-1</sup> )	Yield (g g <sup>-1</sup> )
CB	AB	120	1.65	0.805
WS	AB	2.02	≈ 22.5	≈ 0.03
CS	AB	61		0.92
BK	SSF	24.8	0.79	0.28

## Abbreviations

Feedstock: cane bagasse (CB); wheat straw (WS); corn stalk (CS); bakery waste (BK). Fermentation strategy: anaerobic batch (AB); solid-state fermentation (SSF).

## References

1. R. K. Saxena, S. Saran, J. Isar, and R. Kaushik, "Production and Applications of Succinic Acid," in *Current Developments in Biotechnology and Bioengineering: Production, Isolation and Purification of Industrial Products*, New Delhi: Elsevier B.V, 2016, pp. 601–630.
2. EC-DGE, "From the Sugar Platform to biofuels and biochemicals," 2015.
3. T. Werpy and G. Petersen, "Top value added chemicals from biomass. Volume I: Results of screening for potential candidates from sugars and synthesis gas.," 2004.
4. E. Mancini, S. S. Mansouri, K. V Gernaey, and J. Luo, "From second generation feedstocks to innovative fermentation and downstream techniques for succinic acid production," *Crit. Rev. Environ. Sci. Technol.*, vol. 0, no. 0, pp. 1–45, 2019.
5. D. S. Gunarathne, I. A. Udugama, S. Jayawardena, K. V. Gernaey, S. S. Mansouri, and M. Narayana, "Resource recovery from bio-based production processes in developing Asia," *Sustain. Prod. Consum.*, vol. 17, pp. 196–214, 2019.
6. C. S. K. Lin et al., "Food waste as a valuable resource for the production of chemicals, materials and fuels. Current situation and global perspective," *Energy Environ. Sci.*, vol. 6, no. 2, 2013.

# A Numerical and Experimental Investigation of Industrial Cyclones

(December 2019- December 2022)



## Contribution to the UN Sustainable Development Goals

The purpose of this project is to provide a CFD tool which can be used to optimize a part (cyclone preheaters) of cement production and isolation material production industries to be more energy efficient and less pollutant (CO<sub>2</sub>, NO<sub>x</sub>, and particulate matter) emissive. These can assist to have more sustainable consumption and production patterns (SDG 12). Moreover, optimizing cyclone preheaters will reduce operating and maintenance costs leading to an economic growth (SDG 8).



**Mohamadali Mirzaei**

momirza@kt.dtu

### Supervisors:

Weigang Lin,  
Peter Arendt Jensen,  
Haosheng Zhou  
(Rockwool), Sam  
Zakrzewski (FLSmidth)

## Abstract

The focus of this PhD project is to improve the understanding of phenomena occurring in industrial-scale cyclone preheaters using Computational Fluid Dynamics (CFD) simulations. So far, after choosing appropriate models, they were applied on a lab-scale cyclone operating under a similar condition as industrial cyclone preheaters that proved their validity. Then, the same models were applied on a pilot-scale cyclone preheater where several computational issues arose that we tried to overcome.

## Introduction

Cyclones are extensively used as cyclone preheaters in the building material industry to preheat raw material (raw meal), which is of great importance to the thermal performance of the entire system of production. To optimize the design and operation of cyclone preheaters, in-depth knowledge of the multiphase flow is required, however, considering either experimental or numerical investigations; little work has been done on industrial cyclone preheaters. Despite their deceitful simplicity, cyclones preheaters are complicated to design and hardly optimized, since the flow field within them is extremely complex. This project aims to better understand this complex flow field by developing a validated CFD model capable of predicting important performance parameters of cyclone preheaters including separation efficiency, pressure drop, heat exchange and erosion. Then this CFD model can be used to optimize the design and operation of industrial cyclone preheaters.

- Provide detailed measurements of flow pattern, temperature profile and erosion rate in full-size industrial cyclones to be used as validation data for simulations
- Understand the flow patterns, heat transfer, and separation efficiency as well as erosion inside industrial cyclones

## Modeling methodology

Choosing appropriate turbulence model (capable of capturing the naturally unstable and fluctuating flow field) and multiphase model (capable of capturing phase interaction and particle motion, and accounting for potential particle-particle interactions) is the key for a successful CFD simulation of cyclone preheaters. Considering superiority and inferiority of various turbulence models tested for simulation of cyclones (some of them listed in Table 1) and regarding the industrial-scale geometry used in our study and its complexity, Reynolds Stress Model (RSM) and a version of k- $\omega$ -sst turbulence models seems to be feasible options for the simulation of cyclones in our study. Primary simulations proved the capability of these models in capturing flow field in cyclones. Regarding the robustness of k- $\omega$ -sst and their superiority over RSM in terms of computational cost

## Main objectives

- Develop a generic CFD model that is able to simulate industrial-scale cyclone preheaters and validate the model for various industrial cyclone configurations.

that is of great importance in our case, k- $\omega$ -sst is preferred.

**Table 5.** Qualitative evaluation matrix of turbulence models used in the literature for the simulation of cyclones

Model	k- $\omega$ -sst-cc	RSM	LES
Mean flow field	++	++	++
Fluctuating flow field	-	+	++
turbulence anisotropy	--	++	++
robustness	++	-	--
resolution	-	+	++
efficiency	++	~	--

Considering superiorities and inferiorities of multiphase models suitable for dense particle-laden flows (listed in Table 2), although Dense Discrete Phase Model (DDPM) is an ideal option for the present study, although might not be as accurate as Discrete Element Model (DEM), because of its ability to model particle-particle interaction, its ability to provide particle trajectories and erosion information, its ability in handling polydispersed particles, and its superiority over DEM in term of computational efficiency<sup>1</sup>.

**Table 6.** Qualitative model evaluation matrix of three available four-way coupling multiphase models

Model	TFM	DEM	DDPM
Particle-particle interaction	+	++	+
Particle trajectory	--	++	++
Erosion study	--	++	++
Polydispersity	-	++	++
resolution	+	++	+
efficiency	-	--	+

## Results and Discussion

Before applying chosen models on large and industrial-scale cyclone preheaters that is our ultimate goal, models were first applied on a small-scale generic cyclone (a cyclone studied experimentally by other authors working under solid loads similar to our industrial-scale cyclone preheaters). The purpose was to validate the model, to ensure that the model is capable of predicting performance parameters of cyclones, and to get familiar with challenges, limitations, and special treatments these model require for numerical convergence.

By comparing results obtained from simulations on a lab-scale cyclone with experimental data (see Figure 1), the validity of used models for simulation of cyclones working under high solid loads is proven. Therefore, these models can be applied with more confidence on industrial-scale cyclone

preheaters. Moreover, although RSM provided more accurate results, considering the superiority of k- $\omega$ -sst-cc turbulence model in terms of computational cost and stability, and considering its acceptable results, k- $\omega$ -sst-cc turbulence model can and should be tested on industrial scale cyclones before testing RSM turbulence model.

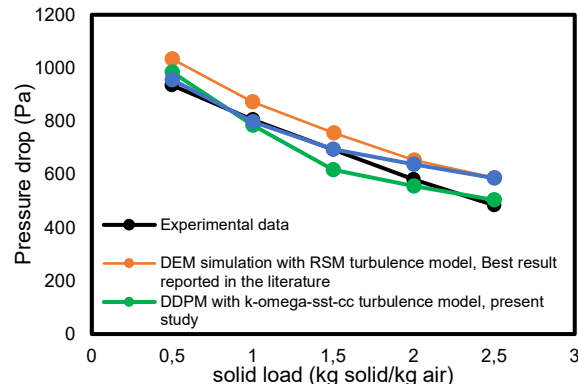


**Figure 19.** Comparison of the pressure drop obtained from DDPM and two turbulence models (present study), DEM (published by Chu et al.<sup>2</sup>), and experiments at different solid loading ratios.

## Conclusion and future work

So far, it is proven that chosen models (RSM and a version of k- $\omega$ -sst as turbulence models and DDPM as multiphase model chosen due to their superiority over other models in our interested areas of present case) are able to predict the pressure drop over a lab-scale cyclone from experimental work in literature. Future work will focus on the application of the same models to a pilot-scale cyclone with experimental data available. It is expected that new challenges will arise, such as being enormously computational expensive, issues with handling very fine particles (below 5 micron which are included in particle size distribution of studied pilot-scale cyclone), instability of solution, and so on which we are trying to overcome.

## Acknowledgement

This project is a part of Probu project, funded by Innovation foundation of Denmark, DTU Chemical Engineering, FLSmidth A/S and ROCKWOOL International A/S.

## References

1. Hwang, I. S., Jeong, H. J. & Hwang, J. Numerical simulation of a dense flow cyclone using the kinetic theory of granular flow in a dense discrete phase model. *Powder Technol.* 356, 129–138 (2019).
2. Chu, K. W., Wang, B., Xu, D. L., Chen, Y. X. & Yu, A. B. CFD-DEM simulation of the gas-solid flow in a cyclone separator. *Chem. Eng. Sci.* 66, 834–847 (2011).

# Evaluation of optimization potentials and capacity liberation options in a full-scale industrial wastewater system using a Digital Twin

(February 2018 - January 2021)

6 CLEAN WATER AND SANITATION



## Clean water and sanitation

Wastewater treatment is a fundamental pillar for society since it provides a key resource for public health, economic development and environment wellbeing. In this project, we aim to create a Digital Tween (DT) of the largest industrial wastewater treatment plant in Northern Europe. Among others benefits, DT allow *in silico* testing and assessment of new scenarios without the need of spend time and resources realizing them in real life. Nevertheless, the conclusions achieved in computer simulations must be practically reproduced (i.e. piloting) prior to application in wastewater treatment plant. Those scenarios can be directed towards improving the operation costs of the wastewater treatment plant, or increase its total processing capacity.



**Vicente T.  
Monje López**  
vtml@kt.dtu.dk

**Supervisor:**  
Xavier Flores-Alsina  
Helena Junicke  
Krist V. Gernaey

## Abstract

This abstract shows the preliminary results of applying a digital twin (DT) concept to a full-scale industrial wastewater treatment system (WWS) in operation at the Novozymes production facilities in Kalundborg (Denmark). The DT provides a virtual replica of the plant outline and will enable more informed decisions about how to optimize: Energy recovery, chemical use, operational procedures and capacity liberation. The proposed approach is tested using a dataset comprised of five weeks (06 May 2019 to 10 June 2019). Simulation results show that plant measurements and model predictions range between 5-20 %. The proposed approach is capable to reproduce and describe COD, N, P and particulate removal processes; energy consumption and sludge production. The study will demonstrate a functional plant-wide model of the largest industrial wastewater treatment plant in Northern Europe, including model-aided evaluation of different capacity liberation options.

## Full-scale system description

The plant layout consists of a initial buffer tank for influents mixing and homogenization, a primary clarifier for solids removal, a pre-acidification tank for conversion of the heterogeneous organic mixture to short chain fatty acids, two anaerobic granular sludge reactors with two external recirculation tanks which remove organic carbon in form of short chain fatty acids and converts them into a mixture of methane, carbon dioxide and hydrogen sulfide, an activated sludge system comprised of seven aerobic/anoxic units for organics and nitrogen, five secondary clarifiers for biomass recirculation and solids removal, three dissolved air flotation units for non-settable solids removal, two chemical inactivation tanks using calcium oxide for biomass inactivation, and a dewatering station comprised of twelve centrifuges where sludge is thickened prior to transportation to

a neighboring biogas facility. Additional details about the plant design and operational conditions can be found in Figure 1. The liquid influents and the reject water coming from dewatering of sludge may be treated anaerobically, aerobically, or using a combination of both.

## Digital twin: Main mathematical process model

The digital twin is based on: (1) a biological model, (2) a physico-chemical model and (3) different model interfaces. The biological models comprise an anaerobic digestion model (ADM) and an activated sludge model (ASM). The ADM is used to describe influent conditions, buffer tank, primary clarifier, pre-acidification tank, anaerobic bioreactors, inactivation tank and dewatering, while the ASM describes the activated sludge, secondary

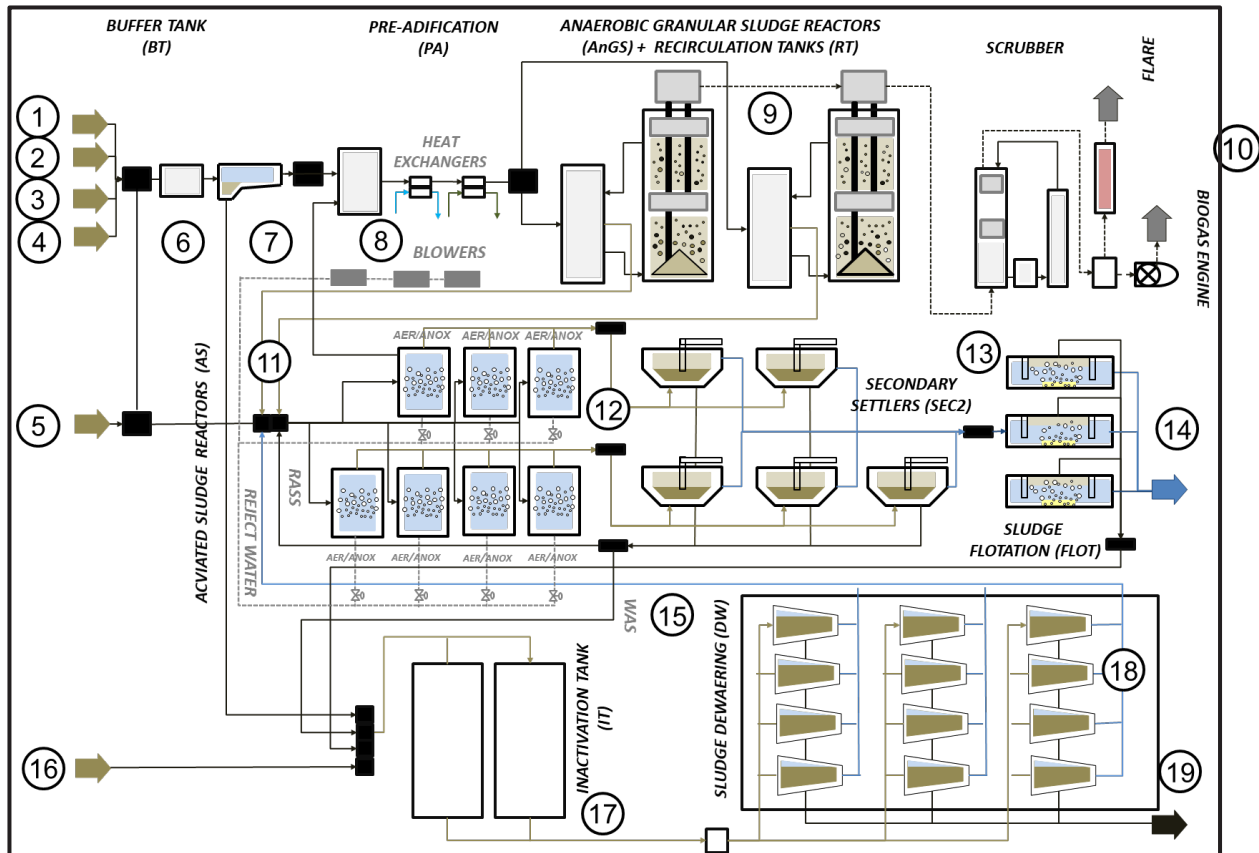


**Figure 1.** Flow diagram of the wastewater treatment plant under study. Measured and model-predicted streams: **1**, Influent factory 1; **2**, Influent factory 2; **3**, Ethanol stream A; **4**, Ethanol stream B; **5**, Influent factory 3; **6**, Buffer tank effluent; **7**, Primary clarifier overflow; **8**, Pre-acidification tank effluent; **9**, Anaerobic digesters effluent; **10**, desulfurized biogas; **11**, Activated sludge influent; **12**, Activated sludge effluent; **13**, Secondary clarifiers overflow; **14**, Dissolved air flotation effluent; **15**, Returned activated sludge; **16**, Biomass influent; **17**, Inactivation effluent; **18**, Reject water effluent; **19**, Dewatered biomass effluent.

clarifiers and dissolved air flotation units. The physico-chemical model includes an aqueous phase + precipitation model and a gas transfer model. Finally, the model interfaces connecting the different moduls. The outputs of the ASM/ADM at each integration step are used as inputs for the PCM module to estimate pH, ion speciation/pairing, precipitation potential and stripping. A comprehensive description of these models can be found in Flores-Alsina et al., 2019.

## CONCLUSIONS AND FUTURE WORK

This abstract has shown the huge potential of digitalization when optimizing water systems by partially showing the preliminary results of an academia-industry collaborative project dealing with capacity liberation in a wastewater treatment plant from the biotech industry. Up to date modelling results are promising, showing a deviation from the measurements of between 5 % and 20%. The project will continue with the modelling of the inactivation and dewatering units as well as the results of implementing different optimization /

retrofitting options. CAPEX and OPEX of the different energy/resource recovery and capacity liberation options will be discussed, supported by simulation results obtained with this DT approach. Some of the considered scenarios could be (but not limited to): Anammox technology for to maximize energy recovery in form of methane and reduce energy consumption in the activated sludge; Struvite precipitation for recovery of nitrogen and phosphorous; different biomass inactivation options (technologies, chemicals) and the effect over the entire plant.

## Acknowledgments

The authors would like to thank the Technical University of Denmark, the GreenLogic project and Novozymes A/S for financing and supporting this project.

## References

Flores-Alsina et al. (2019). Water Research. 156,264-276.

# Exploring the Structure and Properties of Water

(May 2020- April 2023)

6 CLEAN WATER AND SANITATION



## Contribution to the UN Sustainable Development Goals

The project is expected to contribute to the development of knowledge of the structure and properties of water at a molecular level through simulations. The structure of water is thought to be at the root why water behaves the way it does and its many anomalous properties. Understanding the structure-property relations of water can have positive impacts on sustainable utilization of water in many areas of human interests, especially clean water and sanitation.



**Aswin Vinod  
Muthachikavil**  
avimu@kt.dtu.dk

**Supervisors:** Xiaodong Liang, Georgios Kontogeorgis

## Abstract

It is often argued that formation of locally favoured structures due to hydrogen bonding lies at the root of water's anomalies. Molecular Dynamics (MD) simulations are employed to look at different molecular level phenomena, like the formation and breakage of hydrogen bonds and ordering of water in the first shell and second shell of neighbours, at different points on the phase diagram of water. The two dimensional PMF of hydrogen bond formation is also computed using MD simulations using iAMOEBA water model.

## Introduction

Water is arguably the most important liquid on our planet. Its properties lay the foundation for the emergence and existence of life on earth. Even though referred to as the universal solvent, water plays roles beyond being a passive solvent [1]. Structures and functions of biomolecules strongly depend on how they interact with water, making water's thermodynamic, dynamic, structural properties crucial for sustenance of life on earth. For example, hydrogen bonds mediated by water molecules provide linkages to allow proteins to achieve their active conformations rapidly. Because of its ubiquity in our environment, water has been one of the most widely studied substances. The interest of the scientific community in water rises from its importance in almost every area of human development. If there is one molecule which is of common interest to a wide range of research areas like environmental sciences, geosciences, planetary sciences, biology and industrial applications, it must be water [2]. In most of these cases, water is at non-ambient conditions of pressure or temperature, or may even be under confinement or interfacial conditions. Therefore, modelling of water has been of interest to the scientific community to predict the structure and properties of water, including conditions that cannot be probed through experiments. Water is amongst the most studied substances given its importance in

almost all fields of life. Some of its properties like the triple point and density are even considered as international standards [1]. However, many of its properties are anomalous, and do not fall in line with the theory of liquid state of matter. The idea of viewing water as a mixture of two different structures is quite old and dates back to 1883 [3]. However, it started getting attention again in late twentieth century [4, 5] because it gives a simple and intuitive understanding of the origin of anomalous properties of water [6]. One form favors order by maximizing Hydrogen bonds and thereby limiting the number of neighbors to create a low-density environment and the other form favors disorder squeezing molecules tighter leading to a high density environment. The two forms of water are normal liquids and have properties in line with the general theories of liquids. For example, their individual densities decreases continuously with temperature [7]. However, the competition between these two forms of liquids leads to the apparent anomalous maximum density point in water.

## Simulation methods

iAMOEBA, a polarizable water model that accurately captures the properties of liquid water was used in the simulations. Other simple, point charged water models like the TIP4P/2005 were also used for some studies. Five nanoseconds long simulations were performed using a system size of

256 water molecules. The data from the first nanosecond was not considered for the subsequent analysis. The simulations were run using two open source software- Tinker 7.1 and Gromacs 2020.

### Hydrogen bond in water

A combination of distances and angles that define the relative orientation of water molecules with respect to each other are often used to define hydrogen bonds in molecular simulations. The distance between the Oxygen and the hydrogen ( $r$ ) and the Donor-Hydrogen-Acceptor angle ( $\theta$ ) were used in this study to define hydrogen bonds. However, a sharp distinction between hydrogen bonded and non-hydrogen bonded water molecules is difficult. Given the arbitrariness of the cut-off, most literature published use the same cut-off for defining a hydrogen bond, at different conditions of temperature and pressure, and even different models of water. As a step towards making a definition for hydrogen bonds, the two dimensional Potential of Mean Force was calculated for iAMOEBA water along the  $r$ -  $\theta$  surface at 298 K and 1 atm. The difference between two points on the surface gives the free energy difference when changing the orientation between the two points. The results are shown in figure 1. It is observed that there is a minimum at around 1.75-2 Å and 155-180°. This minimum of about -4.2 kT can be interpreted as the free energy change of formation of hydrogen bond in iAMOEBA water.

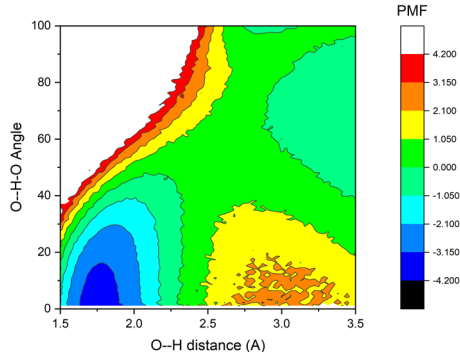


**Figure 20:** The Potential of Mean Force (PMF) surface of hydrogen bond formation in iAMOEBA water at 298 K and 1 atm.

### Structure of water

Studies have reported the existence of two forms of structural environments in water. The structure of water is explored using the distribution of O-O-O angle in water. The distribution of this parameter in water is shown in figure 2. A bimodal distribution with two peaks is observed in simulations, with one peak at approximately 109 degrees, which corresponds to the internal angle of a tetrahedron, and is suggestive of a tetrahedral environment in water. The other peak forms at lower angles and indicates a more tightly oriented environment. These two structural forms corresponds to the low

density and the high-density structural environments. Further, it is also observed in figure 2 that the peak corresponding to tetrahedral organization decreases with increase in temperature.

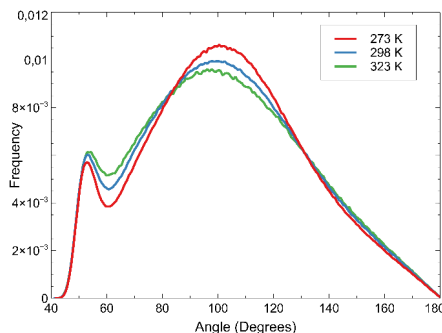


**Figure 2:** The distribution of O-O-O angle in water.

### Conclusions and future work

The polarizable iAMOEBA water model is able to capture the two structural forms of water in molecular simulations. The free energy surface of hydrogen bond formation has also been calculated using this water model. The 2D PMF computed from simulations are proposed to be studied at different physical conditions, and to be used for 'defining' hydrogen bonds in water. A model that takes into account the hydrogen bond in water explicitly is also proposed to be developed, which is expected to improve the accuracy of prediction of properties of water.

### Acknowledgements

I would like to thank PetroChina Research Institute of Petroleum Exploration and Development and the Department of Chemical and Biochemical Engineering, DTU for providing the financial aids for the project.

### References

1. J.F Ouyang and R. Bettens, CHIMIA Int. J. Chemistry, 69(3) (2015) 104-111.
2. B. Guillot, J. mol. liq., 101(1-3) (2002) 219-260.
3. H. Whiting, A new theory of cohesion applied to the thermodynamics of liquids and solids. American Academy of Arts and Sciences, 1883, p.353-466.
4. CM Davis Jr and TA Litovitz, J. Chem. Phys., 42(7) (1965) 2563-2576.
5. M. Vedamuthu, S. Singh, and G.W. Robinson, J. Phy. Chem. , 98(9) (1994) 2222-2230.
6. L.G.M. Pettersson. A two-state picture of water and the funnel of life, International Conference Physics of Liquid Matter: Modern Problems, 2018, p. 3-39.
7. P. Gallo, K. Amann-Winkel, C. A. Angell, M.A. Anisimov, F. Caupin, C. Chakravarty, E. Lascaris, T. Loerting, A.Z. Panagiotopoulos, J. Russo, Chemical reviews, 116(13) (2016) 7463-7500.

# An integrated multi-scale framework for bioprocess design, control and analysis

(August 2019- July 2022)



## Contribution to the UN Sustainable Development Goals

Developing integrated tools in the chemical and biochemical industry for monitoring and control of bioprocesses leads to more efficient handling of available resources. Since the importance of the bio-manufacturing industry is increasing steadily, innovations in this area have a high potential to yield new job opportunities, which can impact economic growth positively. This project aims at development of a more fundamental understanding of key processes in bio-manufacturing, such as flocculation, which then forms the basis for development of improved bio-manufacturing process monitoring and control



**Nima**

**Nazemzadeh**

nimnaz@kt.dtu.dk

**Supervisor:** Martin P. Andersson, Seyed Soheil Mansouri, Krist V. Gernaey

## Abstract

Control and monitoring of chemical and biochemical processes containing solid phases (flocs, crystals, or solid particles) are challenging tasks, due to a lack of a fundamental understanding of the process phenomena, and the lack of reliable real-time process data. Flocculation is a complex process taking place across various length scales. Since the mechanism of this process is not very well understood, industry resorts to manual/heuristic monitoring and control. Flocculation often undergoes process variations during operation, which can make heuristic control inefficient in preventing potential product losses. In this project, a multi-scale hybrid modeling framework is being developed that integrates a machine learning algorithm with common knowledge of the process (i.e. a first-principles model) to model this process.

## Introduction

Flocculation processes have a wide range of applications in many industries, including water/wastewater treatment, papermaking, production of pharmaceuticals, mineral processing, food industry, and many more. Despite the broad application of flocculation, a lack of fundamental/causal understanding of the process mechanism combined with lack of on-line measurement methods makes the modeling, control, and monitoring of the process challenging for both academic and industrial practitioners. The complexity of the flocculation process comes from the fact that it is a stochastic process that takes place across a broad length scale, starting from a non-observable scale (nano-scale) and going all the way beyond microscale. The lack of knowledge that arises from this complexity, makes industry resort to a heuristic control in the production line. The heuristic control may turn into a time-consuming procedure and causes product losses. For instance, in polyelectrolyte flocculation of cells from a fermentation broth, it has been shown that by overdosing polymer, all the cells will be removed from the broth to form a brain floc [1]. Hence, the polymer overconsumption in the broth will have

interactions with the enzyme. These interactions will lead to denaturation of the enzyme and finally cause an undesired enzyme loss. This could potentially be avoided by controlling the amount of flocculants added to the broth [1].

In this study, a hybrid approach that uses first-principles models combined with machine learning algorithms is utilized to model flocculation processes. The first-principles models for flocculation processes are considered to be a population balance model (PBM) combined with the Derjaguin-Landau-Verwey-Overbeek (DLVO) theory [2]. The PBM is used to model the dynamic evolution of particles with different sizes in the system, while the DLVO theory is used to provide the kinetics of flocculation processes with more accurate estimates of collision efficiencies of the particles by calculating interaction energies between the particles in the system.

## Specific Objectives

The main objective of this study is to develop a hybrid multi-scale framework for modeling flocculation processes. In this section, the hybrid modeling framework is an extension of the framework developed by Nielsen et al. 2020 [3]. The

hybrid modeling framework contains six main steps as system specification, setting up the model structure, data acquisition, data pre-processing, model training/validation, and model prediction (test). Figure 1 demonstrates an overview of the framework. A structure similar to the framework of Nielsen et al. 2020 is used to build up the hybrid multi-scale framework. The DLVO calculations of collision efficiencies are incorporated as a first-principles model to estimate agglomeration kinetic parameters more accurately. The application of such modeling framework is demonstrated with a flocculation case study, which has agglomeration and breakage of particles as dominant process phenomena. Note that the same concept allows us to incorporate the kinetic model for other processes such as crystallization, which has nucleation, growth, and shrinkage as relevant phenomena.

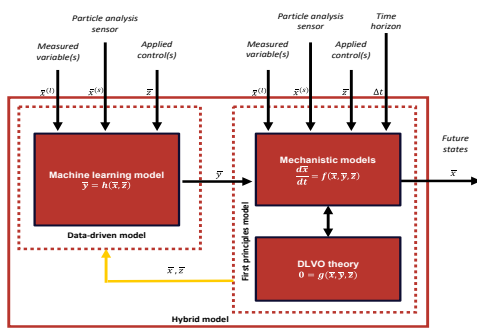


**Figure 1:** Overview of the hybrid modeling framework

## Results and discussion

A laboratory-scale flocculation case of silica particles in water is investigated in this section. An experimental setup is prepared to measure the process variables and the particle size distribution during the process operation. pH is considered as the process variable to be measured by an in-line measurement method. An in-line sampling method is used to measure the pH by providing the flocculation tank with a pH probe. However, an at-line sampling method in close proximity to the tank is utilized to measure the particle size distribution. To measure the particle size distribution, a dynamic optical scanning device (oCelloscope developed by BioSense Solutions ApS) is used which is integrated with ParticleTech Analyzer software (developed by ParticleTech ApS). The software uses image segmentation algorithms to identify the particles and their sizes in the system. By applying the hybrid multi-scale modeling framework proposed in the previous section, end-of-batch predictions are carried out for two different batches of experiments; one shows agglomeration and the other breakage as dominant process phenomena. The alignment between the experimental data and

model predictions shows that the model can quite accurately predict the end-of-batch behavior of the system by only considering the process pH and size distribution of particles at the beginning and at a time-point in the middle of the operation.

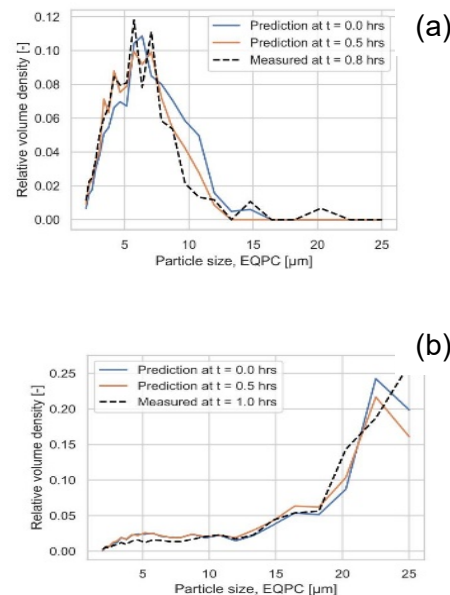


**Figure 2:** End-of-batch predictions for an experimental batch dominated by a) breakage, b) agglomeration

## Conclusion

In this project, the aim is to use a hybrid modeling approach, which incorporates a population balance model and DLVO theory as the first-principles models for flocculation processes, we can quite accurately predict the dynamics of the system. Such modeling framework can then be implemented to develop a model predictive controller in order to avoid potential process variations and eventually reduce potential product losses in this process.

## Acknowledgment

We would like to thank the Department of Chemical and Biochemical Engineering at DTU, Novozymes A/S and Greater Copenhagen Food Innovation program (CPH-FOOD) for co-financing this research and also for their support during this project.

## References

1. C.R. Pearson, M. Heng, M. Gebert, C.E. Glatz, Biotechnol. Bioeng. 87 (2004) 61–68.
2. H. Yotsumoto, R.H. Yoon, J. Colloid Interface Sci. 157 (1993) 434–441.
3. R.F. Nielsen, N. Nazemzadeh, L.W. Sillesen, M.P. Andersson, K. V. Gernaey, S.S Mansouri, Comput. Chem. Eng. 140 (2020), 106916.

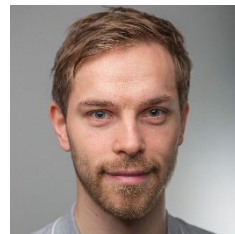
# Novel Catalysts and Reaction Pathways to Complex Nitrile Molecules

(September 2018- August 2021)



## Contribution to the UN Sustainable Development Goals

Responsible production is about utilizing resources in the best way and minimizing toxic chemicals. This project aims at developing a process that can be used instead of the existing which is based on fossil carbon. In an electrified future, the reactants can be produced in an environmentally friendly way and the successfully developed process succeeds at minimizing a toxic byproduct which is inevitable in the existing process.



**Kasper  
Rode Nielsen**

karon@kt.dtu.dk

**Supervisor:** Jakob Munkholt Christensen, Anker Degn Jensen, Thoa Thi Minh Nguyen, Rasmus Munksgård Nielsen

## Abstract

This project is about improving a catalyst for the production of acetonitrile from ammonia and methanol. Acetonitrile is a very important chemical but as of now it is only produced as a byproduct from another process. The work has been about improving a Co-Sn/Al<sub>2</sub>O<sub>3</sub> catalyst. The results show that the visual (i.e. structural) features of the catalysts depend on the preparative procedure. Also the amount of carbon deposition on the surface of the catalysts during reaction seems to be affected.

## Introduction

Acetonitrile (CH<sub>3</sub>CN) is an important solvent in the chemical and pharmaceutical industry and the demand for it is growing [1]. Today, acetonitrile is only produced as a byproduct from the production of acrylonitrile and the supply is thus highly connected to the demand for acrylonitrile. This created an imbalance between the supply and demand for acetonitrile during the financial crisis in 2008 and thus it was clear that an on-purpose process for the production of acetonitrile is needed [2].

Different methods for doing this have been investigated, including for example ammonoxidation of ethane, ethylene [3] and ethanol [4] and reaction between syngas and ammonia [5].

This project explores the reaction between ammonia and methanol which proceeds according to Equation 1.



The reaction is interesting because it involves the formation of a chemical bond between two carbon atoms.

At Haldor Topsøe A/S, an Al<sub>2</sub>O<sub>3</sub>-supported bimetallic catalyst with cobalt and tin has been found to catalyze this reaction [6] but the catalyst

still needs to be improved in order to achieve a high acetonitrile selectivity and minimize the amount of the toxic byproduct hydrogen cyanide. The stability of the catalyst is also under investigation.

## Specific Objectives

The objectives of the project are:

- Improvement of the catalysts in terms of catalytic activity, selectivity and stability
- Elucidation of the structural and compositional properties that govern the catalytic behavior and gaining insight into the mechanisms of the syntheses
- Development of kinetic expressions for the reactions
- Economic evaluation of the findings

## Experimental

All catalysts were prepared using the incipient wetness technique by first dissolving the cobalt and tin precursors in demineralized water and then impregnate this liquid on spheres of Al<sub>2</sub>O<sub>3</sub>. The spheres were subsequently taken through a heat treatment to drive off volatile impurities.

The catalytic experiments were performed in a fixed bed reactor which was made from quartz shaped as a u-tube. The effluent stream was analyzed by a gas chromatograph having both

flame ionization detectors and a thermal conductivity detector.

Fresh and spent catalysts were characterized with X-ray diffractometry, scanning electron microscopy (SEM), transmission electron microscopy and temperature-programmed reduction and oxidation (TPR/TPO).

## Results and Discussion

In one series of experiments, the catalyst for the synthesis of acetonitrile was prepared in different ways (method 1 and method 2). The results indicate that it is possible to produce catalysts with different properties depending on the preparative method. Figure 1 shows two catalysts which have been prepared in similar ways but with slight differences.



**Figure 21:** Two Co-Sn/Al<sub>2</sub>O<sub>3</sub> catalysts with the same amount of Co and Sn but with slightly different preparation methods. Left: method 1. Right: method 2.

The blue color of the one using method 2 shows that blue pigments such as CoAl<sub>2</sub>O<sub>4</sub> are more dominating in this sample.

The SEM images also reveal that there is a compositional difference between the two catalysts. Figure 2 shows the micrographs.

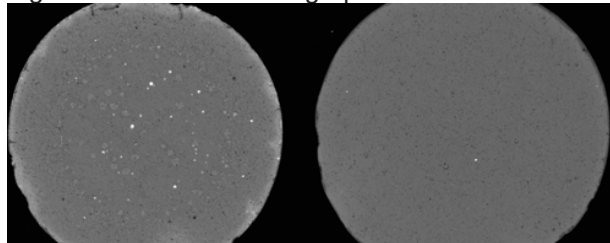


**Figure 2:** SEM micrographs of two Co-Sn/Al<sub>2</sub>O<sub>3</sub> catalysts with the same amount of Co and Sn but with slightly different preparation methods. Left: method 1. Right: method 2.

Evidently, the catalyst prepared with method 1 contains more bright areas. These are seen both in the center and on the perimeter of the sphere. Further analysis clarified that these bright areas contain more tin relative to the more gray areas.

The same two catalysts were also taken through a temperature-programmed oxidation experiment after the catalytic reactions. This was done in order to analyze the carbon which deposits on the surface of the catalyst during the reaction. The catalysts were heated to 1000 °C with a heating rate of 5 °C/min in a flowing (100 Nml/min) stream

comprising 2 vol% O<sub>2</sub> in He. During the experiment, the CO<sub>2</sub> concentration in the effluent was monitored.

Figure 3 shows the result of that for the two catalysts.

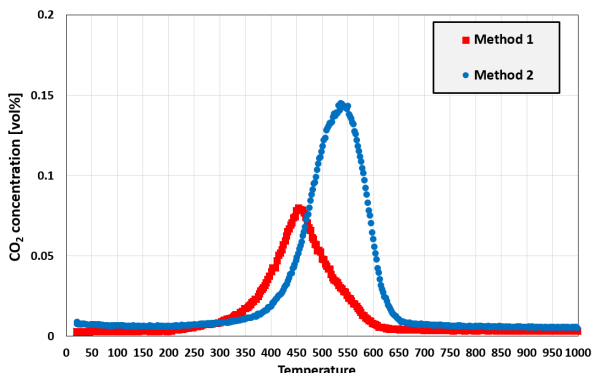


**Figure 3:** The CO<sub>2</sub> concentration of the effluent stream from the TPO experiment with the two catalysts prepared with method 1 and method 2.

In the figure, it can be seen that the one prepared with method 2 not only produces more carbon, the carbon also seems to be more stable because it requires higher temperatures to be removed.

## Conclusions

So far, it can be concluded that the preparative procedure of the acetonitrile catalyst has an impact on the performance. This can be seen on both the structural/compositional characteristics. Moreover, carbon also seems to deposit on the surface of these catalysts but the stability and amount is not the same.

## Acknowledgements

The work on the project is done mainly in the lab of Haldor Topsøe A/S which also provides raw materials for the catalysts and the reactions. DTU CEN has been helpful in providing access to transmission electron microscopy equipment.

## References

1. Global Market Insights, Acetonitrile Market Size, Industry Analysis Report, Regional Outlook, Application Development Potential, Price Trends, Competitive Market Share & Forecast, 2020 – 2026, 2020.
2. E. Rojas, M. O. Guerrero-Pérez, M. A. Bañares, Catal. Comm. 10 (11) (2009) 1555-1557.
3. E. Mannei, F. Ayari, E. Asedegbegha-Nieto, M. Mhamdi, G. Delahay, Z. Ksibi, A. Ghorbel, Chem. Pap. 73 (3) (2019) 619-633.
4. F. Folco, J. Velasquez Ochoa, F. Cavani, L. Ott, M. Janssen, Catal. Sci. Technol. 7 (1) (2017) 200-212.
5. L. M. Eshelman, W. N. Delgass, Catal. Today 21 (1) (1994) 229-242.
6. P.E. Højlund Nielsen, R.M. Nielsen, B.K. Olsen, Patent No. WO2018141821 A1 (2018).

# Catalytic Methanol Synthesis

(November 2017 – October 2020)

7 AFFORDABLE AND CLEAN ENERGY



## Contribution to the UN Sustainable Development Goals

Powering the world with fossil resources is unsustainable and changes toward renewables are required. Methanol produced locally from CO<sub>2</sub> at mild conditions can promote an energy efficient transition because it is a good energy carrier, but it requires development of methanol catalysts with high activity at mild conditions. Improved understanding of methanol synthesis and the role of reactants and products can enable sustainable methanol production and promote carbon neutral energy at a competitive price.



**Niels Dyreborg**

**Nielsen**

ndni@kt.dtu.dk

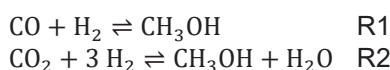
**Supervisors:** Jakob Munkholt Christensen and Anker Degn Jensen

## Abstract

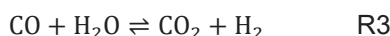
Methanol synthesis is an important industrial process (80-90 million tons demand in 2018) and occurs by syngas (CO/CO<sub>2</sub>/H<sub>2</sub>) conversion over a Cu/ZnO/Al<sub>2</sub>O<sub>3</sub> (CZnA) catalyst at 200-300°C and 50-100 bar [1]. However, fundamental knowledge about the reaction mechanism and the role of the CO in the syngas is not yet fully understood. This project aims at addressing these issues to facilitate feasible, sustainable methanol production from renewable generated H<sub>2</sub> and industrially captured CO<sub>2</sub>. This project is part of the Villum Center for the Science of Sustainable Fuels and Chemicals.

## Introduction

Hydrogenation of CO and CO<sub>2</sub> (R1 and R2) constitute two routes to methanol over supported Cu.



Moreover, the simultaneously occurring water-gas shift (WGS) reaction (R3) has to be considered.



On Cu/ZnO-based catalysts kinetic [2] and isotope labelling studies [3] clearly demonstrate that CO<sub>2</sub> is the main carbon source, but for pure Cu catalysts theoretical models [4] suggest the CO route to be rapid in contrast to high activity from CO<sub>2</sub> found in low and high-pressure experimental studies [2]. This combined with conflicting studies using Cu/ZnO/Al<sub>2</sub>O<sub>3</sub> reporting CO to be detrimental [4] and beneficial [5] to the activity calls for research. Finally, the supremacy of the conventional type Cu/ZnO/Al<sub>2</sub>O<sub>3</sub> catalyst and the influence of products on the catalytic activity are clarified.

## Specific Objectives

- Measure methanol activity in H<sub>2</sub>/CO/CO<sub>2</sub> = 68/29/3 at 250°C, 50 bar to determine the turnover frequency per Cu site (TOF)
- Unravel the carbon source and role of CO at conventional methanol synthesis conditions

- Investigate the supremacy of Cu/ZnO/Al<sub>2</sub>O<sub>3</sub> and role of products on the activity

## Results and Discussion

Syngas switching experiments between CO<sub>2</sub>/H<sub>2</sub> and CO/H<sub>2</sub> for various catalysts were applied to determine the main carbon source [2]. Figure 1 shows that CO<sub>2</sub> is the main carbon source for Cu catalysts with catalytic properties similar to intrinsic Cu (Raney Cu and unsupported Cu) and supported Cu catalysts with and without zinc (Cu/Al<sub>2</sub>O<sub>3</sub> and Cu/ZnO/Al<sub>2</sub>O<sub>3</sub>). Additional switching experiments between CO<sub>2</sub>/H<sub>2</sub> and CO/CO<sub>2</sub>/H<sub>2</sub> for the aforementioned Cu catalysts showed that CO is detrimental to the activity at low conversion. For Cu/MgO, R1 is faster than R2 due to a bifunctional mechanism at the interface between the basic oxide (MgO) and the metal, where CO derived formate activation occurs while CO<sub>2</sub> inhibits these CO active centers.

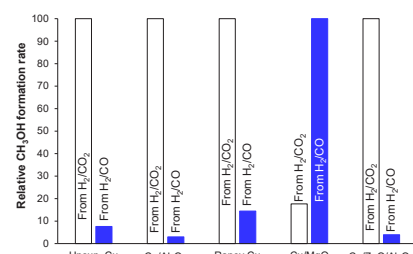


**Figure 1:** Relative methanol rate in H<sub>2</sub>/CO<sub>2</sub> (white) and H<sub>2</sub>/CO (blue) over Cu based catalysts at 50 bar, 523 K in H<sub>2</sub>/CO<sub>x</sub>/inert = 68/3/29 at low conversion.

Milder operating conditions is a prerequisite for a widespread, decentralized methanol plants close to renewable energy sources/applications. Current methanol production is restricted to high temperature ( $> 500$  K) to maintain high kinetic activity and to effectively remove inhibiting water. Figure 2 shows that even low water concentrations ( $>300$  ppmv) profoundly decreases the productivity and makes mildly operated methanol production from  $\text{CO}_2$  (R2) a great challenge. Water-free methanol production by R1 over highly active  $\text{Cu}/\text{MgO}$  constitutes a promising way of small-scale methanol production [2].

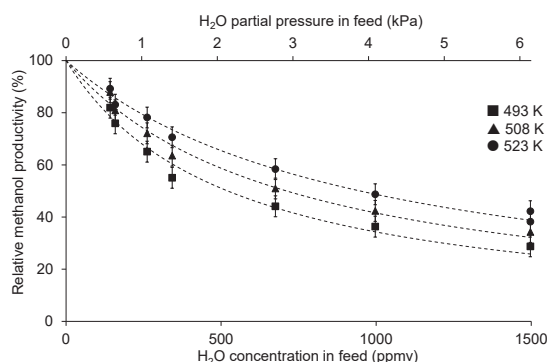


**Figure 2:** Relative productivity over  $\text{Cu}/\text{ZnO}/\text{Al}_2\text{O}_3$  as a function of added water content to the feed gas ( $\text{H}_2/\text{CO}/\text{CO}_2 = 67.6/29.6/2.8$ ) at 41 bar.

Conventional methanol production takes place at higher conversion with significant water production (R2). While CO is detrimental at low conversion, it effectively displaces the worse inhibitor (water) through the WGS reaction (R3) [6]. Figure 3 shows the transition from CO exerting a negative role ( $<1$ ) at low conversion to a gradually more positive role ( $>1$ ) at higher conversion.

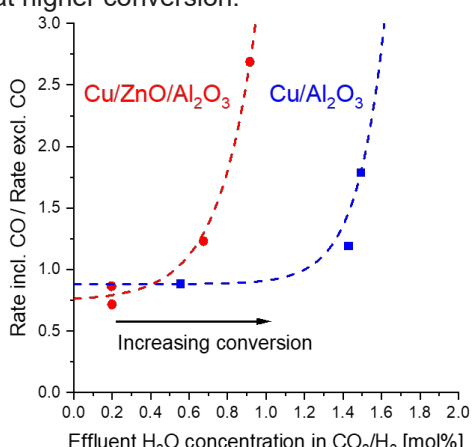


**Figure 3:** Relative methanol rate between feed gas with and without CO as function of the water concentration in  $\text{CO}_2/\text{H}_2$ .  $T = 523$  K,  $P = 50$  bar,  $\text{CO}_2/\text{X}/\text{H}_2 = 3/29/68$  with  $\text{X} = \text{N}_2$  or CO.

Recent results [6] from our group in collaboration with Haldor Topsøe reveal that a methanol-assisted

autocatalytic reaction dominates for conventional methanol synthesis  $\text{Cu}/\text{ZnO}/\text{Al}_2\text{O}_3$ . Figure 4 shows the autocatalytic reaction, where produced methanol accelerates the formation of additional methanol, resulting in substantial TOF increase. Similar mechanism is evident for  $\text{Cu}/\text{SiO}_2$  though at much lower TOF values, while  $\text{Cu}/\text{Al}_2\text{O}_3$  shows no prevalence for such a mechanism.

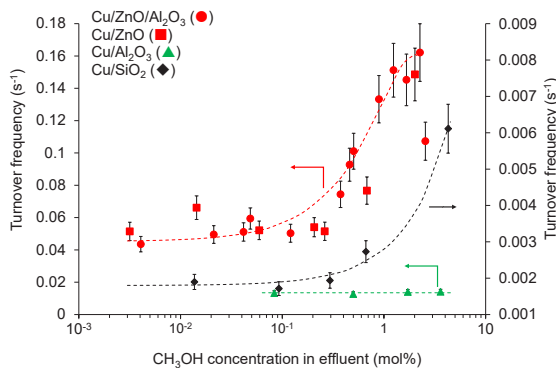


**Figure 4:** TOF variation upon changes to the methanol concentration in the effluent induced by varying the gas space velocity ( $3 \times 10^3$ - $4.3 \times 10^7$  NL kg  $\text{h}^{-1}$ ) at 50 bar, 523 K.

## Conclusions

$\text{CO}_2$  is the main carbon source for methanol synthesis over Cu.  $\text{Cu}/\text{MgO}$  compose a promising candidate for low temperature and water-free methanol production at decentralized plants. CO is detrimental role at low conversion but exerts a beneficial role at higher conversion due to effective scavenging produced water by WGS. The supremacy of  $\text{Cu}/\text{ZnO}/\text{Al}_2\text{O}_3$  has recently been related to an autocatalytic mechanism with methanol catalyzing further methanol formation.

## Acknowledgements

This work was supported by a research grant (9455) from VILLUM FONDEN.

## References

1. J. Sehested, J. Cat. 371 (2019) 368-375
2. Nielsen et al., Cat Lett. 150 (2020), 1427-1433
3. Chinchen et al., Appl. Catal. 30 (1987), 333-338
4. Studt et al., ChemCatChem 7 (2015), 1105-1111
5. Klier et al., J. Catal., 74 (1982), 343-360
6. Nielsen et al., J. Catal. Submitted Sep. 2020
7. Thrane et al., Angew. Chem. Int. Ed., 59 (2020), 18189-18193

## List of Publications

- N. Nielsen et al., Dansk Kemi 7, 2019, 16-18
- N. Nielsen et al., Cat Lett. 150 (2020), 1427-1433
- N. Nielsen et al., Cat. Lett. 150 (2020) 2447-2456
- N. Nielsen et al., Surf. Sci. 703 (2021), 121725
- N. Nielsen et al., J. Catal. Submitted Sep. 2020
- J. Thrane, S. Kuld, N. Nielsen et al., Angew. Chem. Int. Ed., 59 (2020), 18189-18193

# Novel Strategies for Control and Monitoring of Bio-Processes using Advanced Image-Analysis

(September 2018- August 2021)



## Contribution to the UN Sustainable Development Goals

The transition to a more sustainable production in chemical and biochemical industries is in these years challenged by the requirement of rapid process development. This causes processes to be designed and controlled sub-optimally, leading to increased utility consumption and higher product losses due to process variations. The model-based tools developed in this project can help facilitate sustainable design and control without slowing down process development. This is done by combining traditional physicochemical models with machine-learning.



**Rasmus Fjordbak Nielsen**

rfjoni@kt.dtu.dk

**Supervisor:** Krist V. Gernaey, Seyed Soheil Mansouri

## Abstract

This project intends to generate an array of tools that can help facilitate sustainable process design and control towards rapid process development. This is done by combining traditional physicochemical models with machine-learning, forming so-called hybrid models. The models are trained using time-series data obtained from both traditional and novel process sensors, and can among other things be used for inexpensive model-based design and model predictive control.

## Introduction

When developing the design and control for chemical and biochemical processes at industrial scale, there is often a requirement for a rapid process development. This often causes the sustainability requirements to be down prioritized, which causes the final processes to be designed and operated sub-optimally.

This dilemma could potentially be solved using process modelling in the process development phase, as this can reduce the number of experiments that need to be carried out, and thereby also save time and money. However, in cases where the process dynamics are not well understood or not well-defined mathematically, it may require too much effort to use traditional first principles modelling for characterizing the process dynamics. Instead, one may consider using data-driven modelling, commonly known as machine learning. However, to use such an approach, it may require too much process data and thereby also be an infeasible solution for the initial development of a new process.

In-between the traditional first principles modelling, and data-driven modelling is the tradeoff-concept called hybrid modelling. This approach utilizes the prior process knowledge in the form of first principles models and combines it with a

machine learning model to model the unknown or less well-known process dynamics.

## Hybrid modelling framework

Various processes have been examined and modelled using a hybrid model structure as illustrated in Figure 1, originally used for modelling of particle processes, including crystallization and flocculation processes [1].

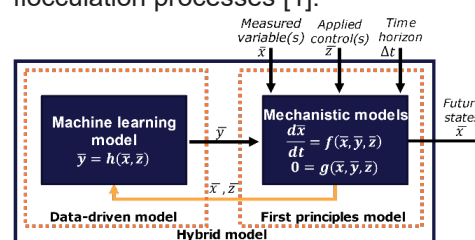


**Figure 22:** Hybrid model structure

The hybrid model consists of a set of mechanistic models for the measured process variables,  $\bar{x}$ , that depends on one or more control actions,  $\bar{z}$ . The mechanistic model furthermore depends on a number of hidden process states,  $\bar{y}$ , that are either not mathematically well-defined or unknown, and thereby need to be estimated using process data. These process states are estimated using a machine learning model, given the current process states,  $\bar{x}$ , and the control actions,  $\bar{z}$ . The model is

trained using time-series data with a sampling frequency of  $\Delta t^{-1}$ .

By utilizing a combination of backpropagation and automatic differentiation, this type of model can be updated in real-time using consumer grade computer hardware, allowing the generation of a true digital twin of the process at a relative low cost.

### A self-updating control strategy

The possibility of updating the hybrid process model in almost real-time, also allows for a self-updating control strategy, where a continuously updated hybrid model can be used for model predictive control. Ideally, if the hybrid model is not overfitted nor underfitted, this type of self-updating control should converge to the optimal control after having collected enough data from the process. An illustration of the self-updating control strategy can be seen in Figure 23, based on batch operation.

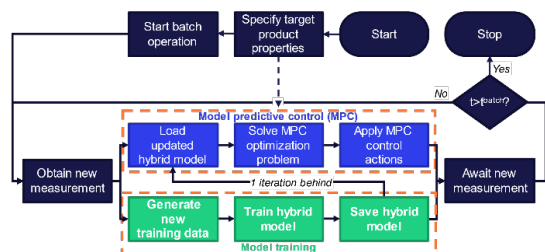


**Figure 23:** Self-updating control strategy [2]

First, one or multiple control target(s) of the end-of-batch product properties are specified. These properties must be either related directly to the modelled process variables  $\bar{x}$ , or a derivative of these. When the process is operated, measurements are collected of these process variables, and subsequently used for training the hybrid model and to solve the model predictive control problem.

### Results

The self-updating control strategy has been demonstrated for a theoretical case study of a lactose cooling crystallization, where disturbances were added to multiple critical process parameters, including the seeding properties and the initial solute loading.

The measured process variables were here the crystal size distribution, the solute concentration, and the crystallizer vessel temperature. These measurements can all be obtained through commercially available on-line/at-line sensors. To measure crystal size, one could for instance use dynamic image analysis in an on-line setting (e.g. ParticleTech solution [3]), where crystals are pumped to a flow-cell situated in a confocal microscopy, whereafter the images are analyzed using advanced image analysis, resulting in an almost real-time measurement of the current crystal size distribution.

To model the crystallization, a population balance model and a solute mass balance model were set

up as the mechanistic models in the hybrid model. A deep neural network was trained to estimate nucleation and bin-specific growth rates for the crystallization process, using the current particle size distribution, the solute concentration, vessel temperature and cooling-rate as inputs.

The target end-of-batch product properties were here specified to be the final mean crystal size and the final vessel temperature. To compare, a simpler reference control (linear cooling profile) was applied in parallel with the same process disturbances, where the reference control was tuned such that it would result in the desired end-of-batch product properties if no disturbances were added.

After the four batch operations, the self-updating model predictive control would start outperforming the conventional control, and as expected gradually improved further as more data was collected [2].

### Conclusions

It has here been demonstrated how a hybrid model can be used to speed up the development of process control. This can easily be extended to account for sustainability criteria, and thereby help facilitating sustainable process control without slowing down process development.

### Acknowledgements

This work partly receive financial support from the Greater Copenhagen Food Innovation project (CPH-Food), Novozymes, from EUs regional fund (BIOPRO-SMV project) and from Innovation Fund Denmark through the BIOPRO2 strategic research center (Grant number 4105-00020B).

### References

1. R.F. Nielsen, N. Nazemzadeh, L.W. Sillesen, M.P. Andersson, K.V. Gernaey, S.S. Mansouri, Comp. Chem. Eng. 140 (2020) 106916.
2. R.F. Nielsen, K.V. Gernaey, S.S. Mansouri, in: S. Pierucci, F. Manenti, G. Bozzano (Eds.), Proceedings of the 30<sup>th</sup> European Symposium on Computer Aided Process Engineering, Elsevier B.V., 2020, p. 1177-1182
3. ParticleTech Solution, 2020. URL: <https://particletech.dk/particletechsolution>

### List of Publications

1. R.F. Nielsen, N.A. Kermani, L.C. Freiesleben, K.V. Gernaey, S.S. Mansouri, in: A.A. Kiss, E. Zondervan, L. Özkan, 29th European Symposium on Computer Aided Process Engineering Proceedings, Elsevier B.V., 2019, p. 1435-1440
2. R.F. Nielsen, N. Nazemzadeh, L.W. Sillesen, M.P. Andersson, K.V. Gernaey, S.S. Mansouri, Comp. Chem. Eng. 140 (2020) 106916.
3. R.F. Nielsen, K.V. Gernaey, S.S. Mansouri, in: S. Pierucci, F. Manenti, G. Bozzano (Eds.), 30th European Symposium on Computer Aided Process Engineering Proceedings, Elsevier B.V., 2020, p. 1177-1182

# Further Development of the Primitive Electrolyte Equation of State Approach

(January 2020- December 2022)

9 INDUSTRY, INNOVATION  
AND INFRASTRUCTURE



## Contribution to the UN Sustainable Development Goals

The core of this project is to better understand electrolyte thermodynamics, and to do this more accurate and predictive thermodynamic models have to be developed. The thermodynamic models are mathematical models that can be used to predict thermodynamic properties. Having better models means that less experiments are needed which can cut down on cost and resources. Having better understanding of thermodynamics can help drive innovation of processes where electrolytes are present.



**Martin Due  
Olsen**

maduel@kt.dtu.dk

**Supervisor:** Nicolas von Solms, Georgios Kontogeorgis, Xiaodong Liang

## Abstract

In this work the Electrolyte-Cubic plus Association (e-CPA) model has been parametrized for sodium chloride to be able to describe various properties including mean ionic activity coefficients, osmotic coefficients and density. The results in terms of figures comparing the modelling results with experimental data shows that this is achieved in a large temperature range, and concentrations up to the solubility limit. This is done in an attempt to better understand electrolyte thermodynamics.

## Introduction

The purpose of this study is to obtain knowledge of electrolyte thermodynamics. Electrolytes are present in diverse industrial applications used within most sectors related to chemical engineering [1]. Gaining further and better understanding of electrolytes is therefore of high importance. This can be done by developing more accurate models and models with a better predictability. The non-electrolyte thermodynamic models have shown great improvements which have not been carried over to electrolyte thermodynamics and modelling electrolytes have therefore not gotten the same attention despite the importance in industrial applications. In this project the equation of state (EoS) model Electrolyte Cubic plus Association e-CPA is applied to various electrolyte systems. This is a so-called primitive model, which means that the solvent is considered a sort of background material that interacts with the ions through its static permittivity and the solvent is not explicitly considered as individual molecules. e-CPA is an EoS that combines a non-electrolyte model with an electrolyte model. The non-electrolyte contribution is from CPA [2] which have shown excellent results for many complex non-electrolyte compounds including water. The electrolyte part is a Debye-Hückel (DH) term that covers the long range

interactions of ions and a Born term which describes the solvation of the ions.

## Specific Objectives

The current work on this has been to investigate many different properties of a single salt (sodium chloride) with the use of e-CPA. To accomplish this a new parameter set for sodium chloride has been estimated, which is capable of calculating the activity coefficients, osmotic coefficients at the same time as volumetric properties like density. The e-CPA model has previously been applied to various systems and various parameter sets have been published from the department [3,4,5]. The previous parameter sets were relying on using a volume translation parameter to be able to somewhat reasonably get the volumetric properties. The new parametrization does not include a volume translation parameter but is still able to calculate the volumetric properties.

## Results and Discussion

A few results are shown in figures 1-3 for the activity coefficients, osmotic coefficients and the density. In all figures the results shown are for aqueous sodium chloride systems at various concentrations and temperatures. It should be noted that the considered temperatures in all three cases are at

298.15 K, 373.15 K and 473.15 K. This means that all these properties are able to be well described in a reasonably large temperature span.

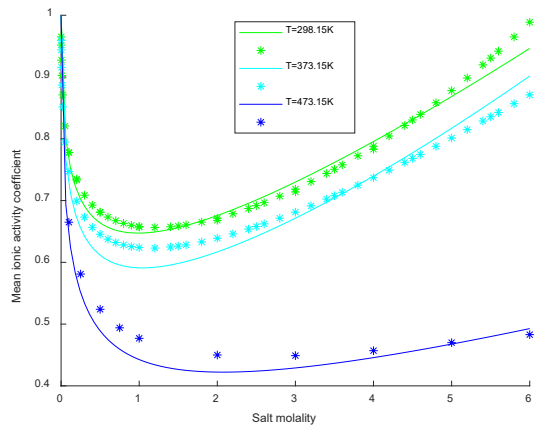


**Figure 24:** The activity coefficients of sodium chloride in water calculated with model (lines) with the new parameters compared to exp. data (\*).

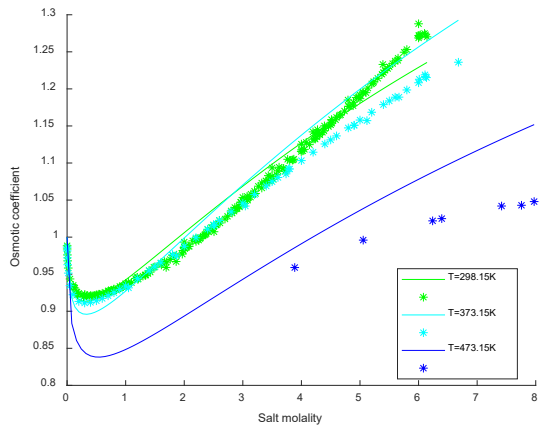


**Figure 2:** The osmotic coefficients of sodium chloride in water calculated with e-CPA (lines) with the new parameters compared to exp. data (\*).

## Conclusion

The new parametrization of e-CPA for sodium chloride has been shown to be able to produce great results for several different properties within a large temperature range. This is accomplished without the use of a volume translation parameter,

which has some unwanted effects on some properties.

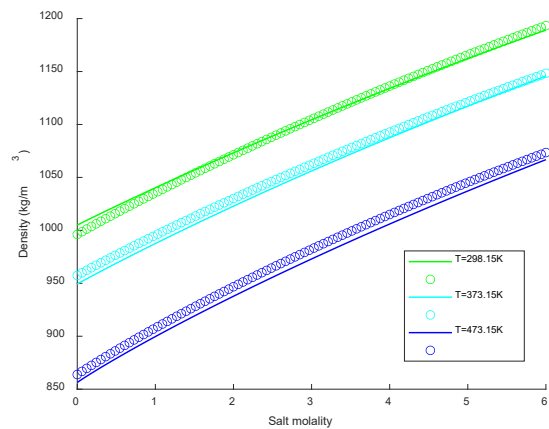


**Figure 3:** The density of sodium chloride in water calculated with model (lines) with the new parameters compared to a correlation of density (o).

## Acknowledgements

The authors wish to thank the European Research Council (ERC) for funding of this research under the European Union's Horizon 2020 research and innovation program (grant agreement No 832460), ERC Advanced Grant project "New Paradigm in Electrolyte Thermodynamics".

## References

1. Kontogeorgis, G.M., Folas, G.K., Thermodynamic Models for Industrial Applications: From Classical and Advanced Mixing Rules to Association Theories, 2010, John Wiley and Sons
2. G.M. Kontogeorgis, E. C. Voutsas, I. V. Yakoumis, and D. P. Tassios. Ind. Eng. Chem. Res. 35 (1996), 11, 4310–4318
3. Schlaikjer, A., Thomsen, K, Kontogeorgis, G.M., 2017, Simultaneous Description of Activity Coefficients and Solubility with eCPA, Ind. Eng. Chem. Res., 56, 1074-1089
4. B. Maribo-Mogensen, K. Thomsen, G. M. Kontogeorgis, 2015, AIChE Journal, 61, 2933-2950
5. A. Schlaikjer, K. Thomsen, and G. M. Kontogeorgis, .Fluid Phase Equilibria, 470 (2018), 176–187

# Phosphorus Chemistry in Biomass Combustion

(December 2019 - November 2022)

7 AFFORDABLE AND  
CLEAN ENERGY



## Contribution to the UN Sustainable Development Goals

Ensuring access to affordable, reliable, sustainable and modern energy for all requires substituting fossil fuels currently widely used for heat and power production by other alternatives. One such alternative is phosphorus rich biomass. However, phosphorus in biomass can cause severe operational problems in combustion processes. Understanding the phosphorus chemistry taking place during biomass combustion will provide a better basis for designing new, and optimizing existing processes able to combust phosphorus rich biomass.



**Emil  
Lidman Olsson**  
eliol@kt.dtu.dk

**Supervisors:** Hao Wu,  
Peter Glarborg,  
Kim Dam-Johansen

## Abstract

Phosphorus in biomass can cause severe operational problems in combustion processes. This PhD project aim to provide a better understanding of the phosphorus chemistry taking place during biomass combustion. As an initial step, the decomposition of the model compound phytate has been studied in order to understand the release of phosphorus to the gas phase. Phytate, being the salt form of phytic acid, is present in many different plants and often contains most of the phosphorus in the plant. Different forms of phytic acid can be used as model compounds to understand how phosphorus behave in different thermal processes. In this work, the decomposition behavior of a sodium phytate has been studied using thermogravimetric analysis to understand how phosphorus will behave in a combustion process.

## Introduction

In the search for alternative fuels to replace the fossil fuels currently widely used for the generation of heat and/or power, the interest for different biomass, especially residues from agricultural and industrial processes, has increased. Some of the biomass residues available in large quantities, such as by-products from animal industry, biodiesel or bioethanol production, or in the form of sewage sludge from waste water treatment contain high levels of phosphorus (P). However, in combustion units, P is reported to have caused operational problems such as bed agglomeration in fluidized bed systems [1], severe deposit formation in grate-fired plants [2] and deactivation of SCR catalyst [3].

In order to address the challenges induced by P species, it is desired to achieve an improved understanding of the P related chemistry in biomass combustion, including the decomposition of organic P compounds, condensed phase transformations, the release of P to the gas phase and reactions taking place in the gas phase. Even though several studies focusing on the interaction between P species and the bed material used in fluidized beds have been undertaken, little is known about the decomposition mechanisms of the organophosphorus species in biomass. In the case

of grate-firing, little is also known about the subsequent release of P species to the gas phase. Some studies of the homogenous gas phase reactions involving P have been undertaken, but only with simple compounds, not involving the often problematic alkali metals present in biomass [4].

In wheat bran and rapeseed cake, being typical residues from biodiesel and bioethanol production respectively, most of the P is present in the form of phytate [5]. Phytate is the salt form of phytic acid, shown in Figure 1. Each phytate unit can coordinate several different cations and common in biomass

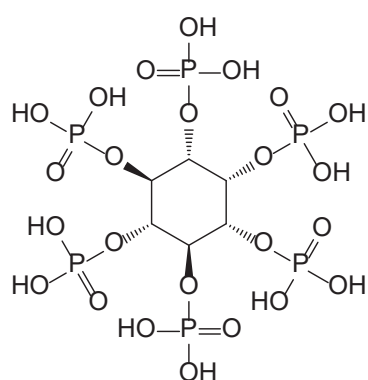


**Figure 1:** Chemical structure of phytic acid

are sodium (Na), potassium (K), Magnesium (Mg) and Calcium (Ca). Phytate, complexed with some of the aforementioned cations should therefore be a good model compound for studying the behavior of P during biomass combustion.

### Specific Objectives

The overall purpose of this PhD project is to provide a better understanding for the high temperature P chemistry taking place during biomass combustion. Starting with studies of the model compound phytate, the aim is to identify the mechanisms responsible for decomposition of phytate and the subsequent release of P under different conditions.

### Results and Discussion

The mass loss of a sodium phytate salt produced from rice containing a Na:phytate ratio of 5:1 was investigated in a thermogravimetric analyzer. The sample was heated in a  $\text{Al}_2\text{O}_3$  crucible up to 1280°C in 10 NmL/min  $\text{O}_2$  and 190 NmL/min  $\text{N}_2$ . The preliminary result is shown in Figure 2.

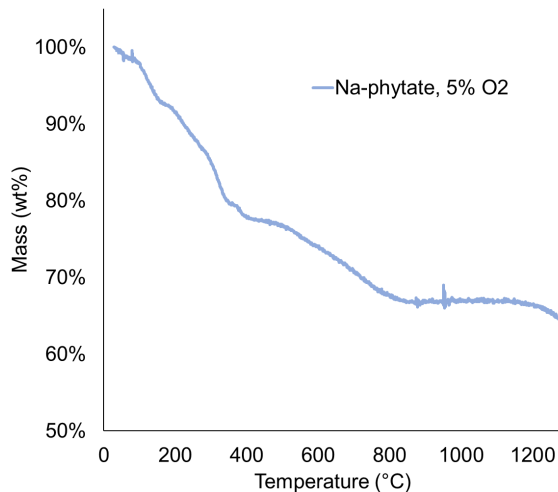


**Figure 2:** Preliminary TGA (thermogravimetric analysis) measurement of Na phytate (Na:phytate ratio of 5:1) at 5%  $\text{O}_2$  and a heating rate of 10°C/min.

The initial decrease, up to about 100°C can be attributed to the release of water from the sample. Above 100°C, up to about 400°C, inter- and intramolecular condensation of the phytate structure results in additional release, also in the form of water molecules. From 400°C to 800°C, the formed carbon structure is probably reacting with

the oxygen in the carrier gas causing it to be released in the form of CO and/or  $\text{CO}_2$ , while P remains in the form of sodium phosphates. The sample mass remains merely constant from 850°C up until about 1200°C, where it starts falling again. Considering the ratio Na:P of 5:6, it is reasonable to believe that sodium metaphosphate,  $\text{NaPO}_3$ , is formed.  $\text{NaPO}_3$  exhibit a low vapor pressure and seem not to evaporate from the sample in considerable quantities until the temperature is above 1200°C.

P rich biomass commonly contains significant amounts of K, Mg and Ca. It is not unreasonable to expect K phytates will behave similarly to the corresponding Na phytate. But in combination with Ca and/or Mg, the formed phosphates might be captured in more stable alkali - alkali earth metal - phosphates, preventing the release of P to the gas phase.

### Conclusions

In an oxidizing atmosphere, the release of P from the investigated phytate depends on the volatility of the formed phosphate.

In future work, the behavior of phytate in other atmospheres, e.g. inert and reducing should also be investigated in order to understand the fate of these compounds in pyrolysis and gasification processes. It also remains to be verified if a similar behavior of P is observed for real biomass. The behavior of other model compounds is currently being investigated.

### Acknowledgements

The project has received financial support from the Sino-Danish Center for Education and Research, and from Technical University of Denmark (DTU) for collaboration with DTU's alliance partners.

### References

1. Grimm A, Skoglund N, Boström D, Öhman M. Energy and Fuels 2011;25:937–47.
2. Wu H, Castro M, Jensen PA, Frandsen FJ, Glarborg P, Dam-Johansen K, et al. Energy and Fuels 2011;25:2874–86.
3. Castellino F, Rasmussen SB, Jensen AD, Johnsson JE, Fehrmann R. Appl Catal B Environ 2008;83:110–22.
4. Korobeinichev OP, Shwartsberg VM, Shmakov AG. Russ Chem Rev 2007;76:1094–121.
5. Frank AW. Phytic Acid. Chem Plant Phosphorus Compd 2013:75–134.

# Experimental Investigation of CH<sub>4</sub>/CO<sub>2</sub> Mixed Hydrate Phase Behavior During CH<sub>4</sub> Recovery and CO<sub>2</sub> Storage

(July 2018- June 2021)

7

AFFORDABLE AND  
CLEAN ENERGY



## Contribution to the UN Sustainable Development Goals

Large amount of methane-rich gas hydrate reservoirs, discovered in permafrost and deep ocean sediments, are seen as a source of cleaner energy and alternative to fossil fuels. Methane production from such deposits is currently being investigated using different production methods. Recently CO<sub>2</sub> rich gas injection into these reservoirs is proposed as a potential method to recover methane from hydrate deposits. This method is a carbon neutral method as it produces Methane and stores carbon dioxide in hydrates simultaneously without destabilizing the hydrates. This PhD project is focused to understand many unknown associated with this technique. (Jyoti S Pandey)



**Jyoti Shanker  
Pandey**  
jyshp@kt.dtu.dk

**Supervisor:**  
Prof Nicolas von Solms,  
Prof Alexander Shapiro

## Abstract

In this study, we investigate the formation and dissociation pattern of CH<sub>4</sub>/CO<sub>2</sub> mixed hydrate in porous media. Phase transitions of CH<sub>4</sub>/CO<sub>2</sub> mixed hydrate in sediments will continuously take place during recovery of CH<sub>4</sub> gas by CO<sub>2</sub> injection. The recovery efficiency of CH<sub>4</sub> gas depends on the amount of liquid water present in the pore space and the recovery efficiency can be aided by pressure depletion. In this scenario, it is important to evaluate the composition of the hydrate that dissociates and possibly reforms during pressure reduction in the presence of both CO<sub>2</sub> and CH<sub>4</sub>. We formed CH<sub>4</sub>/CO<sub>2</sub> mixed hydrate from gaseous CH<sub>4</sub> and liquid/gaseous CO<sub>2</sub> to mimic the scenario where a CH<sub>4</sub> hydrate reservoir has been injected with CO<sub>2</sub>. Pore and core scale investigation will be carried.

Pore scale investigation is done using a high-pressure, water-wet, silicon-wafer based micromodel with a pore network of actual sandstone rock. Mixed hydrate was formed at reservoir conditions from either a two phase system (liquid water and CH<sub>4</sub>/CO<sub>2</sub> gas mixture) or a three phase system (liquid water, CH<sub>4</sub> gas, and liquid CO<sub>2</sub>). A stepwise pressure reduction method was later applied to record multiple dissociation pressure points for a given mixed hydrate system, and the molar concentration of CH<sub>4</sub>/CO<sub>2</sub> corresponding to each dissociation point was calculated. The effect of hydrate and fluid saturation on fluid flow during dissociation was also analyzed.

## Introduction

Gas hydrates are ice-like crystal compounds formed when water and gas come together at high-pressure and low-temperature conditions. Many gases are known to form a hydrate, but the most exciting gases for research purposes are methane (CH<sub>4</sub>) and carbon dioxide (CO<sub>2</sub>). Methane gas is naturally found in hydrate form in colder regions, such as the permafrost region in Alaska, Siberia, and deep ocean sediments, as in the South China Sea, Gulf of Mexico, and Japan Sea.

These methane hydrate deposits are considered a potential source of gas recovery in the coming years, and my research is focused on recovering methane gas by injecting CO<sub>2</sub> gas that replaces CH<sub>4</sub> and allows CO<sub>2</sub> storage in the same place. Hydrate formation in sediments is a complex phenomenon,

and it is important to understand the pore-scale mechanisms to exploit it on a large scale.

Micromodel-based, pore-scale experiments are very useful experimental tools to observe the fluid flow behavior within pore space. Micromodel is also known as microfluidics, includes microchip mimicking rock pore structure at the micrometer scale. With the help of pore-scale visualization, we could understand the hydrate formation and dissociation behavior and correlate the microscale experiments with core-scale findings. Micromodel chips will also help to visualize the effect of different pore sizes and the effect of salinity on formation and dissociation mechanisms. In general, flow within micromodel is laminar, hence transportation of liquid is predictable and easily observable due to the transparent nature of the microchip. Experiments

are performed in a controlled manner using controlled flow rates and pressure.

### Specific Objectives

The primary purpose of this research is to understand gas hydrate formation and dissociation in the porous medium. My research involves pore level (micrometer) to core-scale (centimeter) experiments to understand methane gas hydrate formation and dissociation behavior. I also study the influence of different parameters, including initial water/gas saturation and sediment properties, on methane recovery and CO<sub>2</sub> storage.

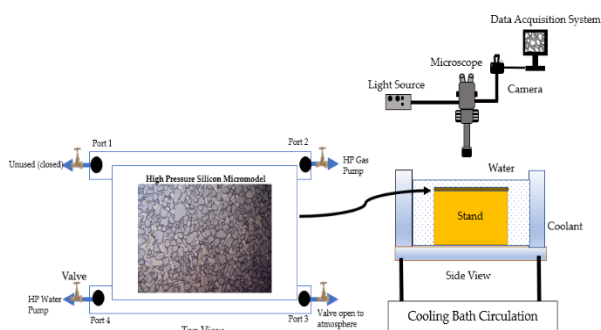


**Figure 1:** Micromodel chip saturated with water and gas (left) and experimental setup (right)

### Methodology

#### Pore Scale Experiment

In this study, a silicon-based micromodel is used for hydrate formation and dissociation visualization. Micromodel is built by a glass plate anodically bonded with a silicon wafer. Anodic bonding procedure leads to water wet micromodel. The water wet nature of solid grain induces the curve interface between water and gas and easy to differentiate between different fluid phases. The model consists of average pore diameter of 100 μm and a constant vertical height of 25 μm. Pore shape and size are based on thin section analysis of the sandstone. This reproduction of actual pore bodies, pore neck, and coordination number makes the model suitable for the fluid flow and phase equilibrium phenomenon. Micromodel based images are acquired, and segmented images are generated to calculate the two-dimensional fluid saturation.

#### Initial Results

Understanding of initial hydrate saturation is very critical of the selection of correct production technique. Hydrate saturation and water saturation plays a crucial role during the dissociation in the permafrost region. Very high and very low hydrate saturation both show a negative effect on the rate of hydrate dissociation due to the presence of a high

self-preservation effect. (Figure 2)

Due to different hydrate melting mechanisms, hydrate dissociation rates and patterns are different for hydrate shells and hydrate crystals. When pressure front arrives at the pore space, hydrate shells start to dissociate from the center of the pore to corner due to differences in thickness while

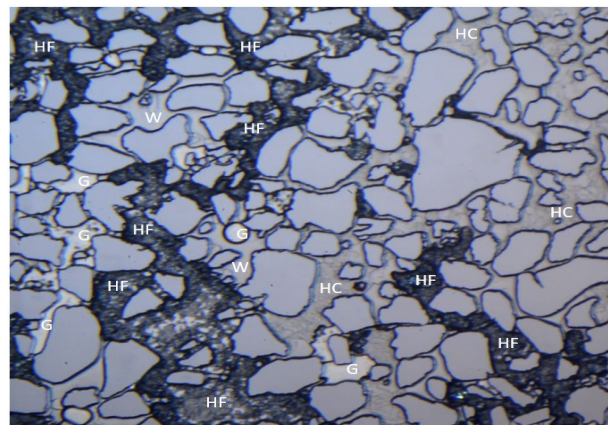


**Figure 2:** Example of High gas hydrate saturation in micromodel. HF refers to hydrate film, HC refers to hydrate crystals, G refers to free gas, and W refers to water.

hydrate crystals melt uniform, releasing the free gas which further dissociates neighbor hydrates. Gas only began to mobilize in the former case, when hydrate shells are completely melted while it is not the case with hydrate crystals.

#### References

1. B. Tohidi, R. Anderson, M. Ben Clennell, R. W. Burgass, and A. B. Biderkab, "Visual observation of gas-hydrate formation and dissociation in synthetic porous media by means of glass micromodels," *Geology*, vol. 29, no. 9, pp. 867–870, 2001.
2. D. Katsuki, R. Ohmura, T. Ebinuma, and H. Narita, "Visual observation of dissociation of methane hydrate crystals in a glass micro model: Production and transfer of methane," *J. Appl. Phys.*, vol. 104, no. 8, 2008.
3. L. P. Hauge, J. Gautepllass, M. D. Høyland, G. Ersland, A. Kovscek, and M. A. Fernø, "Pore-level hydrate formation mechanisms using realistic rock structures in high-pressure silicon micromodels," *Int. J. Greenh. Gas Control*, vol. 53, pp. 178–186, 2016.

# Real-Time Evaluation of the Settlement of Marine Biofouling

(December 2019- November 2022)



## Contribution to the UN Sustainable Development Goals

Developing new and more reliable evaluation methods for better prediction of practical behavior of fouling control coatings will improve and ease the screening task of different fouling control coatings. Improvement of the screening will help the development of fouling control coatings towards new and environmentally friendly coatings. This will reduce the release of harmful biocides into the ocean, while still protecting the ships and other off-shore constructions from the undesired problems caused by marine biofouling.



**Morten  
Lysdahlgaard  
Pedersen**

mlyped@kt.dtu.dk

**Supervisors:** Kim Dam-Johansen, Huichao Bi, Claus Erik Weinell, Weigang Lin

## Abstract

Quick and reliable evaluation of fouling control coatings, is essential in the movement towards new and environmental friendly coatings. The detection and classification of different types of biofouling using image analysis is a step towards an objective and valid evaluation method. The program *ilastik* is used to train a pixel classification model, which provides a simple segmentation. The segmentation is used to determine the percentage of different types of biofouling covering the exposed panels. Utilizing the guidelines of the European Chemicals Agency these percentages are used to calculate a fouling resistance rating.

## Introduction

The purpose of this project is to develop new evaluation methods for quick and reliable testing of fouling control coatings. Fouling control coatings are used to protect against marine biofouling, which is defined as the undesirable accumulation of microorganisms, plants, and animals on artificial surfaces immersed in seawater [1]. For ships, biofouling can cause problems such as increased weight, speed reduction, and loss of maneuverability. To compensate for the speed reduction the fuel consumption is increased, which means increased emission of environmentally harmful compounds [2, 3]. One of the conventional methods for testing fouling control coatings is to immerse samples in strategic placed test sites. During and after the exposure, the samples are visually inspected, to evaluate the resistance against biofouling. The European Chemicals Agency provided a guideline [4] on how to calculate a fouling resistance rating. The rating focus on four main categories of biofouling light slime, dense slime, macroalgae, and animals. From the visual inspections, a percentage of the coverage of each of these categories on the sample is determined. This percentage is the basis for the fouling resistance rating and it is highly subjective.

## Specific Objective

This project aims to achieve a reliable and objective way of evaluating the fouling resistance. One way to achieve this is through the utilization of image analysis, such as pixel classification. The idea is to train the system to recognize or label different kinds of biofouling. Thereby, be able to estimate a percentage of the different fouling categories covering the test sample, which is used in the calculation of the fouling resistance rating.

## Method

Over the summer of 2020, 56 acrylic panels of size 100x200mm were immersed at the newly established CoaST Maritime Test Centre at Hundested harbor. The panels were coated with Hempel's Hempthane HS 55610, which is a polyurethane topcoat without any fouling control properties. This paint was chosen as the purpose was to follow the fouling growth and investigate the type of biofouling found in Hundested harbor. The panels were immersed over three months and every week, they were taken out of the water for inspection. The inspection consisted of both a visual inspection and documentation of the fouling development. At each inspection, the panels were

individually placed in a Falcon Eyes Photo Bow FLB 616AB photo box, and pictures of the panels were taken by a Canon EOS 250D camera, with a Canon EF LENS 50mm 1:1,8 STM. The camera was controlled through the EOS Utility program on the computer, using the following manual settings, 1/250, F2.5, ISO 100, data format RAW (CR3). The pictures were then resized and converted to a TIFF format using python. A group of the pictures have been used to label and train a pixel classification model using the program ilastik. The trained model is used on another group of pictures to get a simple segmentation of the different labels, which are barnacles, mussels, microalgae, macroalgae, and the background. From the segmentation, it is possible to calculate a coverage percentage of the different fouling categories on the panels, which can be used in the calculation of the fouling resistance rating according to the European Chemicals Agency standard.

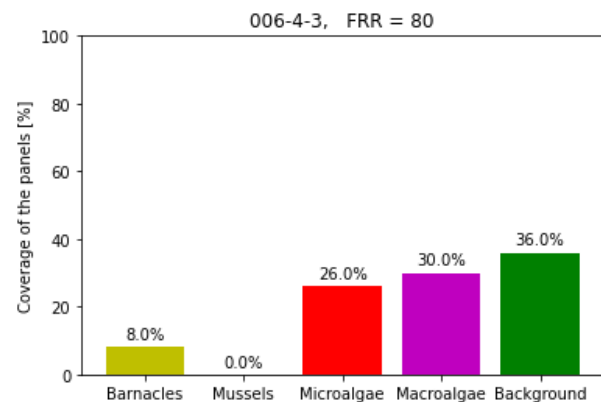
## Result and Discussion

Figure 1 illustrates the picture, which is given as input the pixel classification model after it has been resized and converted to a TIFF file. Based on the labeling and training performed in ilastik, a simple segmentation is calculated. The segmentation is used to determine the percentages shown in the bar chart in Figure 2. The percentages are then used according to the European Chemicals Agency guidelines, to calculate the fouling resistance rating (FRR) given in the title of Figure 2. The fouling resistance rating is given as a number between 0 and 100, where 100 is the best.



**Figure 25:** Here is a picture of the panel, after resizing and converting it to a TIFF. It is the type of pictures used in the pixel classification model.

The pixel classification model is trained on 80 pictures and tested on 50 pictures. The result seems promising, but there is still some wrong classification, which needs to be looked into. Therefore, the training needs to be revisited and improved, to obtain an even better classification. Furthermore, a deeper and more detailed analysis of the segmentation result needs to be performed, to verify the classification.



**Figure 2:** The result from the simple segmentation is shown here as a bar chart, presenting the percentage for each fouling category. In the title, the fouling resistance rating (FRR) is given.

## Conclusion

It is shown, that pixel classification can be trained to distinguish between different types of biofouling. Thereby, enabling the possibility to determine a percentage of the fouling covering the exposed panels. This method provides an objective and reliable determination of the coverage percentages of the biofouling, which is the baseline for the fouling resistance rating.

## Acknowledgement

A special thanks to the Sino-Danish Center (SDC) for partially founding of this project. Another thanks to the Hempel Foundation for the financial support to CoaST (The Hempel Foundation Coating Science and Technology Center).

## References

1. D. M. Yebra, S. Kiil, K. Dam-Johansen, Progress in Organic Coatings, 50 (2) (2004) 75-104.
2. M. A. Champ. Science of the Total Environment, 258 (1-2) (2000) 21-71.
3. A. Abbott, P. D. Abel, D. W. Arnold, and A. Milne. Science of the Total Environment, 258 (1-2) (2000) 5-19.
4. European Chemicals Agency, Transitional Guidance on the Biocidal Products Regulation, 2014.

# Ecological Control Strategies for Biobutanol Production

(January 2018- December 2020)

7 AFFORDABLE AND  
CLEAN ENERGY



## Contribution to the UN Sustainable Development Goals

For a smoother transition towards a bio-based society, no longer dependent on current liquid fossil fuels, sustainable alternatives to energy sources like gasoline and diesel need to be implemented. Due to their similarities, butanol can already today be used as direct replacement for gasoline. In this project we aim at producing butanol from butyrate, a low-value substrate and often disposed of in biotech processes, contributing therefore to the recovery of waste products into added-value commodities.



**Tiago  
Pinto**

[tiapi@kt.dtu.dk](mailto:tiapi@kt.dtu.dk)

**Supervisor:** Xavier Flores  
Alsina, Krist V. Germaey,  
Helena Junicke

## Abstract

For a smoother transition towards a bio-based society, no longer dependent on current liquid fossil fuels, sustainable alternatives to energy sources like gasoline and diesel need to be implemented. Due to their similarities, butanol can already today be used as direct replacement for gasoline. Due to their microbial diversity, mixed microbial cultures (MMC) can overcome the limitations of pure cultures and potentially become the predominant bio-based production platform for biobutanol. Butanol can be produced using only butyrate and hydrogen ( $H_2$ ), common intermediates during the decomposition of organic residues, as is the case for industrial waste streams. By consuming a cheap feedstock alternative that avoids competition with food production, we contribute to a more circular and sustainable fuel bioeconomy.

## Introduction

Accounting for nearly 65% of the world's consumption [1], liquid fossil fuels are the major target for renewable and sustainable research. The search for renewable liquid fuels capable of replacing e.g. gasoline and diesel has in many cases focused on biorefinery approaches. In recent years, biorefineries have expanded their use of renewable feedstocks to now include resources that were once seen as waste. Research on renewable liquid fuels is now also focused on waste valorization and recovery [2].

Bioethanol and biobutanol are the two top contenders for liquid fossil fuel replacement. But of the two, biobutanol is a much more interesting biofuel, with a higher energy density, can be blended with gasoline to any ratio without engine modification, a low solubility in water, and higher boiling and flash point making it safer than bioethanol [3].

The most common process for biobutanol production is the Acetone-Butanol-Ethanol (ABE) fermentation by anaerobic bacteria, mostly belonging to the *Clostridia* family. Although pure cultures of *Clostridium* can achieve high yields, they have strict pure substrate requirements. In this

context, mixed culture biotechnology is seen as a promising solution over pure strain culture due to its many advantages: non-sterile conditions, mixed and/or waste substrates, ecological selection, and continuous operation processes [4, 5].

## Specific Objectives

The focus of the project is to enrich butanol-producing microorganisms through directed ecological selection in a continuously stirred tank reactor, starting from non-defined microbial communities fed on butyrate and hydrogen. By engineering the environment rather than the organism, we move towards the use of low-value feedstock for the production of a valuable chemical such as butanol, as opposed to the use of higher value substrates e.g. glucose, contributing to the progress of circular bio economy.

## Results and Discussion

To ensure process consistency, batch fermentations in Schott bottles closed with butyl rubber stoppers were first conducted to determine possible limitations of the selected MMCs. It was found that anaerobic butyrate conversion was selectively inhibited under the chosen operational

conditions ( $\text{pH}$  5.5 and  $p_{\text{H}_2}$  of 1.5 bar), and production of butanol from butyrate was favored (Figure 1). Other studies have also shown this to occur [6].

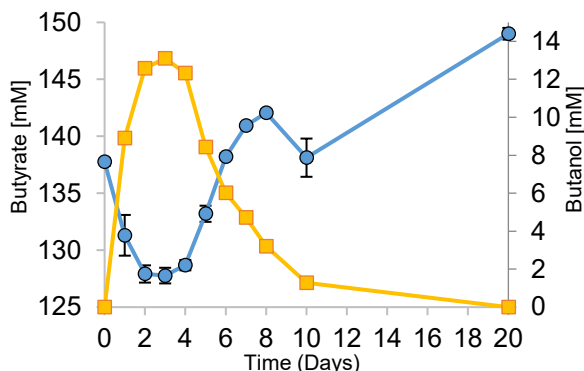


**Figure 26 –** Butyrate (blue) and butanol (yellow) profiles in Schott bottles.

Interestingly, after 3 days of fermentation, butanol production stopped and even reverted (Figure 1). Pathway reversibility is likely to occur for reactions that proceed very close to thermodynamic equilibrium.

If conditions are favorable, the reverse reaction to butanol production from butyrate is possible. For that, the pH would have to be higher than the initial pH set for each experiment ( $\text{pH}$  5.5). Due to the nature of the experiment, pH control when using Schott bottles is not much feasible, and as such when butyrate was consumed it increased the pH of the fermentation to close to  $\text{pH}$  6.5 leading to worse conditions for butanol formation and better conditions for butanol conversion into butyrate.

Moving forwards to a system where pH control is possible at the desired set point, first butanol production is still observed and second plenty of other secondary metabolites are produced (Figure 2). Multi-product formation highlights not only the versatility of mixed microbial cultures but also how such systems can be specifically tailored to improve one or more desired products.

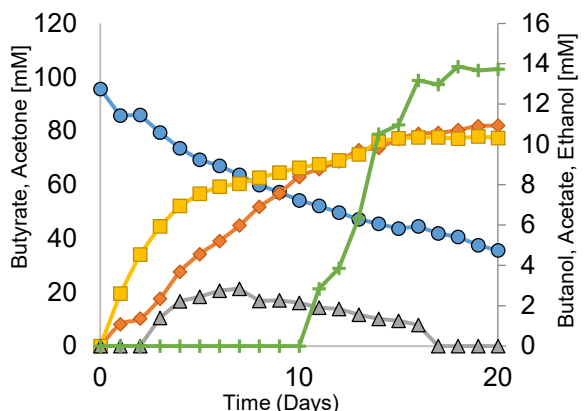


**Figure 27 –** Butyrate (blue), butanol (yellow), acetone (orange), acetate (grey) and ethanol

(green) profiles for butyrate conversion in a bioreactor system.

Continuous fermentation is the next step in proving the feasibility of biobutanol production from butyrate and hydrogen by mixed microbial cultures.

## Conclusions

Butanol production from butyrate and hydrogen is feasible under the set of conditions initially hypothesized. pH control showed to be of critical importance, and when scaling up the current system to bioreactors ( $> 2\text{ L}$ ) this will become more feasible and expected to help achieve better yields. The butanol concentrations obtained in this work were about three times larger than previously reported [8], hinting at future applications of MMC for continuous butanol production from waste streams.

## Acknowledgements

This work is supported by the European Union's Horizon 2020 research and innovation programme under the Marie Skłodowska-Curie grant agreement number 713683 (COFUNDfellowsDTU), by the Danish Council for Independent Research in the frame of the DFF FTP research project GREENLOGIC (grant agreement No. 7017-00175A), by the Novo Nordisk Fonden in the frame of the Fermentation-Based Biomanufacturing education initiative, and by the Danida fellowship Center under the project ERASE (18-M09-DTU).

Acknowledgements also to Farah Ali El-Zouheiri (MsC) for her contribution in the GREENLOGIC project.

## References

1. Key world energy statistics. Int Energy Agency 2017.
2. S.S. Mansouri, I.A. Udagama, S. Cignitti, A. Mitic, X. Flores-Alsina, K.V. Gernaey. Current Opinion in Chemical Engineering, 18 (2017) 1-9.
3. N. Abdehagh, F. Tezel, J. Thibault, Biomass and Bioenergy, 60 (2014) 222-246.
4. R. Kleerebezem, M.C. van Loosdrecht. Current Opinion in Biotechnology, 18 (3) (2007) 207-212.
5. I.A. Udagama, L.A.H. Petersen, F.C. Falco, H. Junicke, A. Mitic, X.F. Alsina, S.S. Mansouri, K.V. Gernaey. Food and Bioproducts Processing, In Press, Available 31 October 2019.
6. H. Junicke, M.C. van Loosdrecht, R. Kleerebezem. Applied Microbiology and Biotechnology, 100 (2), (2016) 915-925.
7. K.J.J. Steinbusch, H.V.M. Hamelers, C.J.N. Buisman. Water Research 42 (2008) 4059-4066

# Multiscale Modeling of Liquid-Liquid Phase Transfer Catalysis

(November 2019 - October 2022)



## Contribution to the UN Sustainable Development Goals

Phase transfer catalysis is an intensified reactive extraction process with wide applications. It allows for waste reduction, waste valorization, lower solvent use, lower energy consumption, higher yields, etc. Providing a better mechanistic understanding of this process would promote a systematic and more widespread adoption of the technology. This in turn has a huge potential for a positive impact in terms of sustainable and responsible consumption and production of resources.



**Abhimanyu  
Pudi**

abpudi@kt.dtu.dk

**Supervisor:** Martin Andersson, Seyed Soheil Mansouri

## Abstract

An integrated and multiscale modelling architecture is developed to describe phase transfer catalysis. It is then applied to a case study of hydrogen sulfide valorization. Recovery and conversion of hydrogen sulfide from an aqueous alkanolamine solution to value-added organic products improves economics and sustainability of sour gas desulfurization by providing a waste-to-value pathway toward resource recovery and circular economy. The model results match well with the experimental data, motivating the further application of this modelling approach towards other biphasic processes and similar systems.

## Introduction

Phase transfer catalysis (PTC) is a general methodology applicable to a wide variety of reactions in which the reactions take place in heterogeneous two-phase systems (organic-aqueous) with negligible mutual solubility of the phases. This type of two-phase system offers numerous advantages, such as high yields and purity of the products, operational simplicity, mild reaction conditions, suitability for large-scale synthesis, and an environmentally benign nature of the reaction system [1–3].

However, the downside of PTC is the need to quantify exacting reaction conditions and parameters that are difficult to uncover and, in some cases, are counterintuitive [4]. Although there has been some progress in terms of mathematical modeling of PTC systems [5–7], availability of accurate thermodynamic parameters still proves a major limitation as the chemical domain in the group contribution methods, such as UNIFAC, is inherently limited to the portion of the chemical design space for which every binary interaction parameter is available.

In this respect, COSMO-based models, such as COSMO-RS [8,9], are valuable alternatives for describing liquid-phase thermodynamics since they do not require any binary interaction parameters.

Furthermore, COSMO-RS allows for easy integration of quantum chemical calculations into a process modeling framework, greatly expanding the envelope of chemical species that can be modeled at a high level of accuracy.

The primary objective of this work is to develop a rigorous and multiscale mathematical model to describe PTC and demonstrate its application to desulfurization of sour natural gas which has been an increasing concern for the energy industry due to the high economic and environmental cost of the existing technologies. Application of PTC to this problem can effectively overcome these issues by providing a waste-to-value pathway toward resource recovery and circular economy.

## Modeling Framework

The present work employs sequential multiscale modelling by using different tools for different scales of time and space to model and predict the behaviour of the PTC system. The use of quantum chemistry and COSMO-RS makes the framework much more generic in terms of its application in comparison to other thermodynamic models.

The algorithm is illustrated in Figure 1. With Python as the high-level interface, three different tools are employed at three different levels of space and time: (a) Turbomole at the molecular/electronic

level, (b) COSMOtherm at the thermodynamic level, and (c) Pyomo at the reactor level.

For each species in the system, geometric optimization calculations are performed in Turbomole using density functional theory (DFT) to obtain their ground-state and gas-phase energies and screening charge density profiles. These are then transferred to COSMOtherm that uses COSMO-RS to obtain partition coefficients, activity coefficients, and chemical equilibrium constants, which are all parameters for the PTC model. These parameters are then sent to Pyomo where the equations for equilibria, kinetics, and balances are solved to model the system behaviour.

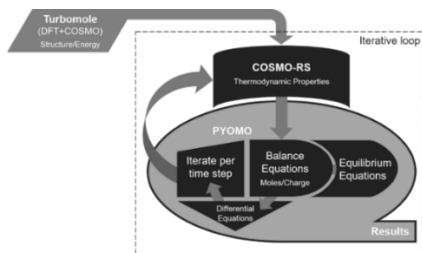


**Figure 28:** Modeling Framework and Solution Algorithm

### Application and Validation

Hydrogen sulphide ( $H_2S$ ) is a highly toxic chemical that is found as an impurity or an inhibitor in many petrochemical, chemical and biochemical processes. In fact, it is classified as a hazardous industrial waste. Environmental and/or process constraints often require the removal of this compound to trace amounts. This is usually accomplished by capturing  $H_2S$  in an aqueous alkanolamine solvent and later oxidizing the separated, pure  $H_2S$  to elemental sulfur. This is generally an expensive process, owing largely to the capital- and energy-intensive stripper column and multistage Claus process.

PTC offers an alternative to this process by replacing the expensive stripper column. One major advantage of this route is the ability to target a wide variety of products, instead of only elemental sulfur or inorganic sulfates. The  $H_2S$ -rich aqueous phase exiting the absorber is put in contact with an organic phase (here toluene) containing benzyl chloride (BC) to produce benzyl mercaptan (BM) and dibenzyl sulphide (DBS) in the presence of a PT catalyst such as tetrabutylammonium bromide (TBAB). TBAB reacts with the inorganic sulfide anion in the aqueous phase to produce the active catalyst species. This species then partitions into the organic phase transporting the hydrosulfide ion to participate in the nucleophilic substitution reactions with BC.

The modelling framework is applied to this system and compared to the experimental data reported by Singh et al. [10]. The developed model can solve for equilibrium but is not yet capable of describing the dynamic behaviour of the reactor. The equilibrium results obtained from the model and the experiment

at 333 K are shown in Table 1. The excellent match in the numbers reported in the table demonstrates the success and strong applicability of the PTC modelling framework developed in this work.

**Table 7: Performance Evaluation**

Criterion	Experiment	Model
BC Conversion	94%	93%
DBS Selectivity	86%	83%

### Conclusion

Quantum chemistry and statistical thermodynamics can help us understand and model multiphase extraction-reaction processes, such as phase transfer catalysis, that haven't been successfully modeled with the existing modeling approaches. In this work, a rigorous multiscale modelling framework to describe the behavior of a phase transfer catalysis system is presented. Integration of computational chemistry into a process model provides a broad chemical domain to explore new solvents, catalysts, and reactions. Current results look promising and demonstrate the strength of this approach. Future work will focus on the development of a dynamic model.

### Acknowledgements

This project is funded by the Danish Hydrocarbon Research & Technology Centre and the Sino-Danish Center.

### References

1. M. Mąkosza, M. Fedoryński, *Catalysis Reviews - Science and Engineering* 45 (2003) 321–367.
2. D. Albanese, *Catalysis Reviews - Science and Engineering* 45 (2003) 369–395.
3. S. Shirakawa, K. Maruoka, *Angewandte Chemie - International Edition* 52 (2013) 4312–4348.
4. S.D. Naik, L.K. Doraiswamy, *AIChE Journal* 44 (1998) 612–646.
5. J.A.B. Satrio, L.K. Doraiswamy, *Chemical Engineering Science* 57 (2002) 1355–1377.
6. C. Piccolo, A. Shaw, G. Hodges, P.M. Piccione, J.P. O'Connell, R. Gani, *Computer Aided Chemical Engineering* 30 (2012) 757–761.
7. A. Anantpinijwatna, M. Sales-Cruz, S.H. Kim, J.P. O'Connell, R. Gani, *Chemical Engineering Research and Design* 115 (2016) 407–422.
8. A. Klamt, *Journal of Physical Chemistry* (1995).
9. A. Klamt, V. Jonas, T. Bürger, J.C.W. Lohrenz, *Journal of Physical Chemistry A* (1998).
10. G. Singh, P.G. Nakade, D. Chetia, P. Jha, U. Mondal, S. Kumari, S. Sen, *Journal of Industrial and Engineering Chemistry* 37 (2016) 190–197.

# Investigation and improvement of zinc-rich coatings

(April 2019-April 2022)



## Contribution to the UN Sustainable Development Goals

Metal lost due to corrosion has been an industrial issue with high cost implications, which is estimated to be 2.5–4% of the gross world's production. Zinc-rich coatings are one of the most effective protective coatings widely used in industrial and marine environments. A high zinc content is required in the zinc-rich coatings to ensure the protective ability. This project aims to reduce the loading of relatively expensive and toxic zinc.



**Chunping  
Qi**

chuqi@kt.dtu.dk

**Supervisor:** Kim Dam-Johansen; Hao Wu; Claus Erik Weinell

### Abstract

Zinc-rich coating is one of the effective coatings for corrosion protection. In this work, the effect of Fe on the performance of zinc-rich coating was studied with different replacement amount of iron powder. The coatings properties were investigated by electrochemical tests and salt spray test. It was revealed that the Fe-modified zinc-rich coatings with a small replacement of zinc dust by iron powder have comparable anticorrosive properties compared with the blank zinc-rich coating.

### Introduction

Zinc-rich coating is widely used for corrosion protection of steel in industrial (e.g. bridges, pipeline) and marine (e.g. ships, offshore platforms) environments. The protective ability of zinc-rich coating is based on two primary mechanisms: in the initial stage, active zinc particles in the coating act as sacrificial anode (cathodic protection stage), and at longer period of its service life, zinc corrosion products are formed sealing the microholes of the coating (barrier protection stage) [1]. Typically, in order for cathodic protection to take place, a high zinc content (over 80 wt% in the dried film) is essential to ensure high electrical conductivity of coating film, i.e. zinc particles should be electrically contact with each other and with steel substrates. However, such a high zinc content in coatings often results in a poor adhesion and decreased mechanical properties. Besides, zinc and its compounds are recognized as toxic to aquatic life. Considering these facts together with the relatively high cost and low utilization ratio of metallic zinc pigment, many efforts have been made to develop zinc-rich coatings with competitive anticorrosive performance at reduced zinc loading. Many substituents such as zinc alloy, conductive polymers/composites (e.g. polypyrrole, polyaniline, polyaniline/graphite oxide composites), conductive fillers (e.g. graphite, carbon black, carbon fibers, Fe<sub>2</sub>P), lamellar fillers (e.g. mica, micaceous iron oxide), unmodified/modified carbon nanotubes and

graphene (oxides), inhibitors, ionic liquids, and nanoparticles (e.g. Zn, Al, SiO<sub>2</sub>) have been investigated to reduce the zinc content and improve the coating performance [2-6]. However, the replacement amount of these substituents and the improvement of coating performance is very limited due to the influence of electrical conductivity.

### Objectives

The main objective of this project is to find good conductive substituents to replace part of zinc dust in zinc-rich coatings. The cathodic protection and barrier effect of the coatings will be studied.

### Results and discussion

In this section, iron powder is used as a conductive substituent of zinc dust in the zinc-rich coating. Five coatings, the blank zinc-rich epoxy coating (ZRE, 82 wt% Zn in the dry film), Fe-modified ZRE coatings with 5, 10, 20 and 43 wt% of Fe, respectively, replacing the same amount of Zn in the coating, were prepared to study the effect of iron powder on the performance of the zinc-rich coating.

The anticorrosive properties of the coatings were evaluated by accelerated salt spray test. From Figure 1, the first three samples show small difference on the surface appearance (with less red rust and no blisters formed) after 40 days of exposure, while severer corrosion were observed at scribe areas of 20Fe-ZRE and 43Fe-ZRE, and

many blisters were formed around scribes for the 43Fe-ZRE.

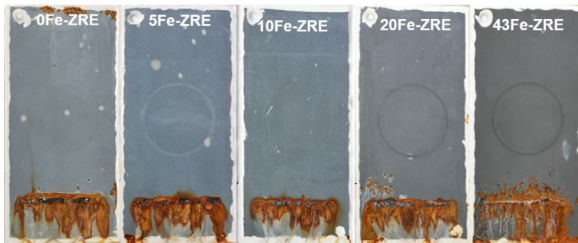


**Figure 1.** Photographs of the prepared coatings after exposure for 40 days.

The cathodic protection duration (period during which OCP is less than 0.86 V vs. SCE) could be estimated from the open circuit potential test. As shown in Figure 2, among five samples, 0Fe-ZRE and 10Fe-ZRE show longer cathodic protection duration (about 17 days), and 43Fe-ZRE has only barrier protection without cathodic protection for the low Zn content. The reason might be that at low Fe content, the partial replacement of Zn particles ( $D_{50}=10.5 \mu\text{m}$ ) with smaller Fe particles ( $D_{50}=8.1 \mu\text{m}$ ) gives better particles packaging and thereby better electrical connectivity. However, due to the inherent more positive potential of Fe, and on the other hand, Fe accelerates the activation and corrosion rate of Zn in the coating, with the further increase of Fe content, the OCP becomes positive, and thereby shortening the cathodic protection duration.

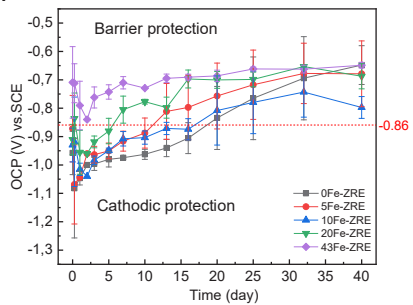


**Figure 2.** The OCP variation of the prepared coatings versus exposure time. The dotted line (-0.86 V) represents the thermodynamic protection limit.

Electrochemical behavior of coatings were investigated by impedance spectroscopy (EIS) measurements. The charge transfer resistance ( $R_{ct}$ ) is to characterize the corroding reaction and the impedance modulus at the lowest frequency ( $|Z|_{0.01\text{Hz}}$ ) can be used to analyze the barrier property of the coating. The decrease of  $R_{ct}$  at the initial period of exposure indicates better activation and oxidation of zinc, and thus better cathodic protection. At late stage, higher impedance modulus indicates the coating has better barrier protection. As shown in Figure 3, 0Fe-ZRE, 5Fe-ZRE, 10Fe-ZRE have comparable anticorrosive properties, while 20Fe-ZRE shows a relatively

higher  $R_{ct}$  at the beginning and lower  $|Z|_{0.01\text{Hz}}$  for long time, and 43Fe-ZRE has significantly lower  $R_{ct}$  and  $|Z|_{0.01\text{Hz}}$  during the whole test period, indicating the worst cathodic and barrier protection, which is consistent with the salt spray testing result.

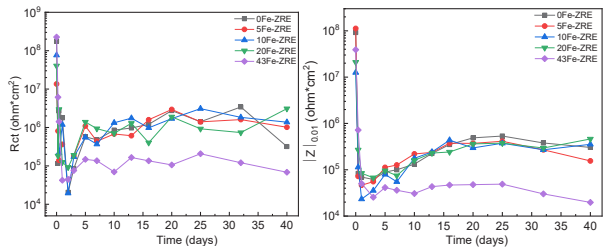


**Figure 3.** The charge transfer resistance (left) and impedance modulus (right) of the prepared coatings.

## Conclusion

Salt spray test and electrochemical tests show that the Fe-modified ZRE coatings have comparable anticorrosive properties when the replacement amount of Fe is no more than 10 wt%.

## Acknowledgements

This project is funded by China Scholarship Council (CSC) and Hempel Foundation.

## References

1. Abreu, C. M., Izquierdo, M., Merino, P., Novoa, X. R., & Perez, C. (1999). A new approach to the determination of the cathodic protection period in zinc-rich paints. *Corrosion*, 55(12), 1173-1181.
2. Ge, T., Zhao, W., Wu, X., Lan, X., Zhang, Y., Qiang, Y., & He, Y. (2020). Incorporation of electroconductive carbon fibers to achieve enhanced anti-corrosion performance of zinc rich coatings. *Journal of Colloid and Interface Science*, 567, 113-125.
3. Arman, S. Y., Ramezanzadeh, B., Farghadani, S., Mehdipour, M., & Rajabi, A. (2013). Application of the electrochemical noise to investigate the corrosion resistance of an epoxy zinc-rich coating loaded with lamellar aluminum and micaceous iron oxide particles. *Corrosion science*, 77, 118-127.
4. Cao, X., Huang, F., Huang, C., Liu, J., & Cheng, Y. F. (2019). Preparation of graphene nanoplate added zinc-rich epoxy coatings for enhanced sacrificial anode-based corrosion protection. *Corrosion Science*, 159, 108120.
5. Hayatdavoudi, H., & Rahsepar, M. (2017). Smart inhibition action of layered double hydroxide nanocontainers in zinc-rich epoxy coating for active corrosion protection of carbon steel substrate. *Journal of Alloys and Compounds*, 711, 560-567.
6. Kowalczyk, K., & Spychaj, T. (2014). Zinc-free varnishes and zinc-rich paints modified with ionic liquids. *Corrosion science*, 78, 111-120.

# Cyclic Distillation Technology

(December 2018 - November 2021)



## Contribution to the UN Sustainable Development Goals

Distillation is an important separation process that is used in chemical and biochemical industry all over the world. It is also a process that often takes place in large columns with many trays and have significant energy requirements. Cyclic distillation is a process intensification that can reduce the energy consumption and number of trays compared to a conventional distillation. This way cyclic distillation can then be a cheaper and more environmentally friendly alternative to conventional distillation.



**Jess Bjørn  
Rasmussen**

jesbra@kt.dtu.dk

**Supervisor:**  
Jakob Kjøbsted Huusom,  
Jens Abildskov,  
Xiangping Zhang,  
Seyed Soheil Mansouri

### Abstract

Cyclic distillation has been shown to be a promising process intensification that have higher tray efficiency compared to conventional distillation. It is a rather old technology, from the early 1960's, but there is still a substantial need for developing and maturing the theory before the process can be a viable alternative to conventional distillation in industry.

### Introduction

Cyclic operation of a distillation process is a process intensifying alternative to a conventional distillation process. Unlike the conventional distillation with continuous counter-current liquid and vapor flows, the phase flows in cyclic distillation are separated in two periods: one where the liquid holdups are kept stationary on the stages, while vapor is sent up through the column, and one, where the liquid holdup on each stage is drained to the stage immediately below. The two periods are called the vapor flow period (VFP) and the liquid flow period (LFP), respectively. After the liquid flow period a new cycle, beginning with a vapor flow period, is started.

There are two methods of draining the liquid holdups on the trays: simultaneous and sequential draining, each of which requires a special tray design [1]. For the simultaneous draining, the vapor flow is interrupted after the vapor flow period in order to allow all the trays to drain to the tray immediately below all at once, whereas for the sequential draining, the trays are drained one by one starting from the bottom. By draining with the sequential method, it is not necessary to interrupt the vapor flow.

By separating the phase flows, as described above, increased tray efficiency and throughput compared to conventional distillation processes can be achieved, as first shown by Cannon in 1961 [2]. With higher tray efficiencies, fewer trays are

necessary and thus smaller columns can be made. Furthermore, a cyclic distillation process can reduce the energy requirements compared to a conventional distillation [1], thus making the distillation process more environmentally friendly by both reducing the size and energy of the column. Cyclic distillation is, despite being almost 60 years old, still a technology that is under development. Recently a mass and energy stage balance model has been developed for cyclic distillation [3] as a continuation of the mass balance stage model proposed by Pätruč et al. [4]. Currently, most of the available models for cyclic distillation are only for the simultaneous draining method [1].

### Specific Objectives

The objective of this project is to further develop the necessary theory and models to properly describe a cyclic distillation process with either simultaneous or sequential draining. With more advanced models that includes considerations of energy transfer, it would be possible to simulate a distillation process in more details, for example for column design, reactive cyclic distillation processes or process control studies. More detailed models would also make the process more interesting as an alternative to conventional distillation for industrial use.

### Results and Discussion

The recently developed model [3] is a general stage model that can account for heat and mass transfer

in LFP and VFP and allows for feed and side draws at any stage. Furthermore, an additional energy term is included that allows the model to easily account for heat of mixing, heat of reaction or heat integration on any tray if necessary. Figure 1 shows the stage model with inlets and outlets in VFP and LFP for simultaneous draining.

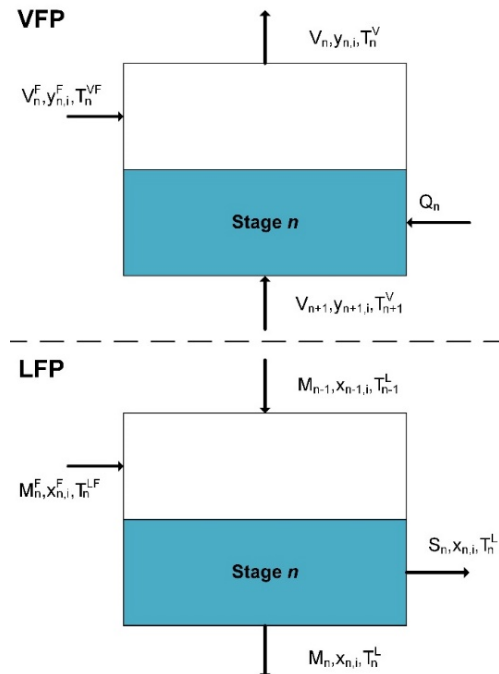


**Figure 1:** Stage in cyclic distillation with simultaneous draining during VFP (top) and LFP (bottom).

With this mass and energy balance stage model a reactive cyclic distillation case is investigated for the production of methyl tert-butyl ether (MTBE). The reactive distillation of MTBE in conventional columns is well studied [5]. In this reaction isobutene and methanol reacts and forms MTBE in a reversible reaction. This reaction is relatively fast and can therefore be described either by reaction kinetics or chemical equilibrium. By doing the same reaction and separation for the MTBE case in a cyclic distillation column, as in a conventional column, it is possible to improve the reaction and separation in such a way that the column design and performance can be improved, with reduced number of stages and reduced energy requirements.

So far, only a model for the simultaneous drained cyclic distillation has been made and no detailed models for sequential draining is available in literature. It would therefore be interesting to set up an equivalent model for sequential draining. This would make it possible to simulate either draining method and compare the two models.

Comparisons between the two draining methods have been made, so far only with simple models for an ammonia three staged stripping case with linear equilibrium. These comparisons showed the duration of the VFP and the LFP are very important when designing a cyclic distillation. The longer VFP, where all stages undergo mass transfer between vapor and liquid, the higher degree of separation. However, a long VFP also means low throughput or very wide columns. A benefit in the sequential draining could be that during LFP it is only the draining and the filling trays, where no mass transfer between vapor and liquid occurs. On the other hand, the sequential draining of all trays is more time consuming, especially when having many trays, since the draining is done one tray at a time.

## Conclusions

Cyclic distillation is a promising alternative to conventional distillation, with higher tray efficiencies that can lead to reduced energy consumption and smaller distillation columns.

It is still an emerging technology, which needs to be further developed. A general stage model has been developed for simultaneous drained cyclic distillation that includes both the mass and energy transfer. With this model a case study regarding reactive cyclic distillation for MTBE is made. A reduction in both number of trays and energy for the process was possible with cyclic operation compared to conventional operation.

Comparisons between the simultaneous and sequential draining methods have been carried, but only for a simple case.

There is still many different aspects of cyclic distillation that need to be investigated, such as reactive distillation, comprehensive design algorithms and process control configurations.

## Acknowledgements

This project is partially funded by the Sino-Danish Center for Education and Research (SDC).

## References

1. C.S. Bîldea, C. Pătruț, S.B. Jørgensen, J. Abildskov, A.A. Kiss, *J. Chem. Technol. Biotechnol.* 91 (5) (2016) 1215-1223.
2. M.R. Cannon, *Ind. Eng. Chem.* 53 (8) (1961) 629.
3. J.B. Rasmussen, S.S. Mansouri, X. Zhang, J. Abildskov, J.K. Huusom, *AIChE J.* 66 (8) (2020) e16259
4. C. Pătruț, C.S. Bîldea, I. Litâ, A.A. Kiss, *Sep. Purif. Technol.* 125 (2014) 326-336.
5. R. Jacobs, R. Krishna, *Ind. Eng. Chem. Res.* 32 (8) (1993) 1706-1709.

# Experimental study and modelling of PET plastic recycling process

(December 2018- December 2021)



## Contribution to the UN Sustainable Development Goals

Heavy production and widespread application of plastic materials create an enormous amount of residues. Plastic residues are mainly landfilled, incinerated, dumped or leaked. Increasing amount of plastic residues poses serious economic and environmental problems. In light of 12<sup>th</sup> UN sustainable development goal, urgent action is needed to ensure that plastic production do not lead to the over exploitation of resources or harm the environment. Thus, a sustainable and industrial way to recycle plastics is in great demand for substantially reducing waste generation through prevention, reduction, recycling and reuse.



**Amirali  
Rezazadeh**

amirax@kt.dtu.dk

**Supervisor:** Hariklia N. Gavala, Kaj Thomsen, Philip L. Fosbøl, Ioannis V. Skidas

## Abstract

We are contributing to the development of a profitable process to recycle Poly-Ethylene Terephthalate (PET) plastics and close its life cycle. The plastic recycling process streams contain mainly terephthalic acid, disodium terephthalate, sodium hydroxide, water and ethylene glycol, which are the products of the de-polymerization reactions. In order to design this recycling process, a thermodynamic model built on an experimental study is needed. Thus, physical and thermodynamic properties of this system were explored experimentally. Subsequently, the thermodynamic behavior of this system was simulated with Extended UNIQUAC model.

## Introduction

An efficient, sustainable, environment-friendly, and less energy demanding way to industrially recycle polyethylene terephthalate (PET) is in high demand [1]. Along with massive production and widespread application of PET, an enormous amount of waste has been created. This waste of PET products do not have any side effects on the human body and does not create a direct hazard to the environment. Nonetheless, since it is highly resistant to atmospheric and biological degrading agents, it will remain as a substantial volume fraction in the waste stream, considered as noxious material [2]. Increasing amount of PET wastes poses severe economic and environmental problems. Recycling plastics and PET materials to produce new products can lead to saving up to 50-60% of capital in comparison with making the same product from the virgin resin [3].

Chemical recycling is the most sustainable method to recycle PET materials. There are three main mechanisms for chemical recycling of PET: glycolysis, methanolysis, and hydrolysis. Hydrolysis is a method in which PET is depolymerized to terephthalic acid ( $H_2TP$ ) and ethylene glycol (MEG) in aqueous acidic, alkaline or neutral environment. Caustic soda can be used for breaking down PET

to terephthalic acid in alkaline environment and this process is called alkaline hydrolysis [4]. The main components in alkaline hydrolysis are ethylene glycol, terephthalic acid, disodium terephthalate ( $Na_2TP$ ) in presence of sodium hydroxide ( $NaOH$ ) and water [5].

Studies on experimental determination of properties of  $Na_2TP$  are quite scarce, and in general, there is a lack of thermodynamic data in order to create a modeling basis for PET recovery. Therefore, we conducted various experiments to explore this electrolyte system. Accordingly, the Extended UNIQUAC model was adopted to estimate the thermodynamics of this chemical complex.

## Specific Objectives - Experimental study:

The solubility of disodium terephthalate in aqueous sodium hydroxide and in aqueous sodium hydroxide - ethylene glycol mixtures was determined experimentally. This study was performed by temperature analysis, gravimetry and titration. The experimental results were compared to existing literature data.

The solubility of the disodium terephthalate above concentrations of the eutectic point has no considerable dependence on temperature. A

complete opposite trend is observed for freezing points at concentrations below the eutectic point. Ethylene glycol has a strong influence on the phase behavior of the system. The solubility and freezing points decrease as a function of the ethylene glycol concentration.

### Modelling:

To design a closed chemical process to recycle PET, the entire operation should be simulated and modelled. The process simulation is working based on a thermodynamic model being able to estimate the behavior of the chemical system. To do so, we adapted the Extended UNIQUAC model, which is widely applicable for electrolyte systems, to PET recycling processes. The model adaption was carried out by correlating the model parameters based on existing experimental data. Besides, the missing standard state properties of all the present ions in the whole operation were calculated based on experimental results.

The parameterization of standard state properties and the parameters of the Extended UNIQUAC model was carried out in ESTIM, which is an in-house correlation tool patented in DTU.

The developed model is consistent, and it can well reproduce all experimental data. It means the model can work efficiently and precisely for the simulation of the whole process and designing the production of pure terephthalic acids and ethylene glycol from PET polymers.

### Results and Discussion

The developed Extended UNIQUAC model can effectively estimate different thermodynamic characteristics of the electrolyte solution. Some of the results are presented here.

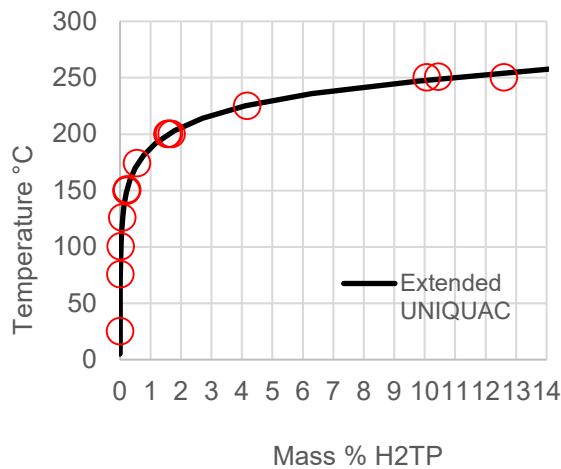


Figure 1, Solubility curve of  $H_2TP$  at water.

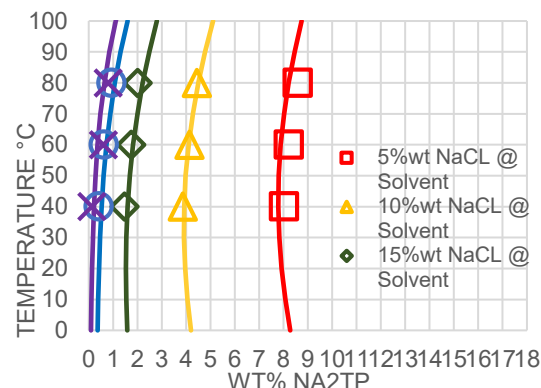


Figure 2, Solubility curve of  $Na_2TP$  at water-sodium chloride.

### Conclusions

The model development was based on the experimental data. The model can efficiently reproduce the Solid-Liquid and Vapor-Liquid phase diagrams of disodium terephthalate and terephthalic acid in a chemical system having various composition of sodium chloride, sodium hydroxide and ethylene glycol. In all cases, there are quite small differences between modelling and experimental results. Furthermore, the model can efficiently reproduce the titration experiments.

The modeling results are being used for simulating a closed downstream process for chemical recycling of Poly-Ethylene Terephthalate (PET) by ASPEN Plus.

### Acknowledgments

This work was part of the DEMETO project supported by the European Horizon 2020 research grant of 768573 and a Ph.D. fellowship from department of Chemical and Biochemical Engineering.

### References

1. L. Bartolome, M. Imran, B. G. Cho, and W. A. Al-Masry, "Recent developments in the chemical recycling of PET," in *Material Recycling-Trends and Perspectives*, InTech, 2012.
2. D. Paszun and T. Spychaj, "Chemical recycling of poly (ethylene terephthalate)," *Ind. Eng. Chem. Res.*, vol. 36, no. 4, pp. 1373–1383, 1997.
3. V. Sinha, M. R. Patel, and J. V Patel, "PET waste management by chemical recycling: a review," *J. Polym. Environ.*, vol. 18, no. 1, pp. 8–25, 2010.
4. H. Alter, "Disposal and reuse of plastics," *Wiley-Interscience, Encycl. Polym. Sci. Eng.*, vol. 5, pp. 103–128, 1986.
5. M. Crippa and B. Morico, "PET depolymerization: a novel process for plastic waste chemical recycling," in *Studies in Surface Science and Catalysis*, vol. 179, Elsevier, 2019, pp. 215–229.

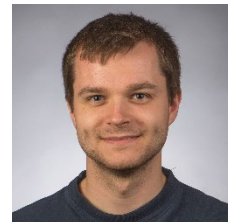
# Cracking of Sugars for Production of Chemicals

(November 2017- November 2020)



## Contribution to the UN Sustainable Development Goals

Responsible production and consumption of chemical products are vital elements in sustainable development, as the current production is heavily based on non-renewable fossil resources. Platform molecules are important in the chemical industry as they are products that can be produced efficiently and used in several other chemical conversions and applications. For a chemical industry based on renewable feedstocks, new platform molecules will be needed. In this project, sugars are investigated for their conversion to glycolaldehyde, a potential platform molecule, used for further conversion to useful products such as ethylene glycol.



**Christian Bækhøj  
Schandl**

chrbsc@kt.dtu.dk

**Supervisors:** Christian Mårup Osmundsen, Martin Høj and Anker Degr Jensen.

### Abstract

In this project, a process utilizing spraying of a liquid sugar solution, into a fluidized bed reactor is investigated. When an aqueous solution of glucose is used, this “sugar cracking” process can selectively produce oxygenates, with the main product being glycolaldehyde, a C<sub>2</sub>-oxygenate with yields as high as 74 wt%. Glycolaldehyde can be used for further sustainable production of useful products such as ethylene glycol. The project work is focused on obtaining a mechanistic understanding of the sugar cracking process to reduce the risk during process scale-up.

### Introduction

Biomass represents the most readily available source of renewable carbon and is considered a promising feedstock for sustainable production of chemicals and fuels. While other renewable resources such as solar, water and wind can be used to produce heat and power, biomass can potentially be used for production of chemicals as well as renewable liquid, solid and gaseous fuels.

Production of chemicals from biomass, particularly the conversion of sugars to value-added chemicals are of interest. Hexoses are carbohydrates with six carbon atoms, and they are the most abundant monosaccharides in nature, among which fructose and glucose are the most economical and suitable feedstocks for chemical production [1]. Glucose is produced from hydrolysis of starch, and fructose can be produced from base catalyzed isomerization of glucose or by hydrolysis of inulin or sucrose [2].

It has previously been shown that fast pyrolysis can be used to convert glucose to glycolaldehyde in high yields (>50 wt%) along with other chemicals by spraying an aqueous solution of glucose into a fluidized bed operated at 500 – 600 °C [3]. This method of sugar conversion is called “sugar cracking”.

Glycolaldehyde can be hydrogenated in a second step to produce ethylene glycol (EG), which is a large commodity chemical with an annual

production capacity of 34.8 million tons (2016). EG is primarily used in the synthesis of polyester fibres and PET bottles (> 80%), while other uses include antifreeze [4].

### Specific Objectives

The main objectives of this project is to build a mechanistic understanding of the sugar cracking process to reduce risk during scale-up. This includes

- Investigation of the effect of operating conditions
- Obtain a deeper understanding of the chemical reaction network and important physical aspects of the process
- Development of a kinetic model that can predict product yields

### Experimental

A simple schematic of the laboratory setup for the sugar cracking process is shown in Figure 1. The bubbling fluid bed reactor is loaded with particles and is fluidized with nitrogen. The aqueous glucose solution is sprayed into the hot reactor operated at 525 °C and 1 atm using a spray atomizer. The feed is rapidly heated and the glucose molecules are cracked to produce smaller fragments. The product vapors are carried out of the reactor and are passed through a condenser, where the liquid product is condensed. The condensed

liquid product is analyzed using HPLC to quantify the yield of oxygenates.

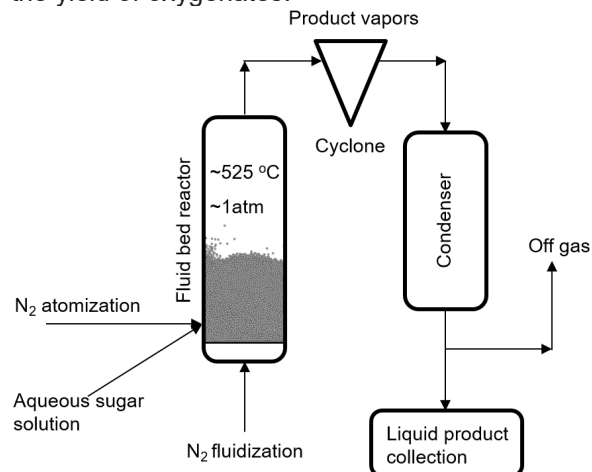


**Figure 1:** Simple schematic of laboratory setup for the sugar cracking process.

### Kinetic model

It is of interest to build a kinetic model that can predict the product yields from the process. Seshadri & Westmoreland [5] calculated reaction kinetic parameters for a number of reactions related to glucose pyrolysis using gas-phase quantum-chemistry and statistical-mechanics calculations. Based on these calculations, a reaction network has been set up assuming instantaneous evaporation of the aqueous glucose droplet and heating to the reactor temperature. The model solution as a function of residence time is shown in Figure 2.

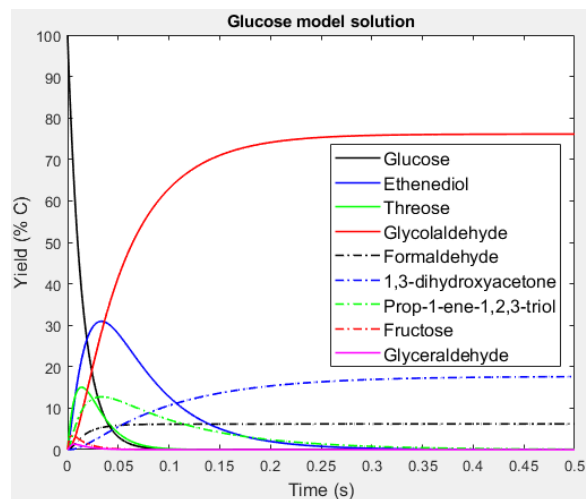


**Figure 2:** Example product distribution from kinetic modelling of glucose decomposition.

### Experimental Results

An example of the product distribution from lab-scale sugar cracking of glucose is shown in Table 1. Here it can be seen that glycolaldehyde is produced in yields as high as 74 wt%, and the main

by-products are pyruvaldehyde (9 wt%) and formaldehyde (7 wt%), along with minor byproducts such as acetol and glyoxal.

**Table 1:** Comparison of experimental and model yields in wt% carbon.

	Exp.	Model
C3	Pyruvaldehyde	9%
	Acetol	2%
	1,3-dihydroxyacetone	0% 17%
C2	Glycolaldehyde	74% 77%
	Glyoxal	2% N/A
C1	Acetic acid	1% N/A
	Formaldehyde	7% 6%
	Sum	95% 100%

### Discussion

From table 1 it can be seen that the yields of glycolaldehyde and formaldehyde calculated by the model agrees well with the experimental data. However, the model is limited with respect to the C3-products. The model predicts 17 wt% yield of 1,3-dihydroxyacetone, whereas pyruvaldehyde and acetol are the experimentally observed C3-oxygenates.

However, it should be noted that the model includes only few secondary decomposition products, and further decomposition of glycolaldehyde and other oxygenate products are not included.

### Conclusions

Sugar cracking of glucose is a promising process for production of chemicals from a renewable source. Glycolaldehyde can be produced with yields as high as 74 wt%. Glycolaldehyde can be hydrogenated in a second step to produce EG, which is a large commodity chemical.

### References

1. X. Tong, Y. Ma, and Y. Li, *Appl. Catal. A Gen.* 385 (1-2) (2010) 1-13.
2. F. W. Lichtenhaler, *Acc. Chem. Res.* 35 (9) (2002) 728-737.
3. P. A. Majerski, J. K. Piskorz, and D. S. A. G. Radlein, US 7,094,932 B2 (2006).
4. Plastics Insight, 2018. [Online]. Available: <https://www.plasticsinsight.com/resin-intelligence/resin-prices/mono-ethylene-glycol-meg/>
5. V. Seshadri and P. R. Westmoreland, *J. Phys. Chem. A* 116 (49) (2012) 11997–12013.

# Optimization of geopolymmer cement technologies

(April 2019- April 2022)

13 CLIMATE ACTION



## Contribution to the UN Sustainable Development Goals

The global production of Portland cement is around 4 billion tonnes per year and contributing an 8% to the total CO<sub>2</sub> anthropogenic emissions yearly. Even though the cement industry has improved significantly the energy efficiency of the process, approximately half of the CO<sub>2</sub> emissions derive from the burning of limestone (CaCO<sub>3</sub>). Therefore, decarbonized cements such as geopolymers should be used. They have demonstrated that they can lower the carbon emissions of the cement industry up to 80%.



**Isabel  
Pol Segura**

isapol@kt.dtu.dk

**Supervisor:** Peter Arendt

Jensen

**Co-supervisor:** Anne Juul

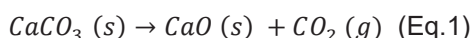
Damø

## Abstract

The international scientific community has addressed the environmental issues associated with Portland cement production and there is a global environmental goal to reduce their CO<sub>2</sub> emissions. This study focuses on the optimal development of geopolymers, low CO<sub>2</sub> binders that could replace partially or totally, Portland cements. Several properties of this new binder need to be tested and compared to Portland cement, to ensure the same quality and performance.

## Introduction

Geopolymers are decarbonized alternative binders to Portland cement (PC). The usefulness of those alternative materials is that they lower the CO<sub>2</sub> emissions associated with the production of Portland cement (PC). Currently, the global production of OPC is around 4 billion tonnes per year [1] and contributing an 8% to the total CO<sub>2</sub> anthropogenic emissions [2, 3, 4, 5]. Even though the cement industry has improved significantly the energy efficiency of the process, approximately 50% of the CO<sub>2</sub> emissions in cement production derive from the calcination of limestone (Eq. 1) at 750°C [3].



Moreover, the global cement demand is expected to increase in the following years due to the growth of population and the rapid infrastructural development of emerging economies [6]. In this way, the cement and concrete industry have decided to take actions in the global reduction of CO<sub>2</sub> emissions and decarbonized cementitious binders such as geopolymers have started gaining attention. Geopolymer cements constitute an attractive substitute as they could have comparable performance to Portland cement, and they have proved to reduce the CO<sub>2</sub> emissions between a 20 to 80% compared to PC [7], depending on the raw materials and processing used.

## Specific objectives

The aim of this study is develop a calcined clay-geopolymer cement that can reduce the CO<sub>2</sub> emissions associated with cement production and that has similar properties and performance as PC. Moreover, a geopolymer production process will be designed for an industrial scale. This will include optimization of clay calcination technology.

## Experimental methods

Geopolymers can be synthesized by the reaction of an aluminosilicate-based material and an alkaline reagent under the presence of water. Table 1 shows the raw materials used for the production of clay-based geopolymer cements.

**Table 1:** Raw materials used in the geopolymers

Aluminosilicate	Calcined clay
Alkali activator	Sodium hydroxide

The raw materials are then blended with distilled water and casted in formworks. After 1 day the specimens are demolded and they are left to cure at room temperature until their properties are tested.

## Results and discussion

In this study, nine different geopolymer formulations were prepared and their compressive strength was measured after 3, 7 and 28 days following the EN 196-1 standard.

The strength development curves of the 9 different formulations are presented in Figure 1. It can be seen that for all the formulations most of the strength is already reached after 3 days. This means that these cements have an early strength development and a fast setting time.

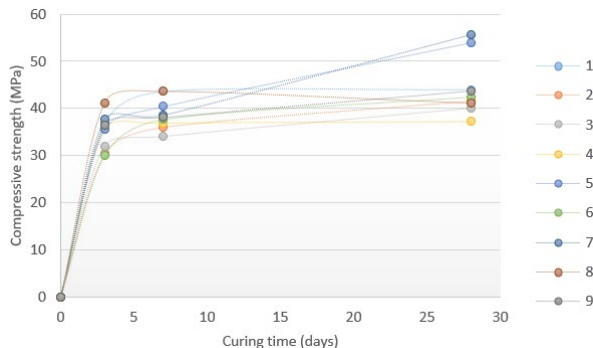


**Figure 1:** Strength development curves of 9 different geopolymer formulations

It can also be seen that geopolymer mixes 5 and 7 lead to the highest compressive strengths after 28 days, with 54 and 55.6 MPa, respectively. When comparing those two mixes (5 and 7) to a standard PC cement (CEM I 52.5), it can be seen in Figure 2 that they have similar strength development curves. Moreover, they reach a compressive strength higher than the targeted compressive strength of 52.5 MPa after 28 days.

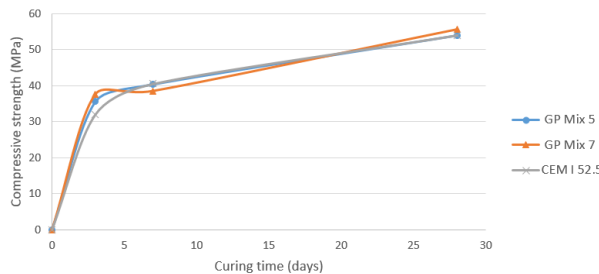


**Figure 2:** Comparison of strength development curves between mix formulations 5, 7 and a CEM I 52.5.

## Conclusions

Calcined clay geopolymers can reach compressive strengths similar to the high strength class cement, CEM I 52.5. This means that geopolymer cements have the potential to replace PC. However, more properties should be tested in order to ensure the good performance and durability of geopolymers, as well as the development of new standards that can embrace this new material.

## References

1. Pavithra, P. ea, et al. "A mix design procedure for geopolymer concrete with fly ash." *Journal of Cleaner Production* 133 (2016): 117-125.
2. McLellan, Benjamin C., et al. "Costs and carbon emissions for geopolymer pastes in comparison to ordinary portland cement." *Journal of cleaner production* 19.9-10 (2011): 1080-1090.
3. Luukkonen, Tero, et al. "One-part alkali-activated materials: A review." *Cement and Concrete Research* 103 (2018): 21-34.
4. Van Deventer, Jannie SJ, John L. Provis, and Peter Duxson. "Technical and commercial progress in the adoption of geopolymer cement." *Minerals Engineering* 29 (2012): 89-104.
5. Peys, Arne, Hubert Rahier, and Yiannis Pontikes. "Potassium-rich biomass ashes as activators in metakaolin-based inorganic polymers." *Applied Clay Science* 119 (2016): 401-409.
6. Maddalena, Riccardo, Jennifer J. Roberts, and Andrea Hamilton. "Can Portland cement be replaced by low-carbon alternative materials? A study on the thermal properties and carbon emissions of innovative cements." *Journal of Cleaner Production* 186 (2018): 933-942.
7. Weil, M., K. Dombrowski, and A. Buchwald. Life-cycle of analysis geopolymers. Woodhead Publishing, 2009. 194-210

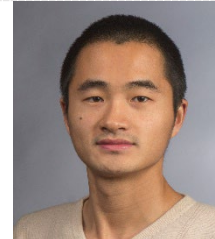
# Stretchable conductive MWCNTs-PDMS composite

(January 2018- December 2020)



## Contribution to the UN Sustainable Development Goals

In this project, a new method is proposed to fabricate stretchable conductive elastomers. The approach is simple, fast, scalable, and cost-effective and can be easily applied to other materials. By this method, a conductive elastomer, with high conductivity can be produced with less conductive material by processes that are easily up-scalable compared to currently used technologies. Therefore, this project contribute to UN Sustainable Development Goal no. 12 --- Responsible consumption and Production.



Jiang  
Shao

jshao@kt.dtu.dk

**Supervisor:** Anders E.  
Daugaard and Anne  
Ladegaard Skov

## Abstract

In this PhD project, a novel, simple, and effective preparation method have been investigated for fabrication of highly stretchable conductive materials, which consists of multi-walled carbon nanotubes (MWCNTs) and poly(dimethylsiloxane) (PDMS). The prepared conductive MWCNT-PDMS materials can be elongated up to 200%. In addition, the prepared materials show high conductivity of  $0.038 \text{ S m}^{-1}$  with only 2.6 phr (parts per hundred rubber) MWCNTs and stable conductivity throughout 160% elongation. Therefore, prepared MWCNTs-PDMS elastomers composes a novel stretchable conductive material with potential applications in soft electronics.

## Introduction

Stretchable conductive materials have gained considerable attention from researchers due to their potential applications in wearable electronics [1]. One key technical challenge in realizing those applications is that material has ability to provide conductivity upon large deformations [2].

Crosslinked PDMS has received considerable attention owing to its biocompatibility, high stability as well as superior elasticity [3]. However, the application of PDMS is restricted by its poor electrical conductivity. Conductive carbon particles such as carbon nanotubes (CNTs) have been extensively used in preparing stretchable conductive materials [4]. One popular approach is direct distribution of conductive nanoparticles in substrates to create percolated particle networks. However, the introduction of percolated particle networks into the polymer matrix significantly increases the stiffness of such materials and conductivity typically decreases with elongation.

Here, we have employed a mixing scheme to prepare heterogeneous bimodal networks to selectively distribute MWCNTs in silicones, which permits distribution of conductive particles in one or in both phases. The purpose of this PhD project is to prepare a stretchable conductive PDMS, which employs the heterogenous bimodal network

preparation method to distribute highly conductive domains throughout low conductive PDMS matrix. Followed by sequential mixing, these high conductivity domains can be mixed with a non-conductive soft PDMS matrix, which combines high conductivity of the internal phase with superior stretchability of PDMS matrix.

## Specific Objectives

The goal of this project is to develop new methods to prepare stretchable conductive materials that can provide conductivity upon large deformation.

## Methodology

Firstly, MWCNTs were entrapped in a hyper-branched short chain PDMS (SC-PDMS) to form high conductive domains. Secondly, hyper-branched long chain PDMS (LC-PDMS) was introduced as the surrounding matrix. Additional MWCNTs were added into LC-PDMS as a "bridge" to connect the highly conductive domains. Thirdly, entrapped MWCNTs and hyper-branched LC-PDMS were mixed together and cured under high temperature to prepare the final composites. Reference samples were also prepared by mixing the conductive particles into the PDMS by roll milling and ultra-sonication.

## Results and Discussion

Figure 1 shows the normalized resistance ( $R/R_0$ , where  $R$  is resistance at certain strain and  $R_0$  is the resistance at zero stress state) of MWCNTs-PDMS composite with 2+0.6 phr MWCNTs (2 phr MWCNTs from the SC domain and 0.6 phr MWCNTs from the LC domain) and reference samples as a function of elongation. It can be seen that the normalized resistance of prepared MWCNTs-PDMS composite decreases with elongation until the strain exceeds 160%. At this point, the normalized resistance of prepared MWCNTs-PDMS composite starts to increase until it finally fractures at 200% strain. However, all the reference samples show an increased normalized resistance under elongation as well as a significantly shorter elongation at break.

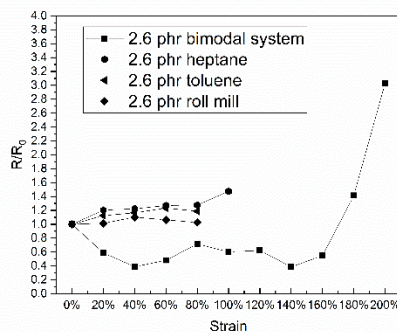


**Figure 1:** Normalized resistance of MWCNTs-PDMS composite with 2+0.6 phr MWCNTs and reference samples under different strains. Reproduced from Journal of Materials Chemistry C. Copyright 2020, Royal Society of Chemistry.

Different from conventional MWCNTs based composites, it is remarkable that the prepared MWCNT-PDMS composite show an increase in conductivity with increased strain. This interesting property can be related to the heterogeneous distribution of conductive particles, which enable new percolated paths to form and reform during elongation, leading to a dynamic system where many new conductive pathways can be established in the material.

During the initial hyper-branching of the SC-domain, the formed structures have a “hairy” appearance as illustrated in the diluted samples in Figure.2c. Apart from having separate domains, this “hairy” appearance of the SC-domains was assumed to be directly related to the reformation of percolated pathways through orientating branches and free MWCNTs during elongation. This assumption was supported by optical microscopy images of samples diluted in PDMS matrix, in their zero stress state and at 100 % elongation, respectively, as displayed in Figure.2.

In Figure.2a, the free MWCNTs are homogenous dispersed in the PDMS matrix (LC-domain). As the

sample is elongated to 100%, the MWCNTs orientate along the force direction (Figure.2b), which demonstrates the assumption that carbon nanotubes are reorganized in the elongated state. However, the SC-domains are hard and cannot deform to the same large extent as illustrated in Figure.2c. Only the branched structures, which exist on the surface of the SC-domains, are able to orientate along the force direction, as shown in Figure.2d. Hence, this formation and reformation of the conductive pathways is believed to come from the combination of MWCNTs, which come from the branches on the surface of the SC-domains, and the free MWCNTs, which exist in the LC-domains.

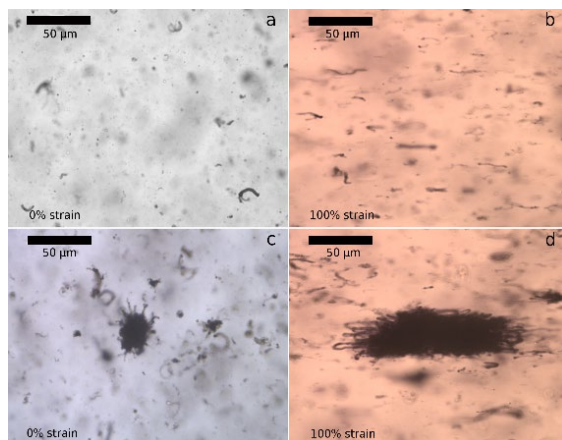


**Figure 2:** Optical microscopy images of microstructures of MWCNTs-PDMS composites at high dilution embedded in PDMS: a) LC-domain dispersed MWCNTs at zero strain. b) LC-domain dispersed MWCNTs at 100% strain. c) SC-domain MWCNTs at zero strain. d) SC-domain MWCNTs at 100% strain.

## Conclusions

The material developed in this PhD project has demonstrated very interesting properties in terms of stretchability and conductivity. This provides a very good basis for broadening this into different forms of materials as well as in testing it for various applications, which is the focus of the last part of the PhD.

## Acknowledgements

DTU Chemical Engineering and China Scholarship Council are acknowledged for financial support.

## References

1. K. Takei, T. Takahashi, J. C. Ho, H. Ko et al. Nature Materials 9 (2010) 821.
2. N. Matsuhisa, D. Inoue, P. Zalar, H. Jin et al. Nature Materials 2017, 16, 834–840.
3. J. Shao, L. Yu, A. L. Skov & A. E. Daugaard. Journal of Materials Chemistry C 8.38 (2020): 13389-13395.
4. J. H. Kim, J. Y. Hwang, H. R. Hwang, H. S. Kim, J. H. Lee, J. W. Seo, U. S. Shin & S. H. Lee. Scientific Reports 2018, 8, 1–11.

# Macroscopic study on depressurization production of hydrate spheres below ice freezing point

(January 2018- December 2020)

13 CLIMATE ACTION



## Contribution to the UN Sustainable Development Goals

The total global energy demand is on the rise rapidly. Ensuring everyone has enough access to energy is of great importance for the development of society. At the same time, the current energy system is facing challenges historically that carbon dioxide and other greenhouse gases are changing the global climate. Natural gas is regarded cleaner and more efficient than other fossil fuels. Accordingly, the generation of natural gas also helps cut reliance on the use of fossil fuels, thus significantly curbs the greenhouse effect.



Meng  
Shi

mshil@kt.dtu.dk

**Supervisor:** Nicolas von Solms; John M Woodley

## Abstract

Depressurization is an attractive technique to extract gas contained within natural gas hydrate sediment. Most researchers have an agreement that gas production behavior from hydrate-bearing sediments is an interfacial decomposition process. A better understanding of the kinetics of hydrate production below zero degrees is essential to reliably predict gas hydrate production potential from natural gas reservoirs. Attributed to the fact of the accumulated property of gas hydrates, the determination of surface area and volume of hydrate particles are always challenging.

To investigate the effects of and driving force on the depressurization production process, the same order of overall volume of spherical methane hydrate samples in a diameter of 11mm, 17mm, and 22mm are prepared to macroscopically simulate hydrate particle in this work. The results showed that the effect of pressure is prominent on the production percentage compared with the surface area-to-mass ratio. With regards to production rates during dissociation, the extent of influence production pressure is consistent with the surface area-to-mass ratio. Driving force and gas diffusion jointly govern the decomposition reaction. The cryogenic SEM image of hydrate samples suggested that bigger hydrate in diameter has a smoother surface which could make ice cluster difficult to attach to the hydrate surface. An ice cluster initially formed on the hydrate surface move occasionally. By this, a randomly distributed ice layer shielding mechanism on different surface area-to-mass ratio was proposed.

## Introduction

Nowadays, energy, the essential not only for achieving the economic, social, and environmental goals but also for sustainable human development. The global energy system now faces many challenges, one perspective is concerning higher levels of consumption, restrictions on access and energy security, another is about the environment, such as climate change, pollution of air and water. For one side of the energy challenge, the discovery of shale gas has considerably changed the global energy framework from traditional coal fuel. But another hydrocarbon resource, natural gas hydrates (NGHs), has the potential to do even more of the energy system. Natural gas hydrates are naturally occurring ice-like solids, which are made of water molecules as the cage forming host and gas molecules as the guest [1]. Natural gas hydrate is globally abundant beneath the permafrost region ranging from about 130 to 2000m, and along the

ocean continental ranging from 100 to 1100 m [2]. More than 99% of natural hydrates are methane hydrates, motivated researchers to consider gas hydrates as a potential energy source.

In recent years two main hydrate research areas have surged in this field, one is fundamentals of hydrate, related to property, quantity, and production potentials; another area is mainly to develop the techniques to economically and safely produce natural gas from NGH reservoir [3,4]. The application of hydrates is also popular in energy recovery, CO<sub>2</sub> capture, and storage, gas separation, water desalination, gas storage and transport, refrigeration, etc. More recently a variety of methods has received considerable attention for natural gas exploration from hydrates. The most widely used, known as depressurization, decreases the system pressure below that required for hydrate formation at a given temperature, which is regarded as the most efficient method.

In this study, we report our findings on how the macroscopic size of MH affects its dissociation. We consider the isothermal dissociation of methane hydrate at a negative temperature to examine the ice-shielding mechanism of hydrate dissociation. The kinetic data of dissociation using the depressurizing method were obtained for different size of methane hydrate pellets. We prepared a different quantity of hydrate pellets with the geometrical mean diameter (GMD) ranging from 11 to 22 mm and characterized by cryogenic SEM. By that, we solved the difficulty of maintaining the uniform size and distribution of hydrate pellets during experiments. In addition, the mechanism of hydrate dissociation from different size was proposed.

## Results and discussion

Different modes of depressurization were employed on a spherical hydrate sample in diameter 17 mm with a quantity of 3. Figure 1 shows the evolution of the production percentage of methane hydrate at different production pressure. The results from different production pressure following a similar pattern that the overall production process was divided into three periods according to production behavior. At the beginning of production, a rapid increase in both production percentage and produced gas was detected as the system pressure reducing. Methane gas was released fast from the excess of free gas in the vapor phase; The second period is the predominant part for hydrate pellets dissociation. Once the system pressure dropped out of hydrate stability zones, ice was generated immediately and CH<sub>4</sub> came out of the hydrate pellets with a slow increment of gas production percentage and produced gas. Production rates display a slight variation before rapid falling. In the final period, production percentage and cumulative gas were gradually approaching constant, with the production rate infinitely close to zero.

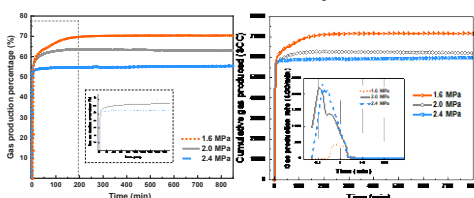


**Figure 1:**(a) Percentage of gas production, (b) Cumulative produced gas and gas production rate for hydrate samples in diameter of 17 mm at production pressures of 1.6 MPa, 2.0 MPa, and 2.4 MPa.

Another factor influencing the hydrate production kinetics is the dimension of hydrate samples that is expressed as a surface area-to-mass ratio. The experimental data of the methane hydrates production in the current study show that the kinetics depended upon the combined effect of the pressure and surface area-to-mass ratio of individual hydrate samples as seen from Figure 2.

The results show that the production percentage significantly depends upon the production pressure (driving force) when on the same size of MH pellets, corresponding to the same surface-to-mass ratio. The pressure dependence acted as the driving force was due to the difference in the fugacity between the gas at the equilibrium and production pressures. However, the final production percentage with the relationship of the surface area-to-mass ratio is not prominent. The effect of gas diffusion may play a more dominant role in this phenomenon.

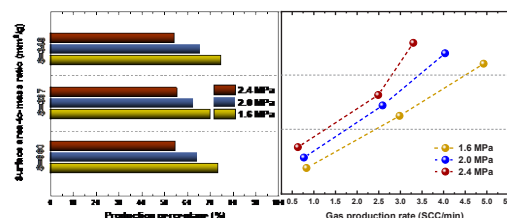


**Figure 2:** The effects of surface area-to-mass ratio and production pressure on production percentage and rate.

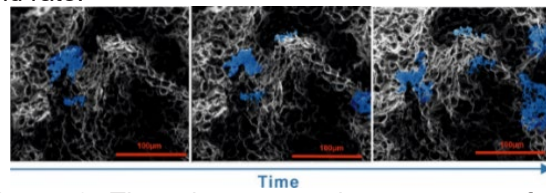


**Figure 3:** The microstructural appearance of the MH sample with time during decomposition.

## Conclusions

The gas production process can be divided into three main periods. Driving force and gas diffusion jointly govern the decomposition reaction. A non-uniform ice rind and the existence of a gas layer between hydrate and ice and this should be taken into account at the simulation of gas hydrate production under freezing point.

## Acknowledgements

This work is supported by the Department of Chemical and Biochemical Engineering, Technical University of Denmark and the State Scholarship Fund of China Scholarship Council.

## References

1. E.D. Sloan, Fundamental principles and applications of natural gas hydrates, *Nature*. 426 (2003) 353–359.
2. M.D. Max, Natural gas hydrate in oceanic and permafrost environments, Springer Science & Business Media, 2003.
3. J.-R. Zhong, Y.-F. Sun, W.-Z. Li, Y. Xie, G.-J. Chen, C.-Y. Sun, L.-Y. Yang, H.-B. Qin, W.-X. Pang, Q.-P. Li, Structural transition range of methane-ethane gas hydrates during decomposition below ice point, *Appl. Energy*. 250 (2019) 873–881.

# High performance production of oligosaccharides by using enzymatic membrane reactors

(December 2018- November 2021)



## Contribution to the UN Sustainable Development Goals

Enzyme membrane reactor (EMR) is a novel technology for high quality oligosaccharides production. By applying enzyme catalysis and membrane separation, EMR reduces consumption of hazardous chemicals, organic solvents and energy in comparison with the traditional process of oligosaccharides fabrication. More importantly, product quality is better controlled in a simultaneous process of bioreaction and products purification, and prevents unexpected side reactions.



Ziran  
Su

zisu@kt.dtu.dk

**Supervisors:**  
Prof. Manuel Pinelo, DTU  
Prof. Jianquan Luo, IPE-CAS; Assoc. Prof Andreas Kaiser, DTU; Assoc. Prof Wenjing(Angela) Zhang,DTU

## Abstract

The PhD project aims at oligosaccharides production by using Enzyme Membrane Reactor (EMR) technology, with the final aim of narrowing the Mw distribution of products which greatly influence their properties and of course their value. Oligodextran with 10-15 monomer units are the initial target products in this project. Enzymes will be immobilized by different novel methods (dopamine or tannic acid coating) onto the membrane that could convert polysaccharides into smaller chains. Enzyme loading efficiency and activity of different immobilization methods will be evaluated. Furthermore, in this study, interactions between enzyme/saccharides and membranes will be investigated to better understand the working patterns on immobilized enzymes.

## Introduction

Oligosaccharides like oligodextran, chitosan-oligosaccharides, fructo-oligosaccharides, heparin-oligosaccharides show different properties (prebiotic activity, etc.) that depend on their molecular weight (Mw) [1-4]. Oligosaccharides with relatively low molecular weight (LMW) have been reported to exert important functions in immunology and therefore are in some cases recommended for animal and human nutrition. These biomolecules have indeed been widely used in medical, food and even cosmetic industry. Traditional production of oligosaccharides includes fermentation/extraction and chemical modification coupled with several steps of purification (Figure 1 [5]). Polysaccharides are normally obtained from plants via extraction, and in some cases such polysaccharides can be obtained from residues e.g. agricultural or urban residues. However, due to the occurrence of impurities in the biomass, fermentation is often conducted for obtaining specific polysaccharides, followed by chemical degradation. In the traditional process of degradation, glycosidic bonds are broken randomly by acid/alkaline agents, generating saccharides with shorter chains and also

certain amounts of waste. Enzyme technology has alternatively replaced chemical degradation for oligosaccharides production due to their specificity on polysaccharides degradation under mild conditions, along with lower generation of wastes and undesired degradations. Combined with membrane technology, oligosaccharides can be generated and separated in-situ in an enzyme membrane reactor (EMR).

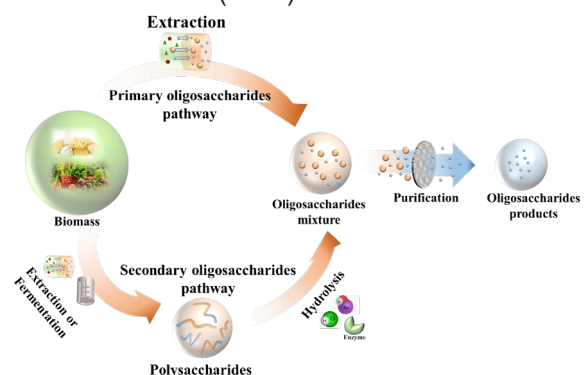


**Figure 1.** Two pathways for oligosaccharides obtainment

In previous works, free enzyme hydrolysis and simultaneous membrane separation has been investigated. High permeate flux with high shear stress on hydrophilic polyether sulfone (PES) membranes was found to improve the oligosaccharide Mw uniformity in the permeate stream [6]. Moreover, enzyme immobilization on membrane is believed to better control both biocoverstion and separation processes, but hydrolysis behavior of immobilized enzymes has not been well studied yet. Therefore, in this project, enzymes will be immobilized onto membrane surface. The hydrolysis behavior of the immobilized enzymes will be analyzed in order to better control the EMR.



**Figure 2.** EMR for oligosaccharides production

### Specific objects

The objects of this project are:

- Enzyme immobilization onto modified membrane via different strategies (Figure 3). The enzymatic membrane will be evaluated by enzyme loading efficiency and enzyme activity.
- Understanding the interaction between bioconversion and membrane separation for better control of oligosaccharides product quality.

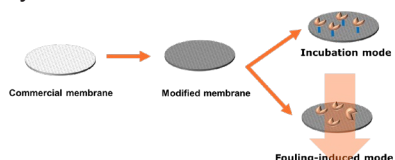


**Figure 3.** Strategies of enzyme immobilization onto modified membrane

### Results and discussion

Strong adhesion of dopamine or tannic acid enables to create a coating layer on the membrane surface that facilitates enzyme immobilization.

. The ‘fouling-induced’ enzyme immobilization mode resulted in a higher enzyme activity, so this strategy should be adopted to develop a high performance EMR for the production of oligosaccharides.

### Conclusion

The type of activity of the immobilized enzymes has been found to be affected by the selected immobilization strategy. This allows to tailor the generation of a certain type of products by promoting different types of immobilization.

With high bioconversion efficiency and selectivity, EMR shows great industrial potential in uniform oligosaccharides production, also at industrial level.

### Future work

Besides membrane modification, the use of electrofibers created by electrospinning are being explored in an attempt to establish a versatile platform for enzyme immobilization that enables smarter design of EMR, particularly in terms of immobilization possibilities. Tailored nanofibers exhibit many advantages due to specific properties (hydrophilicity, porosity etc.) of the electrospun polymers [7]. Electrospun fibers can be specially designed and modified for the purpose of enzyme attachment and encapsulation which will hopefully retain a high percentage of enzyme activity along with high storage stability [8]. In this project, electrospinning nanofibers will be used as immobilization matrixes in the EMRs. Additionally, the modified layer can also help to mitigate the effects of severe fouling [9].

### Acknowledgements

This project is supported by Chinese Scholarship Council

### References

1. E. Olano-Martin, K.C. Mountzouris, G.R. Gibson, R.A. Rastall, Br. J. Nutr. 83 (2000) 247–255.
2. J. Zheng, X. Yuan, G. Cheng, S. Jiao, C. Feng, X. Zhao, H. Yin, Y. Du, H. Liu, Carbohydr. Polym. 190 (2018) 77–86.
3. G. Neeraj, S. Ravi, R. Somdutt, S.K. Ravi, V.V. Kumar, Crit. Rev. Biotechnol. 38 (2018) 409–422.
4. L. Sun, X. Xiong, Q. Zou, P. Ouyang, R. Krastev, J. Appl. Polym. Sci. 134 (2017).
5. Z. Su et al. Separation and Purification Technology. 243 (2020) 116840
6. Z. Su, J. Luo, M. Pinelo, Y. Wan, J. Memb. Sci. 555 (2018) 268–279.
7. P. Lu, S. Murray, M. Zhu, Electrosynthesis Nanofabrication Appl. (2019) 695–717.
8. Z.-G. Wang, L.-S. Wan, Z.-M. Liu, X. Huang, Z.-K. Xu, J. Mol. Catal. B Enzym. 56 (2009) 189–195.
9. K.M. Dobosz, C.A. Kuo-Leblanc, T.J. Martin, J.D. Schiffman, Ind. Eng. Chem. Res. 56 (2017) 5724–5733.

# Combustion Chemistry Studies for Marine Engines

(August 2019 - July 2022)

7 AFFORDABLE AND  
CLEAN ENERGY



## Contribution to the UN Sustainable Development Goals

My PhD project is conducted in collaboration with people from DTU Mechanical Engineering and MAN Energy Solutions that produces diesel engines for the marine industry. There is an ongoing development of greener transportation possibilities on the road with introduction of electrical cars, but this is not a possibility in the ship industry due to the limitation of the electricity interconnection. Therefore, the focus is on optimizing diesel engines with a cleaner combustion or capable of running on fuels produced by green energy.



Lauge  
Thorsen

[lautho@kt.dtu.dk](mailto:lautho@kt.dtu.dk)

### Supervisors:

Peter Glarborg  
Jakob M. Christensen  
Hamid Hashemi

## Abstract

Development of simple kinetic models are important in the development and optimization of maritime diesel engines. In this project, a simple global *n*-heptane kinetic model is evaluated showing promising performances, agreeing within a factor of 2 with a detailed model in predicting the ignition delay time at engine like conditions. This simple *n*-heptane model, combined with a detailed methane model, predicts the ignition delay time of a methane/heptane mixture within a factor of 2.5 compared to the detailed model.

## Introduction

The current environmental challenges set higher demands for engine performances especially for the marine industry. To obtain a cleaner combustion in the diesel engines, it is desired to use natural gas (NG) as fuel instead of diesel oil. However, NG has too long an ignition delay time (IDT) applicable for the two stroke diesel engines. It is desired to overcome this problem by adding diesel as a support fuel to lower the IDT. This demands a knowledge on dual fuel combustion at engine like conditions.

Computational fluid dynamics (CFD) simulations are used as an important tool in the development of improving engines, used to predict e.g. the flow dynamics, pressure increase and heat release. These CFD simulations depends on the chemical kinetic models containing information about the oxidation chemistry during the combustion and its thermodynamics. To obtain the most useful CFD simulations, the used kinetic model should be accurate in predicting the oxidation chemistry and simple to save computation cost. Therefore, it is desired to develop a simple kinetic model with a sufficient performance in IDT predictions.

In this study, methane and *n*-heptane are used as pseudo fuels for NG and diesel, respectively. Detailed kinetic models exists for the methane and *n*-heptane oxidation [1,2], however, especially the detailed heptane model is very comprehensive. This introduces an attention to reduced heptane

models where the global MPL model [3] shows good performances using only 5 species and reactions. In this study, it is investigated whether the IDT of the dual fuel combustion can be predicted using the simple heptane model combined with the methane model, since it have been indicated that in dual fuel methane/heptane mixtures the heptane is fully converted before the methane oxidations starts [4].

## Specific Objectives

- Implement the MPL model using the Chemkin software
- Evaluate the MPL model against experimental shock tube data and a detailed heptane model (NUI model)
- Combine the simple MPL model with the detailed methane model
- Evaluate the combined model against experimental data and detailed heptane model (NUI model)

## Results and Discussion

The combustion is simulated using the Chemkin Pro 19 software in a closed homogeneous and adiabatic batch reactor, and the IDT is estimated as the time from start to the time where a drastic pressure increase is observed indicating the ignition. In figure 1, the global heptane MPL model is compared to the detailed heptane NUI model and experimental data at 42 bar and stoichiometric heptane/air conditions.

The NUI and MPL models show to follow the experimental data. The MPL model over predicts the IDT compared to the NUI model despite around the negative temperature coefficient (NTC) region from 850 to 1000K. This is expected due to the simplicity of the MPL model that does not include the peroxy chemistry of the heptane oxidation that are responsible for this NTC region. Despite the NTC effect, the MPL model sufficiently predict the experimental data within a factor of 2.

Investigations of the pressure dependence on the MPL predictions showed that the MPL model under predicted the IDT dependence at higher temperatures and over predicted the IDT dependence at lower temperatures, compared to the NUI model and experimental data, when the pressure was decreased. The opposite was observed when the pressure was increased. Similar investigations performed for the equivalence ratio showing that the MPL model over predicted the IDT dependence at higher equivalence ratio and opposite for lower equivalence ratio. Overall, the MPL model showed more sensitivity toward the pressure variations than the equivalence ratio variations.

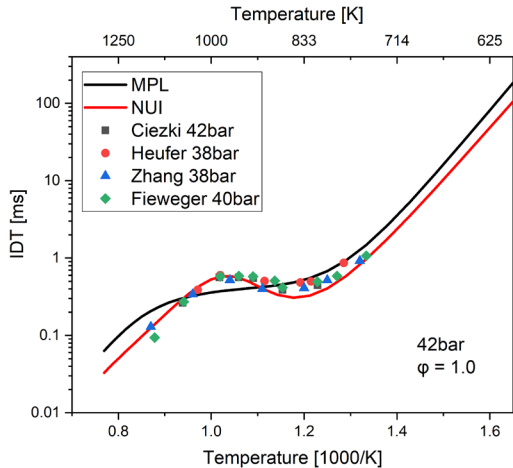


**Figure 29:** Solid lines: Global MPL model [3] and detailed NUI model [2] IDT predictions at 42 bar and stoichiometric heptane/air ratio ( $\phi = 1.0$ ). Symbols: Experimental data from Ciezki and Adomeit (42 bar) [5], Heufer and Olivier (38 bar) [6], Zhang et al. (38 bar) [2] and Fieweger et al. (40 bar) [7] at same initial concentrations.

When combining the methane model with the MPL model, no interactions in the chemistry are introduced, giving the heat release and the products ( $\text{CO}_2$  and  $\text{H}_2\text{O}$ ) to be the only common factors. The results of the combined models (one with a full detailed methane mechanism and one with a reduced methane mechanism) are shown in figure 2 compared to the NUI model and experimental data. No NTC region is observed for the methane/heptane mixture due to the high methane content, which shows no NTC effects. This trend is well predicted by the combined model within a factor of 2 to the NUI model. However, at higher temperatures the combined model over predicts the

IDT up to a factor of 2.5. No difference in the IDT predictions using the full detailed or reduced methane model is observed.

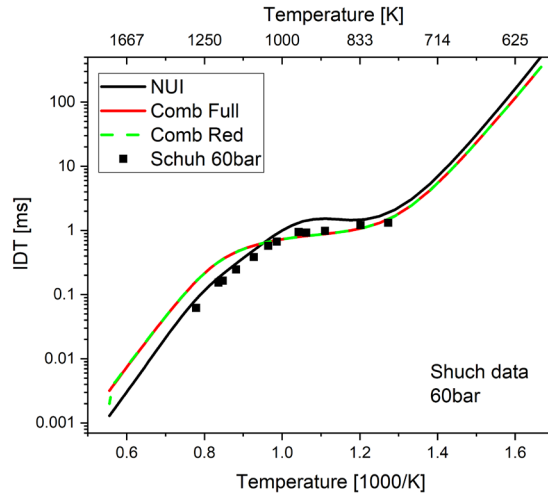


**Figure 2:** Symbols: experimental shock tube data from Schuh et al. [8], at 60 bar, a methane/heptane ratio on 10 and global equivalence ratio on  $\phi_{\text{global}}=0.816$ . Solid lines: NUI model [2], full combined model and reduced combined model IDT predictions of the same dual fuel mixture and conditions.

## Conclusion

This study indicates that it is possible to combine a reduced methane model with a global *n*-heptane model and sufficiently predict the ignition delay time (IDT) of methane/heptane mixtures at high pressures.

## Acknowledgements

The work is carried out at the Combustion and Harmful Emission Control (CHEC) research center at DTU. The project is funded by the Independent Research Fond Denmark (IRFD). The author would like to thank Cirkeline Mjølna (bachelor student) for close collaboration.

## References

1. H. Hashemi, J. M. Christensen, S. Gersen H. Levinsky, S. J. Klippenstein, P. Glarborg, Combust. Flame 2016, 172, 349–364.
2. K. Zhang, C. Banyon, J. Bugler, H. J. Curran, A. Rodriguez, O. Herbinet, F. Battin-Leclerc, C. B'Chir, K. A. Heufer. Combust. Flame 2016, 172, 116–135.
3. U. Müller, N. Peters, A. Liñán, Symp. (Int.) on Combustion 1992, 24, 777–784.
4. J. Liang, Z. Zhang, G. Li, Q. Wan, L. Xu, S. Fan, Fuel 2019, 235, 522–529.
5. H. K. Ciezki, G. Adomeit, Combust. Flame 1993, 93, 421–433.
6. K. A. Heufer, H. Olivier, Shock Waves 2010, 20, 307–316.
7. K. Fieweger, R. Blumenthal, G. Adomeit, Combust. Flame 1997, 109, 599–619.
8. S. Schuh, A. K. Ramalingam, H. Minwegen, K. A. Heufer, F. Winter, Energies 2019, 12, 3410.

# Novel Catalysts for the Selective Oxidation of Methanol to Formaldehyde

(November 2017- October 2020)



## Contribution to the UN Sustainable Development Goals

Catalysis is the science of making reactions happen under milder conditions and promoting specific products. Improvements in selectivity and activity can lower the material loss to unfavorable byproducts, and decrease the energy usage. Formaldehyde is a major chemical made from catalytic oxidation of methanol. In this process, specific challenges are fast catalyst deactivation and increasing power usage from gas blowers due to deposition of (toxic) Mo in the end of the catalyst bed. The development of novel materials may help decrease the power and Mo usage.



**Joachim  
Thrane**

joathr@kt.dtu.dk

**Supervisor:** Anker Degn Jensen, Martin Høj, and Max Thorhauge

## Abstract

Novel Mo containing catalysts for the selective oxidation of methanol to formaldehyde have been synthesized, tested for catalytic activity and selectivity, and characterized by various methods including XRD, Raman and SEM. Tests of the catalysts have been performed at 250-400°C for up to 600 h on stream. Most promising were MoO<sub>3</sub> supported on Ca hydroxyapatite (HAP) and the Sr analogue. Industrial sized pellets were prepared for MoO<sub>3</sub>/HAP, which elucidated that diffusion aspects must be taken into account going from powder to pellets.

## Introduction

Formaldehyde is the most significant aldehyde commercially available as it is an irreplaceable C<sub>1</sub> building block for higher-valued products due to its high reactivity [1]. The annual global production of formaldehyde is expected to increase with a CAGR of 4.8-5.8% and reach a market of 36.6 million tons by 2026 [2,3]. Formaldehyde is mainly produced through either the silver process or the Formox process [1].

In the Formox process, the formaldehyde is formed by catalytic oxidation of methanol over an iron molybdate catalyst (MoO<sub>3</sub>/Fe<sub>2</sub>(MoO<sub>4</sub>)<sub>3</sub>), which achieve high selectivities (92-95%) at high conversions (>99%) [1]. The catalyst, however, is not stable during reactions conditions due to formation of volatile molybdenum compounds [4]. It is thus of interest to develop novel, more stable catalysts for the oxidation of methanol to formaldehyde.

## Specific Objectives

The overall objective of the PhD project is to investigate and develop new catalysts for the selective oxidation of methanol to formaldehyde. This was done through the following parts.

Part 1: To make an extensive investigation of promising materials in the existing literature.

Part 2: Testing of alkali earth metal molybdates as catalysts for the selective oxidation of methanol to formaldehyde.

Part 3: Investigation of MoO<sub>3</sub> supported on hydroxyapatite and the Sr analogue by catalytic testing and various characterization methods.

## Experimental

Catalytic samples were prepared by various methods such as co-precipitation, reflux, sol-gel synthesis and incipient wetness impregnation. The samples were characterized by XRD, N<sub>2</sub>-physisorption, ICP, NH<sub>3</sub>-TPD, CO<sub>2</sub>-TPD, TPR, SEM, STEM, Hg-porosimetry and Raman spectroscopy. Catalytic tests have been performed on a lab scale, fixed bed reactor setup (described in [5]) at temperatures from 250-400°C. Methanol feeding was achieved by saturating the gas mixture in a bubble flask before entering the reactor. The effluent was analyzed for CH<sub>2</sub>O, methanol, dimethyl ether, di-methoxymethane, methyl formate, CO and CO<sub>2</sub> by using a GC with both TCD and FID detectors.

## Results and Discussion

Various samples of alkali earth metal molybdates ( $\text{MMoO}_4$ , M = Mg, Ca, Sr, Ba) were synthesized and tested (Figure 1) and was found to have good selectivity and activity when prepared with excess Mo, however, it was found by Raman spectroscopy that the excess Mo disappeared under operation,

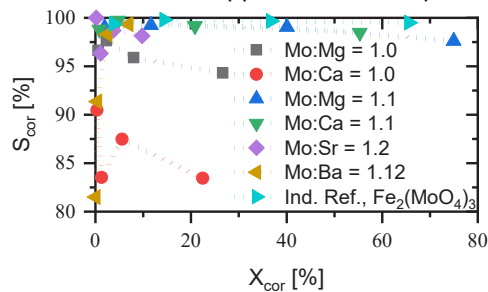


**Figure 1:** Reversible byproducts corrected selectivity towards formaldehyde vs. the corrected conversion obtained by measurements at 250°C, 300°C, 350°C and 400°C. 25 mg catalyst (150-250 µm) diluted in 150 mg SiC. Flow: 150 NmL/min, MeOH/O<sub>2</sub>/N<sub>2</sub> = 5/10/85 %

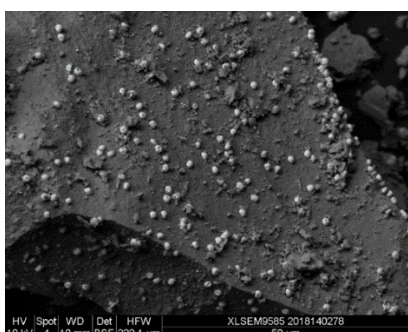


**Figure 2:** SEM image of fresh 10 wt% MoO<sub>3</sub>/HAP.

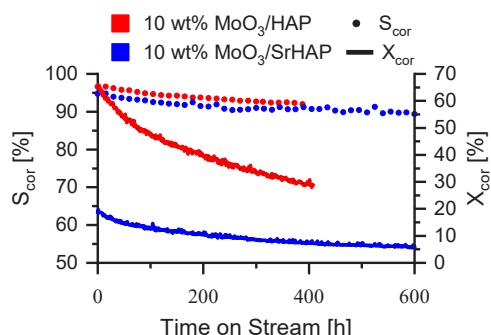


**Figure 3:** Reversible byproduct corrected selectivity and conversion vs. time on stream. 25 mg catalyst (150-250 µm) diluted in 150 mg SiC at 350°C. Flow: 150 NmL/min, MeOH/O<sub>2</sub>/N<sub>2</sub> = 5/10/85 %.

which could also be seen by decreasing activity and selectivity over time. If instead MoO<sub>3</sub> was impregnated on an apatite support such as  $(\text{Ca}_5(\text{OH})(\text{PO}_4)_3$  or  $\text{Sr}_5(\text{OH})(\text{PO}_4)_3$ )  $\text{CaMoO}_4$  and  $\text{SrMoO}_4$  was also observed by XRD after calcination, but much less Mo have been used compared to bulk  $\text{MMoO}_4$  and  $\text{Fe}_2(\text{MoO}_4)_3$ . It was found by SEM (Figure 2), that the  $\text{CaMoO}_4$  was

formed as small particles on the surface of the large support particles. These catalysts have better selectivity, activity and stability, even though crystalline MoO<sub>3</sub> was not measurable by XRD. The selectivity stayed above 89% for over 400 h on stream for a powder test (Figure 3). When testing the catalysts in the form of industrial sized pellets it was found that there is a large dependence on the pellet density (Figure 4) of both selectivity and activity. This is due to diffusion limitations, which must be taken into account when developing an industrial catalyst.

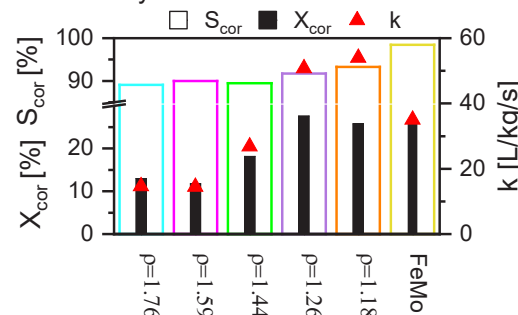


**Figure 4:** Reversible byproduct corrected selectivity, conversion and 1<sup>st</sup> order rate constant as function of pellet density ( $\rho$ ) in g/cm<sup>3</sup> at 350°C for MoO<sub>3</sub>/HAP. 1 pellet (60-91 mg). Flow: 300 NmL/min, 5% MeOH, 10% O<sub>2</sub> and 85% N<sub>2</sub>.

## Conclusions

It has been found that excess Mo on alkali earth metal molybdates give high selectivity and activity but evaporates during operation. MoO<sub>3</sub> impregnated on hydroxyapatite and the Sr analogue gives selective catalysts for the oxidation of methanol to formaldehyde with good stability. The pellet density have a significant influence on the activity and selectivity of MoO<sub>3</sub>/hydroxyapatite catalysts.

## Acknowledgements

This project is part a collaboration between the CHEC research center at Department of Chemical and Biochemical Engineering at DTU and Haldor Topsøe A/S. Funding from Independent Research Fund Denmark (DFF – 4184-00336) is gratefully acknowledged.

## References

1. A. W. Franz et al., Formaldehyde, Ullmann's encyclopedia of industrial chemistry, 2016, p. 1-34.
2. <https://www.prnewswire.com/news-releases/global-formaldehyde-market-2018-2022-300633054.html>, Accessed: 10.11.2018
3. <https://www.transparencymarketresearch.com/formaldehyde-market.html>, Accessed: 10.11.2018
4. B. I. Popov, V. N. Bibin, B. K. Boreskov, *Kin. i Kat.* 17, 371 (1976).
5. M. Høj, A. D. Jensen, J.-D. Grundwaldt, *Appl. Cat. A: Gen.* 451, 207 (2013)

# Theory, Simulation and Models for Electrolyte Systems with Focus on Ionic Liquids

(03. 2018 – 03. 2021)

7 AFFORDABLE AND CLEAN ENERGY



## Contribution to the UN Sustainable Development Goals

Electrolytes are indispensable elements in energy storage since the positive and negative electrodes are interconnected by an electrolyte solution that determines the charge transport during the charge/discharge process. Ideal electrolytes should fulfill the following requirements: *i.e.*, wide voltage window, excellent electrochemical stability, high conductivity, high ionic concentration, environmental friendliness. The design of electrolytes with simulations, theories and models for a good performance is helpful to guide the synthesis of electrolytes, so as to realize the efficient use of energy.



Jiahuan Tong

jito@kt.dtu.dk

**Supervisor:** Nicolas von Solms, Xiaodong Liang, Suojiang Zhang

## Abstract

Ionic liquids are used as electrolytes in high-performance lithium-ion batteries, which can effectively improve battery safety and energy storage capacity. All atom molecular dynamics simulation (MD) and experiment were combined to investigate the effect of lithium concentration on the performance of electrolyte in four IL solvents ( $[C_nmim][TFSI]$  and  $[C_nmim][FSI]$ ,  $n=2,4$ ). The IL electrolytes exhibit higher density and viscosity, meanwhile larger lithium ion transfer numbers as the concentration of LiTFSI increases. Furthermore, in order to explore the effect of the concentration of lithium salt on the ionic associations of  $Li^+$  and anion of IL, the microstructures of the lithium salt in various IL electrolytes at different concentrations were investigated. The structural analysis indicated strong bidentate and monodentate coordination were found between  $Li^+$  and anion of IL electrolytes. Both cis and trans isomerism of  $[FSI]^-$  were observed in  $[FSI]^-$ -type IL electrolytes systems, furthermore, the existence of the ion cluster  $[Li[anion]_x]^{(x-1)}$  in IL electrolytes, and the cluster became more closed and compact as the concentration of LiTFSI increases.

## Introduction

With the popularity of personal portable electronic devices, new energy vehicles and renewable energy are developing rapidly. The electrochemical energy storage system with high energy density, high cycle stability and high power density is facing enormous challenges, and has gradually become the main research direction in the world. Lithium ion batteries have dominated the battery market since their successful commercialization in the early 1990s due to their high voltage, high specific energy and long cycle life.<sup>[1]-[2]</sup> However, the battery performance and composition requirements are becoming more and more stringent as the application requirements continue to improve. The safety of lithium ion battery has been exposed and increasingly prominent, it is difficult to meet the requirements of lightweight, high-capacity, long-life electronic equipment, electric vehicles and other technologies. Therefore, the development of a new generation of green battery system with high performance and

environmental protection has become a common challenge for the international community.

Electrolyte, as a key component of lithium battery, not only plays a role in conducting lithium ions and conducting internal circuit, but also is one of the important factors that determine battery capacity and cycle stability. Excellent battery electrolyte generally has the following characteristics: (1) good chemical and electrochemical stability, does not react with the electrode in the operating voltage range; (2) high lithium ion transport capacity; (3) good compatibility with positive electrode and lithium metal negative electrode; (4) excellent electronic insulation performance; (5) low cost, low toxicity, environmental protection, etc. However, the most widely used organic solvent electrolyte in industry cannot meet all the above comprehensive performance currently. Therefore, optimization and design of electrolyte composition and formula has become one of the best ways to promote the rapid development of lithium ion batteries.

## Research Progress of Project

### 1. Model development of electrolyte system

In order to maintain different salt concentrations in this work, 100 pairs of LiTFSI are placed in periodic boundary simulation boxes with different number of ILs, respectively (Table 1). The initial configurations of all simulated models were built by using Packmol package. All the MD simulations were performed using Gromacs software. The Verlet algorithm was used to integrate Newton's equations of motion. Meanwhile, the van der Waals and electrostatic interaction were treated with Lennard-Jones potential and the Particle Mesh Ewald (PME) algorithm, respectively. For each system the canonical ensemble (NVT) and the isothermal isobaric ensemble (NPT) are relaxed for the first 10ns and the next 60ns, respectively. Furthermore, the NPT ensemble and the microcanonical ensemble (NVE) are carried out for 50ns and 10ns to achieve the configurational equilibria. In the process of simulation, the trajectory is recorded every 0.1ps with time step of 1.0 fs for further analysis.

**Table 1.** Compositions of simulation systems

Ionic liquids	Structure	Number of ILs				Number of LiTFSI
		0.3mol/L	0.5mol/L	1.5mol/L	2.0mol/L	
[C <sub>2</sub> mim][TFSI]		964	551	140	88	100
[C <sub>2</sub> mim][FSI]		1540	882	223	141	100
[C <sub>4</sub> mim][TFSI]		900	515	130	82	100
[C <sub>4</sub> mim][FSI]		1327	760	192	121	100

### 3. Physicochemical properties

In Figure 1, it is also obviously shown that the density trends with concentration of LiTFSI are linear, meanwhile viscosity are almost exponential for all IL electrolytes in this work. Previously reported by our group, due to their strong interactions between Li<sup>+</sup> and TFSI<sup>-</sup>, adding lithium salt LiTFSI to electrolyte will lead to the increase of density. Meanwhile, it is found that for a common cation ([C<sub>2</sub>mim]<sup>+</sup> or [C<sub>4</sub>mim]<sup>+</sup>), [TFSI]<sup>-</sup>-type IL electrolytes have higher density and viscosity than [FSI]<sup>-</sup>-type IL electrolytes. However, for a common anion ([TFSI]<sup>-</sup> or [FSI]<sup>-</sup>), the density of the IL electrolytes decreases as the length of the side chain increased, and the viscosity is reversed. In addition, according to the function of the viscosity and concentration of lithium salt, it can be seen that the viscosity of the [FSI]<sup>-</sup>-type IL electrolytes changes slowly compared with the [TFSI]<sup>-</sup>-type electrolyte.

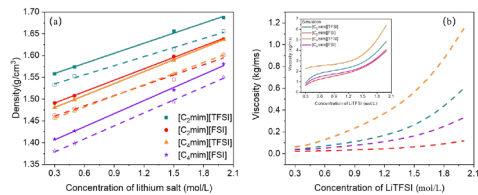


**Figure 1.** Density (a) and viscosity (b) vs concentration of LiTFSI for all ionic liquid electrolytes (The dashed line and open points are the result from experiment and the solid line and filled points are from MD simulation)

### 4. Microstructural analysis

In order to explore the relationship between the structure and properties of electrolyte, the electrolyte solvation of the cation Li<sup>+</sup> was discussed in the organic and ILs solvents to reveal the solution interactions between solute and solvent by radial distribution function (RDF),

$$g(r) = \frac{\langle \sum_{i,j} \delta(r - r_{ij}) \rangle}{N\rho} \quad (1),$$

where  $N$  is the number of particles,  $\rho$  is the number density,  $r_{ij}$  is the spatial distance.

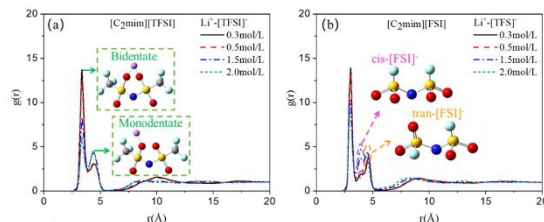


**Figure 2.** Radial distribution function of Li ion and anion of [C<sub>2</sub>mim][TFSI] and [C<sub>2</sub>mim][FSI] ( $n=2,4$ ) for four concentration of lithium salt LiTFSI at 298K.

### 5. Conclusion

The physicochemical properties of all IL solvent electrolytes were calculated and measured at the first. Simulation results showed that the density and viscosity increases with the increased concentration of LiTFSI for all LiTFSI-ILs electrolytes. As shown in the simulation results, higher values both in density and viscosity of LiTFSI-ILs electrolytes were detected as the concentration of LiTFSI increases. Later, we investigated the effect of the concentration of lithium salt on the ionic associations of the ions Li<sup>+</sup> and ILs by evaluating the radial distribution function and ionic coordination number. Further, the ionic cluster [Li[anion]<sub>3</sub>]<sup>2-</sup> in the IL electrolytes has been found by analyzing the coordination of lithium ion and anion of ILs.

### References

1. L. Zhou, K. Zhang, Z. Hu, Z. Tao, L. Mai, Y.M. Kang, S. L. Chou, J. Chen. *Adv. Energy. Mater.*, 2018, **8**, 1-23.
2. H. Zhang, H. Zhao, M. A. Khan, W. Zou, J. Xu, L. Zhang. *J. Mater. Chem. A*, 2018, **6**, 20564-20620.

# Development of Digital Twins in Water Treatment Systems

(October 2020 - September 2023)



## Contribution to the UN Sustainable Development Goals

Water treatment systems are an integral part of modern society that facilitate handling and treatment of wastewater. Most water treatment systems rely on a series of complex physicochemical and biological operational units which prompts the requirement for digital tools in order to improve process understanding. The digital twin developed within this project will provide process engineers with an ability to visualize and monitor current conditions as well as ask questions and predict real-world scenarios that improves the basis of decision for potential changes.



**Sebastian Topalian**

sebtop@kt.dtu.dk

**Supervisor:** Krist V. Gernaey, Xavier Flores-Alsina, Damien Batstone (University of Queensland)

## Abstract

The main objective of this PhD project is the development of a decision support tool based on mathematical models to evaluate resource recovery options from industrial / urban wastewater streams in line with the circular economy and sustainability goals. The decision tool will be operating as a digital twin and will be working as a replica of physical systems that combine physical data (measurements) with real-time, in-situ data (sensors) to simulate water treatment functions.

## Introduction

Mathematical modelling is commonly used to increase process understanding of complex chemical and biochemical phenomena, and it is also employed within the field of wastewater treatment. Wastewater treatment modelling is commonly used during design, control, diagnosis, optimization and teaching. These models have demonstrated to be extremely useful to evaluate promising technologies before full-scale implementation. In this way, undesirable options may be identified at an early stage and only the solutions with the highest rate of success will be put into practice.

Modern water treatment systems contain a series of integrated process units and modelling entire water treatment systems requires the integration of several independent process models into one system wide model. Constructing these models for water treatment systems requires a deep understanding of the underlying chemistry and biochemistry in order to properly tune the parameters for the different processing units in the model. Water treatment systems exist for both municipal and industrial systems, where the industrial systems presents an extra challenge, since their content varies drastically from that of municipal systems and from industry to industry.

## Objective & Scope

The objective of the project is to develop digital twins for municipal and industrial water treatment systems in Denmark and Australia with our partners from the Advanced Water Management Centre at the University of Queensland.

Developing and employing digital twins for plantwide optimization requires the following steps:

- 1) Sensor installation and maintenance
- 2) Data collection and reconciliation
- 3) Model development and adaptation
- 4) Integration of individual processing unit models to one system wide model
- 5) Scenario generation and evaluation for plantwide control strategies

The main focus will be on steps 2-5 since most of the industrial partners are responsible for step one and they actively maintain their sensors.

Furthermore, the digital twin development process is to be thoroughly documented in order to describe all the necessary steps from data reconciliation to plantwide evaluation, so third party users can easily develop their own digital twins. This will be achieved by publishing journal articles and distributing open-source software.



# Slide-ring silicone networks for dielectric elastomer actuators

(December 2018- December 2021)

9 INDUSTRY, INNOVATION  
AND INFRASTRUCTURE



## Contribution to the UN Sustainable Development Goals

The advances in lightweight and flexible electromechanical actuators are on the forefront in advancing the fields of soft robotics and biomimetic prosthetics. The development of elastomers with novel network structures opens up the possibility to meticulously tailor actuators that can possess distinct responses depending on the external stimuli. By achieving these features through the intrinsic properties of the actuating materials themselves, it is possible to bypass the need for constructing bulky mechanisms to accomplish similar functions.



**Jakob-Anantu Tran**

[jakant@kt.dtu.dk](mailto:jakant@kt.dtu.dk)

**Supervisor:** Anne Ladegaard Skov, Jeppe Madsen

## Abstract

Slide-ring elastomers consist of mobile cross-links that can freely slide on their axial polymers in a manner similar to a pulley on a zip line. This novel network structure imparts the elastomers with a distinct sliding elasticity not present in conventional elastomers. The use of sliding networks for dielectric elastomer actuators has been limited due to the low compatibility of slide-ring materials and common elastomer platforms such as silicones. Here, a synthetic pathway is proposed for chemically modifying slide-ring cross-linkers and incorporating them in sliding silicone elastomers that exhibit two distinct time dependent viscoelastic profiles.

## Introduction

Slide-ring materials demonstrate a novel type of dynamic network structure consisting of mobile cross-links that can rearrange on a molecular scale axis. The sliding links are formed by ring molecules that have been threaded on linear axis polymers like pulleys on a rope. This supramolecular assembly allows the rings to be used as movable cross-links that can slide on the constrained axis when exposed to external forces, thus evenly distributing the stress within the network (as seen in Figure 1). The rings can also revert to their original position when relaxed due to their air spring like behavior [1]. The sliding elastomers have been proven peculiar in their intrinsic softness while maintaining high deformability and toughness [2]. This reversible and soft nature of slide-ring materials makes them ideal candidates for dielectric elastomer actuators.

The use of slide-ring cross-linkers is generally restricted by the low reactivity of the pure polyrotaxanes as well as miscibility issues [3]. The issues are caused by the dense hydrogen bonding that occurs between the threaded rings and can be solved by chemical modification of the polyrotaxanes.

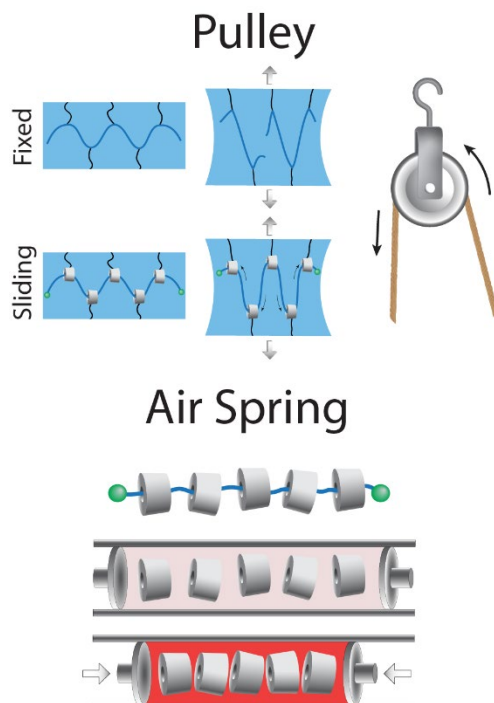


**Figure 1: Pulley and air spring behavior**

Here, we present a synthetic pathway to prepare vinyl functional slide-ring cross-linkers that can be handled with common solvents and incorporated into silicone networks through hydrosilylation. These factors are important in ensuring the versatility and scalability of the slide-ring cross-linkers as the foundation of a new class of sliding silicone elastomers.

## Results and Discussion

Commercially available silylating agents were utilized to chemically modify the slide-ring cross-linkers in order to increase the compatibility between the cross-linkers and silicones. This process was also used to introduce the vinyl cross-linking functional groups that are necessary for the subsequent curing reaction. The general preparative steps for creating sliding silicone elastomers can be seen in Figure 2.

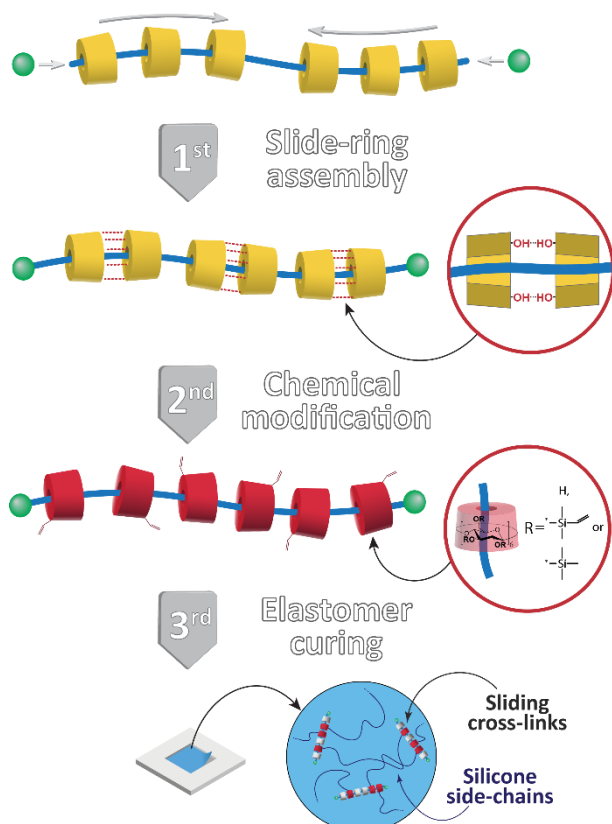


**Figure 2:** General procedure for preparing sliding silicone elastomers

The sliding silicone elastomers exhibited high softness while retaining the favorable dielectric

properties that are characteristic for silicones. Additionally, the sliding elastomers possessed a highly time dependent relaxation mode resulting from the ring sliding that is not present in traditional fixed silicone networks. When the elastomers are extended at a lower speed, they act considerably softer than the stiff response that they exhibit when they are deformed faster (as seen in the Figure 3). It should also be noted that the change is not gradual as would be expected for traditional viscoelastic materials.

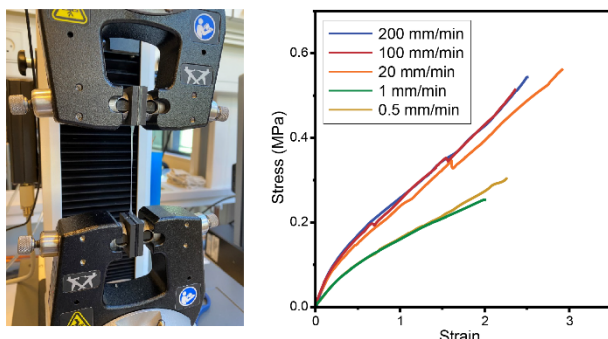


**Figure 3:** Two distinct strain rate dependent viscoelastic responses of the sliding elastomers

This phenomenon demonstrates the possibility of designing more intricate dielectric elastomer transducers with two distinctive modes of behavior determined by the operational speed of the actuators.

## Conclusions

Chemically modified vinyl functional slide-ring cross-linkers were produced with commercially available precursors. The increased processability of the modified cross-linkers allowed them to be used to create sliding silicones with novel material properties not observed in conventional elastomers. The facile nature of the curing chemistry suggest the possibility for exploring a new class of silicone elastomers.

## References

1. K. Kato, Y. Okabe, Y. Okazumi, K. Ito, 51 (2015) 16180–16183
2. K. Minato, K. Mayumi, R. Maeda, K. Kato, H. Yokoyama, K. Ito, *Polymer (Guildf.)*, 128 (2017) 386–391.
3. J. Araki, T. Kataoka, K. Ito K, *Soft Matter*, 4 (2008) 245–9

# Advanced Thermodynamic Models for Water

(November 2019- November 2022)

9 INDUSTRY, INNOVATION  
AND INFRASTRUCTURE



## Contribution to the UN Sustainable Development Goals

Water is the most abundant substance on earth and it is present on numerous everyday applications. Thus, having accurate models for predicting its thermodynamic properties are of high importance to numerous industries. Despite the fact that water is one of the most studied substances, current thermodynamic models are still lacking at accurately describing water. This project aims at developing more advanced thermodynamic models for water that will be able to accurately describe water's unique behavior.



**Evangelos Tsochantaris**  
evtsoc@kt.dtu.dk

**Supervisor:**  
Assoc. Prof. Xiaodong Liang, Prof. Georgios Kontogeorgis,

### Abstract

Water is at the same time the most important and the most anomalous substance on earth. Because of water's unique behavior, the prediction of its thermodynamic properties can prove to be challenging. At the early stages of this project we were able to evaluate the performance of two advanced equations of state that account for hydrogen bonding (PC-SAFT and CPA). The models were not able to predict any of water's anomalies. Thus, significant modifications are needed to the underlying theories. For the modifications it is important to seek out the possible origins of water's unique thermodynamic behavior.

### Introduction

Water is the most important liquid for our existence and plays an essential role in physics, chemistry, biology and geoscience. What makes water unique is not only its importance but also the anomalous behavior of many of its macroscopic properties[1,2]. Just to name a few of these "anomalies", water exhibits a density maximum at 4 °C, decreased viscosity under pressure and high surface tension [1].

Since water is the most common substance and is utilized in a large variety of processes, it is of high importance to have accurate models of water containing systems. Some extremely noteworthy models are equations of state (EOS). Equations of state are mostly simple models capable of fast calculations, they are applicable over a wide range of temperatures and pressures [3].

Besides the well-known cubic EOS, there are also available in recent years molecular EOS that explicitly take into account hydrogen bonding [3]. Two such equations of state are the perturbed chain – statistical associating fluid theory (PC-SAFT) and the cubic-plus-association (CPA) EOS.

For the project, we applied PC-SAFT and CPA on pure liquid water over a wide range of temperatures and pressures in order to properly evaluate their performance and identify the regions in which the models are lacking. The properties that we have investigated are vapor pressure  $P^S$ , density  $\rho$ , residual isobaric heat capacity  $C_p^r$ ,

isochoric heat capacity  $C_V^r$  and speed of sound  $u$ . It is worth noting that there are multiple studies that have used these models for water, especially for the estimation of phase equilibria of water-containing systems. However, few studies investigate all these thermodynamic properties.

### Results and Discussion

As mentioned earlier, water has been studied extensively with PC-SAFT and CPA EOS. Therefore, there are multiple parameter sets for water. So far, we have applied 14 PC-SAFT and 2 CPA parameter sets for the evaluation. The most common procedure for producing these sets is by simultaneously fitting the parameters to vapor pressure and saturated liquid density data. Of course there are authors who have attempted a bit more complex and sophisticated methods for the parametrization process. For instance, Liang et al. [4] have taken into account phase equilibria of water-hydrocarbon mixtures for the parametrization process.

In Table 1 absolute average deviation errors (AAD) of the calculated properties are displayed for one parameter set of each model. Both models show great accuracy for vapor pressure, but they fail to predict the rest of the properties within 5%. Water exhibits quite an unusual behavior for most of these properties, like the density maximum. It is important to investigate whether these models are able to capture water's anomalous behavior.

**Table 8.** Results from PC-SAFT and CPA under saturated conditions

Property	%AAD	
	PC-SAFT	CPA
$P^S$	1.08	1.08
$\rho$	7.46	5.40
$C_P^r$	21.5	12.1
$C_V^r$	22.0	15.0
$u$	26.7	11.6

As it can be observed from Figure 1 and 2 the models are not able to predict the density maximum nor the  $C_P^r$  minimum. These extrema are not the only anomalies in water. The speed of sound also shows maxima with respect to temperature, which are also not predicted by PC-SAFT and CPA. Therefore, it is clear that considerable changes are needed to the models and their underlying theories in order to improve their overall performance.

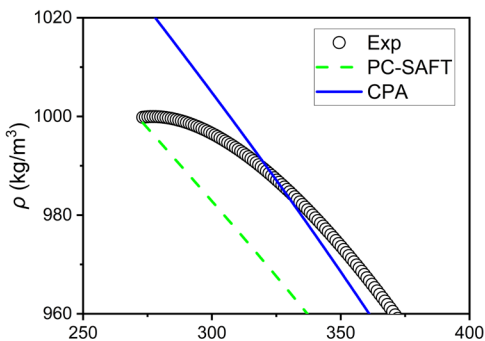


**Figure 30.** Density of pure liquid water at 0.1 MPa. Symbols represent experimental data and lines represent results from PC-SAFT and CPA.

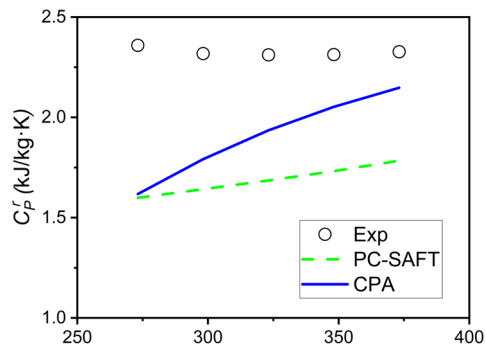


**Figure 31** Residual isobaric heat capacity of water at 0.1 MPa. Symbols represent experimental data and lines represent results from PC-SAFT and CPA.

The current models account for hydrogen bonding, but they do not account for various other phenomena that are also present in water, like polar interactions and hydrogen bond cooperativity. In

addition, the structure of water most likely plays a pivotal role to its unusual behavior. Marshall [5] who modified a similar association model to account for tetrahedral symmetry was actually able to capture the density maximum. However, this model did not show the same accuracy for other thermodynamic properties like the isothermal compressibility.

In order to accurately predict water's unusual properties, it is extremely important to address the cause of this behavior, but the cause is still debated in the scientific community [6]. One noteworthy and highly influential scenario is that there is a second critical point in water, a liquid-liquid critical point (LLCP), and so liquid water consists of two liquid states. These two states are usually referred to as low-density liquid (LDL) and high-density liquid (HDL). This scenario has been supported by many authors, but even amongst them there are disagreements.

### Acknowledgements

The authors wish to thank the European Research Council (ERC) for funding of this research under the European Union's Horizon 2020 research and innovation program (grant agreement No 832460), ERC Advanced Grant project "New Paradigm in Electrolyte Thermodynamics". The authors also wish to thank the Department of Chemical and Biochemical Engineering of DTU for funding the research.

### References

1. L. Pettersson, R. Henchman, A. Nilsson, Water—The Most Anomalous Liquid. *Chemical Reviews* 116 (2016) 7459–7462.
2. P. Debenedetti, H. Stanley, Supercooled And Glassy Water. *Physics Today* 56 (2003) 40–46.
3. G. Kontogeorgis, G. Folas, *Thermodynamic Models for Industrial Applications: From Classical And Advanced Mixing Rules to Association Theories*, John Wiley & Sons, 2010.
4. X. Liang, I. Tsivintzelis, G. Kontogeorgis, Modeling Water Containing Systems with the Simplified PC-SAFT and CPA Equations of State. *Industrial & Engineering Chemistry Research* 53 (2014) 14493–14507.
5. B. Marshall, A Doubly Associated Reference Perturbation Theory for Water. *Fluid Phase Equilibria* 500 (2019) 112252.
6. P. Gallo, K. Amann-Winkel, C.A. Angell, M.A. Anisimov, F. Caupin, C. Chakravarty, E. Lascaris, T. Loerting, A.Z. Panagiotopoulos, J. Russo, J.A. Sellberg, H.E. Stanley, H. Tanaka, C. Vega, L. Xu, L.G.M. Pettersson, Water: A Tale of Two Liquids. *Chem. Rev.* 116 (2016) 7463–7500

# Biogas Upgrading Simulation through Experimental Work and Thermodynamic Modelling

(December 2019- November 2022)

13 CLIMATE ACTION



## Contribution to the UN Sustainable Development Goals

Denmark has a great need to substitute the declining North Sea gas production. Biogas, a sustainable source of energy can potentially replace 10% of the energy needs currently met by fossil fuels. Untreated, it contains 30-40% of CO<sub>2</sub> and needs to be upgraded to bio-methane before being distributed to the natural gas energy grid. The purpose of this project is to create and demonstrate a financially viable technology, which will enable the purification of biogas to grid quality while simultaneously permitting the reuse of CO<sub>2</sub> making the process carbon neutral.



**Sai Hema Bhavya  
Vinjarapu**  
shbvin@dtu.dk

**Supervisor:** Philip Loldrup Fosbøl, Nicolas von Solms

## Abstract

Biogas upgrading is done for the removal of CO<sub>2</sub>. The purpose is to produce clean bio-methane from the biogas. CO<sub>2</sub> capture is a method that can accomplish this task. This project focuses on the chemical absorption process using amine as a baseline. The objective is to develop the basis for new additives, which may enhance the performance of the CO<sub>2</sub> capture technology. Monoethanolamine (MEA) is used as a basis for assessing the ease of benchmarking. The energy required for CO<sub>2</sub> capture can be optimized by the use of new additives termed as vapour reduction additives.

## Introduction

Energy productions of all forms contribute to 72% of greenhouse gas emissions [1]. Demand for energy across the globe is on the rise due to the rapid growth of economies. A majority of the world's energy needs are still met by fossil fuels. Renewable energy sources are expected to account for 34% of all the energy sources by 2050. Even in this scenario, the carbon emissions are projected to be 22% higher than required, to limit the global temperature rise to 2°C [1]. Therefore, there is an increasing urgency in switching to carbon-neutral sources while ensuring their cost-efficiency and economic viability.

One such potential alternative is Biogas. Biogas is produced by anaerobic digestion of organic waste from wastewater sludge, industrial wastes, and agricultural wastes. The composition of biogas depends on the raw organic material used. However, it generally comprises 60-70% Methane, 30-40% CO<sub>2</sub>, and minor impurities of water vapour and H<sub>2</sub>S [1]. Owing to the high CO<sub>2</sub> concentration, biogas has a low calorific value, making it a less appealing replacement to energy-dense fossil fuels. To increase its energy density, this CO<sub>2</sub> is required to be removed. This process of biogas purification is called biogas upgrading and the technology used for achieving this goal is called carbon capture.

Of the numerous carbon capture technologies available, chemical absorption by primary amines is state-of-the-art. Amines like Monoethanolamine (MEA), which are basic, react reversibly with acidic CO<sub>2</sub> gas. The process involves an absorber where CO<sub>2</sub> from the biogas dissolves in MEA, releasing pure bio-methane. The CO<sub>2</sub>-rich solvent then enters a desorber where it is heated to regenerate MEA and a pure CO<sub>2</sub> stream. The regenerated MEA is recycled to the absorber and the pure CO<sub>2</sub> obtained is either sequestered or utilized as a raw material. MEA has a high absorption capacity of CO<sub>2</sub> and a high reaction rate, which make it a suitable solvent.

Conventionally, the CO<sub>2</sub>-rich solvent is heated to 105°C by lean-amine before being pumped to the top of the desorber, which is at 110°C. The reboiler at the bottom of the column is at 120°C. A high-energy requirement is the main limitation of this technology. The heat required for the solvent's regeneration is given as the sum of three terms [3]:

$$Q_{reb} = Q_{sens} + Q_{vap, H2O} + Q_{abs, CO2} \quad (1)$$

where, Q<sub>sens</sub> is the sensible heat required to raise the temperature of the solvent to that of the reboiler's, Q<sub>vap, H2O</sub> is the heat of evaporation required to produce the stripping steam in the reboiler, and Q<sub>abs, CO2</sub> is the heat of absorption of CO<sub>2</sub> into the solvent. The equivalent amount of heat released by the exothermic absorption of CO<sub>2</sub> should be supplied to desorb it. The energy required

for regeneration accounts for 70-80% of the whole process. Additionally, the high-temperature conditions result in degradation of the solvent leading to corrosion of the equipment. All of these result in significant operating costs. These disadvantages inhibit the wide-scale implementation of the process.

### Specific Objectives

The objective of the project is to develop and demonstrate a financially viable solvent technology for biogas upgrading. This will be an extension of the existing MEA-based carbon capture. In order to optimize the regeneration of the solvent, new additives, known as vapour reduction additives are being investigated. Typically, a 30 wt% aqueous MEA solvent is used for the capture process. The high water content implies a high heat of vaporization, increasing the heat of regeneration and solvent losses. The vapour reduction additives (VRAs) are designed to replace water, thereby reducing the solvent's vapour pressure. This abates the amount of water evaporated along the column, thereby decreasing the energy requirements at the condenser situated at the top of the desorber. Further, the size requirements of the desorber are expected to decrease resulting in a decline in both capital and operating costs. The following are the different aspects that would be investigated in the course of the project:

- Determination of physical properties like density, viscosity, heat of absorption.
- Fitting of experimental data to a thermodynamic model to determine the parameters of the species.
- Transfer of the thermodynamic model and parameters to Aspen Plus for simulation.
- Rate-based modelling of the system.
- Pilot-scale campaigns of the new solvents.

### Results and Discussion

To calculate the performance of CO<sub>2</sub> capture in aqueous mixtures of MEA and VRAs, simulators need accurate models capable of calculating the equilibria and thermal properties of the system. Therefore, the Extended UNIQUAC model developed by Kaj Thomsen [5] is extended to estimate the essential thermodynamic properties of this solvent system. This is done in several stages where parameters are fit to experimental data of various binary, ternary, and quaternary systems. The following is the data previously fit to the binary MEA-H<sub>2</sub>O system employing the Extended UNIQUAC model:

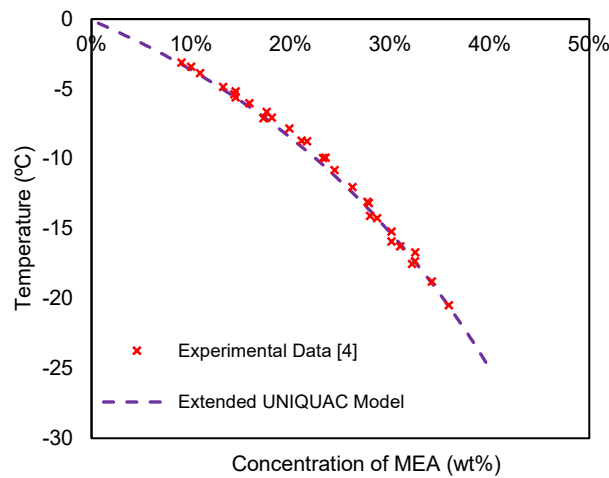


**Figure 1:** Experimental and modelled solid-liquid phase diagram for MEA- H<sub>2</sub>O system [6].

### Conclusion

Energy reduction of the solvent regeneration process plays a crucial role in the extensive establishment of biogas upgrading plants. The new solvent technology has the potential to meet these requirements. This project focuses on demonstrating this prospective.

### Acknowledgements

This project is co-funded by the Danish Government through the EUDP (Energy Technology Development Program) Agency.

### References

1. Global Energy Perspective 2019. (n.d.). Retrieved July 23, 2019, from <https://www.mckinsey.com/industries/oil-and-gas/our-insights/global-energy-perspective-2019>
2. Zhou, K., Chaemchuen, S., & Verpoort, F. (2017). Alternative materials in technologies for Biogas upgrading via CO<sub>2</sub> capture. Renewable and sustainable energy reviews, 79, 1414-1441.
3. Oexmann, J., & Kather, A. (2010). Minimising the regeneration heat duty of post-combustion CO<sub>2</sub> capture by wet chemical absorption: The misguided focus on low heat of absorption solvents. International Journal of Greenhouse Gas Control, 4 (1), 36-43.
4. Chang, H. T., Posey, M., Rochelle, G. T. (1993). Thermodynamics of Alkanolamine-Water Solutions from Freezing Point Measurements. Ind. Eng. Chem. Res, 32, 2324–2335
5. Thomsen, K. (1997). Aqueous electrolytes : model parameters and process simulation. (Ph.D Thesis).
6. Sadegh, N. (2013). Acid Gas Removal from Natural Gas with Alkanolamines : A Modelling and Experimental Study (Ph.D Thesis).

# Synergistic Optimization Framework for the Process Design of Biorefineries

(November 2018 - October 2021)

9 INDUSTRY, INNOVATION AND INFRASTRUCTURE



## Contribution to the UN Sustainable Development Goal

Lignocellulosic biomass is the most abundant and one of the most sustainable resources on earth. By utilizing it as feedstock for an integrated biorefinery, biofuels, platform chemicals and energy can be produced. This complies with the concept of a circular economy and promotes sustainable economic growth, independent from fossil resources. This work aims to synthesize biorefinery processes in a conceptual manner to exploit this potential fully and to facilitate the implementation of such biorefineries on a global scale.



**Nikolaus  
Vollmer**  
[nikov@kt.dtu.dk](mailto:nikov@kt.dtu.dk)

**Supervisor:**  
Gürkan Sin, Solange I.  
Mussatto (DTU  
Biosustain), Krist V.  
Gernaey

## Abstract

The scope of this work comprises the development of a synergistic optimization framework for the process synthesis and design of biorefineries by a hybrid optimization approach. By combining domain knowledge in the form of mechanistic models and process systems engineering techniques as superstructure optimization and simulation-based optimization, current gaps in the conceptual process design of novel bioprocesses can be closed and the implementation of biorefineries facilitated and expedited.

## Introduction

A key approach in expediting the transition towards a bio-based economy is the conceptual design and implementation of integrated second-generation biorefineries (iSGB) [1]. Despite tremendous efforts in research as well as various industrial initiatives, the number of active iSGBs worldwide is low, mainly due to their deficient economic robustness [2]. A conceptual design approach for these iSGBs is Superstructure Optimization (SSO), which yields an optimal candidate process topology (CPT), but which is inherently limited by the initial search space and the fidelity of the unit operation models [3,4]. This contrasts highly with the complexity of fermentation processes and disregards recent advances in synthetic biology for the optimization of the cell factories [2]. From a biotechnological perspective, this hurdle is surmounted by a design approach, in which the products are specified *a priori* and subsequently the cell factory and the process are tailored towards the product and finally the feedstock is specified [5]. Furthermore, by following a simulation-based optimization (SBO) approach, complex models of cell factories can be employed in the search for an optimal process design. Despite being computationally demanding, the second benefit from it is the possibility to include uncertainties into the process design with models of complex biological systems [6].

## Methodology

In this work, we therefore propose a novel synergistic framework for the synthesis and design of iSGBs: based on a hybrid approach integrating surrogate-based SSO with SBO: it harnesses both the power of the SSO for process synthesis and the potential of SBO for detailed design optimization. The framework itself capitalizes thorough knowledge regarding biotechnology and synthetic biology in order to guide decisions for both SSO and SBO, which results in a consolidated framework and an expedited evaluation process.

The first step of the proposed framework involves defining possible products for an iSGB and subsequently developing high-fidelity mechanistic models for compulsory unit operations in the iSGB. In the following step, these models are combined with other optional unit operation models in a superstructure. The complexity of the superstructure is heavily reduced by removing binary decision variables for compulsory unit operations and thus downsizing the search space. In order to solve the underlying mixed-integer nonlinear program (MINLP) of the superstructure, a surrogate-based approach, using different surrogate model types [7], is employed to identify several promising CPTs. In the next step, these candidates are subjected to detailed design optimization under uncertainty in a novel SBO framework [6], which directly uses the high-fidelity

process models instead of their surrogates to optimize the process under the objective of key performance indicators (KPI). The resulting optimized CPT is a base-case process design for an iSGB and can be analyzed further regarding economic or sustainability aspects.

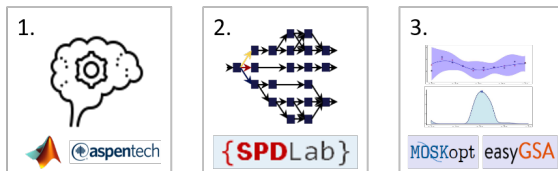


**Fig. 1:** Schematic representation of the framework

In this study, we apply the proposed framework in a case study to the process synthesis and design of a xylitol biorefinery. Xylitol is a platform chemical sugar substitute with manifold beneficial health properties. It can be produced by microbial fermentation and the current chemical production process is relatively expensive, which makes it an ideal product for an iSGB [8]. As the hemicellulosic fraction in lignocellulosic biomass consists mainly of xylose, it is selected as substrate for a fermentation process towards xylitol. Consequently, succinic acid, another high-potential platform chemical- is selected as value-added co-product of a fermentation process with the cellulosic fraction as substrate [9]. In order to meet the high energy demand of the iSGB, the lignin fraction is chosen as substrate for a combustion process. The chosen feedstock for the base case is wheat straw.

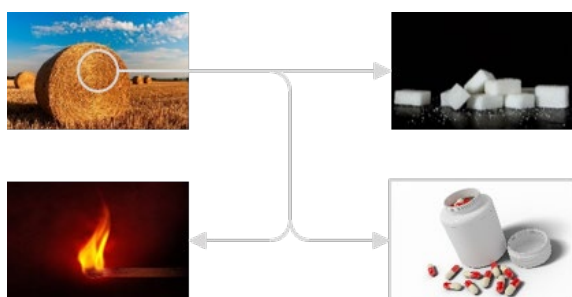


**Fig. 2:** Wheat straw as feedstock and possible set of products

The compulsory unit operation models for the xylitol biorefinery are the biomass pretreatment for the fractionation and depolymerization of the hemicellulosic fraction, as well as the fermentation processes for xylitol and succinic acid. Thus, based on domain knowledge, a detailed pretreatment model for dilute acid pretreatment is developed, as it proves to be the pretreatment with the highest hemicellulose monomer yield for the given case. Subsequently, both fermentation models are built based on domain knowledge of cell factories for fermentation in biomass hydrolysate media. This includes information about the physiology and the

optimization of the cell factory by synthetic biology tools. Furthermore, mechanistic models for different downstream unit operations, the enzymatic hydrolysis and a model for the combustion process of lignin are developed and validated. All models are analyzed towards robustness by a comprehensive Monte Carlo-based uncertainty and sensitivity analysis. Based on this, surrogate models are developed and validated. For the SSO a state-task network representation is selected and the surrogate models are utilized for the composition of the superstructure. Solving the resulting MINLP then yields the CPTs. In the last step they are subjected to SBO including the uncertainties in the model, input and design parameters for the unit operations. The selected KPI are the net present value, the discounted cash flow of return, as well as the minimum selling prices of the products.

## Conclusions

The result of this hybrid approach is then a consolidated base-case process for a xylitol biorefinery, which can be easily extended towards the evaluation of further products, process integration or value chain optimization. The resulting process itself is evaluated against both criteria of being economically viable and sustainable. With these criteria fulfilled, the process itself can be implemented. Hence, the presented hybrid approach can substantially assist the conceptual process design of further iSGBs in order to facilitate their implementation throughout industry as core part of a bio-based economy.

## Acknowledgements

This project is part of the Fermentation-Based Biomanufacturing Initiative and funded by the Novo Nordisk Foundation (NNF17SA0031362).

## References

1. F. Cherubini, Energy Conversion and Management 51 (2010) 1412-1421.
2. A.J.J. Straathof et al., Trends in Biotechnology, 37 (10) (2019) 1042-1050.
3. Q. Chen and I. Grossmann, Annual Review of Chemical and Biomolecular Engineering 8 (2017) 249-283.
4. L. Mencarelli et al., Computers & Chemical Engineering 136 (2020) 106808.
5. T. Chaturvedi et al., Energies 13 (6) (2019) 1493
6. R. Al et al., Computers & Chemical Engineering 142 (2020) 107118.
7. K. McBride and K. Sundmacher, Chemie Ingenieur Technik 91 (3) (2019) 228-239.
8. F. Hernández-Pérez et al., Critical Reviews in Biotechnology 39 (7) (2019) 924-943.
9. E. Mancini et al. Critical Reviews in Environmental Science and Technology 50 (18) (2019) 1829-1873.

# Linear viscoelastic and nonlinear extensional rheology of diamine neutralized entangled poly(styrene-co-4-vinylbenzoic acid) ionomer melts

(June 2018 - May 2021)



## Contribution to the UN Sustainable Development Goals

Polymer gels and networks are widely used in our daily life. Permanent networks can resist flow and creep, but they show limited processability and recyclability. Physical networks are more processable and recyclable but they creep at long time. The idea behind this project is to combine distinct features of permanent and physical networks in double dynamic networks, so as to make the product ideal for applications. In this way, we prolong the lifetime of polymer networks and contribute to a responsible production.



**Wendi Wang**

wendiw@kt.dtu.dk

### Supervisor:

Anne Ladegaard Skov  
Qian Huang  
Ole Hassager

## Abstract

Ionomers are a family of polymers with a small amount of ionic groups covalently attached to the polymer backbone, and have been widely used in everyday life. The processing of ionomers is challenging due to brittle fracture even in the melt state. In this work, we provide a new strategy of preparing flowable, stretchable and extensible ionomers. Diamine neutralized entangled poly(styrene-co-4-vinylbenzoic acid) ionomers are used as an example. They are studied and compared to non-ionic parent polymer by small amplitude oscillatory shear and nonlinear uniaxial extension measurements.

## Introduction

Ionomers are a family of polymers where a small amount (<10 mol%) of ionic groups is covalently attached to the polymer backbone (see Fig.1). They have been used in a variety of applications, such as membranes, packaging and films, compatibilizers, shape memory materials, and self-healing materials.[1,2] However, the processing of ionomers may be challenging due to ionic clusters formed by ion dipole interaction. The presence of ionic clusters has been confirmed by dynamic mechanical analyses and X-ray scattering.[3,4] As a result, ionomers usually have long relaxation times and are difficult to process even at high temperature.

To achieve better processability, it is important to avoid ionic cluster formation. This is usually realized by using lower ion concentration and weaker counter ion species, so that the relaxation time is shortened.

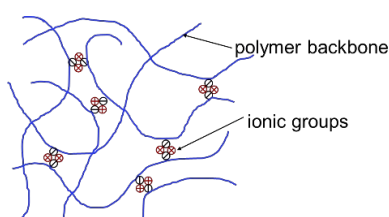


**Fig.32** Schematic presentation of ionomers

## Specific Objectives

In this work, we aim to provide a new strategy to prepare ionomers with good flowability, stretchability and extensibility. Entangled poly(styrene-co-4-vinylbenzoic acid) with 5 mol% acid ( $M_w=85\text{kg/mol}$ , number of entanglements  $Z=6.4$ ) was neutralized with diamines of two different molar masses. The linear viscoelastic behavior and nonlinear extensional behavior of the neutralized materials are studied and compared to those of their parent polymer.

## Materials

Poly(styrene-co-4-vinylbenzoic acid) (PS-co-PVBA) containing 5 mol% carboxylic acid prepared according to reference [5] has been separately mixed with two Jeffamines of different molar mass at stoichiometric ratio of acid and amine group. Weight-average molar mass ( $M_w$ ) and glass transition temperature ( $T_g$ ) for the parent polymer and the resulting neutralized ionomers are listed in Table 1.

**Table 9** Data for parent polymer and neutralized ionomers

Material	$M_w$ [kg/mol]	$T_g$ [°C]
PS-co-PVBA	85.4	105
PS-co-PVBA+ED900	87.7	66
PS-co-PVBA+D2000	85	25

A blend of polystyrene 77 kg/mol and Jeffamine D2000 is prepared as control sample.

## Results and discussions

### 1. Material characterization

The neutralized ionomers are transparent, whereas the control sample without ionic interaction is white as a result of phase separation. The ionomers are characterized by FTIR-ATR spectroscopy as seen in Fig.2. It is observed that the carbonyl-stretch around  $1700\text{ cm}^{-1}$  almost disappears by adding diamine. In addition, the C-O stretch of Jeffamine bonds around  $1100\text{ cm}^{-1}$  is clearly seen in the ionomers and is absent in the parent polymer.

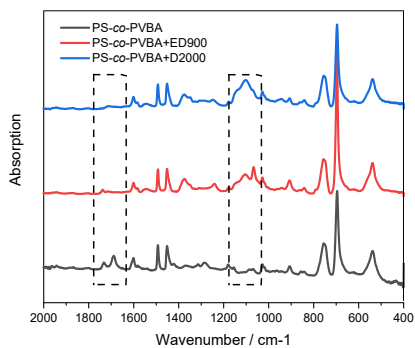


**Fig.33** IR spectrum for parent polymer and ionomers

### 2. Rheological properties

In Fig.3, linear viscoelastic measurements of all three materials are plotted in van Gorp-Palmen-plot with phase angle as a function of reduced complex modulus. In the reduced van Gorp-Palmen plot, the influences from chemical constitution, tacticity and monomer composition in copolymers are eliminated.[6] Hence the difference in  $T_g$  is compensated. Moving from high to low value of  $G^*/G_c^*$ , the phase angle drops and passes a minimum. After the minimum, the phase angle is larger with longer diamine length, thus a faster terminal relaxation, suggesting no ionic clusters inside the materials. This feature facilitates processing considerably.

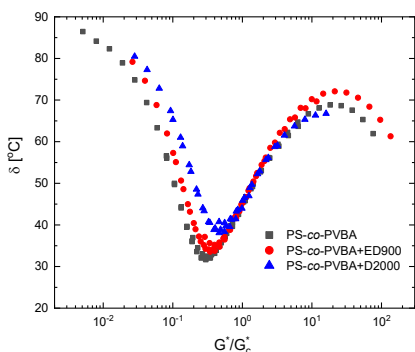


**Fig.34** Van Gorp-Palmen plot for all samples

Fig.4 shows the comparison of normalized nonlinear extensional behavior of all three materials.

The sample PS-co-PVBA was stretched faster than the inverse Rouse time, so that the chains are oriented and stretched. The neutralized ionomers are stretched to match this extension behavior. While the strain hardening is similar until Hencky strain 2.8, the Weissenberg numbers ( $Wi$ ) are different. Sample PS-co-PVBA+ED900 has a lower  $Wi$  than sample PS-co-PVBA, indicating an effectively stronger strain hardening owing to the ionic interaction. Hence, a more stretchable material is achieved. Sample PS-co-PVBA+D2000 has a slightly higher  $Wi$  than PS-co-PVBA; the strain hardening effect is compromised by the presence of the longer Jeffamine chain D2000. At larger strain, the ionomers display a reproducible stress overshoot, but finally reach a steady state without brittle fracture, indicative of good extensibility.

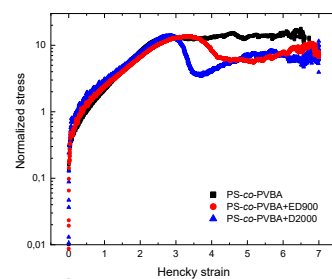


**Fig.35** Nonlinear extension behavior for all samples

## Conclusion

We provide a new strategy for preparing flowable, stretchable and extensible ionomers. Better flowability and processability are achieved by preventing ionic cluster formation using diamine chains. In nonlinear extensional measurements, better stretchability is achieved, manifesting as higher strain hardening compared to non-ionic parent polymer. Good extensibility up to Hencky strain 7 is obtained.

## Acknowledgement

This project has received funding from the European Union's Horizon 2020 Programme for Research and Innovation under the Marie Curie grant agreement number 765811(DoDyNet).

## References

- Shabbir et al., J. Rheol. 61 (2017) 1279-1289
- Zhang et al., Macromol. React. Eng. 8 (2014) 81-99
- Bazuinet et al., J. Polym. Sci. Part B Polym. Phys. 24 (1986) 1137-1153
- Zhang et al., Macromolecules. 50 (2017) 963-971
- Wang et al., Macromolecules. 52 (2019) 9261-9271
- Trinkle et al., Rheol Acta. 41 (2002) 103-113

# Particle deposition in high temperature processes

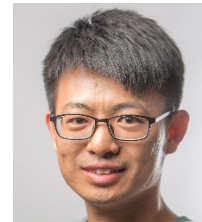
(April 2019- March 2022)

12 RESPONSIBLE CONSUMPTION AND PRODUCTION



## Contribution to the UN Sustainable Development Goal

The global energy consumption has increased during the past decades due to industrialization and urbanization. To reduce the use of fossil fuels, waste-derived fuels are increasingly used in mineral-based industrial high temperature processes. However, the use of waste derived fuels in these processes is challenged by deposit formation induced primarily by the high content of alkali and chlorine in waste. To facilitate the efficient use of waste-derived fuels in mineral-based industrial high temperature processes, it is desirable to improve the understanding and develop countermeasures for particle deposition.



**Xiaozan Wang**  
xiwang@kt.dtu.dk

**Supervisor:** Hao Wu  
Peter Arendt Jensen  
Kim Dam-Johansen

## Abstract

Mineral particle deposition on industrial high-temperature reactor surfaces, such as cement calciners and stone wool melting furnaces, may cause operational problems. Achieving an improved understanding of particle deposition is essential for reducing unwanted deposit formation and maximize industrial production efficiency. In this work, the influence of mineral feed particle properties and operating conditions on particle deposition is investigated in an entrained flow reactor using cement and stone wool raw materials.

## Introduction

Particle deposition occurs in many mineral-based industrial high temperature processes, such as cyclone-based stone wool production process and cement production process. In these processes, it is often not the fuel ash but the mineral feed that mainly causes deposit formation, and the deposition typically occurs on refractory lined surfaces. In some cases, moderate deposition is wanted and helps to decrease heat loss. However, excessive deposition may lead to blockage of flue gas channels, and sometimes even cause unscheduled plant outage<sup>1</sup>.

Particle deposition in combustion systems using biomass and coal has been studied extensively through laboratory and pilot-scale experiments, full-scale measurements, and modelling<sup>2</sup>. However, particle deposition in mineral feed based industrial high temperature processes, which usually involves different temperature and gas atmosphere conditions, different surface properties, and deposition locations, has only been studied limitedly. An improved understanding and modelling capability of particle deposition in industrial high temperature processes is wanted.

- To develop a chemical engineering model to predict deposit formation processes;
- To illustrate that the developed particle model is applicable to describe the particle deposition in industrial-size reactors;

## Methods

The mineral particles were mixed with air and injected into a 2 m long electrically heated furnace, as illustrated in Figure 1. The deposit is formed on an air-cooling steel probe, which can be take out from the bottom of the setup via side port.

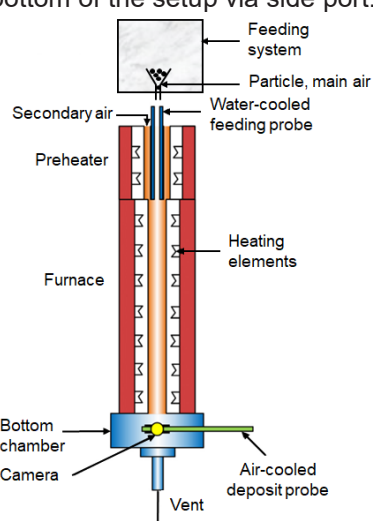


**Figure 1:** Schematic drawing of the pilot scale entrained flow reactor<sup>3</sup>

## Specific objectives

The specific objectives of this project are:

- To obtain an improved fundamental understanding of particle deposition in cement and stone wool production processes;

## Results and discussion

The influence of furnace temperature and deposit probe surface temperature on the deposit formation rate, using cement bypass dust, is presented in Figure 2. The furnace temperature ranges from 1000 °C to 1400 °C. For each furnace temperature, experiments were carried out with two probe surface temperatures, by running the experiments with and without air-cooling of the deposit probe.

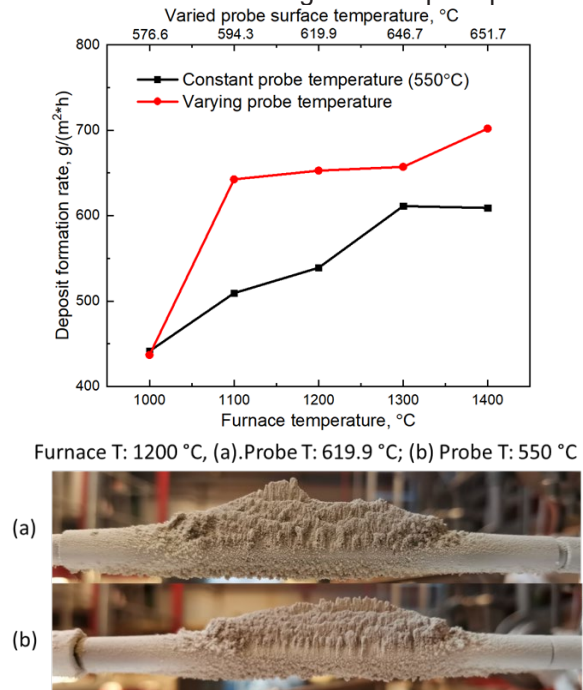


**Figure 2:** Effects of furnace temperature and probe surface temperature on deposit formation rate of cement bypass dust. Experiments were conducted with a particle feeding rate of 100g/h, an average gas velocity of 2.7 m/s in the reactor, and an experimental duration of 1 h.

It is observed that a higher furnace temperature leads to a higher deposit formation rate. The deposit formation rate on the probe without cooling is higher than that with cooling. Based on the morphology of the deposits, it can be inferred that the dominant deposition mechanism is particle inertial impaction.

Experiments with different duration (5, 7.5, 15, 30, 60 minutes) were also conducted. The obtained deposition rates and pictures of the deposits are shown in Figure 3.

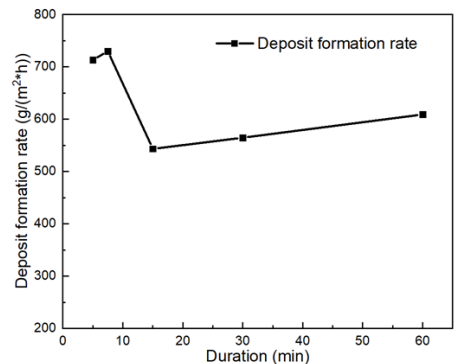


**Figure 3:** Effect of experiment duration on deposit formation rate. Experiments were conducted with cement bypass dust, with a furnace temperature of 1400°C, flue gas temperature 1099°C, gas velocity 2.7 m/s, probe surface temperature 550°C, feeding rate of 100g/h.

In Figure 3, it can be found that the deposit formation rate at 5 and 7.5 minutes are higher than the subsequent ones. This is mostly likely because both condensation and inertial impaction contribute significantly to early stage deposition formation, while condensation becomes less important for deposit formation after 15 mins.

## Conclusions

In the present study, the effects of furnace temperature, probe surface temperature and experiment duration on cement bypass dust deposition rate were investigated. Both higher furnace and probe surface temperature lead to a higher deposit formation rate. The deposit formation rate in the early stage is higher than at later stages.

## Acknowledgement

This project is funded by China Scholarship Council (CSC), Technical University of Denmark (DTU), and the ProBu project funded by Innovation Fund Denmark, ROCKWOOL A/S, FLSmidth A/S and DTU.

## References

1. Zbogar A, Frandsen F, Jensen PA, Glarborg P. *Prog Energy Combust Sci.* 2009;35(1):31-56.
2. Wu H, Bashir MS, Jensen PA, Sander B, Glarborg P. *Fuel.* 2013;113:632-643.
3. Laxminarayan Y, Jensen PA, Wu H, Frandsen FJ, Sander B, Glarborg P. *Proc Combust Inst.* 2019;37(3):2689-2696.

# Hydrodynamics of circulating fluidized beds

(March 2019 - February 2022)

9 INDUSTRY, INNOVATION  
AND INFRASTRUCTURE



## Contribution to the UN Sustainable Development Goals

The political, societal, and environmental demand for replacement of fossil-based products with sustainable sources of production fosters new industrial infrastructures and technological advances through innovation. The use of bio-based materials, such as sugar, has shown promising potential as a candidate for superseding fossil-based feedstocks in production of chemicals. This drives the need for development of new skillsets, economic growth, and job opportunities that will help to keep Denmark abreast of the green transition.



**Frederik Zafiryadis**  
flza@kt.dtu.dk

**Supervisor:** Hao Wu,  
Anker Degn Jensen  
Morten Boberg Larsen,  
Haldor Topsøe A/S  
Elisabeth Akoh Hove,  
Haldor Topsøe A/S

## Abstract

Thermal cracking of sugars in a circulating fluidized bed system is a novel technology for producing intermediate oxygenate products, which can be further converted into a variety of bio-based chemicals. The technology has the potential to enable economically and environmentally sustainable production of bio-based chemicals for use in e.g. plastic production. The project aims at developing a computational fluid dynamics model to predict the hydrodynamic and reactive behavior of the fluidized bed system. The developed model is compared and validated with both cold- and hot-flow, pilot-scale measurements to predict the behavior and optimize the design of a full-scale plant.

## Introduction

Thermal cracking of sugars is performed in a fluidized bed. In the sugar cracking process, an aqueous sugar solution is fed and exposed to the catalyst particles in a circulating fluidized bed (CFB). The hydrodynamics of such CFB system are complex and play a critical role in successful design and operation of the plant.

Over the last few decades, computational fluid dynamics (CFD) has been used for evaluating, designing, and scaling-up CFB reactors [1]. Several modeling approaches have emerged, treating the challenges of modeling particle-particle and particle-gas interactions in different ways. The hybrid Eulerian-Lagrangian multiphase particle-in-cell (MP-PIC) method has gained increased attention over the last years due to its ability to model large-scale systems with polydisperse particles at acceptable computational costs [2]. The method has been adopted for modeling of risers, downers, bubbling beds, strippers etc. of different types of systems. However, only a few full-loop MP-PIC, CFB simulations have been reported in literature [1,3,4]. Additionally, even for cold-flow systems under inert conditions, the accuracy of the simulations are highly case sensitive, and only a limited amount of work has been conducted on improving the prediction accuracy of the models. This study aims at closing this gap in the literature

by experimentally investigating the hydrodynamics of the CFB system in pilot-scale. Using the experiences and obtained data as foundation for validating the CFD model of the system, accurate predictions of a full-scale facility can be made for improving system design and mitigating the risk in scaling-up the technology.

## Specific objectives

The PhD project is part of the OxyCrack project in collaboration with Haldor Topsøe A/S, for which the main objective is development of the sugar cracking technology from lab-scale through pilot-scale to commercial-scale. The main purpose of this contribution to the OxyCrack project is to improve the understanding of the hydrodynamics of the CFB system and to develop a CFD model, capturing both the hydrodynamics and the cracking reactions of the system. The PhD project is comprised of four main tasks:

1. Experimental investigation of the hydrodynamics in a cold-flow, pilot-scale CFB system.
2. Development and validation of a CFD model (using Barracuda Virtual Reactor ® by CFD Software) describing the hydrodynamics of the investigated CFB system.

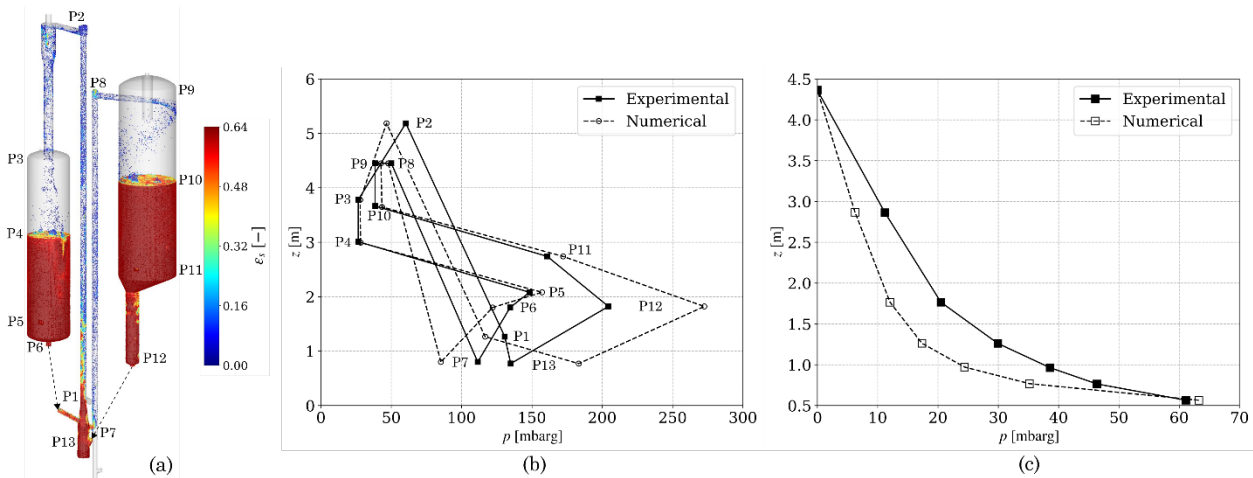


**Figure 36:** CFD Barracuda VR simulation results for specific cold-flow, pilot-scale CFB operating condition. (a) instantaneous particle volume fractions. (b) time-averaged system pressure distributions. (c) time-averaged pressure profile across height of the reactor riser (P1-P2).

3. Expansion of the CFD model to cover cracking reaction kinetics in a hot-flow, pilot-scale CFB system.
4. Prediction and evaluation of proposed full-scale sugar cracker design using the validated CFD model.

## Results and discussion

The cold-flow, pilot-scale CFB at DTU Chemical Engineering consists of a reactor and a regenerator loop. Each loop is comprised of a riser, primary and secondary cyclones, a bubbling bed, and a transfer line for connecting the two loops. Furthermore, a gas stripper is located below the regenerator bubbling bed. In the first phases of the study, only the cold-flow system consisting of the particle and gas phase at ambient conditions is considered. Detailed information on the hydrodynamics of the system in terms of particle velocities, residence times, voidage, and pressure distributions throughout the system can be obtained and analyzed using the proposed CFD model, allowing for direct comparison with experimental data. An excerpt of relevant results for a specific set of operating conditions is included in the following. Fig. 1a displays the predicted instantaneous distribution of particles in the system. A high degree of particle packing is found in the bubbling beds, stripper, and reactor riser conditioning zone. Dilute, fast fluidization regimes are observed in the two risers, while bubble coalescence and splashing at the freeboard is found in the two bubbling beds. Fig. 1b depicts time- and cross-sectional-averaged gauge pressures measured and predicted at different locations in the system. Fig. 1c compares the predicted and measured gauge pressure profile across the height of the riser (P1-P2), normalized by the pressure at the top. Overall, a good agreement is found between simulation and experiment, in the upper parts of the system and in the reactor loop. Pressure drop across the entire

height of the riser is estimated within 3% by the CFD model, although the model overpredicts the pressure drop over the lower part of the riser. Additional efforts are required to remedy some of the observed inconsistencies between experimental data and numerical predictions, before the reactive conditions can be simulated.

## Conclusions

The study addresses the challenge in scaling-up of CFBs for use in cracking of sugars to produce biochemicals. A full-loop CFD model simulating the behavior of the cold-flow in a pilot-scale CFB system has been developed, showing promising results in terms of pressures and particle distributions. Improvements to the cold-flow model are needed to increase its accuracy before extensions of the model to include chemical reactions and a third (liquid sugar feed) phase can be made.

## Acknowledgements

This PhD project is part of the Combustion and Harmful Emission Control (CHEC) Research Centre at DTU Chemical Engineering. The project is by the Innovation Fund Denmark (Project 7045-00009A), and carried out in collaboration with Haldor Topsøe A/S.

## References

1. S. Kraft, F. Kirnbauer, H. Hofbauer, Particuology 36 (2018) 70-81.
2. S. Pannala, M. Syamlal, T.J. O'Brien, Computational Gas-Solids Flows and Reacting Systems, Engineering Science Reference, Hershey, U.K., 2011, p. 279.
3. R.K. Thapa, A. Frohner, G. Tondl, C. Pfeifer, B.M. Halvorsen, Computers and Chemical Engineering 92 (2016) 180-188.
4. Q. Tu, H. Wang, Powder Technology 323 (2018) 534-547.

# Agglomeration in Fluidized Bed Gasification of Wheat Straw

(May 2018- May 2021)

7 AFFORDABLE AND CLEAN ENERGY



## Contribution to the UN Sustainable Development Goals

Biomass is a renewable energy resource and is considered as a substitute for fossil fuels. About 15% of the current global energy supply is contributed by biomass, and it is estimated that up to 33–50% of the global primary energy consumption will be provided by biomass by 2050. Fluidized bed combustion and gasification are widely applied technologies for biomass utilization. However, agglomeration strongly affects the operation of a fluidized bed and may lead to defluidization and unscheduled plant shutdown. Therefore, an improved understanding of agglomeration is important for an efficient utilization of biomass in fluidized bed reactors.



**Liyan  
Zhao**

liyzh@kt.dtu.dk

**Supervisor:** Hao Wu  
Kim Dam-Johansen  
Weigang Lin

## Abstract

Bed agglomeration affects the operation and efficiency of fluidized bed gasification of biomass. In this work, the agglomeration during gasification of wheat straw using different gasification agents (air and steam) was studied in a lab-scale fluidized bed reactor at 850 °C using silica sand as bed material. The results suggest that a high concentration of steam in the bed could accelerate the agglomeration by increasing the amount of liquid phase and lowering the viscosity of straw ash.

## Introduction

Bed agglomeration in fluidized bed combustion of biomass is mainly attributed to the presence of a molten phase, i.e. a low melting point alkali containing compounds, which is originated from the interactions of the alkali species from biomass and bed materials (mainly SiO<sub>2</sub>) [1]. However, the agglomeration tendencies and mechanisms during biomass gasification are still not fully understood. An improved understanding of agglomeration is wanted in order to develop effective countermeasures for bed agglomeration and defluidization.

## Experimental

Experiments were performed in a lab-scale fluidized bed reactor. Wheat straw (WS) with a size range of 2 - 4 mm and silica sand (SiO<sub>2</sub> > 97wt.%) with a size range of 355 – 500 µm were used as fuel and bed material, respectively. The proximate analysis of WS is shown in Table 1. 500 g of sand was loaded in each experiment. During the experiments, the fluidizing gas, which consists of air, steam and nitrogen, was introduced at the bottom of the reactor. The air and steam concentrations in the fluidizing gas were in the range of 2.5% to 25% (v/v) and 0 to 50% (v/v), respectively. The fuel was continuously fed into the reactor until the occurrence of defluidization, which was indicated by a sudden decrease or increase of the pressure

drop. The corresponding feeding rate of wheat straw was around 0.11 kg/h. The bed temperature during all experiments was 850°C. The defluidization tendencies under different atmospheres were evaluated by the amount of the injected fuel that caused defluidization.

**Table 10: Properties of wheat straw**

Proximate analysis (wt. %, ar)	Moisture			Ash		
	8.5			6.7		
Ultimate analysis (wt. %, db)	C	H	N	O*	S	Cl
	42.8	6.1	0.8	42.9	0.1	0.1
Inorganic composition (wt. %, db)	Al	Ca	K	Mg	Si	P
	0.2	0.3	1.0	0.1	1.1	0.1

\* Calculated by difference

## Results and Discussion

Compared to air gasification (Experiment A-C), the presence of 25% steam in fluidizing gas (Experiment D-F) reduces the amount of straw fed for inducing defluidization when other operating parameters are kept constant. This indicates that the presence of a high concentration of steam would promote the agglomeration. This result is in agreement with the results from Ma *et al.* [2]. When the steam concentration is further increased from 25% to 50%, the amount of straw fed for causing defluidization further decreases at low oxygen concentration (0 and 0.5%), while remains stable at high oxygen concentrations (2% and 5.25%).

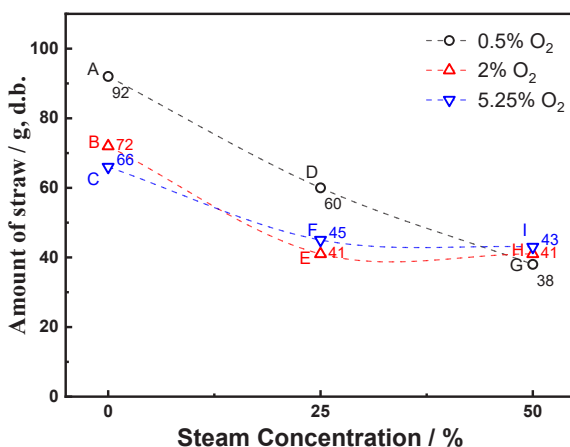


**Figure 37:** The amount of the fed straw that caused defluidization at different conditions. Conditions:  $T_{bed}=850\text{ }^{\circ}\text{C}$ ; fuel feeding rate  $\approx 0.11\text{ kg/h}$  (db); fluidizing gas flow rate = 11.5 NL/min; carrier gas flow rate = 15.5 NL/min; 0.5kg of silica sand with a size range of 355-500  $\mu\text{m}$ .

The impact of steam on the thermodynamic equilibrium calculation of K-species distribution is presented in Figure 2. The addition of 25 % steam in fluidizing gas could lower the KCl (g) concentration, while increase the  $\text{K}_2\text{Si}_4\text{O}_9$  (liq) concentration, implying that a conversion of KCl (g) to  $\text{K}_2\text{Si}_4\text{O}_9$  (liq) is promoted by presence of steam. The calculation results are in agreement both with the experimental results and what has been reported in the literature [3]. This interaction is further enhanced by increasing the steam concentration.

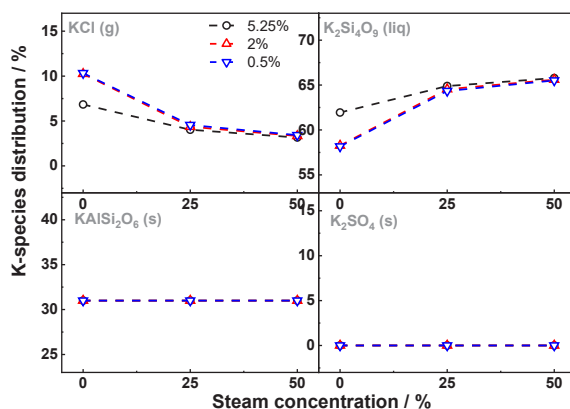


**Figure 38:** The impact of steam on the thermodynamic equilibrium calculation of K-species distribution at 850  $^{\circ}\text{C}$ .

The impact of steam on melting temperature of  $\text{K}_2\text{Si}_4\text{O}_9$ , which is one of main sticky components in straw ash, is shown in Figure 3.  $\text{K}_2\text{Si}_4\text{O}_9$  pellet becomes hemisphere after heating at 850  $^{\circ}\text{C}$  for 3 hours under 100% air condition (Figure 3-b), indicating that its hemispherical temperature of  $\text{K}_2\text{Si}_4\text{O}_9$  under air condition is around 850  $^{\circ}\text{C}$ . This results is consistent with the reported value [4].

However, the  $\text{K}_2\text{Si}_4\text{O}_9$  pellet spread out over the crucibles under 50% steam & 50%  $\text{N}_2$  after heating at 850  $^{\circ}\text{C}$  for 3 hours (Figure 3-c), suggesting that the viscosity of  $\text{K}_2\text{Si}_4\text{O}_9$  is significantly lowered by the presence of high concentration steam.

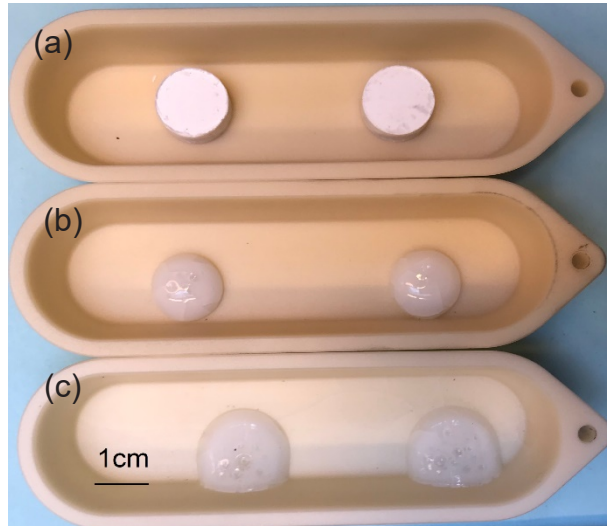


**Figure 39:**  $\text{K}_2\text{Si}_4\text{O}_9$  pellets (a) before and after heating for 3 hours at 850  $^{\circ}\text{C}$  in horizontal oven at (b) 100% air and (c) 50% steam and 50%  $\text{N}_2$ , gas flow rate = 3NL/min.

## Summary

The composition of the fluidizing gas strongly affects the defluidization tendency during biomass gasification. A high steam concentration promoted the defluidization in fluidized bed during steam/air gasification of wheat straw. This trend may be explained by two reasons. The evaporation of KCl is hindered by the interaction between KCl and silica sand induced by the high concentration steam, thus increasing the liquid amount in the bed at operating temperature. In addition to ash chemistry, high concentration steam may lower the viscosity of straw ash, making it easier for the ash to migrate to the surface of the agglomerates and causes the formation of a thick liquid film.

## Acknowledgement

This project is funded by China Scholarship Council (CSC) and Technical University of Denmark (DTU).

## References

1. B. Gatternig and J. Karl, Energy Fuels, 29 (2) (2015) 931–941.
2. T. Ma; C. Fan; L. Hao; S. Li; W. Song; W. Lin, Energy Fuels, 30 (8) (2016) 6395–6404.
3. C. Sevonius; P. Yrjas; M. Hupa, Fuel, 127 (2014) 161–168.
4. Y. Laxminarayan, 2018, Technical University of Demark

# Tubular membrane reactors for immobilization of enzymes

(March 2018- May 2021)



## Contribution to the UN Sustainable Development Goals

With the current global focus on minimizing waste, pollutants and the use of toxic materials in the entire production cycle, this project aims at finding alternative and more sustainable production methods by combination of polymers and enzymes. Particularly, this project targets production of high-value chemicals, such as active pharmaceutical ingredients (APIs). The project focuses on development of new tubular bioreactors, spanning new enzyme immobilization methods as well as gas-liquid phase reactions in continuous flow.



**Libor  
Zverina**

libzve@kt.dtu.dk

### Supervisors:

Anders Daugaard  
John Woodley  
Manuel Pinelo

### Abstract

Oxidation plays a crucial role in synthesis of fine chemicals and production of APIs. Enzymatic oxidation is a greener alternative to a conventional chemo-catalytic approach and opens the potential for new reactions. However, inefficient use of expensive enzymes and oxygen limitations represent particular challenges for oxygen-dependent biocatalytic reactor design. In this work, we combine a porous monolith inside a flow-through reactor with a gas-permeable wall for enzymatic oxidations. We target low and efficient enzyme consumption, and cheap, sustainable oxygen delivery.

### Introduction

Porous monolithic reactors are quickly emerging as an attractive path to viable continuous-flow enzymatic reactions [1]. For preparation of a porous monolith, polymerized high internal phase emulsion (polyHIPE) is nowadays receiving particular attention. PolyHIPE materials offer very facile scalability, good flow-through properties and low pressure drop. Moreover, their characteristic highly porous structure and large specific surface area make them perfect candidates for immobilization of enzymes [2].

As a platform for enzyme immobilization, thiol-ene polymerization products have proven to be extremely versatile [3]. Particularly, introduction of off-stoichiometric thiol-enes allows for easy control of the surface chemistry to provide a very specific environment for enzymes on surfaces [4]. As such, thiol-ene surfaces in combination with polyHIPEs provide a good basis for preparation of a multifunctional immobilization system, with a large specific surface area.

Interestingly, most monolithic reactor studies focus on immobilization strategies of proteolytic enzymes such as trypsin. Studies on oxygen-dependent enzymes in continuous flow monolith reactors are rare.

### Specific Objectives

The objective of the project is to prepare a tubular continuous flow biocatalytic reactor for enzymatic oxidations (figure 1).

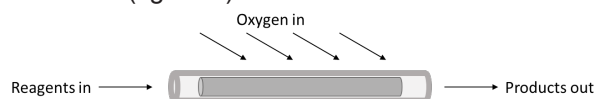
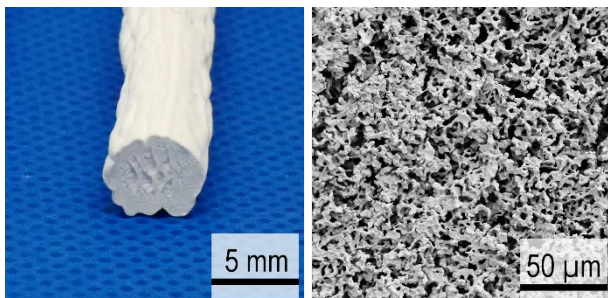


Figure 1: Monolithic flow-through reactor for enzymatic oxidations.

### Results and Discussion

A new tubular reactor was constructed consisting of a highly porous thiol-ene polyHIPE monolith, which was inserted into a gas-permeable polydimethylsiloxane (PDMS) tubing.

The porous monolith was prepared from a high internal phase emulsion combined with off-stoichiometric thiol-ene polymerization. Using excess of thiol groups in the monomer composition results in a monolith with thiol-functional surface, which has previously been proven beneficial for enzyme immobilization [3]. Moreover, the thiol functionality opens up the possibility for further modifications of the surface chemistry to tailor the reactor for a specific enzyme system. After molding, curing, washing and drying, a solid piece of cylindrical monolith was prepared (figure 2).



**Figure 2:** Photograph (left) and scanning electron micrograph (right) of the monolith.

The monolith exhibits a rough and open porous structure (figure 2), which can be observed already on a macroscopic scale. This texture provides a high surface area that is readily available for enzyme adsorption. Furthermore, the SEM picture clearly shows a highly porous and open structure on a microscopic scale. This represents a great potential for using such monolith for enzyme immobilization.

To demonstrate the monolith's ability to immobilize protein, a solution of bovine serum albumin (BSA) ( $0.5 \text{ mg mL}^{-1}$ ) was passed through the monolith at a constant flow rate of  $0.1 \text{ mL min}^{-1}$ . The protein concentration of the feed and the eluate was determined using the Bradford assay. By comparison of the feed and eluate concentration over time, the amount of immobilized BSA and immobilization yield were calculated as shown in figure 3.

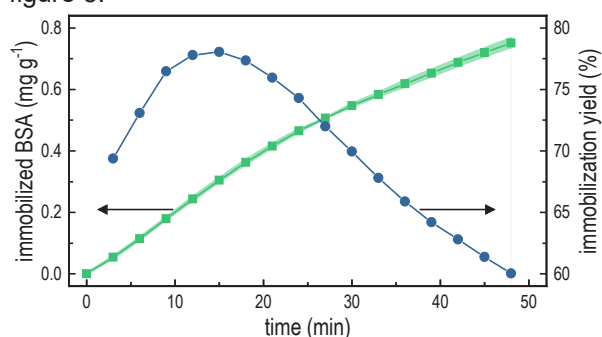


**Figure 3:** Amount of immobilized BSA per gram of monolith and immobilization yield over time.

The amount of immobilized BSA on the monolith steadily increased with time. The immobilization yield reached its maximum already after 15 min, where 78 % of the fed BSA was immobilized, corresponding to  $0.3 \text{ mg g}^{-1}$ . These results suggest that the monolith is well suited for enzyme immobilization.

Next, a commercial PDMS tubing was selected and its oxygen permeability was determined at different flow rates by passing deoxygenized water through different lengths of tubing. During the test, the concentration of dissolved oxygen in the water at the outlet was measured using an optical needle probe.

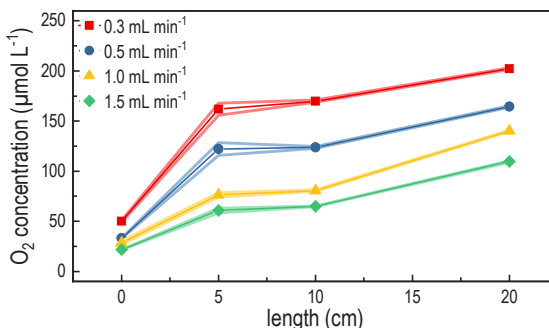


**Figure 4:** Concentration of dissolved oxygen in deoxygenized water after passing through a PDMS tube of various lengths at different flow rates.

As can be seen from data in figure 4, the oxygen level substantially increased already at the short tube length of 5 cm and it continued to increase as the length of the tube increased. The oxygen delivery is sufficiently high even at very high flow rates above  $0.5 \text{ mL min}^{-1}$ , which confirms the applicability of PDMS as an outer membrane contactor in oxygen-dependent enzymatic reactors.

## Conclusions

A new tubular reactor was constructed. The core element of the reactor was a porous monolith based on a thiol-ene polymerization of a high internal phase emulsion. The prepared monolith provides a structure with a large surface area for enzyme immobilization. The monolith was fitted into a highly oxygen-permeable PDMS tube, which ensures a fast and efficient supply of oxygen inside the reactor. This reactor will be applied for enzymatic oxidations under continuous flow conditions using a selection of oxidative enzymes.

## Acknowledgements

The authors wish to thank The Danish Council for Independent Research, Technological Production grant no. DFF – 7017-00109 for financial support.

## References

1. J. Britton, S. Majumdar, G.A. Weiss, Chem. Soc. Rev. 47 (2018) 5891–5918.
2. M.S. Silverstein, Prog. Polym. Sci. 39 (2014) 199–234.
3. C. Hoffmann, M. Pinelo, J.M. Woodley, A.E. Daugaard, Biotechnol. Prog. 33 (2017) 1267–1277.
4. C. Hoffmann, C. Grey, M. Pinelo, J.M. Woodley, A.E. Daugaard, P. Adlercreutz, Chempluschem. 85 (2020) 137–141.

## List of Publications

- L. Zverina, M. Koch, M.F. Andersen, M. Pinelo, J.M. Woodley, A.E. Daugaard, J. Memb. Sci. 595 (2020) 117515.





**Department of Chemical and Biochemical Engineering**

Technical University of Denmark

Building 228A

Søltofts Plads 228A

DK-2800 Kgs. Lyngby

Denmark

Phone: +45 4525 2822

E-mail: [kt@kt.dtu.dk](mailto:kt@kt.dtu.dk)

Web: [www.kt.dtu.dk](http://www.kt.dtu.dk)

March 2021 ISBN: 978-87-93054-91-2

**Editor in chief**

Professor Kim Dam-Johansen,

Head of Department

**Editors**

Peter Szabo,

Associate Professor

Wenhao Hu,

PhD student

**Print**

STEP PRINT POWER

**Cover and design**

Meile Adinaviciute,

Graphic designer



